

**THE COMPOSITION OF ATMOSPHERIC AEROSOL OVER THE
EASTERN MEDITERRANEAN: THE COUPLING OF GEOCHEMICAL AND
METEOROLOGICAL PARAMETERS**

DOCTOR OF PHILOSOPHY

in

Chemical Oceanography
Middle East Technical University
Institute of Marine Sciences

by

NILGÜN NEZİHE KUBİLAY

İÇEL/TÜRKİYE

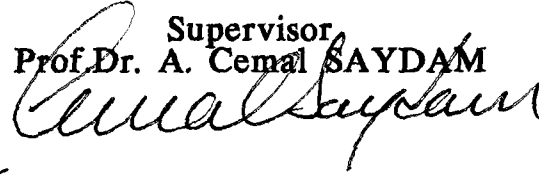
56619

February, 1996


**M.Ö. YÜKSEKÖĞRETİM KURULU
DOKÜMANTASYON MERKEZİ**

I certify that I have read this thesis and in my opinion it is fully adequate, in scope and quality, as a dissertation for the degree of Doctor of Philosophy.

Supervisor
Prof.Dr. A. Cemal SAYDAM



Member of
Examining Committee
Prof.Dr. Gürdal TUNCEL



Member of
Examining Committee
Prof.Dr. Ümit UNLUATA

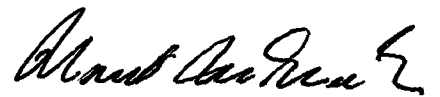
Member of
Examining Committee
Prof.Dr.Selim KAPUR



Member of
Examining Committee
Prof.Dr.Alec GAINES



Certified that this thesis confirms to the formal standards of the Institute.



Office of the President
Prof.Dr. Ümit UNLUATA

ABSTRACT

THE COMPOSITION OF ATMOSPHERIC AEROSOL OVER THE EASTERN MEDITERRANEAN: THE COUPLING OF GEOCHEMICAL AND METEOROLOGICAL PARAMETERS

KUBILAY, Nilgün Nezihe

Ph.D., in Marine Sciences

Supervisor: Prof. Dr. A. Cemal SAYDAM

February 1996, 219, pages

From August 1991 to December 1992 samples of 339 aerosols arriving at a rural site on the Turkish coast of the eastern Mediterranean (Erdemli) were collected by a hi-vol pump and analyzed by the flame and flameless modes of an atomic absorption spectrophotometer for their elemental composition (Al, Fe, Mn, Co, Cr, Ni, V, Zn, Pb, Cd, Mg, Ca and Na). Moreover, three dimensional (3D), three days backward trajectories of the air masses arriving daily at the Erdemli site at 900, 850, 700 and 500 hPa barometric pressure levels have been calculated. The calculation of the backward trajectories was achieved by utilizing the operational model on the computer of the European Center for Medium Range Weather Forecast (Reading, England). The model uses the gridded wind fields produced and archived at the center.

Study of the back trajectories provided a rigorous interpretation of the trace metal concentrations observed in the aerosols. The classification of the air-mass trajectories into geographical sectors showed them to be representative of the mean annual conditions and consistent with the air flow climatology statistics of the eastern Mediterranean. The scale and

permanence of the flow features dictate the average or preferred atmospheric pathways of atmospheric constituents. However it is shown that average conditions or patterns can be misleading since they do not depict the high degree of temporal variability in the atmospheric system. Smaller-scale meteorological features, such as the intensity of vertical-exchange processes or the occurrence of precipitation exerted significant influence on the observed atmospheric concentrations.

The results indicate that the seasonal variability of the atmospheric concentrations of the elements measured at the Erdemli site was related to the occurrence of precipitation. During winter precipitation scavenging decreased the atmospheric concentrations to their minimum values whereas, during dry summer months the lack of precipitation and steadiness in the atmospheric flow, resulted in the accumulation of aerosols in the atmosphere. During transitional seasons, although there was still precipitation, the elements associated with mineral aerosol particles exhibited sporadic but intense concentration peaks. 3D trajectories as well as satellite imagery showed that, throughout the transitional seasons, incursion of Sahara dust governed the fluctuation in the atmospheric concentrations of the elements. Assuming trace metals and other species found in Sahara dust to be soluble in precipitation and seawater, they would be important to marine cycles and consequently to marine biosystems in the eastern Mediterranean during spring and autumn. The vertical dimensions of the trajectories were particularly useful for the identification of the meteorology associated with dust transport.

Although the airflow patterns showed Europe to be a potential source for the long-range transport of material to the sampling site, it was impossible to identify geochemical evidence that differentiated it from the highly variable local background.

The results obtained from factor analysis and from enrichment factors show that the aerosols over the sampling site were affected by anthropogenic, marine and crustal sources. The enrichment diagram of Pb

was used to interpret the chemistry of this enriched element in eastern Mediterranean aerosols.

Estimates of the atmospheric deposition fluxes have emphasized elements indicating mineral dust (Al, Fe, Mn) and anthropogenic emissions (Pb, Cd, Zn). Although the fluxes of elements have been estimated it is stressed that the derivation of the total deposition figures for the entire Mediterranean, especially for anthropogenic elements, is unwarranted.

Keywords: aerosol, eastern Mediterranean, trace metals, enrichment factors/diagrams, factor analysis, sources, 3-D air mass back trajectories, long-range transport, atmospheric vertical motions, Sahara, fluxes.



ÖZ

DOĞU AKDENİZ ÜZERİNDEKİ ATMOSFERİK PARÇACIKLARIN YAPISI: JEOKİMYASAL VE METEOROLOJİK PARAMETRELERİN BİLEŞKESİ

KUBİLAY, Nilgün Nezihe

Doktora Tezi, Deniz Bilimleri

Tez Yöneticisi: Prof. Dr. A. Cemal SAYDAM

Şubat 1996, 219 sayfa

Ağustos 1991 ve Aralık 1992 tarihleri arasında Doğu Akdeniz'in Türkiye kıyısındaki kırsal bölgeye (Erdemli) ulaşan hava kütlelerinden 339 adet aerosol örnekleri toplanmıştır. Örnekler yüksek debili hava pompası kullanılarak toplanmış ve elemental analizleri (Al, Fe, Mn, Co, Cr, Ni, V, Zn, Pb, Cd, Mg, Ca, Na) atomik soğurma spektrofotometresi ile alevli ve elektro-termal atomlaştırma teknikleri kullanılarak yapılmıştır. Buna ilaveten örnekleme bölgesine (Erdemli) 900, 850, 700, ve 500 hPa barometrik basınç seviyelerinde ulaşan hava kütlelerinin üç günlük geriye dönük üç boyutlu (3D) yörüngeleri hesaplanmıştır. Hava kütlelerinin geriye dönük yörüngelerinin hesaplanmasında ECMWF'in (Avrupa Orta Ölçekli Hava Tahmin Merkezi, Reading, İngiltere) bilgisayarında kullanıcıya açık bulunan model kullanılmıştır. Bu model gene merkezde hazırlanmış ve arşivlenmiş rüzgar elemanlarını kullanarak istenilen tarihlere ait geriye dönük hava kütleleri yörüngelerini hesaplayabilmektedir.

Geriye dönük hava yörüngelerinin hesaplanması aerosollerdeki metal derişimlerinin deęişim sebeplerinin yorumlanmasına açıklık kazandırmıştır. Hava kütlelerinin coęrafik bölgelere göre sınıflandırılması sonucunda elde

edilen bilgilerin literatürdeki Doğu Akdeniz'e ulaşan hava akımları istatistiği ile uyumlu olduğu dolayısıyla bölgeye ulaşan yıllık ortalama hava akım yönlerini temsil ettiği görülmüştür. Ayrıca, ortalama meteorolojik koşulların, atmosferik sistemler içerisinde ani ve geçici değişimleri izah etmekte yarıltıcı ve yetersiz kaldığı da gösterilmiştir. Daha küçük ölçekli meteorolojik şartların, hava kütlelerinin düşey yönde hareket yoğunluğu veya havanın yağışlı olması gibi, aerosollerdeki element derişimlerini önemli ölçüde etkilediği görülmüştür.

Elde edilen sonuçlar, Erdemli'de toplanan aerosollerde ölçülen elementlerin derişimlerindeki mevsimsel değişimlerin yağışlarla yakından ilgili olduğunu göstermiştir. Kış ayları boyunca etkin olan yağışların atmosferi yıkaması elementlerin aerosoller içerisinde derişimlerini en alt düzeye indirmektedir. Yaz ayları süresince yağış olmaması ve hava kütlelerinin durağan olması aerosollerin atmosferde birikmesine ve dolayısıyla içerdikleri elementlerin derişimlerinin artmasına neden olmaktadır. Geçiş mevsimlerinde (bahar ve sonbahar aylarında) yağışlar devam etmesine rağmen alüminyum-silikat yapısında zenginleşmiş elementlerin derişimlerinde ani yükselmeler görülmüştür. Üç boyutlu hava kütlelerinin yörüngeleri ve uydudan elde edilen görüntüler elementlerin derişimlerinde bu aylarda görülen değişimlerin bölge atmosferinin Sahra çölünden taşınan toza maruz kalmasından kaynaklandığını göstermiştir. Sahra tozlarında bulunan metallerin ve diğer elementlerin yağmur ve deniz suyunda çözüldüğünü varsayarsak, bunların, bilhassa ilkbahar ve sonbahar aylarında Doğu Akdeniz'deki elementlerin döngüleri ve eko-sistemi üzerinde önemli ölçüde etkin olabileceğini söylemek mümkündür. Hava yörüngelerinin düşey yöndeki hareket boyutunun, atmosferik taşınımından sorumlu meteorolojik olayların tanımlanabilmesi açısından oldukça önemli olduğu saptanmıştır.

Hava kütlelerinin yörüngelerinin coğrafi bölgelere göre gruplandırılması sonucunda, Avrupa kıtasının bölgeye uzun mesafeli aerosol taşınımında potansiyel bir kaynak olabileceği görülmüştür. Fakat Doğu Akdeniz atmosferine has çok değişken olan metal derişimleri arasında

Avrupa kıtasından gelen hava kütlelerinin etkisini belirleyebilecek karakteristik bir özellik bulunamamıştır.

İstatistiksel analizler ve zenginleşme katsayılarının hesaplanmasından elde edilen sonuçlar örnekleme bölgesi atmosferinin antropojenik, denizsel ve toprak kaynaklı aerosollerin etkisinde olduğunu göstermiştir. Kurşun için elde edilen zenginleşme diyagramları, Doğu Akdeniz atmosferindeki aerosollerde antropojenik kaynaklı bu elementin dağılımının tanımlanmasında faydalı olduğu gösterilmiştir.

Atmosferden denize olan toprak kaynaklı aerosollerin çökeltme akılarının hesaplanması için Al, Mn ve Fe gibi elementler kullanılmıştır. Atmosfer yoluyla denize ulaşan kirlilik miktarının önemini vurgulanması amacı ile de antropojenik emisyonların göstergesi olan Pb, Cd ve Zn için çökeltme akıları hesaplanmıştır. Her ne kadar elementlerin atmosferden denize olan akıları hesaplanmış isede bu değerlerin tüm Akdeniz havzasına yayılmasının, özellikle antropojenik kaynaklı elementler için şüpheli sonuçlar verebileceği vurgulanmıştır.

Anahtar kelimeler: aerosol, doğu Akdeniz, iz metaller, zenginleşme faktörü/diyagramı, faktör analizi, kaynaklar, üç boyutlu hava yörüngeleri, uzun mesafeli taşınım, hava kütlelerinin düşey hareketleri, Sahara, çökeltme akıları.

ACKNOWLEDGMENTS

I am deeply grateful to my supervisor Prof. Dr. A. C. Saydam for his valuable comments and sincere guidance. Working under his supervision was very rewarding in various aspects that are not limited to the thesis subject.

I wish to extend my special gratitude to Prof. Dr. E. Özsoy (who as a co-director of the Project Land-3 of ICSC-World Laboratory with headquarters in Lausanne, Switzerland and the Mediterranean Research Center in Erice, Italy supplied a fellowship) for making part of this study possible.

I want to add my appreciation to Prof. Dr. A. Gaines and Prof. Dr. G. Tuncel for their careful reviews of the manuscript.

I would like to thank Assist. Prof. Dr. S. Yemenicioğlu who helped me in various ways for achievement of the study.

I would like to thank my colleague Mr. F. Karakoç for his assistance in collection and analysis of the samples.

I extent my warmest thanks to Mrs. G. Latif for her documental support during this study.

And finally, I would also like to express my gratitude to my family for their endless support and understanding.

TABLE OF CONTENTS

	Page
ABSTRACT	ii
ÖZ	v
ACKNOWLEDGEMENTS	viii
TABLE OF CONTENTS	ix
LIST OF TABLES	xii
LIST OF FIGURES	xv
CHAPTER I: INTRODUCTION	1
1.1. Aim of the Study	1
1.2 Sources of Material to the Marine Atmosphere	2
1.3. The Atmospheric Transport of Material to the Oceans	4
1.4. The Case of the Mediterranean Sea	9
1.4.1. Input of Material onto the Mediterranean via the Atmospheric Pathway	9
1.4.2. Geographic and Climatic Overview of the Mediterranean Area	16
CHAPTER II: MATERIALS AND METHODS	25
2.1. Computation of Air Mass Back Trajectories	25
2.2. Atmospheric Aerosol Sampling	26
2.2.1. Sampling Tower	26
2.2.2. Aerosol Collection	28
2.2.3. Sample Manipulation	30
2.3. Aerosol Chemical Analysis	31
2.3.1. Sample Dissolution	31
2.3.2. Atomic Absorption Spectrophotometer (AAS)	32

2.4. Quality Assurance	34
CHAPTER III: RESULTS AND DISCUSSIONS	37
3.1. Atmospheric Transport of Material From the Meteorological Point of View	37
3.1.1. Comparison of the Air Flow Climatology at the Erdemli Site With Different Receptor Sites in the Eastern Mediterranean	37
3.2. Atmospheric Concentrations of Aerosol Elements Collected at the Erdemli Station	46
3.2.1. Mean Concentrations	46
3.2.2. Contributions of Major Sources to the Observed Mean Concentrations	48
3.2.3. Comparison of the Data With the Results of Other Studies	53
3.2.4. Temporal Variation of the Atmospheric Concentrations	63
3.2.4.1. Seasonal Changes	63
3.2.4.2. Elemental Concentrations: Time Series	65
3.3. The Variations in the Atmospheric Concentrations of the Elements and Air Mass Back Trajectories	70
3.3.1. African Dust Reaching the Eastern Mediterranean: A Case Study to Verify Trajectory Calculations	70
3.3.2. Atmospheric Concentrations of the Elements and the Corresponding Air Mass Back Trajectories	76
3.3.2.1. Case Studies	76
3.3.2.2. Influence of Sectors of Air Trajectories on the Elemental Compositions of the Aerosols at the Erdemli Site	104
3.3. Chemical Composition of Aerosols Over the Eastern Mediterranean	
3.3.1. Enrichment Factors	117
3.3.2. The Average Compositions of the End Members of the Aerosols Over the Eastern Mediterranean	125
3.3.2. Enrichment Factor (EF) Diagrams	133
3.4. Statistical Techniques in Studying the Relationships Between the Elements	145

3.4.1. Linear Correlation	145
3.4.2. Factor Analysis	146
3.5. The Atmospheric Input of Trace Elements onto the Eastern Mediterranean	148
3.5.1. Dry and Wet Deposition Fluxes	149
CHAPTER IV: CONCLUSIONS	158
CHAPTER V: RECOMMENDATIONS FOR FUTURE RESEARCH	166
REFERENCES	169
APPENDIX	191



LIST OF TABLES

	Page
Table 1.1. Primary sources of atmospheric tracers and trace elements (after Church et al., 1990)	4
Table 1.2. Atmospheric dissolved versus fluvial dissolved inputs to the global ocean (units, 10^9 g y^{-1})	6
Table 1.3. Comparison between total input of Rhone river and atmospheric input to the Gulf of Lyon	12
Table 2.1. Concentrations of elements observed in BCR standard reference material (RM 142) by AAS	35
Table 2.2. The reproducibility of the AAS technique	36
Table 3.1. Summarized statistics of the elemental concentrations for the whole sampling period	47
Table 3.2. Percent contribution of the major sources to the observed mean atmospheric concentrations of the elements	52
Table 3.3. Geometric mean concentrations of trace metals in aerosols from a number of representative marine environments	54
Table 3.4. The geometric mean concentrations of trace metals in aerosols over the Mediterranean Sea and surrounding coastal sites. Percentages of the non-crustal metal concentrations are given in parentheses	61
Table 3.5. Summarized statistics of the seasonal elemental concentrations	
(a) Winter (November, December, January, February; wet season)	63
(b) Summer (June, July, August, September; dry season)	64
(c) Transitional seasons (March, April, May and October; wet seasons)	64

Table 3.6. The average composition of mean crust, various rocks types, soil and bulk sea water	121
Table 3.7. Seasonal geometric mean enrichment factors (EFs) of the metals (number in parenthesis are the ranges of Efs)	124
Table 3.8. EF_{crust} values of the elements in the samples collected from outbreaks of desert dust	127
Table 3.9. EF_{crust} values of the elements in samples representative of the European end Member	128
Table 3.10. Mean EF_{crust} for trace metals in aerosols representative of marine environments	130
Table 3.11. EF_{crust} values in aerosols over the land-based stations at the Mediterranean Sea	131
Table 3.12. Enrichment Factors, ranked on the basis of Al concentrations in atmospheric particulates collected in April 1992	132
Table 3.13. Relationships between the elements in the atmospheric particulates	146
Table 3.14. Varimax rotated factor matrix	147
Table 3.15. Total atmospheric depositions of trace elements onto the eastern Mediterranean ($mg\ m^{-2}\ y^{-1}$)	154
Table 3.16. Percent contribution of the four sectors at 900 hPa to the mean seasonal total deposition of the elements	155
Table 3.17. Total atmospheric depositions of trace elements onto the regional seas ($mg\ m^{-2}\ yr^{-1}$)	156
Table A1. The job utilized for retriving air mass back trajectories from ECMWF	192
Table A2. The trajectory data base obtained from the request file given in Table A1	193

Table A3. Classification of the trajectories corresponding to the samples collected during August 1991-December 1992 with respect to their origins and meteorological conditions together with their elemental composition. The geographical coverage of trajectory codings are indicated in Figure 3.1. and the codes used for the type of airflow are as follows:

A: Anticyclonic; C: Cyclonic; I: Isobaric

(For the sake of space the sample numbers are used instead of sampling dates in the concentration tables)

	199
A3.1. August 1991	199
A3.2. September 1991	200
A3.3. October 1991	201
A3.4. November 1991	203
A3.5. December 1991	204
A3.6. January 1992	205
A3.7. February 1992	206
A3.8. March 1992	208
A3.9. April 1992	209
A3.10. May 1992	210
A3.11. June 1992	211
A3.12. July 1992	212
A3.13. August 1992	213
A3.14. September 1992	214
A3.15. October 1992	215
A3.16. November 1992	216
A3.17. December 1992	218

LIST OF FIGURES

	Page
Figure 1.1. Topographical map of the eastern Mediterranean area (after Brody and Nestor)	18
Figure 1.2. Major local wind systems in the Mediterranean (after Brody and Nestor, 1980)	19
Figure 1.3. Areas of cyclogenesis and tracks of cyclones which affect the eastern Mediterranean (after Brody and Nestor, 1980)	20
Figure 2.1. Sample-to-blank ratios of the elemental concentrations in Whatman-41 filter papers	29
Figure 3.1. Sector partitioning for the geographical classification of air mass back trajectories	39
Figure 3.2. The percentage of mean airflow directions at various barometric pressure levels during August 1991-December 1992 at the Erdemli site (a) 900 hPa (b) 850 hPa (c) 700 hPa (d) 500 hPa	40
Figure 3.3. The seasonal distribution of the air flow directions at 900, 850, 700 and 500 hPa barometric levels	42

Figure 3.4. The mean airflow climatologies at different receptor sites located at the eastern Mediterranean area	44
(a) Crete trajectories shown as annual percentages (after GESAMP, 1985).	
(b) Israel trajectories shown as the percentages of the five years' trajectories (after Dayan, 1986). About 10% of the total number of trajectories were missing or could not be accurately classified into the five categories.	
Figure 3.5. The monthly precipitation rates during the year of 1991, 1992 and the mean rates between the period of 1931-1980 at the sampling site. The total yearly precipitation rates are given at the bottom	45
Figure 3.6. The frequency histograms of the log-transformed atmospheric concentrations of the elements and their expected normal distributions	49
(a) Fe; (b) Pb; (c) Na	
Figure 3.7. Locations of the land based aerosol sampling sites around the Mediterranean basin. The transect along which aerosol samples collected on ship was indicated (Chester et al., 1993a)	57
Figure 3.8. Variations in aerosol metal concentrations during August 1991-December 1992 at the Erdemli site, illustrating the large-scale short-term variability. Local daily precipitation amounts are indicated at the bottom	68
(a) Al; (b) Fe; (c) Mn; (d) Ca; (e) Mg; (f) Co; (g) Ni; (h) Cr; (i) V; (j) Pb; (k) Cd, (l) Zn; (m) Na	
Figure 3.9. 3-D, three days backward air mass trajectories arriving at Erdemli, at 900, 850, 700 and 500 hPa barometric pressure levels, at 12 00 UT on 27 March 1992. The pressure profile is shown at right hand side of the figure	71
Figure 3.10. A sequence of METEOSAT vis images from 25 to 31 March 1992	73
Figure 3.11. A sequence of METEOSAT IR images from 25 to 31 March 1992	75

Figure 3.12. The percentage of mean air flow direction at various atmospheric pressure levels during October 1991. (a) 900 hPa; (b) 850 hPa; (c) 700 hPa; (d) 500 hPa	77
Figure 3.13. Air mass back trajectories arriving at Erdemli at 900, 850, 700 and 500 hPa barometric levels on 2 October 1991. The right hand panel illustrates associated vertical motions of the trajectories. (conc. in ng m^{-3})	78
Figure 3.14. Air mass back trajectories arriving at Erdemli at 900, 850, 700 and 500 hPa barometric levels on 3 October 1991. The right hand panel illustrates associated vertical motions of the trajectories (conc. in ng m^{-3})	79
Figure 3.15. A sequence of METEOSAT IR images during 1-3 October 1991	81
Figure 3.16. Air mass back trajectories arriving at Erdemli at 900, 850, 700 and 500 hPa barometric levels on 8 October 1991. The right hand panel illustrates associated vertical motions of the trajectories (conc. in ng m^{-3})	82
Figure 3.17. Air mass back trajectories arriving at Erdemli at 900, 850, 700 and 500 hPa barometric levels. (a) 9 October 1991 (b) 10 October 1991	83
Figure 3.18. Air mass back trajectories arriving at Erdemli at 900, 850, 700 and 500 hPa barometric. The bottom panels illustrate associated vertical motions of the trajectories. (a) 11 October 1991; (b) 12 October 1991	84
Figure 3.19. Air mass back trajectories arriving at Erdemli at 900, 850, 700 and 500 hPa barometric levels on 13 October 1991. The right hand panel illustrates associated vertical motions of the trajectories (conc. in ng m^{-3}).	84
Figure 3.20 Air mass back trajectories arriving at during 17-23 October 1991 (conc. in ng m^{-3}) (a) 900 hPa; (b) 500 hPa	85

Figure 3.21. Air mass back trajectories arriving at Erdemli during 24-28 October 1991 (conc. in ng m^{-3}) (a) 900 hPa; (b) 500 hPa	85
Figure 3.22. Air mass back trajectories arriving at Erdemli at 900, 850, 700 and 500 hPa barometric levels on 29 October 1991. The right hand panel illustrates associated vertical motions of the trajectories (conc. in ng m^{-3})	86
Figure 3.23. The percentage of mean air flow direction at various atmospheric pressure levels during April 1992 (a) 900 hPa; (b) 850 hPa; (c) 700 hPa; (d) 500 hPa	87
Figure 3.24. Air mass back trajectories arriving at Erdemli at 900, 850, 700 and 500 hPa barometric levels on 1 April 1992. The right hand panel illustrates associated vertical motions of the trajectories (conc. in ng m^{-3})	88
Figure 3.25. Air mass back trajectories arriving at Erdemli at 900, 850, 700 and 500 hPa barometric. The right hand panel illustrates associated vertical motions of the trajectories (conc. in ng m^{-3}) (a) 3 April 1992; (b) 4 April 1992	89
Figure 3.26. Air mass back trajectories arriving at Erdemli at 900, 850, 700 and 500 hPa barometric levels on 7 April 1992. The right hand panel illustrates associated vertical motions of the trajectories (conc. in ng m^{-3})	90
Figure 3.27. Air mass back trajectories arriving at Erdemli during 8-12 April 1992 (conc. in ng m^{-3}) (a) 900 hPa; (b) 500 hPa	91
Figure 3.28. Air mass back trajectories arriving at Erdemli at 900, 850, 700 and 500 hPa barometric levels on 13 April 1992. The right hand panel illustrates associated vertical motions of the trajectories (conc. in ng m^{-3})	92

- Figure 3.29. Air mass back trajectories arriving at Erdemli at 900, 850, 700 and 500 hPa barometric levels on 14 April 1992. The right hand panel illustrates associated vertical motions of the trajectories (conc. in ng m^{-3}) 92
- Figure 3.30. Air mass back trajectories arriving at Erdemli at 900, 850, 700 and 500 hPa barometric levels. The right hand panel illustrates associated vertical motions of the trajectories (conc. in ng m^{-3}). (a) 19 April 1992 (b) 20 April 1992 (c) 21 April 1992 94
- Figure 3.31. Air mass back trajectories arriving at Erdemli during 22-29 April 1992 (conc. in ng m^{-3}). (a) 900 hPa; (b) 500 hPa 95
- Figure 3.32. Air mass back trajectories arriving at Erdemli at 900, 850, 700 and 500 hPa barometric levels on 27 April 1992. The right hand panel illustrates associated vertical motions of the trajectories (conc. in ng m^{-3}) 96
- Figure 3.33. Air mass back trajectories arriving at Erdemli at 900, 850, 700 and 500 hPa barometric levels on 30 April 1992. The right hand panel illustrates associated vertical motions of the trajectories (conc. in ng m^{-3}) 96
- Figure 3.34. The percentage of mean air flow direction at various atmospheric pressure levels during October 1992 98
(a) 900 hPa; (b) 850 hPa; (c) 700 hPa; (d) 500 hPa
- Figure 3.35. Air mass back trajectories arriving at Erdemli at 900, 850, 700 and 500 hPa barometric levels on 6 October 1992. The right hand panel illustrates associated vertical motions of the trajectories (conc. in ng m^{-3}) 99
- Figure 3.36. Air mass back trajectories arriving at Erdemli during 12-23 October 1992 (conc. in ng m^{-3}) 100
(a) 900 hPa; (b) 500 hPa

Figure 3.37. Air mass back trajectories arriving at Erdemli at 900, 850, 700 and 500 hPa barometric levels on 24 October 1992. The right hand panel illustrates associated vertical motions of the trajectories (conc. in ng m^{-3})	101
Figure 3.38. Air mass back trajectories arriving at Erdemli at 900, 850, 700 and 500 hPa barometric levels on 26 October 1992. The right hand panel illustrates associated vertical motions of the trajectories (conc. in ng m^{-3})	102
Figure 3.39. Air mass back trajectories arriving at Erdemli during 27-29 October 1992 (conc. in ng m^{-3}) (a) 900 hPa; (b) 500 hPa	102
Figure 3.40. Representative trajectories and their mean elemental concentrations on seasonal basis from the N-W sector (conc. in ng m^{-3}) (a) Western Anatolia; (b) Europe	105
Figure 3.41. Saharan originated trajectories during summer time (conc. in ng m^{-3}) (a) 900 hPa; (b) 700 and 500 hPa	109
Figure 3.42. Representative short range trajectories and their mean elemental concentrations (ng m^{-3}) on seasonal basis from the S-W sector	110
Figure 3.43. North-Africa originated trajectories arriving at 900 hPa to the Erdemli site (conc. in ng m^{-3})	111
Figure 3.44. Representative Middle East originated air-mass back trajectories and their corresponding vertical movements (conc. in ng m^{-3}) (a) 900 hPa (b) 700 hPa and 500 hPa	112
Figure 3.45. Representative North-Africa originated air-mass back trajectories and their corresponding vertical movements (conc. in ng m^{-3}) (a) 900 hPa (b) 700 and 500 hPa	113

Figure 3.46. Air mass back trajectories arriving at Erdemli at 900, 850, 700 and 500 hPa barometric levels on 4 November 1992. The right hand panel illustrates associated vertical motions of the trajectories (conc. in ng m^{-3})	116
Figure 3.47. EF_{crust} values for atmospheric trace metals collected at the Erdemli site. The horizontal bars represent geometric mean enrichment factors, and vertical bars represent the geometric standard deviation (Solid bars for average crust composition and dashed bars for average soil composition)	122
Figure 3.48. EF_{mar} values for atmospheric trace metals collected at the Erdemli site. The horizontal bars represent geometric mean enrichment factors, and vertical bars represent the geometric standard deviations	123
Figure 3.49. Composite enrichment factor diagram for Pb	135
Figure 3.50. EF Diagram of Pb for the samples collected during April 1992	138
Figure 3.51. EF diagrams of Pb constructed on seasonal basis for the aerosols collected at the Erdemli site (a) summer (b) winter (c) transitional seasons	142

CHAPTER I

INTRODUCTION

1.1. Aim of the Study

River input has long been considered to be the major source of chemical elements to the ocean system. However, in recent years it has become increasingly apparent that atmospheric transport plays a central role in the supply of material to the ocean. This atmospheric input is especially important in shelf seas and semi-enclosed seas like the Mediterranean which is closed to potential pollution sources from surrounding countries and subjected to the well-known influx of Saharan dust. From a global change perspective, the driving forces are acting in the atmospheric compartment, induced climatic changes will in turn affect wind regimes, mean air mass trajectories, rainfall and accordingly the atmospheric input of different compounds of biogeochemical significance.

The overall aims of this thesis may be summarised as follows: to provide a time series data set of: (a) the concentrations; (b) the sources; (c) the air/sea fluxes of trace metals in aerosols over the eastern Mediterranean.

One of the main purposes of the present study is to contribute to the understanding of the significance of long-range material transported from remote potential source regions to the eastern Mediterranean. The lack of long-time sampling data sets is one of the major problems and it is very difficult to give more detailed and quantitative information. Previous workers have shown that trace metal concentrations in aerosols vary daily (Dulac et al., 1987; Bergametti et al., 1989b). It is the purpose of this study to operate a land-based station at a coastal site (Erdemli) in order to obtain

better characterization of the geochemical "end-members" in the aerosols and to assess the nature and relative contributions of the different sources to the atmospheric trace metal concentrations. Accordingly, this study was directed towards the investigation of the factors controlling the variability of atmospheric trace metal concentrations over the eastern Mediterranean and towards the complete understanding of the transport processes using a combination of both geochemical and meteorological approaches.

1.2. Sources of Material to the Marine Atmosphere

A suspension of solid and liquid material in a gaseous medium is usually referred to as an aerosol. The particulate material (aerosol) is introduced to the atmosphere by either natural and/or anthropogenic processes. These are divided into two classes according to their generation termed low- and high-temperature generation processes (Chester, 1990a). This division is stressed since the forms in which elements are present in the atmosphere i.e., their speciation, can be strongly dependent on the temperature at which they were released from their parent host. Following this broad classification of the generation of atmospheric particulate material, various researchers have identified both natural and anthropogenic sources of the elements to the world atmosphere listed below (Church et al., 1990; Chester, 1990a).

(a) Natural sources; The surfaces of the earth and the oceans can supply material to the atmosphere both in particulate and gaseous forms. The generation of particulate material from these wide-spread sources occurs during the low-temperature mechanical mobilization of surface deposits and sea salts. Emissions from volcanoes and forest fires are other major natural sources of trace elements in the atmosphere formed from high-temperature processes. These two types of source can release particulate material, e.g. ash, together with gaseous phases that may undergo condensation

reactions and can result in the enrichment of particulate material. The high temperature burning of vegetation and the consequent emission into the atmosphere of particulate and vaporized elements from plant surfaces and soils are counted as natural sources.

(b) Anthropogenic sources; A variety of anthropogenic sources release both particulate and gaseous material into the atmosphere. These include the combustion of fossil fuels, including such additives as the lead in gasoline, the roasting of ores for refining metals, waste incineration, the processing of crustal materials for manufacturing cements, the production of chemicals, agricultural utilization and numerous other industrial and social activities.

To assess the relative importance of natural and anthropogenic sources interference factors (IF) were first calculated for trace metals as the ratio (Lantzy and Mackenzie, 1979);

$$IF = \left(\frac{\text{total global anthropogenic emissions}}{\text{total global natural emissions}} \right) \times 100$$

Global IF values calculated by this method using the most recently available data were tabulated by Church et al., (1990) (reproduced in Table 1.1) to show the primary sources of those atmospheric tracers and trace elements included in the present study. As can be seen from the table IF values for some elements (Na, Mg, Ca and Al) are not given. For these elements the IFs are usually near 100 since their concentrations are contributed equally by natural and anthropogenic sources and they are often used as tracers of sea salt or crustal dust.

Table 1.1. Primary sources of atmospheric tracers and trace elements (after Church et al., 1990).

Element	Primary Sources	Group	Interference Factor
Ca	Sea salt, cement manufacture, crustal	1c	
Mg	Sea salt>crustal		
Na	Sea salt>crustal	1a	
Al	Crustal	1a	
Fe	Crustal, anthropogenic	2,1c	39
Mn	Crustal, anthropogenic	1c	52
Co	Crustal, anthropogenic	1c	63
Ni	Crustal, petroleum burning	1b	180
Cr	Crustal, anthropogenic	1c	161
V	Crustal, oil combustion	1c	320
Cd	Mixed anthropogenic emissions	2,c	760
Pb	Gasoline combustion, volcanic smelters	1b	2400
Zn	Anthropogenic, vegetation	2	78,500

Note: Group 1-Primary sources: 1a.natural, 1b.anthropogenic, 1c.mixed origin.
 Group 2-Tracers, biogeochemically important, atmospherically transported.

1.3. The Atmospheric Transport of Material to the Oceans

Atmospheric and fluvial inputs constitute the primary sources of trace metals and nutrients to surface waters. It is important to assess the magnitude of these fluvial and atmospheric fluxes to ocean surface waters, because, through their conversion to organic matter, these inputs are transported to the ocean interior.

The oceans can act as both a source and sink of materials which are transported by the atmosphere. Particularly on a global basis, the atmosphere plays an important role as a conduit of such substances as

sulfur compounds, trace metals, desert dust, organic materials and other natural and man-made substances.

How a given substance is transported via the atmosphere depends on a number of factors. One of the most important is the form in which the substance is released. A non-reactive gas will be transported much further than an aerosol, all other things being equal. Other factors that influence transport are the elevation of release, the state of the atmosphere, the location of the source with respect to the oceans and the particle size. However, physical transport is not the only factor that influences the lifetime of materials in the atmosphere.

Two other factors beside transport affect the residence time of a substance in the atmosphere. First, chemical transformation can have important effects on the lifetime of a gas or aerosol through photochemical processes or through chemical reactions within clouds. In both cases, the end product will be in a different chemical and/or physical form (obviously, for non-reactive species this process is not important). Second, physical capture or scavenging of particles and gases by cloud droplets may occur, and in this manner substances can be deposited to the oceans.

Traditional estimates of budgets and residence times of trace metals in the oceans have been based on riverine fluxes and have ignored atmospheric inputs. Over the last few decades this view has begun to be modified and systematic studies of atmospheric inputs to the oceans have been undertaken. The most recent and comprehensive estimate of riverine and atmospheric inputs of metals and nutrients has been prepared by GESAMP (1989). The comparison with riverine inputs suggests that the impact of atmospheric deposition on open ocean biogeochemical cycles will be much greater than that for rivers. Although the magnitudes of fluxes (except for Pb) are comparable (Table 1.2.), the various data sets demonstrate that the influence of riverine inputs is not detectable far from the river mouth (Boyle et al., 1982; Shiller and Boyle, 1987; 1991). Probably the dissolved species entering the ocean are directly taken up by

phytoplankton. Both the plankton remains and the original riverine particles are deposited on the continental shelf, where they are subject to diagenetic processes. This results in a secondary input to the ocean, into surface and thermocline waters, depending on the depth of the shelf sediments. This flux has hardly been quantified so that its influence to the open ocean cannot as yet be assessed.

Table 1.2. Atmospheric dissolved versus fluvial dissolved inputs to the global ocean (units, 10^9 g y^{-1}).

Element	Riverine	Atmospheric
N (excluding N ₂ gas)	22-50	30
Pb	2	80
Cd	0.3	1.9-3.3
Cu	10	14-45
Ni	11	8-11
Zn	6	33-170
Fe	1100	3200
P	300*	310

All data from GESAMP (1989).

* Total P input to marine sediment.

The estimates of chemical fluxes whether from rivers or from the atmosphere suffer from uncertainties. For rivers there are major problems of the undersampling of representative systems because, though large rivers dominate the global water balance, such rivers are located in remote regions and have been insufficiently sampled to permit an adequate description of the variation of dissolved and particulate concentrations with season and flow. The atmospheric flux estimates suffer from the same problem of undersampling. In both cases there is a common objective, that of defining the temporal variability of the flux - how the source output varies with climate and human activity. An understanding of this variability is essential if one wishes to characterize the present day flux. The characterization of the temporal and areal variability of the continent-to-ocean wind-borne flux is a

difficult task. In contrast to rivers, which have well-defined channels and are relatively shallow, the winds are global in scope and have significant vertical structure. Thus, in order to quantify atmospheric transport it is necessary to develop comprehensive understanding of the governing meteorological processes, such as wind flow and precipitation patterns and to evaluate their effects on the chemical fluxes. Since the atmosphere is a very dynamic compartment of the earth system the atmospheric concentrations are highly variable in space and time. In order to characterize such variability adequately, daily sampling over periods of one year or longer is necessary but such a long period of sampling is normally impossible at sea on research cruises, so almost all data are derived from coastal or island sampling sites. The lack of time series data is now becoming a major problem in both oceanic and atmospheric science.

It has long been recognized that significant mineral aerosol, particularly soil eroded dust, is transferred through the atmosphere and deposited onto the ocean surface. The long range transport of dust from north Africa to the Atlantic and from Asia to the Pacific has been studied in detail by combining the meteorological conditions with ground measurements (Uematsu et al. 1983, 1985; Blank et al. 1985; Kendall et al. 1986; Talbot et al. 1986, Betzer et al., 1988; Savoie et al. 1989; Prospero 1990; Whelpdale and Moody 1990). The aeolian transport of desert aerosols is a major contribution to oceanic sedimentation and it has been suggested that the aeolian components of the marine and ice-core record could provide information about paleoatmospheric circulation patterns and past climatic conditions on the continents (Prospero, 1981a; Prospero, 1985; Chester 1990b; Mayewski et al., 1993). Driven by large-scale atmospheric motion, dust particles may travel long distances before being deposited. A number of case studies confirm the long range nature of the transport of Saharan dust, dust paths having been detected towards the Black Sea (Kubilay et al., 1995b); the eastern Mediterranean (Dayan et al., 1991; Ganor et al., 1991; Ganor and Mamane, 1982; Ganor, 1994; Kubilay et al., 1994;

Kubilay and Saydam, 1995c; Kubilay et al., 1995a,d); the western Mediterranean (Bergametti et al., 1989a,b; Martin et al., 1990; Dulac et al., 1992); the Netherlands (Reiff et al., 1986); Scotland (Davies et al., 1992b); Sweden (Franzen et al. 1994); across the northern Atlantic (Talbot et al., 1986); to South America (Prospero et al., 1981b; 1987) and toward the Amazon basin (Swap et al., 1992).

There are a variety of hypotheses about the effects of this huge deposition of dust on the sea surface. The main effect that is of interest is the role of dry fallout and rain as a source of such essential elements for biological as N, P and Fe (Duce, 1986). The impact of atmospheric iron on phytoplankton production and the resulting increase in biomass, as initially proposed by Martin and Fitzwater (1988); Duce and Tindale (1991); Donaghay et al. (1991) is now proven through the in situ large scale experiment, "Iron Ex1", carried out in the equatorial Pacific Ocean in November 1993 (Wells, 1994; Martin et al., 1994).

The effects of a dust outbreak on the regional radiative energy budgets of desert and oceanic locations were investigated using a combination of model calculations and satellite observations by Ackerman and Chung (1992). They concluded that over the oceanic regions the presence of dust increased the short-wave radiative scattering which causes cooling. On the other hand, the presence of dust decreased the observed long-range radiation more vigorously on desert areas. This effect of dust on radiation led us to consider the link between dust and climate. Although the ultimate radiative effects of dust are uncertain, there is sufficient evidence to suggest that the effects of mineral dust must be considered when modeling the radiation balance. At the very least, these effects should be estimated for the lower latitudes, which are the major areas of intense dust production and transport. These regions are also the location of the major energy exchanges of the earth's climate system (Schutz et al., 1990).

1.4. The Case of the Mediterranean Sea

1.4.1. Input of Material onto the Mediterranean via the Atmospheric Pathway

The Mediterranean Sea is a midlatitude semi-enclosed sea; it is connected with (and separated from) the Atlantic by the Strait of Gibraltar, with the Sea of Marmara by the Dardanelles and with the Red Sea by the Suez Canal. At its northern boundary there are nations with economies that range from industrial and semi-industrial to agricultural. To the south there are highly productive mineral aerosol sources like North Africa (Sahara desert belt) and Asia (Saudi Arabian and Syrian deserts). Thus the Mediterranean is a classical example of a marine region with a number of contrasting catchment areas which supply material to the atmosphere. It is subjected to considerable stress from the adjacent large population centers and is one of the most fragile ecosystems in the world. The discovery of the existence of sapropels i.e. discrete, black and organic rich layers sedimented in anoxic conditions could be the first signature of anthropogenic effects (Bethoux and Gentili, 1994).

The geochemistry of the whole basin depends on the marine dynamics and the Atlantic, terrestrial and atmospheric inputs. The eastern part of the basin differs from the western part in its meteorology, hydrology and chemistry. The physical circulation characteristic of the eastern basin is well documented and characterized by dynamic current systems flowing through quasi permanent, meso-scale, cyclonic gyres (Rhodes) and a series of anticyclonic eddies (Ozsoy et al., 1989; 1993; Robinson and Golnaraghi, 1993).

The damming of the Nile, previously the major source of material to the eastern Mediterranean, has left the Seyhan, Ceyhan and Manavgat located along southern Turkey as the only riverine sources of material to the eastern basin. These inputs will be reduced as the rivers are used as fresh water

supplies to the Middle East states: indeed, construction has already started to transport Manavgat water by tankers to Israel. Eventually, therefore, only the atmospheric input to the eastern basin will remain to act on the biogeochemistry of the basin, together, of course, with the oceanographic processes.

The productivity of the sea is limited by nitrate in the western part (Woodward et al., 1990), whereas in the eastern Mediterranean productivity is limited by phosphate (Krom et al., 1991). The airflow climatology of the eastern basin shows seasonal behavior whereas the western part does not (GESAMP, 1985). It is also likely that over the eastern Mediterranean mineral aerosol fluxes are at least five times higher than over the western Mediterranean though fluxes of pollutants are lower (GESAMP, 1989).

In the Mediterranean Sea the distribution of dissolved trace metals differs fundamentally from that in the open ocean. First, Cd, Ni, Zn and Cu, which exhibit nutrient-like behavior in the open ocean (Bruland, 1983), have more or less uniform vertical distributions in the Mediterranean Sea (Laumond et al., 1984; Copin-Montegut et al., 1986). Vertical concentration profiles of the dissolved trace metals may show a surface maximum (Cd, Cu and Pb: Laumond et al., 1984; Pb and Cd: Copin-Montegut et al., 1986; Co and Ni: Zhang and Wollast, 1990) though this is not always true (Zn and Cr: Sherrell and Boyle, 1988; Al: Cassetto and Wollast, 1979; Hydes et al., 1988; Chou and Wollast, 1989).

Important questions pertaining to these observations are;

- (i) whether the trace metal distributions are the result of natural or anthropogenic processes,
- (ii) why the nutrient-type metals are not efficiently removed from surface waters,
- and (iii) why their vertical profiles differ from those in the open ocean.

Based on the results of a box-model, Bethoux et al., (1990) concluded that during the last few decades the increase in trace metal concentrations has been caused mainly by anthropogenic input. Such input

is probably most pronounced in the western basin, because of the higher levels of industrialization of the bordering countries. The lack of vertical structure of the trace metal profiles was attributed to the short residence time of deep waters, minimizing the contribution of biogeochemical relative to hydrographic processes (Bethoux et al., 1990). Observational evidence for this explanation is scant, the major impediment being a lack of information on trace metal fluxes into, within and out of the Mediterranean Sea. Neither the biological cycling of trace metals (Buat-Menard et al., 1989) nor the influence of diagenetic processes (Nolting, 1989) has been quantified for the Mediterranean Sea. Lastly, the descriptions of the trace metal distributions were based largely on data from the western Mediterranean Sea, there being no data for the eastern Mediterranean.

EROS-2000 (European River Ocean System), a project of the Commission of the European Union, has attempted to compare riverine and atmospheric fluxes to the north-western Mediterranean. One of the main aims of this program was to determine the relative contributions of materials supplied from the atmosphere and from the rivers. Within the framework of this project, the 5 year assessment of particulate matter by precipitation to the north-western Mediterranean has shown the atmospheric input to be very close in magnitude to the river input and to range from 10 to $27 \text{ t km}^{-2} \text{ yr}^{-1}$, about 90 % being constituted of Saharan mineral dust. With regard to fluvial sediment discharge it has also been shown that 90% settles in estuarine and coastal zones and that 10% finally escapes to the open Mediterranean (Martin et al., 1989; Loye-Pilot et al., 1989). This particulate Saharan dust is particularly rich in elements of ecological concern (e.g. Fe, Si, Mn, Co...) and since it is generally postulated that only dissolved forms of these elements can easily be available as nutrients for biological growth (Finden et al., 1984; Sunda et al., 1983), determination of the partitioning between dissolved and particulate fractions is a very important task with regard to the biological significance of the atmospheric inputs.

The results of a systematic, 16 month, sample collection have quantified the total atmospheric depositions in a coastal area of the north-western Mediterranean. Comparison of the atmospheric input of trace metals with the Rhone river input into the northern part of the western Mediterranean is presented in Table 1.3. Although the total inputs of trace metals by the Rhone River are higher than the total inputs from the atmosphere, It has been stressed that atmospheric inputs cannot be neglected especially as one moves seaward from the river mouth (Guieu et al., 1991a).

Table 1.3. Comparison between total input of Rhone river and atmospheric input to the Gulf of Lyon.

	Atmospheric input t yr ⁻¹			Rhone input t yr ⁻¹		
	Dissolved	Particulate	Total	Dissolved	Particulate	Total
Al	595	318320	318715	1283	37283	38566
Cd	3	7	10	3	39	42
Co	4	58	62	2	7	9
Cu	107	212	319	16	28	44
Fe	135	197800	197935	387	18093	18480
Mn	194	4273	4467	100	318	418
Ni	74	236	310	8	21	29
Pb	6	446	452	24	64	88

(Guieu et al., 1991a and the references cited there in).

It has been verified that partitioning between particulate and dissolved phases in rain depends upon pH: the highest Pb and Cd concentrations were observed at very low pH. Surprisingly, Fe, Cu and Ni behaved differently, the highest concentrations corresponded to the highest pH measured in red rain events (Guieu et al., 1990).

For the case of Fe this could be explained by the existence of different oxidation states of the element under environmental conditions. The different oxidation states have different solubilities and thus, redox

cycling, possibly via photochemistry, may also play a role (Sunda et al., 1983; Siffert and Sulzberger, 1989; Zhuang et al., 1992; Johnson et al., 1994). Throughout atmospheric transport an aerosol may be subject to repeated wetting and drying cycles during cloud formation and dissipation. During these cycles, low pHs may be experienced if, for example, the aerosol acts as a site for SO₂ adsorption. Subsequent oxidation of SO₂, which may even be catalyzed by mixtures of manganese (II) and iron (III) (Takashi and Takeuchi, 1986), can yield very acidic sulfuric acid solutions (Zhu et al., 1992). The pH of the final precipitation may be raised by reaction with bases during or after the wetting/drying cycle and thus does not necessarily reflect the pH conditions the aerosol is exposed to in the atmosphere. The results of a laboratory study of Fe in Saharan aerosol during repeated cycling from high to low pH, thereby simulating cloud processes, has shown that increasing the pH results in almost complete removal of dissolved Fe and that the amount of Fe remaining in solution increases with the number of low pH cycles (Spokes et al., 1994). It has been verified also that the kinetics of the photo dissolution of Fe depend not only on the pH but also on the structural identity of the iron mineral (Xyla et al., 1991; Sulzberger, 1992; Sulzberger and Laubscher, 1995). The importance of these processes for describing inputs to the ocean is that trace metal solubility may depend on the life history and crystalline structure of the aerosol, and thus simple solubility-pH relationships may not be appropriate.

Its ecological importance has motivated researchers to estimate the atmospheric input of nutrients to primary productivity. In the western Mediterranean the atmospheric N input contributes 25% of the new production and this percentage increases to 60% in oligotrophic zones such as the eastern Mediterranean (Loye-Pilot et al., 1989). In summer, when low rates of primary productivity are associated with intense stratification of the water column, the atmospheric input of dissolved phosphorus forms a large

part of the phosphorus exported from the photic zone (Bergametti et al., 1992).

It is noteworthy that Quétel et al., (1993) and Kremling and Streu (1993) found atmospheric inputs from Africa to be the major source of the fluxes of Al and Fe particulates in western Mediterranean and subtropical north Atlantic waters. Quétel et al. (1993) also suggested North African aerosols to be delivered in the form of pulses which may impose non-steady conditions on the biogeochemical processes of the iron in the marine environment. Chester et al. (1990c) have emphasized the need for further investigation of the role played by Saharan dust in the sea water chemistry of the western Mediterranean. They proposed that when Saharan dust is deposited in the mixed layer it can act as a 'sink' rather than a 'source' for trace metals in sea water. The 'source/sink' nature of the role played by Saharan dust is particularly important in determining the concentration of PO_4^{3-} dissolved in the eastern Mediterranean.

The analysis of samples collected at high altitudes over the equatorial Atlantic has revealed that Saharan dust is a significant source of water soluble phosphate in the boundary layer over this oceanic region (Talbot et al., 1986). Such enrichment has also been reported by other scientists who measured the total P over the tropical north Atlantic (Graham and Duce, 1979; Coude-Gaussen et al., 1987). On a global basis weathered crustal material is believed to be a principal source of soluble phosphate in aerosols over the world's ocean (Chen et al., 1985). Actually, the dynamics of phosphorus exchange on detrital particles exposed to solution are complex. Chase and Sayles (1980) resuspended five sediments suspended in the Amazon River in phosphate-free surface seawater and observed rapid (hours) release of P into solution. On the other hand, the great reactivity of phosphate with particles and the high phosphate-absorbing capacity of clay particles possessing a surficial armour of reactive iron and aluminum hydroxides maintains low equilibrium phosphate concentrations in solution (Froelich, 1988). This finding led Krom

et al. (1991) to suggest that removal of phosphate by dust particles may be an important process controlling the concentration of P in the water column of the eastern Mediterranean region. These studies, confirming that dust deposited onto the ocean may provide biologically important elements, led Donaghay et al., (1991) to postulate a variety of marine ecosystem responses to episodic atmospheric inputs of nutrients. Indeed, a study of the nutrients in atmospheric depositions over the northwest Pacific coastal ocean demonstrated a potential link between episodic atmospheric deposition and toxic biological blooms (Zhang and Liu, 1994).

Additional evidence demonstrating the importance of the Sahara has come from geochemical studies of Mediterranean sediments which suggest that material transported from the Sahara is an important source of certain clay minerals (Chester et al., 1977; Tomadin et al., 1984; Correggiari et al., 1989).

The overall amount of mineral aerosol (dust) reaching the Mediterranean basin is large compared to the atmospheric impact on other oceans and since the desert dust intrusions to the basin occur in the form of pulses, these can impose intermittent, non-steady state conditions on the mixed layer in the Mediterranean (Chester, 1986; Chester et al., 1989; Quetel, 1993). The assessment of such an influence demands quantitative knowledge of the atmospheric concentrations and fluxes of the particles over the marine environment. The wide variation found in the daily trace metal concentrations of Mediterranean atmospheric particulates (Dulac et al., 1987; Bergametti et al., 1989b), has highlighted the importance the Co-ordinated Mediterranean Research and Monitoring Program (MEDPOL) attached to a continuous sampling strategy for assessing the inputs of trace elements over the Mediterranean basin (UNEP/WMO, 1989a; 1992).

Knowledge of the dust concentration over the eastern Mediterranean has been limited by ship time (Chester et al., 1977; 1981; 1984) though long term assessments of dust deposition have been provided by the Israeli scientists. According to these measurements, about 25 million

tons of desert dust annually reach the eastern Mediterranean (Yaalon and Ganor, 1979; Ganor and Mamane, 1982). This addition contributes to the characteristics of the typical Mediterranean soil (Yaalon and Ganor, 1973).

The finding that the sediment discharged from western Mediterranean rivers settles in the estuarine zone before it reaches the open sea (Martin et al., 1989) implies long-range, atmospheric transport to be a major source of terrigenous sediment. To our knowledge, however, no direct measurements of the down-column transport of the alumino-silicate associated, trace elements have so far been made in the eastern part of the Mediterranean.

Deposition to the Mediterranean of radionuclides from atmospheric weapon tests over the Pacific (GESAMP, 1985) and from the Chernobyl accident (Fowler et al., 1987; 1990) is another good verification of the long-range transport of material via atmospheric pathways.

Beside the aforementioned effects, increased dust concentrations over the eastern Mediterranean could change the climate by modifying the radiation balance and by the generation of cloud condensation nuclei (Levin, 1993; Gilman and Garrett, 1994). The transport of desert dust also aids the neutralization of acidic rains (Loye-Pilot et al. 1986; Mamane et al. 1987; Loye-Pilot and Morelli, 1988; Losno et al. 1991) and, among the negative effects of dust transport, it is worthy of mention that intensive dust storms may profoundly influence human activities and the economies of the countries of the region (Khalef 1989).

1.4.2. Geographic and Climatic Overview of the Mediterranean Area

In order to assess the transport of material via the atmosphere to the eastern Mediterranean both from anthropogenic and from natural sources, the climatology and meteorology of the region must be well understood.

The eastern Mediterranean is located to the east of the island of Crete and bounded by the coast of Turkey in the north, by Syria, Lebanon and Israel in the east and by Egypt and Libya in the south. The topography of the continental masses surrounding the eastern Mediterranean area is complex (Fig.1.1); it provides both barriers to and channels for airflows that at times bring extremely different air masses to the region. Thus, the topographic features shown in Figure 1.1 may interact with the large-scale atmospheric flow within the boundary layer by influencing both horizontal transport and vertical mixing of the aerosols.

Such well known regional winds (Fig.1.2) as the Etesian, Bora, Sirocco and Poyraz transport aerosols over the Mediterranean from the potential source areas.

The Etesian (the Turkish name is Meltem) is a northerly to westerly wind that occurs during the summer over the Aegean Sea and the eastern Mediterranean where it occurs as a southeastward extension of the Aegean wind regime. The Bora is most common along the Yugoslavian coast but it also occurs over the Aegean Sea; this latter occurrence occasionally extends into the eastern Mediterranean. The meso-scale effects of significant mountain gaps along the southern Turkish coast produce strong regional northerly winds, the Poyraz, especially during the winter season and during some summer months (mainly August). The Sirocco (also known as the Ghibli and Khamsin) is a southeasterly to southwesterly wind over the Mediterranean originating over North Africa. The air comes from the Sahara as a desert wind and is dry and dusty; the inhabitants of North Africa call it Chom (hot) or Arifi (thirsty). When crossing the Mediterranean it picks up moisture as it travels northward, causing rain. In the eastern Mediterranean, the Sirocco originates in the south over the deserts of Libya and the United Arab Republic and over the Arabian deserts to the southeast (see Fig.1.2).

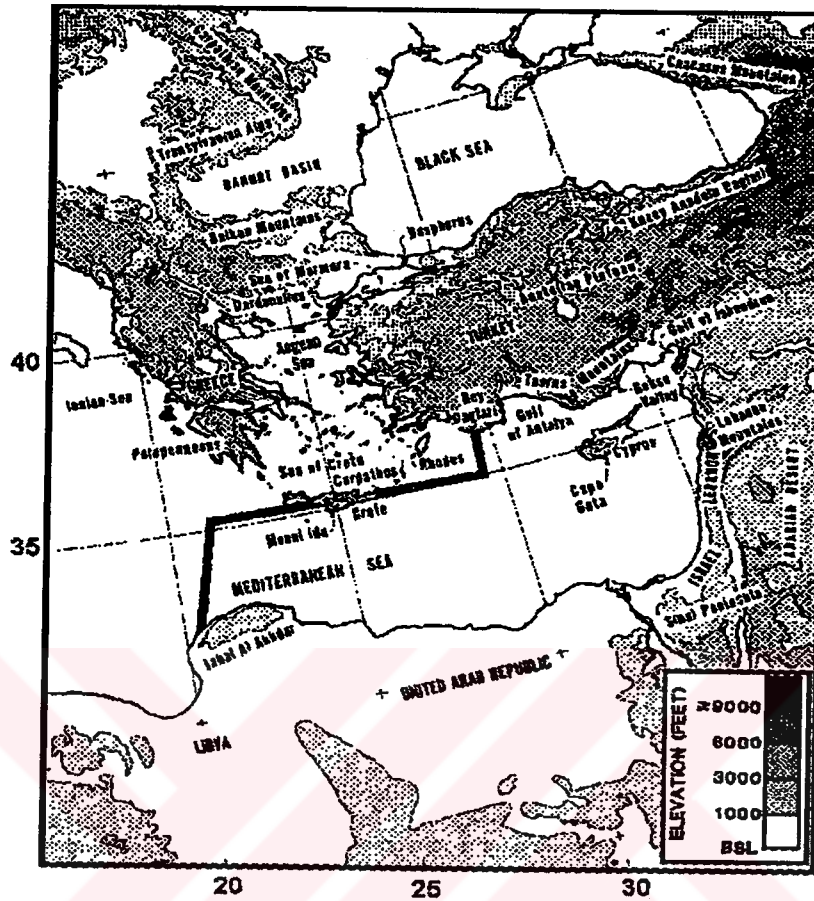


Figure 1.1. Topographical map of the eastern Mediterranean area (after Brody and Nestor, 1980).

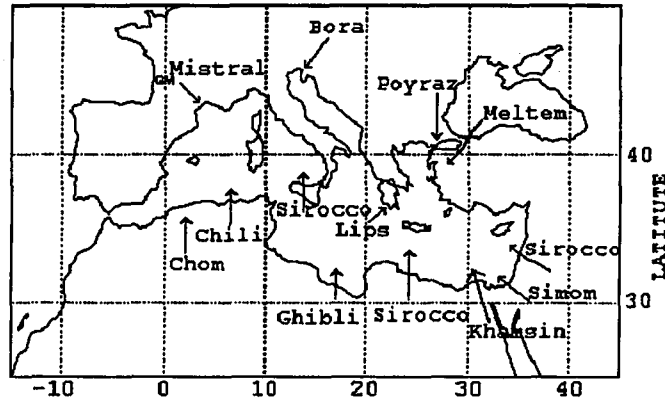


Figure 1.2. Major local wind systems in the Mediterranean
(after Brody and Nestor, 1980).

Eastern Mediterranean depressions usually originate in the Southern Aegean Sea and generally occur in the Cyprus area just south of the Turkish coast during autumn and winter, being most intense from November through April, whereas during spring (March through May) depressions are more effective over north Africa (see Fig.1.3).

Climatological analysis of Mediterranean cyclones has revealed intermonthly variations in their routes which become lost in seasonal pictures (Alpert et al., 1990a,b). Thus, composite seasonal pictures are not faithful representations of the cyclonic routes over such a complex terrain as the Mediterranean.

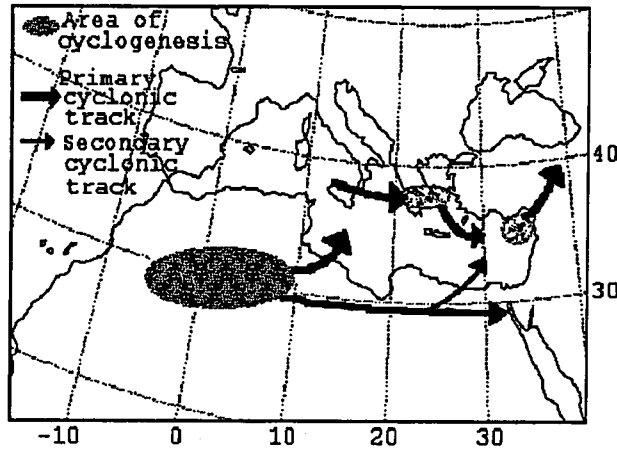


Figure 1.3. Areas of cyclogenesis and tracks of cyclones which affect the eastern Mediterranean (after Brody and Nestor, 1980).

The Mediterranean region is famed throughout the world for its distinctive climate affected by the air-sea interactions and by the surrounding topography. Climatically, the region is characterized by generally warm temperatures, winter dominated rainfall and dry summers. The strong contrast between summer and winter rainfall that characterizes the Mediterranean climate is accompanied by pronounced seasonal cycles in most climatic variables.

The seasonal weather patterns of the eastern Mediterranean are controlled by the monsoonal character imparted by the surrounding land mass. During the winter season (November through February), the Eurasian land mass to the north is very cold in comparison with the sea surface temperature. With the upper level westerlies often found over the Mediterranean, cyclonic activity with unsettled weather and strong winds is common. Precipitation, although mainly associated with these cyclonic disturbances, is also influenced by local orographic effects.

During the summer season (June through September), the monsoonal effect leads to the development of an intense heat trough over southern Asia that extends westward over Turkey. With higher pressure over the relatively cooler sea surface of the Mediterranean, settled and dry weather with westerly winds persists during the summer.

The transitional seasons, spring and autumn, are of very different length. The relatively long spring season (March through May) is noted for periods of unsettled winter-type weather associated with an increased occurrence of North African cyclones; otherwise spring weather is much like summer's. Autumn usually lasts only one month (October) and is characterized by an abrupt change to the unsettled weather of winter (Reiter, 1975; Brody and Nestor, 1980; Ozsoy, 1981; Milliman et al., 1992).

One of the most commonly used techniques for interpreting atmospheric measurements, that is, for evaluating the long-range transport of chemical constituents and for characterizing the mean flow to a specific region of the atmosphere, is through the modeling of atmospheric trajectories (GESAMP, 1985; Merrill, 1985a; Miller and Harris, 1985; Dayan, 1986; Dulac et al., 1987; Martin et al., 1987; 1990). Generally, the models postulate that the tracked air particle follows the mean atmospheric motion and thus permit the calculation of transport pathways forward in time from a source region or backward in time from a receptor. All trajectory calculations rely upon measurements of vertical profiles of pressure, temperature and wind which are made discretely in time and space. Martin et al., (1987) have reviewed the various applications of backward trajectory models and tabulated the advantages and disadvantages of several methods of calculating trajectories for two basic types of models:

- (1) dynamic models, which employ pressure or temperature fields to calculate isobaric or isentropic trajectories, respectively;
- and (2) kinematic models, which employ measured wind fields.

In isobaric trajectory analysis the motion along constant pressure surfaces is tracked. This method is useful only for short times (<1 day) when the air remains on isobaric surfaces (Artz et al., 1985; Merrill, 1985b).

Using case studies, Martin et al., (1987) showed that the introduction of vertical movements into trajectory models had a noticeable influence on the horizontal trajectory of air masses, depending on the meteorological situations. They also compared the 3-D air parcel trajectories arriving in the Mediterranean region with the isobaric paths and showed that, for trajectories of duration more than 48 h, significant differences occur during cyclonic and anticyclonic situations when the vertical motions are modified by wind shear. Their observations clearly indicate that trajectory calculations must utilize the vertical component of wind speed (w) in taking wind shear into account. Subsequently, by coupling geochemical tracers of dust (Al, Si) and satellite imagery, Martin et al., (1990) validated the use of the synoptic, vertical wind component in trajectory calculations defining the real track of African dust transport to the western Mediterranean.

Whenever trajectories are used to interpret atmospheric chemical measurements, the assumptions underlying the method used for calculation must be understood. In addition to model assumptions, it is important to keep in mind that the coarse resolution of input data limits the accuracy of all trajectory models. The meteorological data used in the trajectory models generally possess a selected spatial and temporal resolution. These discrete data must be interpolated both in space and time. After a certain number of hours, the magnitude of the interpolation errors in the location of trajectories increases. The estimates of errors range from 140–290 km after 24 hr to 350–495 km after 72 hr (Whelpdale and Moody, 1990). The important conclusions of these authors for the application of air-mass trajectories to the interpretation of ground-based aerosol and precipitation data so as to identify sources and apportion source emissions can be summarized as;

1. Single trajectories should not be used to determine source-receptor relationships.
2. Trajectory accuracy depends on the type of model and the resolution of data employed.
3. Trajectory accuracy depends on the meteorological conditions being modeled.
4. Trajectories provide more reliable estimates where large area sources are involved.
5. Long-term trajectory climatologies are more reliable than single trajectory calculations.
6. When available, knowledge of conditions along a trajectory (e.g. precipitation) helps interpret chemical measurements.
7. The combined use of multiple chemical tracers (such as, Al, Si) and trajectories may help interpret transport (e.g., Martin et al., 1990).

Most current literature uses satellite-derived images in qualitative investigations of the magnitude, frequency and movements of dust, or for long-term assessment of frequencies and source regions of dust transport (Reiff et al., 1986; Coude-Gaussen et al., 1987; Dayan et al., 1991; Jankowiak and Tanre, 1992).

Over the ocean, the presence of aerosol increases the upward radiance by scattering the short-wave radiation which is propagated downward. Due to the darkness of the oceanic surface, this effect is observed easily and can be modeled straightforwardly. Thus, it has been used to map the global aerosol distribution (optical thickness) over the ocean from the data retrieved by the advanced, very high resolution radiometer (AVHRR) aboard polar-orbiting NOAA satellites (Tegen and Fung, 1994). Over continents, the incident visible flux at ground level is reduced by the presence of dust, yielding a drop in ground temperature. Moreover the radiance emitted by hot arid surfaces is attenuated by the colder atmospheric dust layers. During the night, one finds, on the other

hand, that backscattering and emission by dust particles reduces the cooling of the colder ground surface. Dust over arid areas therefore significantly decreases the brightness temperature during daytime but increases it during night-time and permits the detection of dust over the continents.

By utilizing a time-series analysis of visible (VIS) and thermal infrared radiation (IR) obtained from METEOSAT, Saharan dust transport to the Mediterranean and the spatio-temporal distribution of dust occurrences over the North African continent and Atlantic ocean have been documented by various scientists. Satellite detection of dust above North Africa during the eight years, 1984-1991, generates a dust climatology; an annual cycle in dust producing activity is observed with a maximum in March-May and a minimum in October-December - which in fact is consistent with observations of dust above the Atlantic (Dulac et al., 1992a; Legrand and N'doume, 1992; Legrand et al., 1994; Dulac et al., 1994; Legrand, 1995).

Throughout this study, satellite pictures from METEOSAT VIS and IR channels were provided for certain dust intrusions from surrounding desert areas observed at the Erdemli site (data available from Dr.F.Dulac, Centre d'Etudes de Saclay, L'Orme Des Merisiers, 709, F-91191 Gif-Sur-Yvette Cedex/France and Dr.M. Legrand, Labor. d'Optique Atmospherique, bat.P5-Physique Fondamentale, Universite de Lille-1, 59655 Villeneuve d'Ascq cedex, France). These satellite imageries were used as complementary evidence for the intrusion of desert dust to the eastern Mediterranean.

CHAPTER II

MATERIALS AND METHODS

2.1. Computation of Air Mass Back Trajectories

To obtain the three dimensional (3-D), three day's backward air mass trajectories, the publicly available operational model on the CRAY C90/UNICOS super computer at the European Center for Medium-Range Weather Forecast center (ECMWF, Reading, U.K.) was utilized. To run this model from a remote site and obtain trajectory data for a specified region and date, the job (a request file for a trajectory) given in the Appendix (Table A1) was initialized via internet.

The model uses analyzed wind field components; u and v, zonal and meridional respectively, plus the vertical velocities available in the archive of the center (MARS) in the form of a special, on-line database (Gibson, 1991) gridded every 6 h (00, 06, 12, 18 UT) for standard pressure levels. The grid space is equal to 1.875° for both latitude and longitude. The model recalculates the new position of the air parcel at each 15-min. time step by utilizing linear spatial and temporal interpolations (see Kallberg, 1984 for further details). All calculations are carried out on a regular latitude-longitude grid, with a resolution selected by the user. In this study a resolution of 1.5×1.5 degrees has been used. A coarser resolution may be selected, in order to reduce computer time. The resulting parcel positions (expressed as latitudes and longitudes) together with wind components and pressures have been entered hourly as characters to a result file.

An example of such a result file, obtained by sending a request file (see Table A1) for the date of 27 March 1992 is given in Appendix (Table A2). The second column shows time steps for backtracking and the third, fourth and fifth columns show u, v and w components of the wind in every time step. The sixth and seventh columns represent the position of the air parcel in latitude and longitude respectively at each time step whilst the last column gives the pressure of the tracked air-parcel at its new position.

The data for trajectories arriving at four different barometric levels were obtained daily throughout this study. The hourly latitude and longitude of air parcels have been plotted on horizontal mercator projection maps. Such plots are known as air mass back-trajectories, the actual three-dimensional paths that air parcels follow as they move through space.

The air mass back trajectories provide information only about the source regions of the air masses arriving at the sampling zone. They do not give information on precipitation that the air mass might have experienced throughout its travel - which would be a useful parameter in explaining the variance in the atmospheric concentrations of the measured species. Local precipitation data at the atmospheric sampling site has been used both for the assessment of its effect on the variability of the elemental concentrations in the aerosols and in wet-deposition calculations. The daily amount of local precipitation at the sampling site during 1991 and 1992 was obtained from the Erdemli Meteorological station, formerly part of the Turkish meteorological network and located 10 km east of the tower.

2.2. Atmospheric Aerosol Sampling

2.2.1. Sampling Tower

In an atmospheric sampling program, site selection is critical.

The first step is to define the purpose of the measurements clearly. If the input to a specific location is required then this will obviously dictate the sampling location. If a regional background will be measured it is important to recognize the potential sources of local contamination. Local trace metal inputs will arise from essentially all industrial sources, automobile traffic, cultivated fields, smoke stacks and any other sources of dust such as areas of sand or concrete. Sites selected must be remote from such sources under all wind directions.

Thus a platform for sampling an atmosphere representing a marine region could be a research vessel or remote coastal site (e.g. an island). In many cases practical considerations of manpower ability, electrical power and the cost of site operation will constrain the choice of site and the best available site should then be selected.

Atmospheric sampling from a ship has some advantages, particularly for short-term preliminary studies and quick investigations of a particular geographical area. The problems of shipboard contamination and the difficulty of collecting sufficient air samples to obtain any meaningful statistics at a given location precludes ship sampling for any detailed study of atmospheric transport.

In 1990 a 21 meter high sampling tower was constructed on the northeast coast of the Mediterranean at the harbour jetty of the institute ($34^{\circ}15'18''$ E $36^{\circ}33'54''$ N). After various considerations this site was considered to be the most practical location since it was possible for experts to reach the tower within a few minutes, thereby reducing the risk of contamination.

A wide range of material exists for the construction of a sampling tower. The sampling tower used in this study was constructed from three commercial, 20 foot containers mounted on top of each other. Apart from the first, the side walls of the upper two containers were removed to reduce wind resistance and the tower was secured by steel wires to provide extra strength. The construction material was quite resistant to oxidation by the

marine atmosphere, cheap and easy to obtain. Equipment for atmospheric sampling was located on the top level of the tower.

The vicinity of the sampling tower is surrounded mainly by lemon trees and cultivated land and greenhouses. Populations of 55,000 and 500,000 inhabitants live 7 and 45 km to the east of the tower, respectively. Pulp and paper industry exist 45 km to the west of the tower and a petroleum refinery, soda, chromium, thermic power plant and fertilizer industries are located 45 km east of the sampling tower.

2.2.2. Aerosol Collection

The sampling campaign started in August 1991 and lasted for 17 months. During this period 339 aerosol samples were collected. Put simply, atmospheric aerosols were sampled by passing volumes of air through filters.

A variety of filter types are available and the particular type selected depends on a number of factors, including the chemistry of the substance being determined, the flow rate obtainable through the filter, the efficiency of various filter sizes, their loading characteristics (rates at which the filters clog), the ease of chemical manipulation of the filter (ease of solubility in various solvents) and its cost. The common filters used for high volume sampling include glass fiber, Whatman 41 (cellulose), and Delbag Microsorban (polystyrene). Membrane filters such as Millipore and Nucleopore, which generally have significantly lower flow rates, are also used. Whatman 41 (20.3x25.4 cm) filters are generally recommended for several reasons—a low metal blank, low cost, and ease of handling in analysis. Accordingly, aerosol samples for trace metal analysis were collected during the present study on Whatman-41 cellulose filters (Whatman International Ltd, Maidstone, England).

The sampling program was corrected by 'comprehensive blanks' processed in the same manner as the samples collected on the tower with the exception that no air was drawn through the filters. 'Comprehensive blank' filters were removed from their boxes and mounted in the filter holder, then dismounted and stored in polyethylene bags for later analysis. By contrast, 'filter blanks' were removed from their box under laboratory conditions just prior to analysis. Although from the same selection of filters as the 'comprehensive blanks' these filters were never taken on the sampling tower. Extreme care was taken during the collection and handling of atmospheric samples.

To assess the blank contributions from filter papers, the blank-to-sample ratios for each element are given in Figure 2.1. It can be seen that the contribution from Whatman 41 filter papers was significant only for Ni (20%) and Cr (17%). For other elements the subtracted blank values were less than 10% of the mean concentrations of the elements throughout the 17 months collection period at Erdemli.

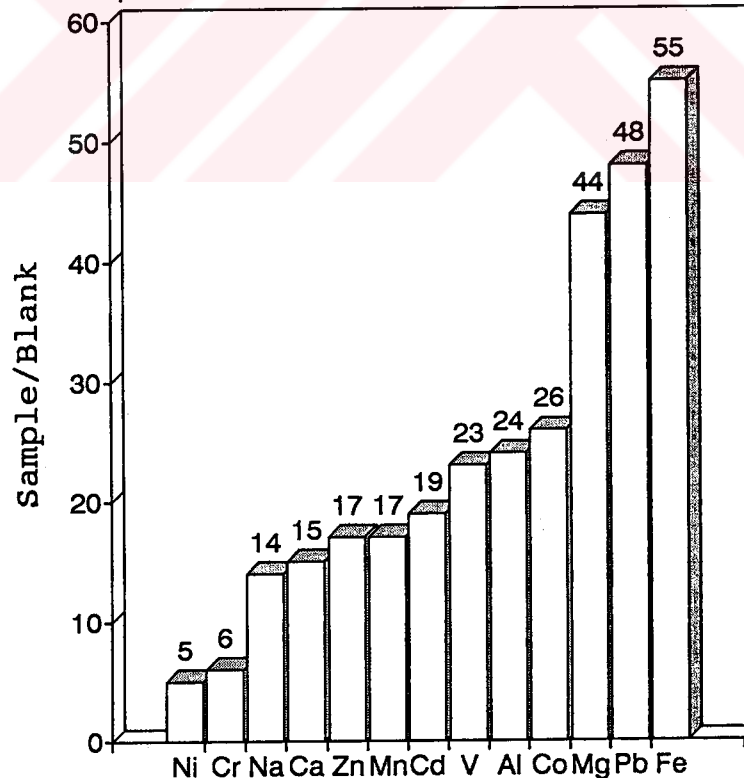


Figure 2.1. Sample-to-blank ratios of the elemental concentrations in Whatman-41 filter papers.

Aerosol samples were collected by a model GMWL-2000 (General Motor Works Inc., OH) high-volume sampler consisting of a heavy duty turbine blower with a high speed motor, flow meter and seamless stainless steel filter holder.

Utilizing paper media, the model GMWL-2000, designed and built for continuous sampling, traps particles as small as 0.01 micron in size. For their protection, all instruments and components were mounted within a reinforced shelter constructed of 0.08" anodized aluminum.

The equipment possessed a flow rate of $1.17 \pm 0.46 \text{ m}^3 \text{ min}^{-1}$ which could be maintained for 24-72 hours. The air flow monitored by a variable orifice meter which was calibrated periodically utilizing a calibration kit (model PN G25) to maintain on-site accuracy. An elapsed-time counter recorded the duration of the sampling. A flow recorder with a clock-driven chart provided a permanent record of the sampling duration. In this way changes in air flow resulting from variations in line voltage or from increasing filter load could be recognized.

The total volume of air sampled was computed from the sampling duration and the average mass flow of air.

2.2.3. Sample Manipulation

Both at the sampling site and in the laboratory extreme care was taken to minimize contamination of the filters by handling during the sampling and analysis of aerosols. All personnel collecting the samples were thoroughly familiar with precautions to be taken during sample collection and handling and were well aware of the many sources of contamination that could have arisen.

All filters were carried to the sampling tower within their boxes. Polyethylene gloves were always worn throughout any manipulating of the filter papers. Filters were unloaded from the box and mounted on the filter

holder using Teflon covered tweezers. At the end of sampling the filter papers were folded over with their exposed face inward and the exposed filter paper was placed in a polyethylene bag on which the date of the sampling was written.

For each sample the duration of sampling was read from the continuous time recorder on the pump and noted. The continuous flow recorder paper was changed for each sample. These records gave the mean flow rate throughout the sampling. Before mounting of a new filter paper, the metal part of the filter holder was cleaned with tissue paper to remove any dust from the previous filter and the pump was assembled for the succeeding run.

2.3. Aerosol Chemical Analysis

2.3.1. Sample Dissolution

In order to determine elemental concentrations in solids by atomic absorption spectrophotometer it is necessary to bring the material into solution. The analysis of aerosol samples collected throughout this study utilized Saydam's (1981) procedure for dissolution.

In the laboratory all filter papers were manipulated in a Laminar Air Flow bench (Clean LAF HF906). PTFE, polytetrafluoroethylene, beakers with a capacity of 50 mL were used to dissolve (digest) the filter matrix and the particles collected on it. Each PTFE beaker was cleaned by refluxing with 65 % HNO₃ MERCK Suprapur® for 6 hours, and subsequently rinsed with Milli Q water. Each filter paper was carefully removed from its storage bag and one fourth of the paper was cut by nylon cord and placed in a PTFE beaker. 25 mL of HNO₃ were added. The beaker was then covered with a PTFE lid and placed on a hot plate at 130 °C to dissolve filter material. The HNO₃ was refluxed for 10-12 hrs. If the solution was not clear, depending on

the sample matrix at the end of 12 hours, 20 mL of additional HNO₃ was refluxed for a further 6-8 hr. The sample was then evaporated, until about 10 mL of HNO₃ was left. 5 mL of 40 % HF MERCK Suprapur[®] was then carefully added to the solution and the samples were digested for a further 6-8 hr. before being evaporated almost to dryness. 5 mL of HNO₃ were added and evaporated almost to dryness. This last step was repeated three times to eliminate any traces of HF left in the solution. The beaker was then allowed to cool and the residue dissolved with Milli Q water. This solution was poured into 25 mL graduated flasks and made up to volume with Milli Q water. The solution was quickly transferred to a labeled polyethylene sample bottle (100 mL) fitted with screw tops for storage prior to analysis. A reagent and filter blank determination was carried out using the same procedures. The solutions were kept refrigerated at 4 °C until analysis.

Since metals are adsorbed on the walls of the container and are not removed by simple rinsing with distilled water, polyethylene sample bottles and all other glassware used in the analysis were left in 10 % HNO₃ solution for 12 hr. to desorb metals from the walls of the containers before use. They were then rinsed 3 times with distilled water and 5 times with Milli Q water and left to dry in a clean hood.

2.3.2. Atomic Absorption Spectrophotometer (AAS)

AAS is a simple and rapid procedure that can be used to determine trace elements in aerosol samples. Throughout this study samples were analyzed directly for those elements of interest by the flame and flameless modes of a computer controlled GBC-906 model (GBC Scientific Equipment Pty Ltd. Australia) atomic absorption spectrophotometer equipped at the factory with a deuterium (D₂) lamp for background correction. Detection limits, sensitivities, optimum ranges and detailed operation instructions were obtained from the users manual of the

instrument provided by the manufacturer (GBC 906 and 908 Operation Manual, 1990).

The analysis of Ca, Mg, Na, Al, Fe, Mn, Zn, and Cr used the flame mode of the AAS with the attachment of an FS3000 autosampler which provided automatic sample changing. The autosampler carousel held 10 standards and 60 samples, with separate positions for 'rinse', 'blank' and 'rescale standard'. Operation of the autosampler was programmed from the computer. The operating instructions for adjusting the controls and developing and operating a suitable flame were followed carefully to obtain accurate and reliable results.

In the flame mode the sample was introduced in the form of homogenous liquid so that thermal and chemical reactions created free atoms. These atoms were excited by a light source emitting a narrow spectral line of characteristic wavelength. The decrease in energy (absorption) was then measured. An air-acetylene flame was used for all the elements except for Al when a nitrous oxide-acetylene flame was used.

For the analysis of Co, Ni, V, Pb and Cd the flameless electro-thermal atomization mode of the AAS was used with the attachment of a PAL3000 autosampler. The PAL3000 provided automatic injection of up to 10 standards for calibration and the automatic analysis of up to 40 samples.

In this mode the flame was replaced by an electrically heated and pyrolytically coated graphite tube. This graphite furnace, by virtue of its small size, ensured a large population of free atoms in the optical path and required extremely small volumes of samples, typically 20 μ L. Due to the greater efficiency of the furnace its sensitivity was 10-200 times (depending on the element) greater than that of flame ionization.

The instrument was calibrated against standards of known concentrations. Stock solutions were prepared from pure compounds. Compounds used to prepare stock solutions, were dried and, after equilibration at room temperature, weighed and dissolved so that the final concentration of the element in the stock solution was 1000 ppm. Working

standards of elements were prepared by dilutions from stock solutions using HNO₃ solution instead of pure water. Concentrations of elements in working standards were arranged so that the concentration of an element in the sample lay between the standards used in the construction of a calibration curve.

From the total procedural chemical blank concentrations and average sampled volume of 1680 m³, the detection limits (defined as twice the standard deviation of the blank values) in aerosol samples (in nanograms per cubic meter) were: Na (30), Mg (25), Ca (30), Al (10), Fe (15), Mn (1.6), Co (0.01), V (0.2), Cr (1.9), Ni (1.3), Zn (2.2), Pb (1), Cd (0.02).

2.4. Quality Assurance

The accuracy of the analytical method and of the standards used was determined by analyzing a reference material issued by the Community Bureau of Reference (BCR) and prepared by the Commission of the European Community within the framework of the preparation of reference materials (RM) for pollution control. The material analyzed was a light sandy soil (RM 142) for which information on certificated concentrations of the elements had been provided. Table 2.1. compares the results of the analysis carried out in this study and those reported by BCR.

Table 2.1. Concentrations of elements observed in BCR standard reference material (RM 142) by AAS.

Element	determined	certified
Cd	0.25±0.08	0.25±0.09
Co	9.03±0.1	(7.9)
Cr	77.3±5.3	(74.9)
Ni	27.2±1.5	29.2±2.5
Mn	529±17	(569)
Pb	35.9±4.6	37.8±1.9
Zn	99.2±8.3	92.4±4.4
Al ₂ O ₃	90.9±5.9	(94.8)
Fe ₂ O ₃	29.5±1.4	(28)
MgO	11.1±0.5	(10.9)
CaO	47.2±2.2	(49.4)
Na ₂ O	6.3±1	(9.7)

Values in brackets are not certified. Concentrations for Cd, Co, Cr, Ni, Mn, Pb, Zn are in $\mu\text{g g}^{-1}$ and for Al₂O₃, Fe₂O₃, MgO, CaO and Na₂O are in mg g^{-1} .

The reproducibility of the digestion and analytical procedure was assessed by seven replicate analyses of subsamples of an atmospheric particulate sample collected by the mesh technique, for which sufficient sample was available. The mesh collection technique samples mainly the soil-sized fraction of aerosols and since it does not quantitatively retain the full spectrum of atmospheric particles, it can not be used to describe the total elemental distribution in atmosphere. The detail of aerosol sampling by this technique was described in another study (Kubilay et al., 1995a). The mesh-collected sample was washed from the mesh in redistilled water and treated in the same manner as the filter samples. Analytical precision for each metal is then defined and reported as the coefficient of variation (c.v.) calculated by dividing the standard deviation of the replicate determinations to the mean concentrations. The results are presented in Table 2.2. As can

be seen from the bottom of the table the percentages of c.v. of each measured element are less than 10.

Table 2.2. The reproducibility of the AAS technique
(concentrations are in $\mu\text{g g}^{-1}$).

Al	Fe	Mn	Cr	Ni	Zn	Pb	Cd	Co	Na	Ca	Mg	V	
30686	23622	398	368	160	298	149	0.2	20.5	34449	68724	30454	93	
32223	25100	389	360	158	320	140	0.21	20.0	35073	69651	32964	107	
34846	22494	396	356	166	305	140	0.21	22.6	35036	68527	30029	98	
33823	24074	386	363	158	310	132	0.22	20.2	35444	67911	30085	100	
31020	24684	375	372	163	300	132	0.23	22.6	36034	66834	30494	94	
30885	24228	376	364	162	289	132	0.20	20.8	34813	65341	30743	102	
30804	25799	385	369	168	305	134	0.20	20.2	35891	60767	31312	110	
X	32043	24286	386	364	162	304	137	0.21	21	35248	66822	30869	101
s.d.	1553	986	8	5	4	9	6	0.01	1.1	531	2792	944	6
c.v.	5	4	2	1	2	3	5	5	5	2	4	3	6

$$\text{c.v.} = \left(\frac{\bar{X}}{\text{s.d.}} \right) \times 100$$

c.v.; coefficient of variation

\bar{X} ; mean elemental concentration

s.d.; standard deviation of mean

CHAPTER III

RESULTS AND DISCUSSIONS

3.1. Atmospheric Transport of Material From the Meteorological Point of View

3.1.1. Comparison of the Air Flow Climatology at the Erdemli Site With Different Receptor Sites in the Eastern Mediterranean

To assess the atmospheric transport of aerosols from their source areas to the Erdemli receptor three dimensional (3D), 3-day back air mass trajectories arriving at 900 (990 m), 850 (1460 m), 700 (3000 m) and 500 (5560 m) hPa final barometric levels and at 12 00 UT were retrieved on a daily basis between August 1991 and December 1992.

The validity of the back trajectories for tracing the source areas of material transported via the atmosphere will be discussed -and established- in Section 3.3.1.; for the present the qualitative validity of the back trajectories will be assumed and they will be treated as straightforward observations which generate a very detailed description on the origin of the air masses over the eastern Mediterranean.

In order to see the mean airflow pattern at the sampling site throughout the duration of the study, the air-mass back trajectories have been classified according to the airflow direction. To do this, the wind rose was divided into four 90° geographical sectors with Erdemli at the center. Each trajectory was assigned to the sector in which it spent most of its three days of travel. In this way the temporal distribution of the mean airflow direction from the potential source areas for the aerosols over the eastern

Mediterranean has been obtained. The sector directions partitioning the back trajectories into four categories were as follows:

(1) Trajectories lying in sectors directed between north and east and therefore revealing aerosols originating in

- (a) continental flow from Eastern Anatolia,
- (b) long range flow from the Commonwealth of Independent States.

(2) Trajectories in sectors directed between north and west and therefore bearing aerosols originating in

- (a) continental flow from Western Anatolia,
- (b) long range flow from the Eurasian mainland (the United Kingdom, Europe, Ukraine) sometimes starting from the Atlantic Ocean and crossing the Mediterranean before reaching the Erdemli site.

(3) Trajectories in sectors directed between south and west and therefore bearing aerosols from

- (a) the Mediterranean Sea,
- (b) North Africa.

(4) Trajectories in sectors directed between south and east, being continental flow from

- (a) Middle East countries,
- (b) the Arabian Peninsula.

Moreover, with this type of classification it would be possible to evaluate the role of long and short range transport on the trace metal distribution in atmospheric particulates over the eastern Mediterranean. Short trajectories may be assumed to include aerosol transport from Eastern Anatolia (sector 1a), Western Anatolia (sector 2a), the Mediterranean (sector 3a) and Middle East countries (sector 4a), whereas long trajectories may bear aerosols from the Commonwealth of Independent States (sector 1b), the Eurasian mainland (sector 2b), North Africa (sector 3b) and the Arabian Peninsula (sector 4b) as well as from the corresponding regions

covered by short range trajectories. Figure 3.1. delineates areal limits to classify each of the samples according to the corresponding airflow direction. Three day back trajectories were associated with close source regions, when limited to the circled area in the figure assigned as short (see Fig. 3.1).

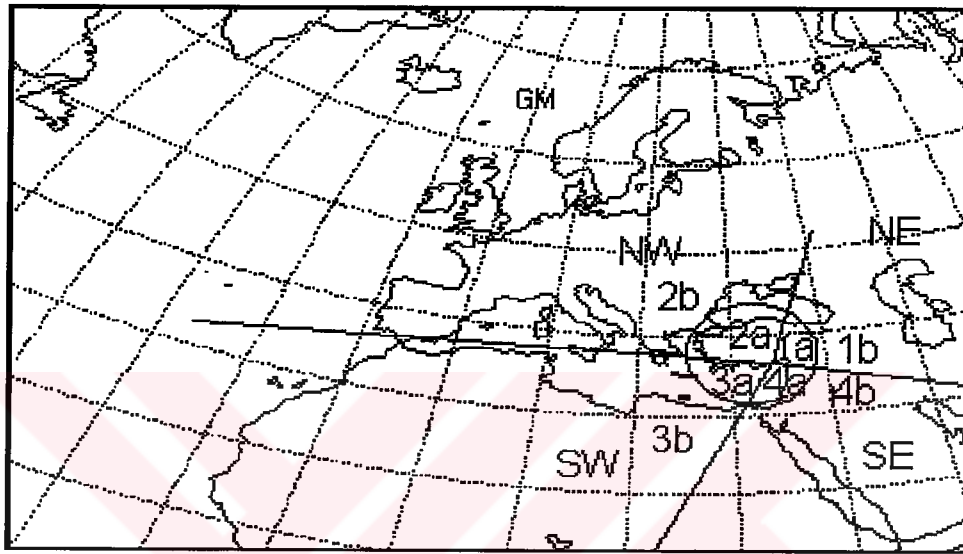


Figure 3.1. Sector partitioning for the geographical classification of air mass back trajectories.

All air mass back trajectories were allotted to one of the geographical sectors shown in Figure 3.1. by the method described below.

The air parcel locations (72, 1-h positions per 3-day trajectory) expressed as latitude and longitude were converted into vectors whose magnitude was defined as the distance to the sampling site and whose direction was defined as the angle from the x-axis showing the east direction at the Erdemli site. The points falling within the sectors (1st sector between 0° - 90° , N-E; 2nd sector 90° - 180° , N-W; 3rd sector 180° - 270° , S-W and 4th sector 270° - 360° , N-E) were then counted and the trajectory was assumed to belong to that sector in which it spent most of its travel time. The result of this classification of each trajectory to its relevant geographical

sector is depicted in Figure 3.2(a-d)- for four different barometric levels - as a percentage of the total of 513 trajectories.

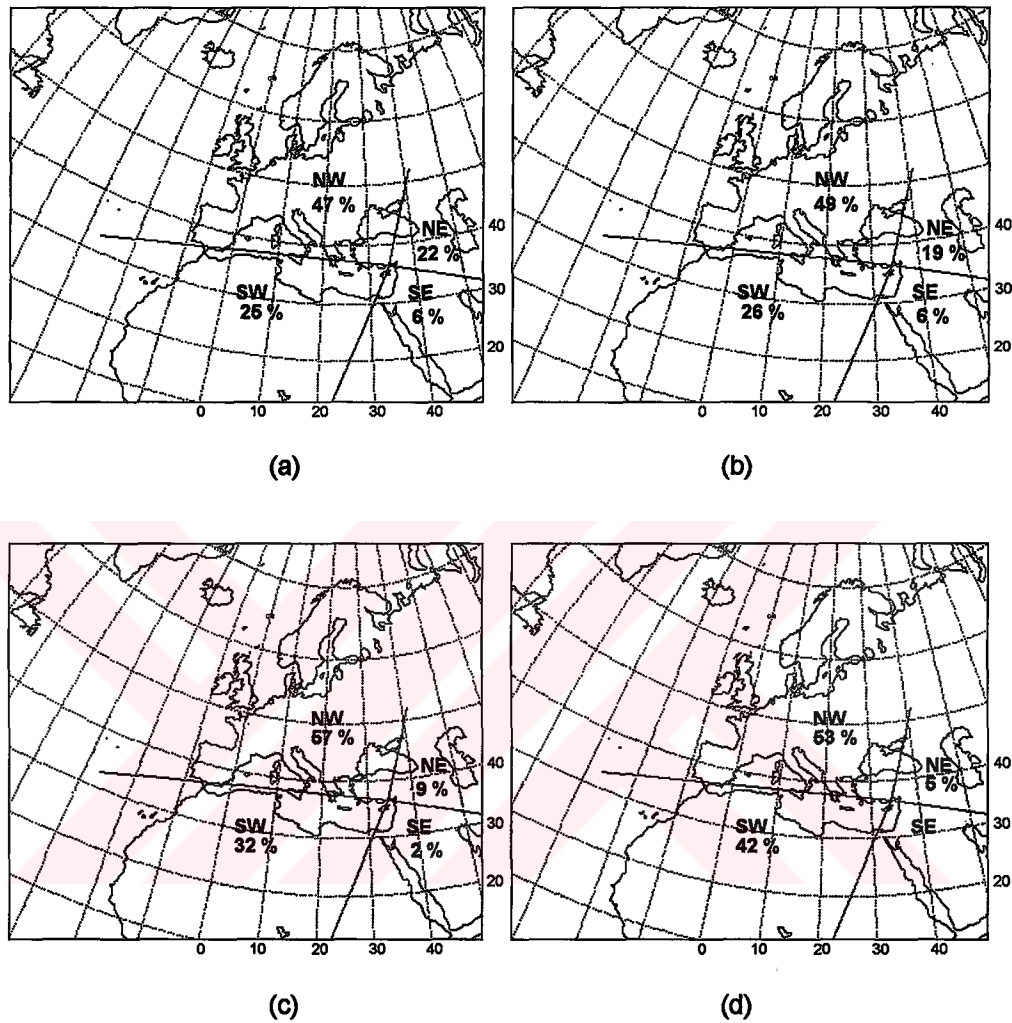


Figure 3.2. The percentage of mean airflow directions at various barometric pressure levels during August 1991-December 1992 at the Erdemli site.

(a) 900 hPa (b) 850 hPa (c) 700 hPa (d) 500 hPa

The classification of the mean air flow directions during the periods August 1991 and December 1992 obtained from the air mass back trajectories arriving at 900 and 850 hPa (boundary layer trajectories) was

quite similar (see Fig.3.2a,b). Although those arriving at 700 and 500 hPa (free atmosphere trajectories) show quite similar results, the percentage of air flow from the S-W sector is higher for those arriving at 500 hPa (see Fig.3.2c,d).

The temporal distribution of the air flow direction at the four barometric levels is shown in Figure 3.3 (a-d) where the trajectories have been grouped into three seasons.

During the summer most of the air flow (%50) within the boundary layer originated from the N-W direction, whereas the remaining %50 percent of the flow originated from both the N-E and S-W directions. The percentages of the flow from the N-W direction within the upper and lower layer trajectories were similar. However, in the upper layer trajectories the percentage of flow from the N-E was smaller and the percentage of flow from the S-W, especially at 500 hPa, was considerably larger than in the lower layer trajectories.

The percentages of the air flow directions within the boundary layer were similar in winter and summer except that during winter there was flow from the S-E. At higher levels in the winter the airflow percentages decreased in the following order N-W>S-W>N-E.

During the transitional seasons about 50 % of the airflow within the boundary layer originated from the N-W and it is in these seasons that the highest percentage of air flow (about 35%) within the lower layer of the atmosphere arose from the S-W. As in winter but unlike summer there was flow from the S-E. In the higher levels of the atmosphere in these seasons the air flow percentages were almost equally distributed between the N-W and S-W directions. The most pronounced seasonality exists for those trajectories having their origin in the S-E direction. Only during winter and transitional seasons did the boundary layer trajectories originate from this sector. Although, at the 900, 850 and 700 hPa levels more trajectories originated from the S-W sector during the transitional seasons than in summer and winter, at the 500 hPa level the percentage of the trajectories

arriving from the S-W was the same in the summer and in the transitional seasons. The same seasonal picture of the variable level mean airflow was observed for the trajectories arriving from the N-W sector (see Fig.3.3a). The greater percentages of the trajectories arriving within the boundary layer originated from the N-E direction during summer.

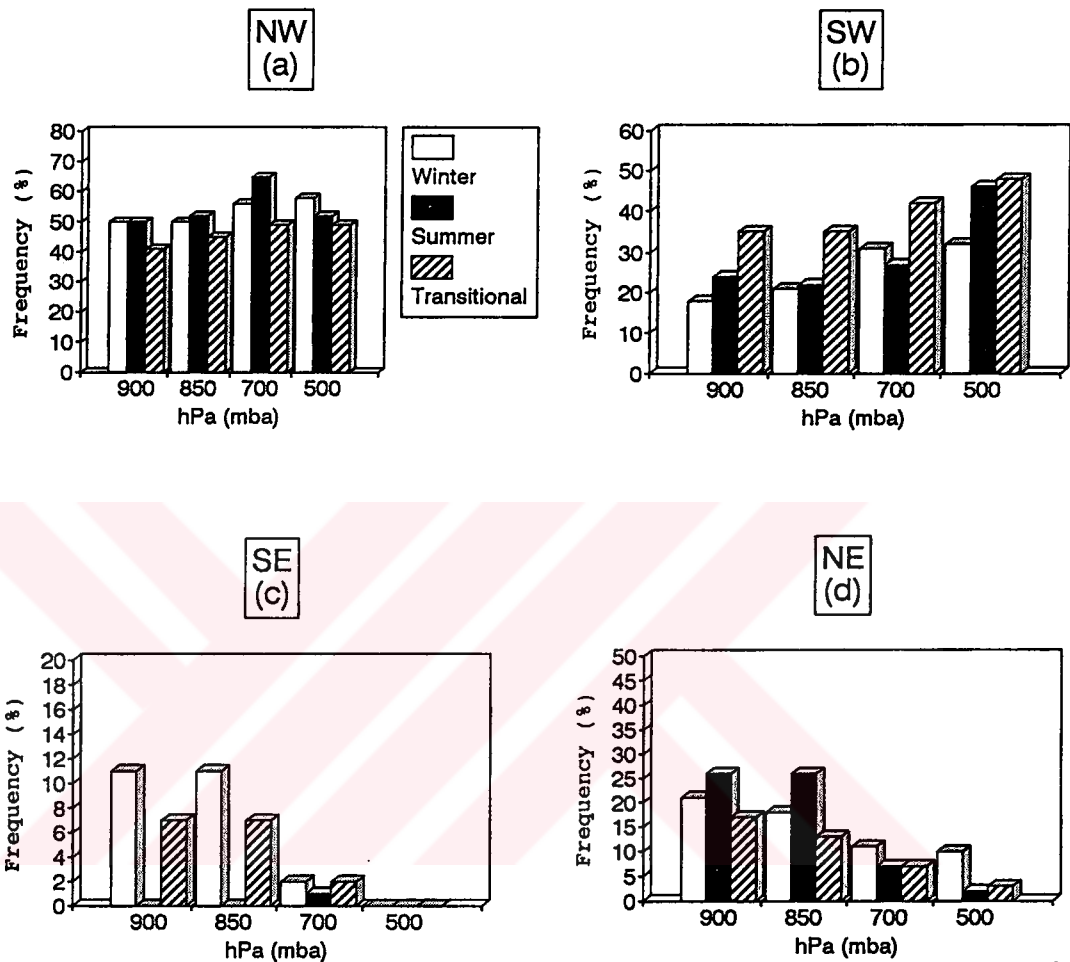


Figure 3.3. The seasonal distribution of the air flow directions at 900, 850, 700 and 500 hPa barometric levels.

(a) N-W; (b) S-W; (c) S-E; (d) N-E

To provide insight about the mean airflow direction to the eastern Mediterranean, five years of back trajectories (January 1978-December 1982) arriving at Israel and nine years of back trajectories arriving at Platanos (Crete) (January 1975-December 1983) have been reported by Dayan, (1986) and by the GESAMP, (1985), respectively (see Fig.3.4.a,b.).

The seasonality observed in the air flow directions in the present study was also reported by Dayan, (1986). Both the earlier calculations of trajectories used wind fields at 850 hPa produced by a global atmospheric model acquired from the National Meteorological Center (NMC) in Suitland, Maryland. This barometric level was taken as the approximate boundary layer between the planetary boundary layer, friction layer, or Ekman layer and the free atmosphere where frictional drag of air along the rough surface of the earth causes a pronounced inflow across the isobars towards the lower pressure. Theoretically, this departure of flow from the geostrophic wind (parallel to isobars) is 45° at the earth's surface, diminishing to 0° about 1000 m above the ground (Planetary boundary layer). The planetary boundary layer depth (PBLD) derived from upper-air rawinsonde data over the eastern Mediterranean basin shows temporal variability between 800 and 1900 m (UNEP/WMO, 1989b).

Most of the continentally derived material (both natural and anthropogenic) that contributes to the atmospheric aerosol composition is initially injected into the PBL. The upper surface of the boundary layer is defined by an inversion, which inhibits the transfer of material to the upper atmosphere (Prospero, 1981a). According to Prospero (1981a), the primary transport path by which material generated close to the continents, i.e. within tens to hundreds of kilometers, reaches the sea surface may be via this marine boundary layer. Over longer distances, however, the major transport path is probably via the free troposphere above the marine boundary layer. Since the long range transport of material generally occurs within the upper level of the atmosphere and the height of an air parcel at a selected isobar is not constant throughout its travel, the calculation of the air mass trajectories at a single barometric pressure level might lead to incorrect conclusions in assessing the transport of aerosol particles to the eastern Mediterranean. Because of this, in this study two trajectories arriving within the boundary layer (900 and 850 hPa) and two trajectories

arriving at the free troposphere (700 and 500 hPa) were calculated for each sample.

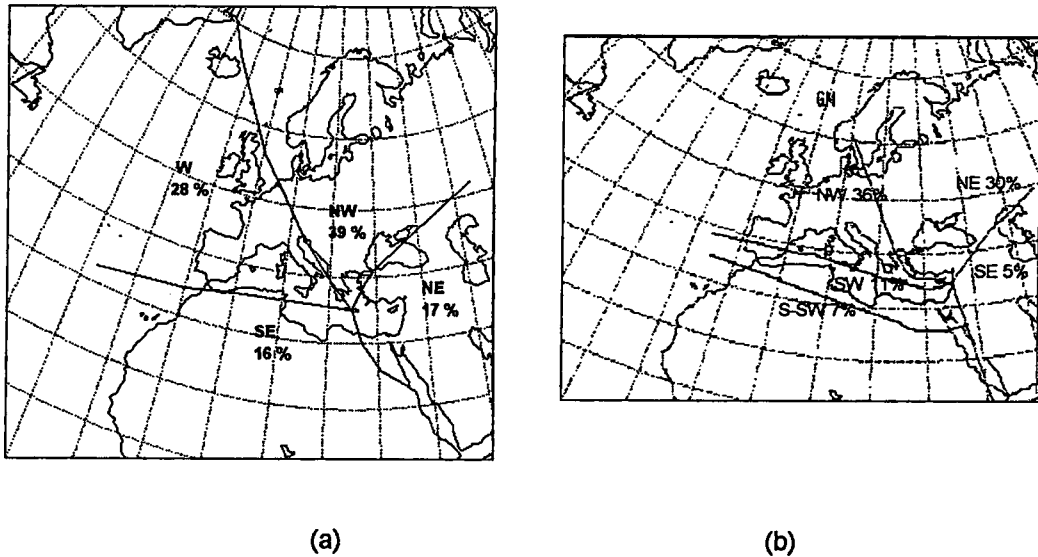


Figure 3.4. The mean airflow climatologies at different receptor sites located at the eastern Mediterranean area.

(a) Crete trajectories shown as annual percentages (after GESAMP, 1985).
(b) Israel trajectories shown as the percentages of the five years' trajectories (after Dayan, 1986). About 10% of the total number of trajectories were missing or could not be accurately classified into the five categories.

Although trajectories were calculated using different sources of data, models and sectoring techniques, the flow climatologies at 850 hPa obtained in both the earlier and the present study (see Figs.3.2b and 3.4a,b) were similar. This provides confidence in the validity of the categorization used to obtain airflows to the eastern Mediterranean region.

To test whether the amount of precipitation occurring during the sampling period was anomalous historical precipitations (50 years mean) recorded at the Mersin Meteorological station (45 km east of the sampling station) were utilized (Devlet Meteoroloji Isleri Genel Mudurlugu, 1984). Figure 3.5. presents monthly mean precipitation during the years of 1991

(empty bars) and 1992 (solid bars) together with the previous climatological means (dashed bars).

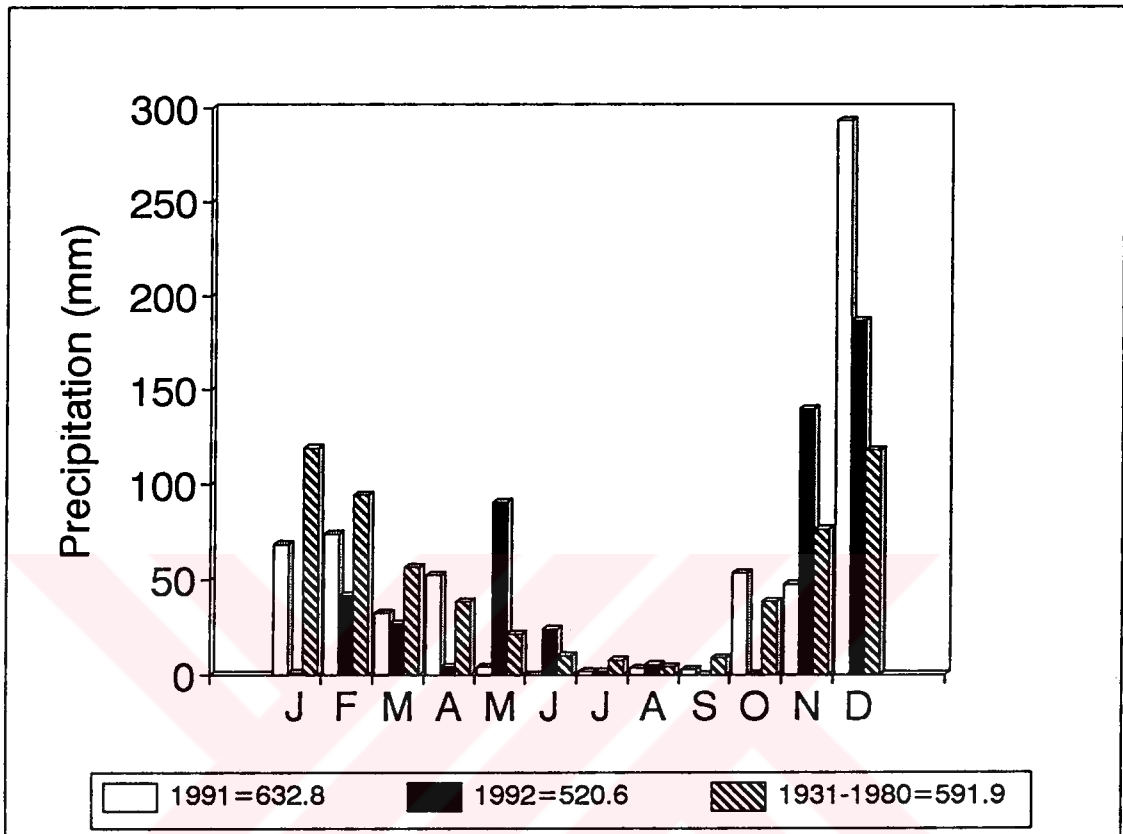


Figure 3.5. The monthly precipitation rates during the year of 1991, 1992 and the mean rates between the period of 1931-1980 at the sampling site. The total yearly precipitation rates are given at the bottom.

The figure confirms that a seasonal pattern of precipitation existed at the sampling site; almost all rain was experienced during winter and the transitional seasons whereas summers were dry and this is consistent with the historical data of the region and is a typical characteristic of the Mediterranean climate.

3.2. Atmospheric Concentrations of Aerosol Elements Collected at the Erdemli Station:

3.2.1. Mean Concentrations

The concentrations of 13 elements (namely Ca, Mg, Na, Al, Fe, Mn, Co, Ni, Cr, V, Zn, Pb and Cd) were determined in a total of 339 samples collected at the Erdemli station from August 1991 to December 1992. The statistics for these samples, including the arithmetic and geometric means and their respective standard deviations, the median values as well as the maximum and minimum concentrations are summarized in Table 3.1.

Most elements are log-normally distributed, i.e. the logarithms of the concentrations are normally distributed, as can be seen from the correspondence between the geometric mean and the median values (see Table 3.1.). The concentration ranges of each element are very wide resulting in high standard deviations of the mean concentrations. This is not unusual for atmospheric trace element data reported for aerosols over the Mediterranean and suggests significant variability of atmospheric concentrations on time scales of the order of one day due to the prevailing synoptic and micro scale meteorological factors and the temporal variation of source strengths (Dulac et al., 1987; Bergametti et al., 1989b; Guerzoni et al., 1989). The geometric standard deviations listed in Table 3.1 range from 2.1 to 3.2 and consequently indicate that the annual mean concentrations are not very representative of the concentrations as they occurred throughout the sampling period. This also illustrates quite dramatically the necessity of collecting a large number of samples over an extended period of time to obtain any meaningful information on the "climatological mean" concentration of any of these metals.

Table 3.1. Summarized statistics of the elemental concentrations for the whole sampling period (339 samples).

	(1)	(2)	(3)	(4)	(5)
Al	1255±2030	685(3.05)	749	21	22560
Fe	1280±2430	685(2.93)	739	35	30393
Mn	20±25	13(2.65)	15	1	306
Ni	7.3±6.1	5.6(2.2)	5.9	0.1	56
Cr	12±11	8.5(2.49)	8.4	0.07	66
Co	0.74±1.1	0.40(3.19)	0.45	0.004	11.2
V	10±9.4	7.8(2.24)	8.4	0.29	123
Zn	27±24	19(2.42)	20	1	205
Pb	54±80	30(2.83)	29	1.4	730
Cd	0.3±0.37	0.19(2.59)	0.2	0.005	3.7
Ca	4730±5160	3140(2.53)	135	230	52840
Na	3360±4740	1900(3.12)	249	44	44960
Mg	1740±1980	1200(2.35)	1270	67	16750

(1) Mean concentration and standard deviation of the mean.

(2) Geometric mean and geometric standard deviation .

(3) Median.

(4) Min. concentration.

(5) Max. concentration.

All concentrations are in ng m⁻³.

The log-normal distributions of the atmospheric concentrations of the elements were verified by a goodness of fit test (Kolmogorov-Smirnov test) using "Statgraphics" statistical software. The Kolmogorov-Smirnov goodness of fit test also called the Kolmogorov-Smirnov one-sample test, assesses the fit of observations to an expected cumulative frequency distribution (Biostatistical Analysis, 1984). This test was applied to all measured species and it revealed that the atmospheric concentrations of elements measured in this study followed log-normal distributions at the 95% confidence level.

The frequency histograms of the log-transformed data and the associated expected normal distribution curves for Fe, Pb

and Na are given in Figure 3.6 (a-c). As can be seen from the figure the distributions of log-transformed atmospheric concentrations of these elements fit quite well to the corresponding expected normal distribution curves.

3.2.2. Contributions of Major Sources to the Observed Mean Concentrations

The aerosols over the Mediterranean Sea, always being near a coastal region, exhibit both crustal and pollutant dominated characteristics. To a first order approximation one can consider that the atmosphere over the Mediterranean is composed of two components, anthropogenic and crust originated particulates.

Rahn (1976) classified atmospheric samples as "marine", "semi marine" and "nonmarine". According to his classification a "marine" location means either that the sample was obtained above the open ocean or that the aerosol was enriched in such marine elements as Na, Ca, Mg, K, Cl etc. "Semi marine" included areas where a city was in a coastal area with a continent on one side and an ocean on the other. This author also concluded that over continental areas, where little sea-salt is found, weathered crustal material is the dominant source of atmospheric Na. Nevertheless, the concentration of Na in the atmosphere over the western Mediterranean, a region that is affected by windblown dust, is slightly, but significantly, affected by mineral aerosol (Dulac et al., 1987). "Nonmarine" included all types of continental sites free of significant marine aerosol.

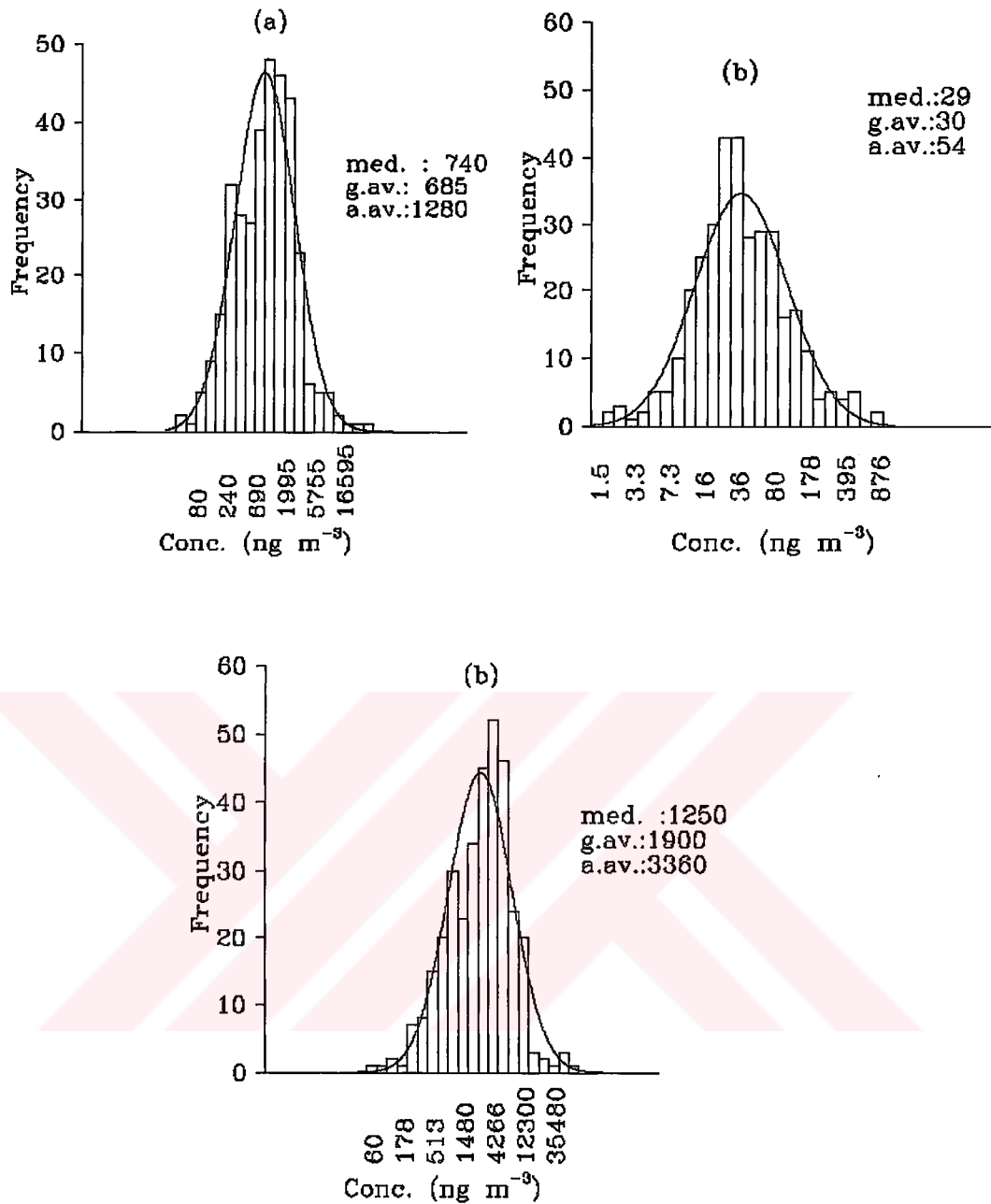


Figure 3.6. The frequency histograms of the log-transformed atmospheric concentrations of the elements and their expected normal distributions.

(a) Fe; (b) Pb; (c) Na

Accordingly, the land based sampling site (Erdemli) occupied throughout the present study should be classified as semi marine and would be expected to demonstrate both marine and nonmarine characteristics under the prevailing meteorological conditions. Thus we are suggesting that, besides continental sources (wind eroded alumino-silicate particles and aerosols derived from anthropogenic emissions), the Erdemli site is influenced by the nearby marine source.

The contributions of these sources to the total concentrations of the elements observed in the aerosols can be estimated by utilizing uniform chemical compositions of crust and of bulk sea water (Rahn, 1976; Schneider, 1987; Chester et al., 1993a). These investigators utilized metal:Al and metal:Na ratios in appropriate reference materials to estimate the relative importance of crustal and marine sources to elemental concentrations. To get a better feeling for the relative importance of marine and crustal contributions to the elements in a typical mixed aerosol, the aerosol of the eastern Mediterranean has been resolved into its crustal and marine components. The crustal fractions of the atmospheric concentrations were calculated by assuming 100% of the Al to be crust derived and utilizing the element to aluminum ratios documented for average crustal rocks. The marine component was calculated from the composition of bulk sea water, assuming all noncrustal Na to be of marine origin. The supposed non-crustal Na (i.e. Na_{mar}) concentrations were calculated from the following formula:

$$Na_{mar} = Na_{air} - Al_{air} \left(\frac{Na}{Al} \right)_{crust} \dots \dots \dots (1)$$

In this thesis, the contributions of the crustal and marine sources to the observed elemental concentration were calculated from elemental abundances in the crust compiled by Taylor (1964) and from the bulk sea water composition reported by Martin and Whitfield (1983) according to the equations given below.

$$X_{\text{crust}} = Al_{\text{air}} \left(\frac{X}{Al} \right)_{\text{crust}} \dots \dots (2)$$

$$X_{\text{sea}} = Na_{\text{mar}} \left(\frac{X}{Na} \right)_{\text{sea}} \dots \dots (3)$$

where X , Al and Na_{mar} represent the atmospheric concentrations of the observed elements and the aluminum and sodium concentrations calculated from eqn.1; the subscripts 'crust' and 'sea' identify the reference material ratios and the subscript 'air' denotes atmospheric concentration. The remaining component of the concentration of each element is simply the difference between the total measured concentration of an element and the sum of its marine and crustal fractions calculated from eqns. 2 & 3. This unexplained component may come from pollution, unknown natural sources or from the crust or sea water via enrichment processes.

The percentage contribution of the two natural sources (crust and sea) to the total atmospheric concentrations of each element, together with the unexplained percentages are presented in Table 3.2. By definition 100% of the Al and 78% of the Na concentrations come from crustal and marine sources respectively. Dulac et al. (1987) emphasized caution in using Na as a tracer of sea-salt particles. Even though their samples represented the marine atmosphere (they collected their samples onboard ship throughout various cruises in the western Mediterranean) they found

the crustal influence on a measured sodium concentration corresponding to a Na/Al ratio of lower than 3 to be more than 20% and was still more than 10% when the corresponding Na/Al ratio was higher than 6.

Table 3.2. Percent contribution of the major sources to the observed mean atmospheric concentrations of the elements.

Elements	Crustal	Marine	Other
Al	100(def.)	-	-
Fe	53	-	47
Mn	65	-	35
Ni	15	-	85
Cr	16	-	84
Co	55	-	45
V	21	-	79
Zn	5	-	95
Pb	0.7	-	99.3
Cd	1.9	-	98.1
Ca	15	5	80
Na	22	78(def.)	0
Mg	21	23	56

As indicated in Table 3.2. the calculated crustal influence on the Na concentration of the whole sample set collected at Erdemli is 22 %, whereas for the 104 samples having Na/Al ratios higher than 6 it becomes 2 % and for the 176 samples having Na/Al ratio lower than 3 it attains 37%. Ca and Mg are the only elements concerned in this study that have been influenced by the marine source. The contributions of the marine source to the concentrations of Ca and Mg, were 5% and 23 % respectively. The marine source contribution to the atmospheric concentrations of these elements increased to 11% and 42 %, respectively, for those samples having Na/Al ratios higher than 6. These two natural

sources, namely crustal and marine cannot explain the concentrations of Zn, Cd and Pb and the concentrations of these elements in the atmosphere can be attributed to anthropogenic emissions (see Table 3.2).

For only 15% of the total samples was the contribution of the crustal source to the observed concentrations of Fe, Mn and Co 100%. In the remaining samples the contribution of other sources was significant. The contribution of other sources to the concentrations of V, Cr and Ni was also significant, indeed it was always greater than the crustal contribution.

3.2.3. Comparison of the Data With the Results of Other Studies

The mean concentrations of the elements in atmospheric particulates exhibit substantial spatial variations which differ markedly from element to element. For comparison of the data obtained in this study with those of previous workers, geometric mean concentrations have been preferred since these correctly reflect the concentrations obtained under normal meteorological conditions whereas arithmetic means are strongly influenced by the presence of a very few high values. The higher arithmetic means might be of interest in other contexts, e.g. in calculations of average deposition during a measurement period.

In general, low atmospheric concentrations are found at remote sites and over the oceans, whereas the highest concentrations are observed at urban sites. Thus, the principal trend in the trace metal observed over marine environments is a decrease in concentrations from coastal areas to pristine oceanic sites (Chester et al., 1991a).

For the purpose of the present discussion, sites have been separated into three groups based on the spatial variation in the mean concentrations of the elements in atmospheric particulates over the marine

regions. These groups are coastal "pollutant dominated", coastal "crustal dominated" and "open ocean" of which some examples are given in Table 3.3.

Table 3.3. Geometric mean concentrations of trace metals in aerosols from a number of representative marine environments (concentrations are given in ng m^{-3}).

Element	Open Ocean			Coastal Seas	
	Tropical North Pacific (Enewetak) ¹	Tropical South Pacific (Samoa) ²	Tropical North Atlantic ³	North Sea ⁴	Arabian Sea ⁵
Al	21	0.72	160	219	1227
Fe	18	0.21	100	230.5	790
Mn	0.29	0.044	2.2	9.1	17
Ni	-	-	0.64	2.5	2
Cr	0.091	-	0.43	3.1	3
Co	0.0076	0.00037	0.08	0.19	0.38
Cd	0.0035	-	-	-	0.045
V	0.082	-	0.54	-	6.3
Zn	0.18	0.06426	4.4	26	10
Pb	0.12	0.01620	9.9	20	4.3

References; 1: Duce et al., (1983); 2: Arimoto et al., (1987); 3: Buat-Menard and Chesselet (1979); 4: Chester and Bradshaw (1991) (close to pollutant sources); 5: Chester et al., (1991a) (close to crustal sources).

The results observed over the Pacific Ocean were obtained through the Sea-Air Exchange (SEAREX) program designed to study the atmospheric transport of naturally occurring and anthropogenic substances to the Pacific Ocean. For this purpose, major field experiments were conducted at remote island sites in the major wind regimes over the Pacific Ocean: the northeast trades over the tropical North Pacific (Enewatak Atoll; $11^{\circ}20' \text{ N}$, $162^{\circ}20' \text{ W}$) and the southeast trades over the tropical South Pacific (American Samoa; $14^{\circ}15' \text{ S}$, $170^{\circ}34' \text{ W}$) (Duce, 1989). The

concentrations of the elements in the atmosphere at Samoa reported by Arimoto et al., (1987) are among the lowest ever observed over open ocean areas and lower than those over the atmosphere at Enewatak reported by Duce et al., (1983). Although these two sites represent truly remote marine environments, the mean atmospheric concentrations of the crustally derived elements (Al, Fe) are two orders of magnitude higher in the Enewatak samples than in the Samoa samples (see Table 3.3.) and this has been attributed to the long-range transport of weathered crustal material from Asia, primarily desert dust from China (Duce et al., 1983). The existence of the truly anthropogenic elements, Zn, Cd, Pb and of the crustal elements in the atmosphere over the tropical Pacific Ocean (at Enewatak Atoll which is 5000 km away from any continental sources) verify the occurrence of long range transport of crustal material from continents to the remote marine region.

The data for samples collected on board ship in the tropical North Atlantic by Buat-Menard and Chesselet (1979) are representative of open North Atlantic atmospheric concentrations. The higher atmospheric concentrations of the elements observed over the North Atlantic than over the Pacific Ocean reveal the atmospheric transport of both crustal and anthropogenic elements to be more effective in the former oceanic area. The elemental analysis of aerosols over the tropical North Atlantic and the trace element fluxes in deep North Atlantic waters show this region to underlie the path of the northeast trades which transport large quantities of Saharan dust (Talbot et al., 1986; Kremling and Streu, 1993).

In contrast to the Pacific and Atlantic oceans, the North Sea is surrounded by some of the most industrialized nations in the world and the atmospheric concentrations of anthropogenic elements (Zn, Pb) reported by Chester and Bradshaw (1991) are the highest of the regions mentioned in the table. A recent study validated anthropogenic processes as being the most important source of particulate trace metals to the North Sea atmosphere and showed the anthropogenic fraction of the North Sea aerosol

to approximate in composition to that of average anthropogenic European trace metal emissions (Chester et al., 1994).

Although in Table 3.3 the Arabian Sea is grouped with the North Sea as being coastal, the concentrations of the crustal elements (Al,Fe) observed over it are one order of magnitude higher than those reported for the North Sea atmosphere and this has been attributed to a significant crustal component from the surrounding arid lands (Chester et al., 1991a).

The geometric means of the atmospheric concentrations of the crustal elements (Al, Fe, Mn and Co) observed for the whole sampling period of the present study (see Table 3.1) resemble those reported for the Arabian Sea atmosphere, whereas the concentrations of the elements derived from anthropogenic processes (e.g. Pb and Zn) resemble those for the North Sea atmosphere. Thus, the atmosphere over the enclosed eastern Mediterranean is affected both from aeolian weathering of crustal material and by anthropogenic activities in the surrounding land masses.

Before attempting to explain the temporal variability of each trace element, one compares the results summarized in Table 3.1. with those from comparable atmospheric sampling programs carried out over the Mediterranean basin. The comparison of the concentrations found at the Erdemli site with those reported for other sample collection sites could be valuable in demonstrating the possible existence of differences in the concentrations of the elements in the atmosphere over the eastern and western parts of the Mediterranean. Table 3.4. compares the geometric mean concentrations of elements in aerosols collected from different land based stations and also on board ship throughout various cruises along a Mediterranean transect (the locations of the land-based stations and the cruise track for the Mediterranean transect are depicted in Fig.3.7). As can be seen from the figure, throughout the EROS-2000 (European River Ocean System) project on the western coast of the Mediterranean more than one coastal,

land-based station provided data on the elemental concentrations of the atmospheric aerosol. However, few aerosols have been analyzed over the eastern Mediterranean, in particular no monitoring data have previously been reported from a coastal station. The present study may therefore be considered as a prototype paralleling the observations of stations occupied along the western Mediterranean coast and providing preliminary data on the temporal variation of the elemental concentrations in the aerosols over the eastern Mediterranean.

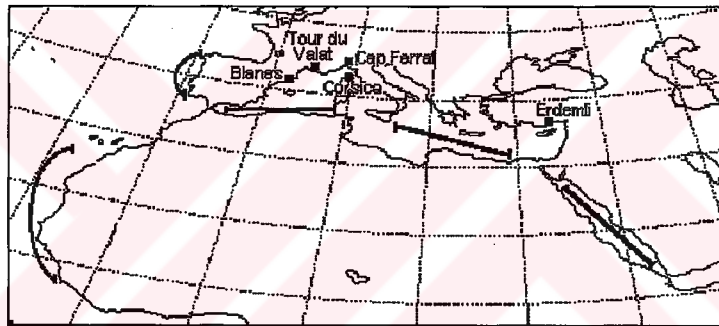


Figure 3.7. Locations of the land based aerosol sampling sites around the Mediterranean basin. The transect along which aerosol samples collected on ship was indicated (Chester et al., 1993a).

The major difference in the composition of atmospheric particulates observed in this study and those located in the western basin is that particulates from the eastern basin have higher

concentrations of crustal elements, specifically, Al and Fe, and lower mean concentrations of anthropogenic elements, specifically, Cd, Zn, Pb.

Particulate Pb is generally considered a reliable indicator of human activity, particularly of car exhaust, which is the major contributor of fine particulate Pb in the atmosphere. Pb is added to petrol as an anti-knock agent and emitted in particulate form, mainly as PbBrCl (Biggins and Harrison, 1979). About 60 % of the total anthropogenic emission of lead in Europe comes from this source (Pacyna, 1984). Emissions of Pb from gasoline combustion seem to have decreased in western Europe due to the diminished use of Pb additives and the introduction of unleaded gasoline. In France, for example, the consumption of leaded gasolines decreased by 50% between 1988 and 1991 and in response Pb concentrations in the atmosphere over the French coast of the Mediterranean declined (Nicolas et al., 1992). Ice-core records in permanent ice fields probably provide the most accurate assessment of the extent and magnitude of atmospheric deposition. The samples of Boutron et al. (1991) in the Greenland ice fields extend back for a continuous sequence of 22 yr. (1967-1989). They reported that, as a result of improved emission controls and product-use patterns introduced in developed countries, Pb concentrations in Greenland snow have decreased by a factor of 7.5 whereas Cd and Zn concentrations decreased by a factor of 2.5.

Lower Pb concentrations were reported for samples collected on board ship throughout the Mediterranean transect (Chester et al., 1993a) and for samples collected at the Mediterranean island of Corsica (Bergametti et al., 1989b) than for the other coastal stations. This suggests emissions from local traffic to be much more pronounced at the latter stations. Although the concentrations of such crustal elements of Al and Fe in the

atmosphere of the Erdemli site are about twice as high as at the western stations the concentration of Mn is comparable for both basins (see Table 3.4).

This element has a mixed origin; its atmospheric concentration is affected by both crustal and anthropogenic sources. The world-wide manganese emission from windblown dust exceeds more than 24-fold the anthropogenic emission of manganese in Europe (Pacyna et al., 1984). In order to estimate the non-crustal contributions of atmospheric metal concentrations (Excess M), the crustal contribution is subtracted from the observed element concentrations, assuming the initial elemental composition of the crust to be similar to that of the Taylor's (1964) compilation of the average crustal composition, using the following relation:

$$\text{Excess M} = M_{\text{atm}} - \left[\left(\frac{M}{Al} \right)_{\text{crust}} \times Al_{\text{atm}} \right]$$

where the subscript "atm" refers to the elemental concentrations (M) in aerosols and (M/Al)_{crust} is the ratio of the weight of element M to that of Al in the average crust.

Excess M values vary somewhat with the location of the sampling site within the atmosphere of the Mediterranean sea. The average non-crustal (Excess M) percentages of each elemental concentration estimated from the above equation utilizing the geometric mean concentrations of the elements are tabulated in Table 3.4. The amount of each trace metal in excess of the crustal material was assumed to be an anthropogenic component either transported to the atmosphere over the eastern Mediterranean or produced within the region. It should be noted at this point that it is extremely difficult to ascertain unambiguously what precise proportions of the trace elements come from anthropogenic and

natural emissions due to variations on the composition of the local crust. The non-crustal contributions to the total mean atmospheric concentrations of the elements Cd, Zn and Pb are almost 100 % irrespective of the sampling location. The observation of concentrations, low compared to those observed at land based stations in the western basin, of such elements as Pb, Cd and Zn indicate that the effect of anthropogenic emissions over the eastern basin to be much less pronounced. This can be explained simply by the presence of the industrialized nations that define the northern border of the western basin. In contrast the eastern basin is bounded by a desert belt to the South and East and semi-industrialized and agricultural countries to the North. The most interesting feature of the Table 3.4. is the highest non-crustal contribution to the mean Fe concentration, of course, is a well known crustal element for the samples collected at the Erdemli site. Al-Momani (1995), reported the non-crustal contribution to the concentration of Fe in precipitation at Antalya (a coastal eastern Mediterranean station) as 35%, in line with the percentage given for the aerosol samples in this study.

The mean elemental concentrations reported for the Mediterranean transect resemble those in the atmosphere above the Erdemli site with the exception of Cr, Ni and Pb concentrations (see Table 3.4). Thus, although the Erdemli site is a coastal land-based station, it is less affected by pollution sources than other comparable stations located on coastal sites on the western part of the Mediterranean. The differences in trace metal concentrations between Erdemli and other sites highlight the need to establish a network of atmospheric collection sites around the Mediterranean basin.

Table 3.4. The geometric mean concentrations of trace metals in aerosols over the Mediterranean Sea and surrounding coastal sites. Percentages of the non-crustal metal concentrations are given in parentheses.

	Erdemli ¹	Blanes ²	Cap Ferrat ³	Tour du Valat ⁴	Corsica ⁵	Med.Sea ⁶
Al	680	390	370	380	168	936
Fe	685(32)	316(16)	320(21)	275(6)	144(21)	707(10)
Mn	12.6(41)	10(57)	11(63)	13(68)	5.3(65)	16(36)
Ni	5.6(89)	5.5(94)	2.8(88)	-	-	4.2(80)
Cr	8.5(90)	1.8(74)	2.5(82)	-	-	3.1(64)
Co	0.40(48)	0.20(41)	-	-	-	-
Cd	0.19	0.60	0.36	0.51	-	0.17
Zn	19	50	41	60	19	12
Pb	30	50	58	56	16	10.5

References; 1: Present study; 2: Chester et al., (1991b); 3: Chester et al., (1990c); 4: Guieu (1991b); 5: Bergametti et al., (1989b); 6: Chester et al., (1993a).

Concentrations are given in ng m⁻³; (-) no data reported.

The observation of high Cr and Ni levels over the eastern basin is probably due to the presence of ophiolitic rocks that frequently outcrop on the coastal hinterland of the basin and are relatively enriched with Cr and Ni bearing minerals (Aslaner, 1973; Tolun and Pamir, 1975). Guerzoni et al. (1989) similarly explained the enrichment of Ni and Cr in aerosols over the Adriatic Sea as arising from ophiolitic minerals in the Balkan area. The geochemical characteristics, the depositional environment and the provenance of surface sediments from the Cilician Basin (the area between Cyprus and southern Turkey) have been well described by various authors and the enrichment of the near-shore sediments in Cr and Ni has been attributed to accumulation of the products of the denudation of particular types of rocks (basic-ultrabasic) in the sediments (Shaw and Bush, 1978;

Emelyanov and Shimkus, 1986). A significantly high Cr content in one sediment sample was explained as due to the existence of major chromite deposits in the central part of the Taurus Mountains flanking the coast. A survey of the recent sediments of the southern Turkish coast has also verified that its characteristics are mainly governed by the rock types (limestone, ultrabasic and intermediate igneous) found on the mountains bordering the coast which are undergoing weathering (Evans, 1972; Ergin et al., 1988).

The higher excess iron concentrations in the aerosol samples reported in this study and in the precipitation samples reported by Al-Momani (1995) with respect to samples collected from the western Mediterranean atmosphere might also be the result of the weathering of basic and ultrabasic rocks which have a high Fe content.

Another possible source of excess Cr in the atmospheric samples is the presence of a factory handling chromium ores at the city of Mersin located 45 km east of the sampling site.

The enrichment of the basin sediments in Cr and Ni can be demonstrated by comparing their element/Al ratios with the same elemental ratio in the crust. The Cr/Al and Ni/Al ratios both in the average crust and in ultrabasic rocks are 0.001 and 0.44 respectively (Taylor, 1964; Emelyanov and Shimkus, 1986). The mean ratios of Cr/Al and Ni/Al in the basin sediments are 0.007 and 0.004 (Shaw and Bush, 1978), whereas the mean of the same elemental ratios in aerosol samples collected throughout the present study are 0.012 and 0.008, respectively (calculated from Table 3.1). It is not yet clear whether the slightly higher ratios found in the atmospheric particulates compared to those in basin sediments should be attributed to local anthropogenic emissions or to a regional geochemical characteristic of the crust.

3.2.4. Temporal Variation of the Atmospheric Concentrations

3.2.4.1. Seasonal Changes

To illustrate the seasonality in the elemental concentrations the sampling period has been divided into the following climatological seasons, winter (November, December, January, February), summer (June, July, August, September) and the transitional seasons, autumn and spring, (March, April, May, October). Summarized statistics reveal minimum seasonal elemental concentrations during winter when the region was rainy, the mean elemental concentrations in the dry summer season are much higher. Although rains continued during the transitional seasons, the arithmetic means of the elemental concentrations and their ranges are higher than during either winter or summer for almost all elements being considered in this study (Table 3.5a-c).

Table 3.5. Summarized statistics of the seasonal elemental concentrations.

(a) Winter (November, December, January, February; wet season)
n=142

	(1)	(2)	(3)	(4)	(5)
Al.....	570±775	340(2.7)	350	21	6110
Fe	615±840	375(2.6)	370	35	6470
Mn	10.3±9.9	7.2(2.4)	7.2	1.1	66
Ni	5.5±4.1	4.3(2.1)	4.5	0.43	34
Cr	9.6±7.8	6.9(2.4)	7.2	0.33	35
Co	0.43±0.64	0.23(3.1)	0.23	0.01	4.3
V	8.3±6	6.5(2.2)	6.9	0.29	42
Zn	18.3±18.3	13(2.4)	13	1	156
Pb	39±45	24(2.8)	26	1.4	400
Cd	0.26±0.29	0.18(2.4)	0.2	0.005	2.75
Ca	2565±2230	1895(2.2)	1855	230	14180
Na	3250±5360	1455(3.6)	1515	50	37800
Mg	1120±1225	780(2.3)	710	70	10260

Table 3.5. Cont.

(b) Summer (June, July, August, September; dry season) n=103

	(1)	(2)	(3)	(4)	(5)
Al	1270±640	1120(1.7)	1090	130	3435
Fe	1370±1070	1140(1.75)	1090	310	8220
Mn	23.9±10.2	21.8(1.56)	22	3.6	75.8
Ni	7.4±3.6	6.7(1.59)	6.4	2.3	19.3
Cr	11.8±9.5	9.4(1.9)	8.4	2.6	59.5
Co	0.83±0.50	0.70(1.77)	0.68	0.16	2.89
V	11.7±7.1	9.6(1.95)	9.4	0.63	32.5
Zn	42±27	34(2.06)	41	1.5	206
Pb	53±67	34(2.32)	30	6.7	390
Cd	0.4±0.52	0.21(3.16)	0.24	0.02	3.65
Ca	5820±4100	4680(1.93)	4680	1000	20780
Na	3950±2315	3225(2.07)	3465	150	11085
Mg	1920±880	1760(1.5)	1733	670	5940

(c) Transitional seasons (March, April, May and October; wet seasons)

n=145

	(1)	(2)	(3)	(4)	(5)
Al	2286±3480	1115(3.3)	1340	100	22570
Fe	2215±4240	970(2.6)	1160	49	30390
Mn	29.7±42.9	16.4(2.4)	19.8	1.0	306
Ni	9.8±9.3	6.6(2.8)	7.8	0.1	56
Cr	16.4±14.5	10.5(3.0)	10.8	0.07	66
Co	1.11±1.91	0.49(3.8)	0.52	0.01	11.2
V	11.9±14.3	8.0(2.5)	8.8	0.4	123
Zn	24±21	18.9(2.0)	19	2.4	169
Pb	80±124	39(3.2)	33	4	730
Cd	0.25±0.23	0.18(2.2)	0.19	0.02	1.43
Ca	6890±7690	4395(2.7)	4290	300	52840
Na	2930±7690	1625(2.7)	1695	44	44960
Mg	2500±3180	1534(2.6)	1455	190	16745

(1) Mean concentration and standard deviation of the mean.

(2) Geometric mean and geometric standard deviation.

(3) Median.

(4) Min. concentration.

(5) Max. concentration.

All concentrations are in ng m⁻³.

The same seasonal pattern, that is higher mean concentrations in summer than in winter have also been reported for the western Mediterranean (Bergametti et al., 1989b). These authors suggested that this seasonal change in atmospheric concentrations could be explained by two factors:

(1) a seasonal change in continental source strength and/or airflow patterns and/or

(2) a different removal rate for atmospheric particles between these two seasons.

They ruled out the first effect since nine years' observation of air flows over the region showed no obvious change from season to season (GESAMP, 1985). They therefore attributed the observed seasonal change of the atmospheric elemental concentrations to the local precipitation rate and episodic inputs of crustal material from North Africa.

Compared to the western area, a marked seasonal change in airflow patterns has been observed in the mean air flow directions to the eastern Mediterranean both in this study (see Section 3.1) and in other studies (GESAMP, 1985; Dayan, 1986). This implies that the seasonality in atmospheric concentrations over the eastern Mediterranean is the consequence of both the factors suggested by Bergametti et al., (1989b).

3.2.4.2. Elemental Concentrations: Time Series

The temporal variation of the atmospheric concentrations during August 1991 and December 1992 is shown in Figs.3.8 (a-m) for the elements Al, Fe, Mn, Ca, Mg, Co, Ni, Cr, V, Pb, Cd, Zn and Na. The figures also depict local rainfall, clearly demonstrating the dramatic decreases observed in elemental concentrations following rain in winter, spring and autumn - but not during summer which is a dry period. The large standard deviations of the mean concentrations presented in Table 3.1. confirm that

the intense, short term variations of atmospheric concentrations are superimposed on a seasonal pattern. That is, during the dry period (June-Sept.) the geometric mean concentrations for the trace metals are higher than those reported for the wet period (Nov.-Dec.) (see Table 3.5a-c) and indicate also that the means are poorly representative of the concentrations as they occur throughout the year. At first sight, the data suggest precipitation to be a major factor influencing the variability of the observed aerosol trace metal concentrations. Indeed, it appears from Fig.3.8 that precipitation is systematically followed by abrupt decreases of the aerosol trace metal concentrations.

The atmospheric concentrations of the major elements (Al, Fe, Si, Ca and Mg) are determined by the long-range transport of crustal aluminosilicate particles (commonly called dust or mineral aerosol) over the marine environment (Rahn, 1976; Guerzoni et al., 1989; Coude-Gaussen et al., 1987, Bergametti et al., 1989a,b; Martin et al., 1990). Al concentrations have often been used as indicators of the atmospheric dust load, itself (Uematsu et al., 1983; Prospero and Nees, 1987; Chester et al., 1991a). Accordingly, in this study the increase in the concentrations of Al has been used as a chemical indicator of the intrusion of dust from the surrounding desert areas which are highly productive sources of mineral aerosol. The time variabilities of Al, Fe, Mn, Co and Ca concentrations depict similar patterns. All these elements possess minimum concentrations during winter when the soil on both the local and the surrounding land masses is damp due to precipitation. During this period weathering of the crustal material decreases and there is a decrease in the atmospheric concentrations of those elements that derive from weathered crustal material. During the transitional seasons the major elements show intense episodic peaks and between these events concentrations diminish to the magnitudes observed in winter. During summer the concentrations of these elements varied less markedly. Compared to winter, summer is a favorable period for local soil particles to become airborne.

Concentrations of Pb, Cd and Zn which derive from pollution, did not show the significant seasonal trends of crustal elements (see Fig.3.8j-l) From simultaneous measurements of lead in aerosol samples collected at a remote coastal station (Corsica), air mass trajectory analyses and precipitation patterns, the variability of aerosol lead concentrations in the western Mediterranean atmosphere on both daily and seasonal time scales has been shown to be due primarily to the scavenging of lead aerosol particles by rain rather than to changes in source strengths (Remoudaki et al., 1991). This finding, together with the results obtained during the present study, indicates that these elemental concentrations are generated in the atmosphere by local emissions rather than by remote sources. The primary anthropogenic source for Pb is gasoline combustion, secondary sources being iron, steel and alloy production as well as refuse incineration, cement production and wood combustion. The largest contribution of Cd and Zn to the atmosphere arises from primary zinc-cadmium smelters located mainly in the former Russian region. Other sources are the combustion of coal and oil, refuse incineration, iron, steel and alloy manufacturing, gasoline combustion, wood combustion, phosphate fertilizers and cement production (Pacyna, 1983).

Ni and Cr showed no significant seasonal trend which could be attributed either to local natural enrichment of the weathered soil or to anthropogenic emissions (see Figs.3.8g,h).

Na, which is universally used as an index for seasalt particles in the atmosphere, shows conspicuous peak intensities in winter periods when storms are more pronounced (see Fig.3.8.m). The classical linear relation between the local wind speed and the atmospheric concentration of Na has been demonstrated for both western and eastern Mediterranean aerosols (Bergametti et al., 1989b; Karakoc, 1995).

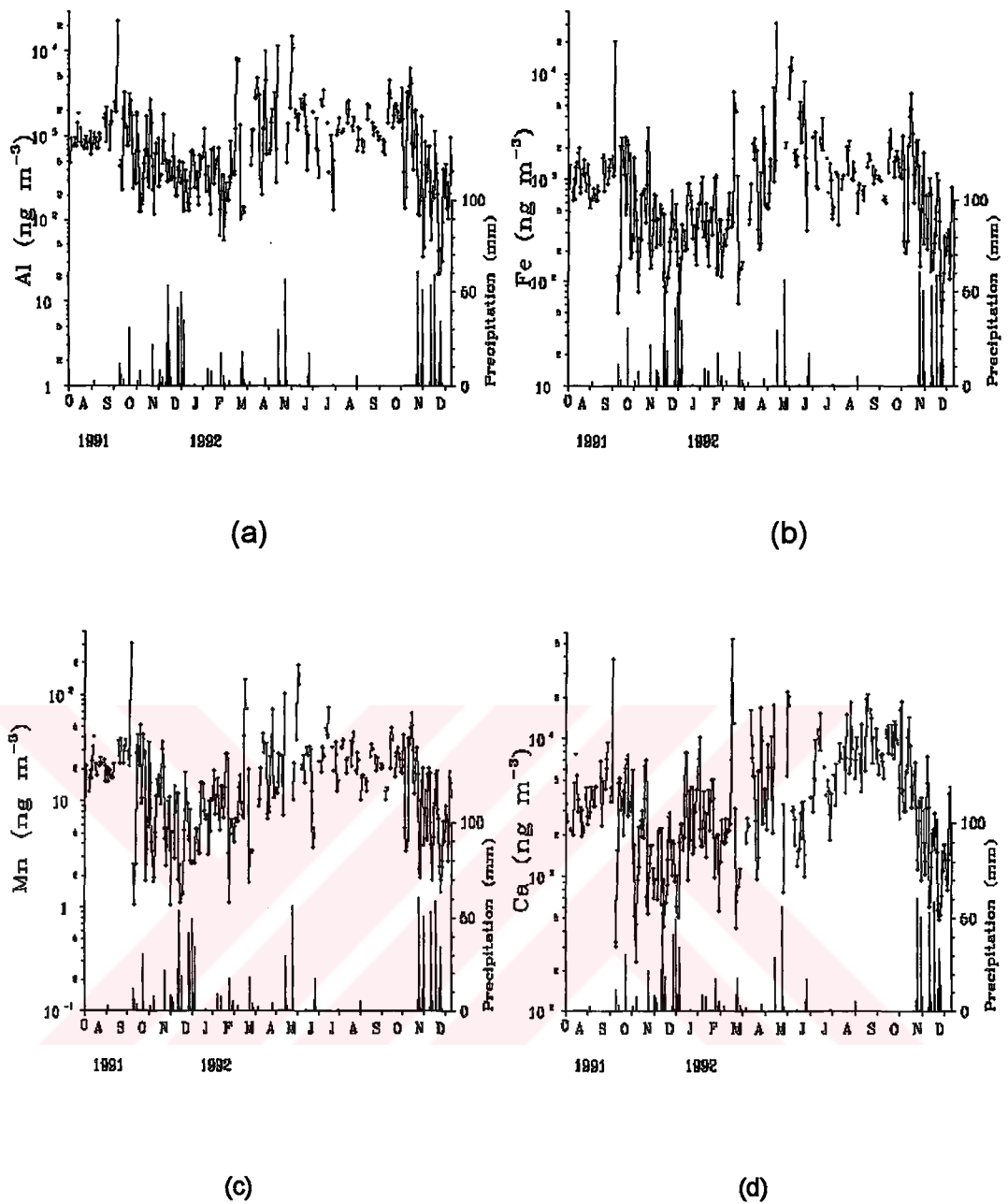
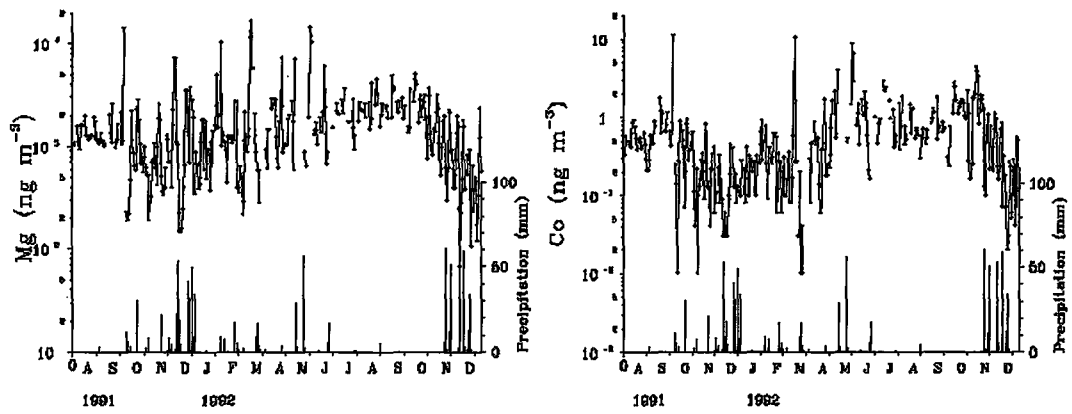


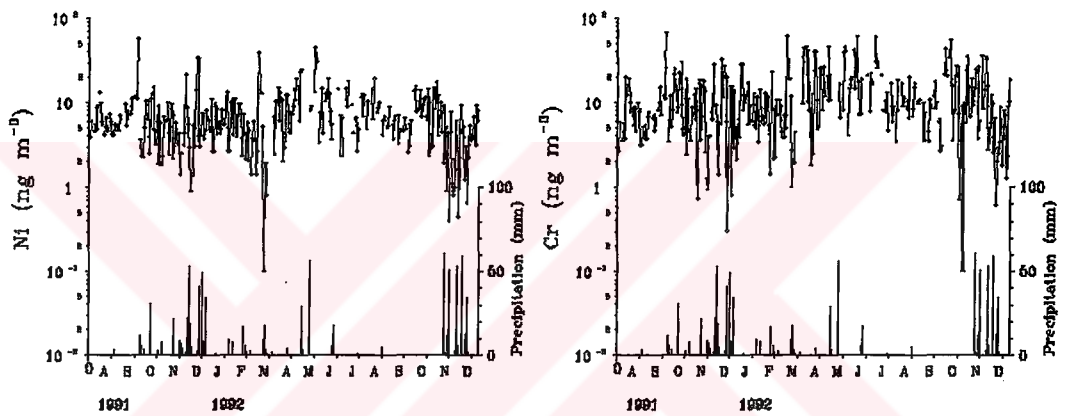
Figure 3.8. Variations in aerosol metal concentrations during August 1991-December 1992 at the Erdemli site, illustrating the large-scale short-term variability. Local daily precipitation amounts are indicated at the bottom.

(a) Al; (b) Fe; (c) Mn; (d) Ca; (e) Mg; (f) Co; (g) Ni; (h) Cr; (i) V; (j) Pb; (k) Cd
 (l) Zn; (m) Na



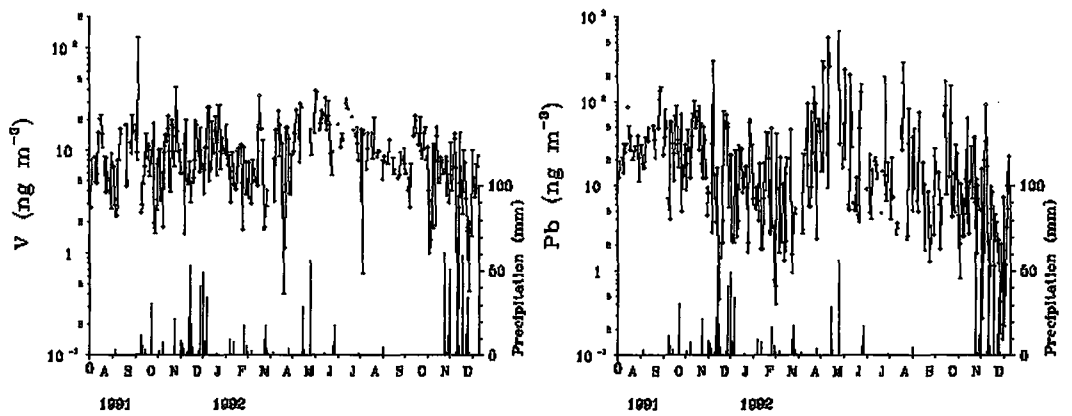
(e)

(f)



(g)

(h)



(i)

(j)

Fig.3.8. Cont.

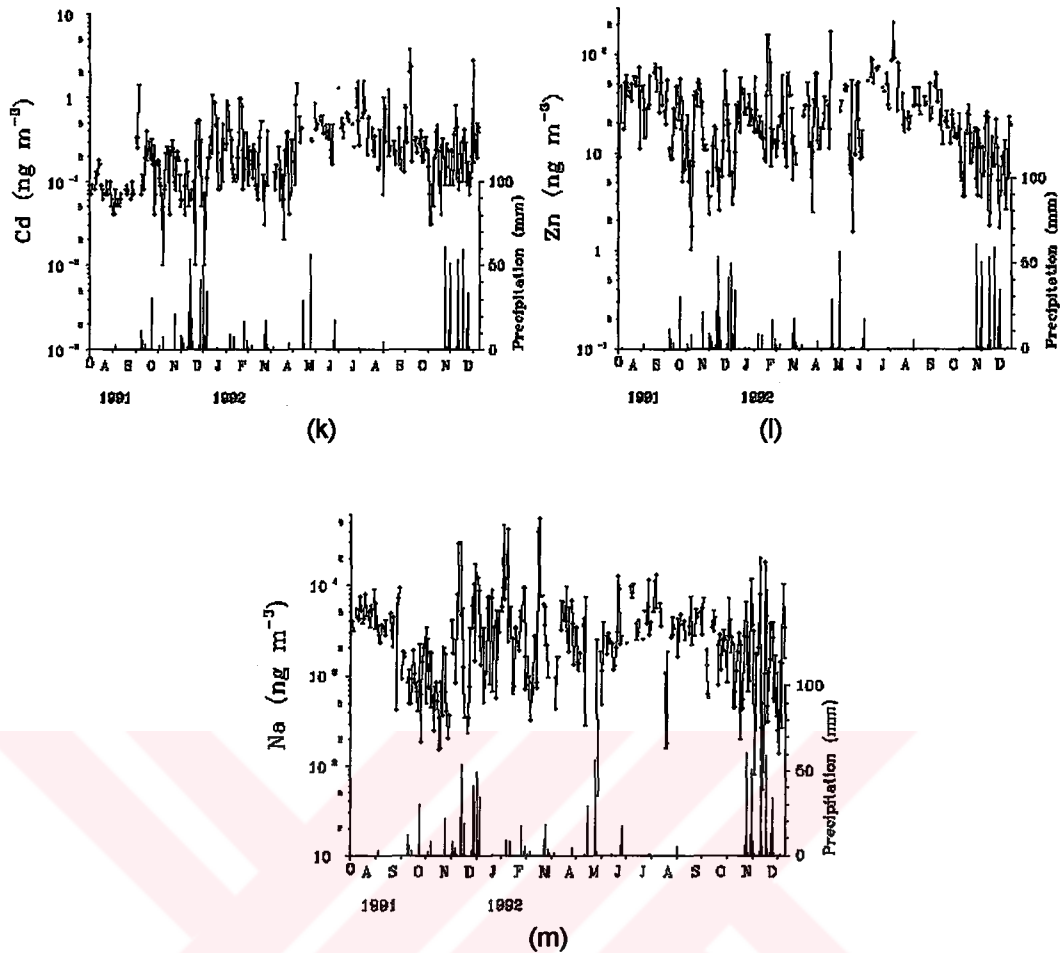


Fig.3.8. Cont.

3.3. The Variations in the Atmospheric Concentrations of the Elements and Air Mass Back Trajectories

3.3.1. African Dust Reaching the Eastern Mediterranean: A Case Study to Verify Trajectory Calculations

The precipitation experienced on 29 March 1992 at the sampling site exhibited typical characteristics of Saharan. This sample was a pronounced outlier so far as its abnormal pH and particulate aluminum concentration was concerned. The appearance of the particulate material was also unusual, being distinctly reddish.

By way of illustration Figure 3.9. shows the back trajectories for 27 March 1992 derived from the data shown in Table A2 in Appendix. The vertical motions of the air parcels in a pressure-time diagram is given in the right hand site of Figure 3.9. The slopes of these curves provide information as to the meteorological conditions prevailing during the atmospheric transport (Martin et al., 1987). One observes that the trajectories arriving at 850 hPa on 27 March 1992 started from elevated sources - which represent an anticyclonic situation - and the trajectories arriving at 900, 700 and 500 hPa started from a low level source representing cyclonic movements at these levels.

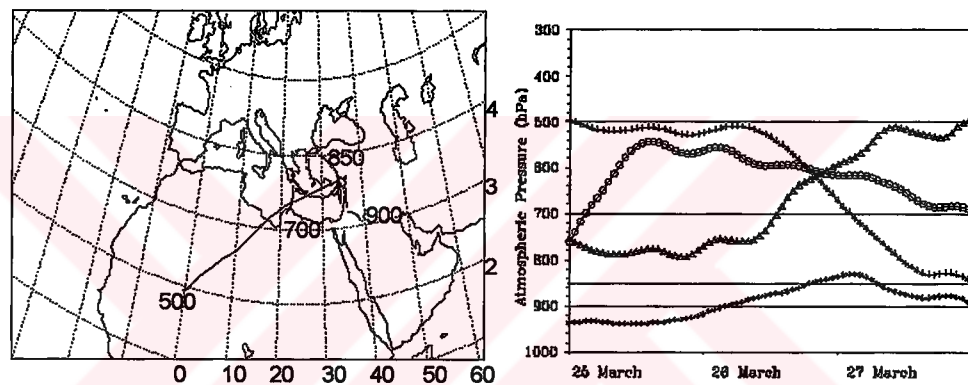


Figure 3.9. 3-D, three days backward air mass trajectories arriving at Erdemli, at 900, 850, 700 and 500 hPa barometric pressure levels, at 12 00 UT on 27 March 1992. The pressure profile is shown at right hand side of the figure.

Since the trajectories provide only qualitative information about atmospheric transport and their validity has sometimes been challenged they should be complemented by measurements of ground-truth. Unfortunately there is no aerosol sample for this event. Due to technical difficulties with the sampling pump beginning from 24th of March till the end of the month aerosol sampling at ground level was discontinued. The only ground-truth observation of this event is the rainwater collected on 29 March

1992. The pH of the rainwater was 7.8 and the concentration of Al (indicator of wind eroded aluminosilicate minerals in atmospheric samples) measured in the particulate of this precipitation was $8020 \mu\text{g L}^{-1}$. These values are higher than the mean pH of the rainwater, 4.93, and the Al concentration in particulates from precipitations, $540 \pm 730 \mu\text{g L}^{-1}$, observed at a land based coastal station (Antalya) 400 km west of Erdemli (Al-Momani, 1995). It has been well documented that precipitations associated with trajectories originating from Saharan desert, both in the western and eastern parts of the Mediterranean, have a high pH due to their high CaCO_3 content (Loye-Pilot et al., 1986; Mamane et al., 1987; Losno et al., 1991).

Thus the alkaline character of the pH and the order of magnitude higher Al concentration in the particulates from the rainwater collected on 29 March (with respect to the mean Al concentration in the particulates sampled by Al-Mamani (1995) at Antalya provide direct geochemical evidence for Saharan dust intrusion and deposition at the Erdemli site.

Meteosat vis images of March 25 to 31 are displayed in Figure 3.10 so as to provide a complete picture of the long-range transport of the atmospheric material over the eastern Mediterranean which originated from North Africa. The clear sky over the sea is in dark blue, clouds are gray or appear with colour dots and dust concentrations increase from light blue to red. Images correspond to 11:30 UT except when indicated (14:30 on the 25th of March). On 25 and 26 of March there was no dust at the Erdemli site and visual inspection of the trajectories for these days indicated trajectories with a N-W origin. On 27 of March the horizontal trajectories of air masses arriving at 900 and 500 hPa together with their vertical movements (see Fig.3.9) show cyclonic movements from North Africa and the Middle East.

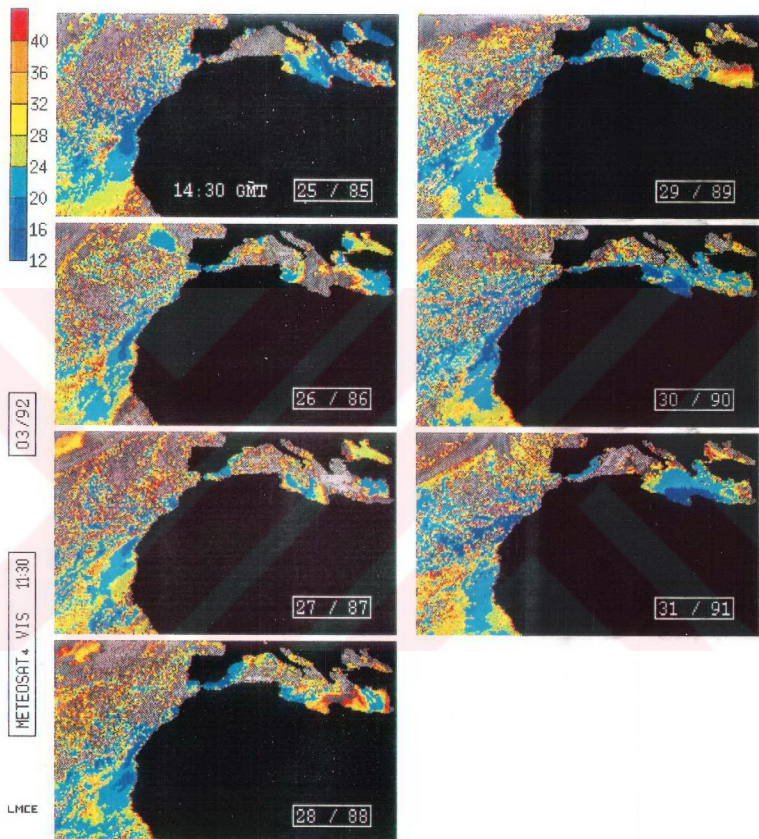


Figure 3.10. A sequence of METEOSAT vis images from 25 to 31 March 1992.

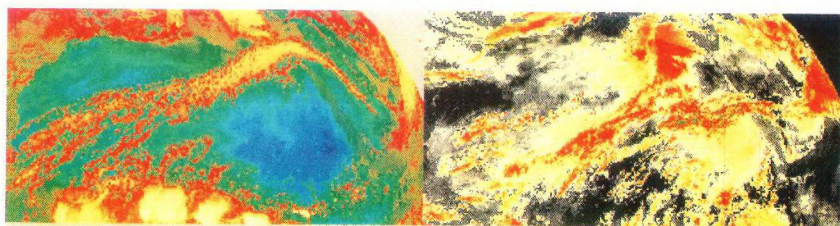
On 28 of March the red colour over the Israeli coast and over a south-north flank from the coast of Libya to Turkey clearly verified that dust was being transported to the Mediterranean both from the Middle East and from the North African deserts

The red colour on 29 of March over the southern coast of Turkey clearly indicates the existence of desert dust in the atmosphere. The transit time of this dust intrusion from North Africa to the sampling coordinates was 2 days.

On the night of 29 March it rained and washed out the atmosphere, thereby lowering the dust load as can be seen from the colors of the images corresponding to the 30 and 31 of March.

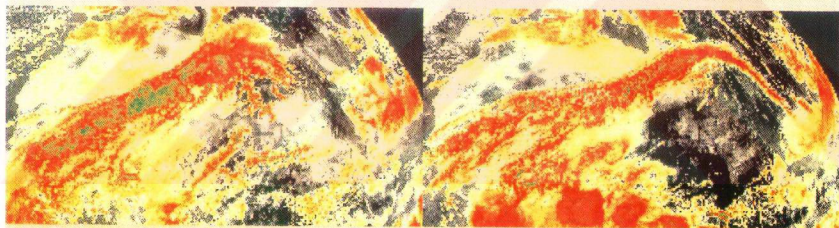
The METEOSAT IR images of 24, 26 and 27 March 1992 shown in Figure 3.11 clearly verify the existence of dust over North Africa and the Middle East. The figure labeled as "ORIGIN" for 27 March represents the original IR image, whereas the figure labeled as "DIF" represents the difference of the original images from a reference image which is supposed to be clean of any dust or water cloud. Dust in the "DIF" images is constituted as smooth yellow unstructured patches, while the reddish structures - which can also be seen on the original image - are clouds. Clear and clean areas appear black, they are apparently associated with anticyclonic airmasses.

Thus, this specific transport of African dust to the sampling zone has been documented and examined more thoroughly using satellite imagery, air-mass back trajectories and surface observations. The correspondence between the results of the different techniques has revealed that trajectory analysis offers opportunities to researchers who need accurate identification of the source regions of the long-range transport of atmospheric material.



ORIGIN 27/03/92

IR DIF 24/03/92



IR DIF 26/03/92

IR DIF 27/03/92

Figure 3.11. A sequence of METEOSAT IR images from 25 to 31 March 1992.

3.3.2. Atmospheric Concentrations of the Elements and the Corresponding Air Mass Back Trajectories

3.3.2.1. Case Studies

The principal finding to emerge from the earlier studies is that the variability of the elemental concentrations in the Mediterranean atmosphere depends on the origin of the air masses arriving at the sampling zone, on source strengths and on precipitation scavenging (Chester et al., 1984; Dulac et al., 1987; Guerzoni et al., 1989; Bergametti et al., 1989b and Chester et al., 1990c). To assess the atmospheric transport of aerosols from their source areas, 3-D air mass back trajectories corresponding to each sample were classified according to the method explained in Section 3.1.1 and are presented in Table A3 in Appendix as their corresponding codes together with elemental concentrations and the amount of daily precipitation rates. By examining the pressure-time diagram of each trajectory the prevailing air flow type was expressed as cyclonic (C), anticyclonic (A) or isobaric (I) and included in the tables.

Dulac et al. (1987) also used 3-D air-mass trajectories to identify source regions for atmospheric particles over the western Mediterranean. The vertical dimension is particularly useful in determining when the air-mass traveled in the boundary-layer where pollutants are predominantly emitted. Further, for several cases of transport, Maring et al. (1987) assessed the influence of the different source regions on Pb inputs, using stable lead isotope analysis and 3-D air-mass trajectories.

The following paragraphs examine the bulk data obtained in October, 1991 and in April, 1992 together with the relevant back-trajectory information in order to illustrate the relative influence of local precipitation and airflow patterns on the daily fluctuations of the atmospheric concentrations of the elements over the eastern Mediterranean. A first glance at the data of both months (see Tables A3.3 and A3.9 in Appendix)

suggests that washout by local rains diminished atmospheric concentrations at the sampling site.

Figure 3.12 classifies the air mass back trajectories at four different barometric levels for October 1991 according to the geographical sectors discussed in Section 3.1.1. In the lower layers of the atmosphere (900 and 850 hPa) air flowed from all four directions but at higher levels (700 and 500 hPa) air flow was confined to the north west and south west directions.

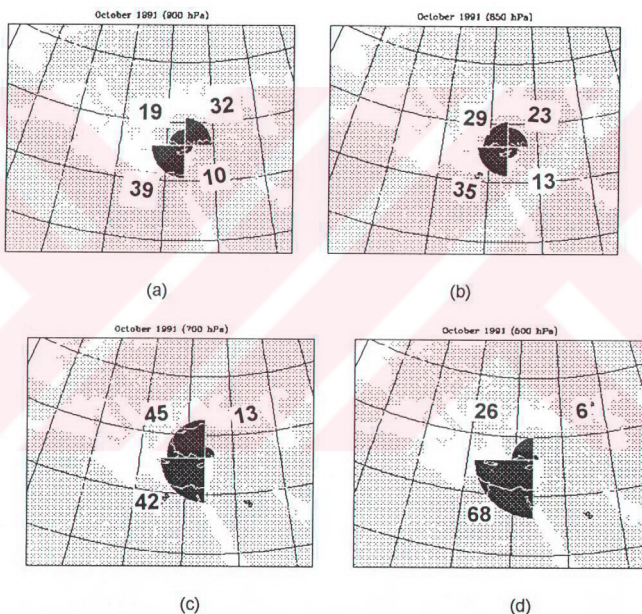


Figure 3.12. The percentage of mean air flow direction at various atmospheric pressure levels during October 1991.

(a) 900 hPa; (b) 850 hPa; (c) 700 hPa; (d) 500 hPa

On 1-2 October the air mass back trajectories at all four levels demonstrate short range continental transport from the north-east (Fig.3.13 presents air mass back trajectories on 2 Oct. and the associated vertical movement of air masses). The permanent downflow of the air masses from their source area to the receptor point and the shortness of the trajectories reveals that the prevailing weather was governed by a regional cell of high pressure. The aridity of the sampling region throughout the three months prior to October (i.e. during July, August and September) implies that dry fallout of the aerosols can have been the only loss mechanism from the atmosphere. Consequently the average elemental composition of the samples collected on Oct.1 and 2 (samples 1 and 2) (also shown in Fig.3.13) is the best approximation to the local averaged elemental concentrations over the previous three months.

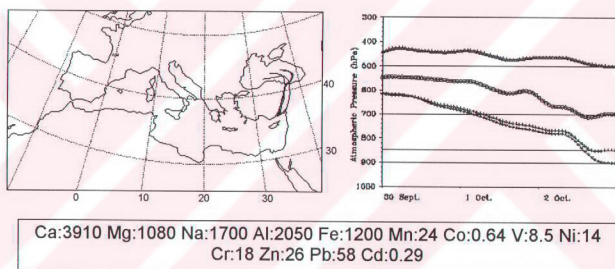


Figure 3.13. Air mass back trajectories arriving at Erdemli at 900, 850, 700 and 500 hPa barometric levels on 2 October 1991. The right hand panel illustrates associated vertical motions of the trajectories (conc. in ng m^{-3}).

The sample collected on 3 of October (sample no. 3) possessed larger elemental concentrations than the average concentrations of samples 1 and 2- by one order of magnitude for the elements Ca, Mg, Al, Fe, Mn and Cd and by two orders of magnitude for the elements V and Co. The observed increases in the concentrations of Ni, Cr and Zn were relatively

low and there was no change in the Pb and Na concentrations. The high concentrations of Cd, usually considered an anthropogenic element, in the crust dominated aerosols from the Sahara desert have also been noted in previous studies of samples collected in the western and the central Mediterranean (Chester et al., 1981; 1984; Dulac et al., 1987; Guerzoni et al., 1989; Tomadin et al., 1989). Dulac et al. (1987) considered that crust-dominated aerosol become enriched with respect to Cd in consequence of the anthropogenic pollution from Zn-Cd metallurgy in North African countries and the production of Cd-containing fertilizers in North Tunisia. Guerzoni et al. (1987), on the other hand, attributed the high concentration of Cd in samples originating from the Sahara to the characteristics of calcite-enriched rock or soil exposed to weathering processes. They explained that part of the Cd enrichment in these samples was the result of Cd association with the calcite minerals.

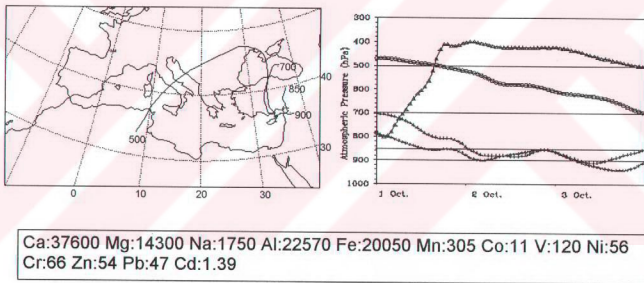


Figure 3.14. Air mass back trajectories arriving at Erdemli at 900, 850, 700 and 500 hPa barometric levels on 3 October 1991. The right hand panel illustrates associated vertical motions of the trajectories (conc. in ng m^{-3}).

The air mass back trajectories for the 3 October showed short range downflowing transport from the S-E and N-E directions, indicating the predominance of the previous days high pressure system at lower barometric levels. On 3 October the air parcel arriving at the sampling point

at 500 hPa originated at 800 hPa over Tunisia three days before (on 1 October) and experienced a mean continuous and upward movement over the lower layer air masses (Fig.3.14). Consideration of the vertical dimension in the three dimensional air mass trajectories, together with the abrupt change seen in the elemental concentrations, reveals that either the intense cyclogenetic activity over Tunisia or the high pressure system in the lower layer of the atmosphere from the Syria-Iraq region caused an uplift of crustal material (dust) into the atmosphere which was then transported to the sampling site by the prevailing wind systems.

To clarify which of the sources (Middle East or North Africa) were active during the time of the sampling, METEOSAT thermal infrared pictures were obtained. They are constituted of a 12 UT thermal infrared original (or primary) image from METOSAT, an "ORIGIN+date", which supplies the minimum geographic information and a time series of three successive, processed, difference images, "IR DIF+date", the last being the observation of the dust at the site where the aerosols were sampled. Dust is shown as smooth yellow unstructured patches, while the reddish structures- that can also be seen on the original image- are clouds. Clear and clean areas appear black, they are apparently associated with anticyclonic air masses (over the northeastern and eastern Sahara) (see Fig.3.15). As can be seen from these satellite images, dust is associated with the clouds in the atmosphere both over Tunisia and over Iran-Iraq. Since the trajectories of the sample collected on 3 October show these two desert regions at different levels, it is not possible to identify a unique source region for the corresponding sample.

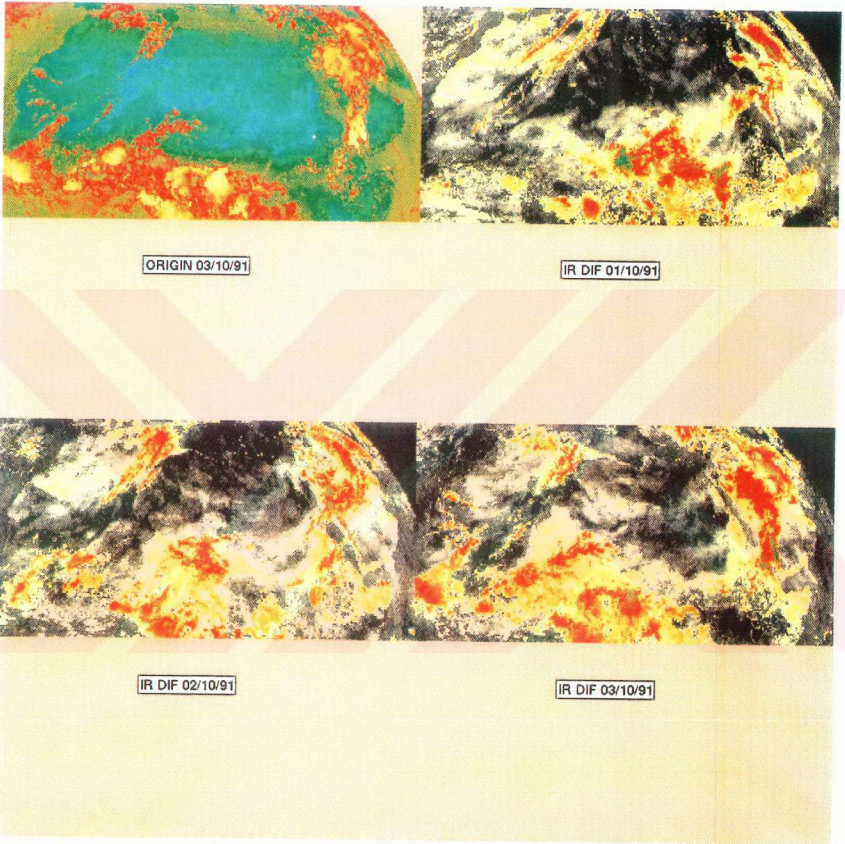


Figure 3.15. A sequence of METEOSAT IR images during 1-3 October 1991.

Local precipitation observed on 4, 5 and 6 October washed-out the dust from the atmosphere. On 7-8 October the air masses at all four levels had their origins over the Mediterranean Sea (short range maritime air masses from the S-W direction) and the weather was subjected to a regional marine low pressure system as may be deduced from the ascending vertical motions of the air masses (Fig.3.16 presents the situation for 8 October 1991 and the average elemental concentrations of the samples collected on 7 and 8 Oct.). As a result, the precipitation, together with the change in airflow direction, decreased the elemental concentrations to low levels.

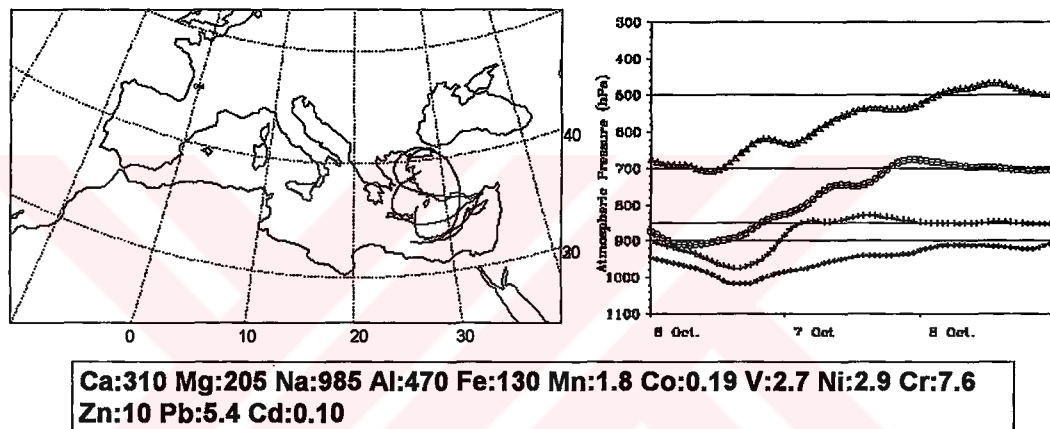
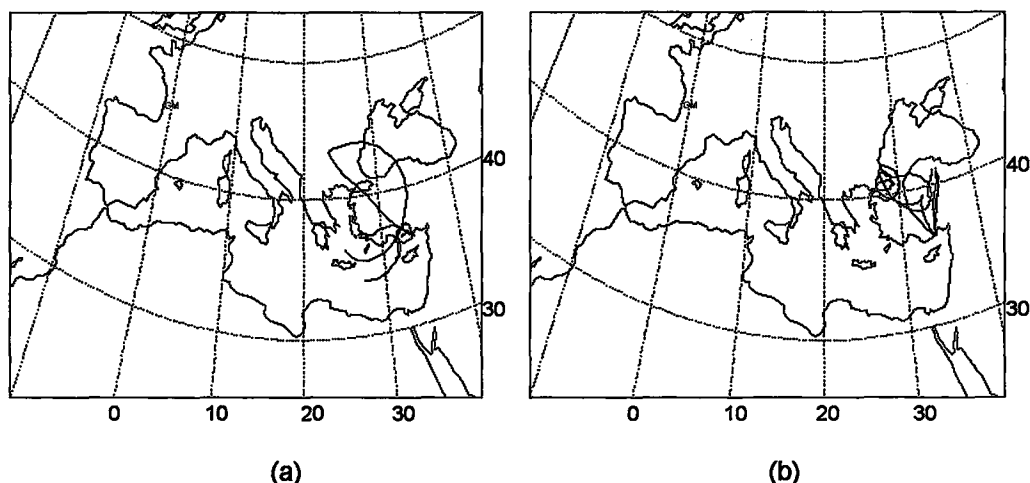


Figure 3.16. Air mass back trajectories arriving at Erdemli at 900, 850, 700 and 500 hPa barometric levels on 8 October 1991. The right hand panel illustrates associated vertical motions of the trajectories (conc. in ng m^{-3}).

Sample 6 was a composite of two days collection (Oct.9 and Oct.10). Since the air mass back trajectories of Oct.9 and Oct.10 arrived at the sampling site both from the local Mediterranean and from the inner part of Anatolia (see Fig.3.17), it is difficult to assign a sample to a specific region when sampling had a duration of more than one day. Hence, utilization of the relatively featureless mean climatological flow pattern to explain change in atmospheric concentrations due to air mass history is uninformative when compared to a typical daily flow pattern such as that depicted in Figure 3.17.

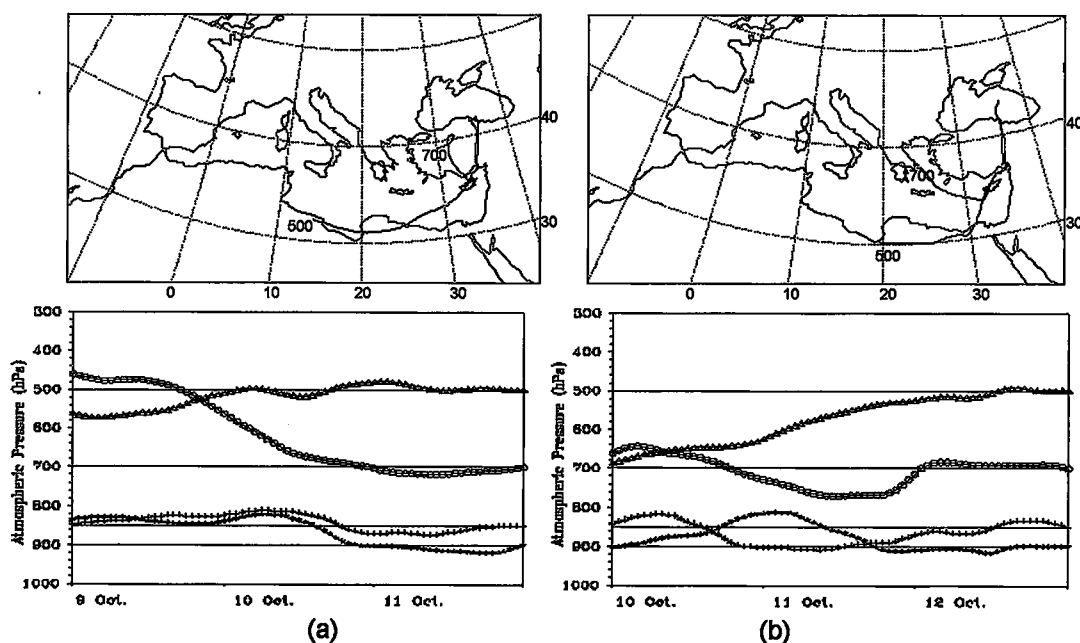


Ca:1535 Mg:215 Na:480 Al:230 Fe:135 Mn:2.5 Co:0.01 V:4.6 Ni:2.2 Cr:5 Zn:8.6 Pb:55 Cd:0.08
--

Figure 3.17. Air mass back trajectories arriving at Erdemli at 900, 850, 700 and 500 hPa barometric levels.

(a) 9 October 1991 (b) 10 October 1991

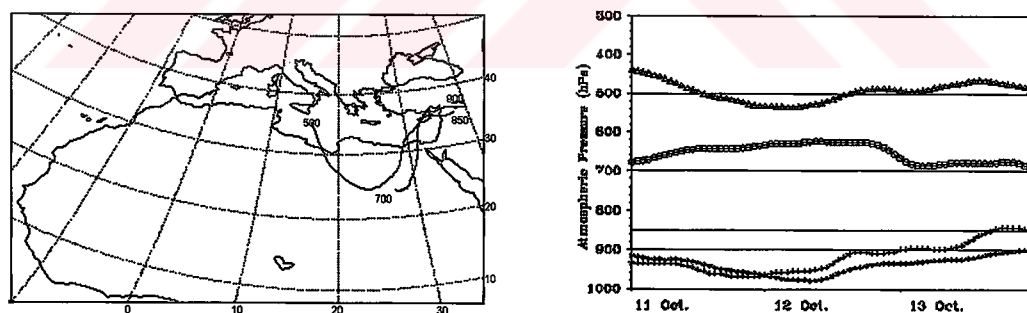
On 11 and 12 Oct. the air mass back trajectories at each different barometric level evolve from similar origins. As can be seen from the bottom panels of Figure 3.18, the air parcels at 500 hPa arrive at Erdemli in a gradually ascending order which can be attributed to cyclogenesis over Libya bearing dust and thereby increasing the elemental concentrations within the aerosol. Peak elemental concentrations associated with the event initiated on 11 Oct. were observed on 13 Oct. (sample no 8). This suggests that additional transport of material from the east (Middle East) resulted in cyclonic transport within the boundary layer of the atmosphere (see Fig.3.19).



Ca:4700 Mg:470 Na:900 Al:1540 Fe:2060 Mn:28 Co:0.27 V:6.8 Ni:4.9 Cr:8.1
Zn:28 Pb:31 Cd:0.19

Figure 3.18. Air mass back trajectories arriving at Erdemli at 900, 850, 700 and 500 hPa barometric. The bottom panels illustrate associated vertical motions of the trajectories.

(a) 11 October 1991; (b) 12 October 1991



Ca:5115 Mg:2170 Na:1875 Al:3215 Fe:2475 Mn:41 Co:0.88 V:14 Ni:10 Cr:21
Zn:22 Pb:24 Cd:0.40

Figure 3.19. Air mass back trajectories arriving at Erdemli at 900, 850, 700 and 500 hPa barometric levels on 13 October 1991. The right hand panel illustrates associated vertical motions of the trajectories (conc. in ng m^{-3}).

From 17th up to 23rd of October short range transport from the local sea or land at 900 hPa was accompanied by long range transport of continental material by 500 hPa trajectories passing over Africa or the north-west region (see Fig.3.20). Indeed, the character of the 500 hPa trajectories persisted until 28th of October but from 24-28th October local transport at 900 hPa was superseded by long range transport of air masses originating mainly over the sea (Fig.3.21).

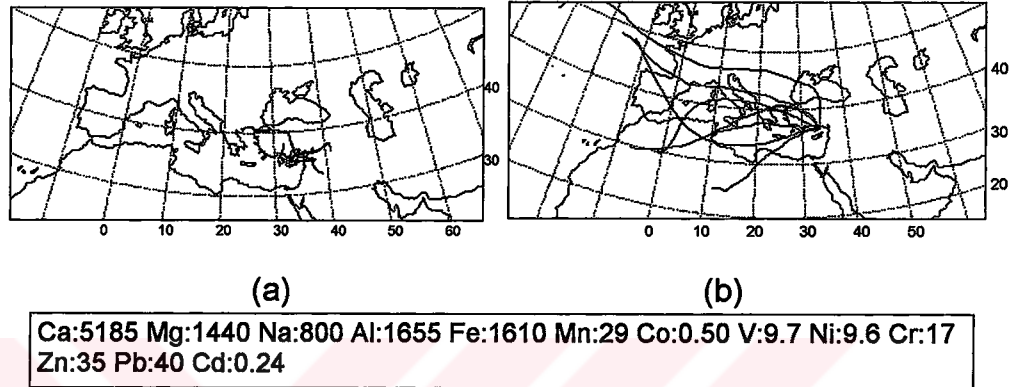


Figure 3.20. Air mass back trajectories arriving at Erdemli during 17-23 October 1991 (conc. in ng m^{-3}).
(a) 900 hPa; (b) 500 hPa

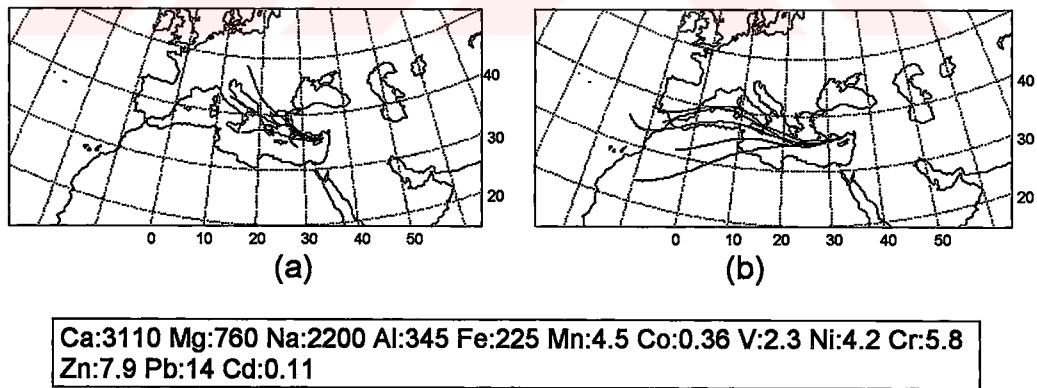
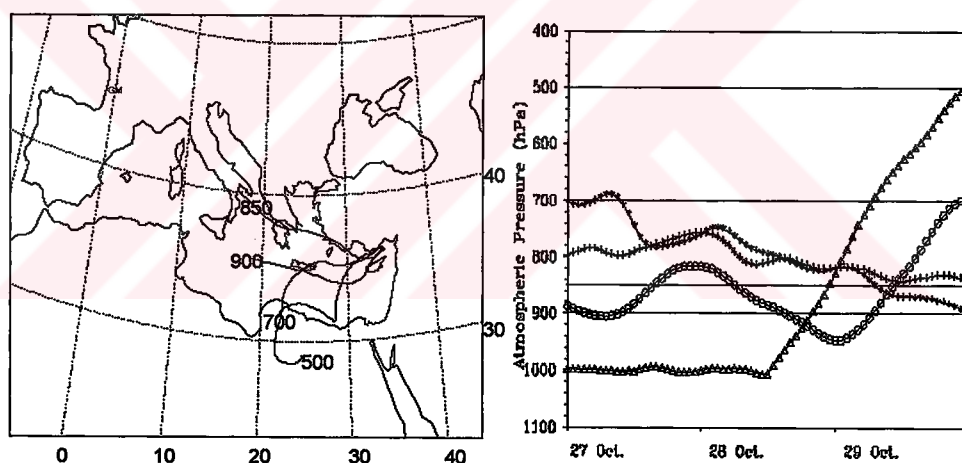


Figure 3.21. Air mass back trajectories arriving at Erdemli during 24-28 October 1991 (conc. in ng m^{-3}).
(a) 900 hPa; (b) 500 hPa

On 29th October the concentrations of the elements V, Co, Al, Fe, Mn, Cr and Pb increased between 2 and 8 fold and the air parcel arriving at 500 hPa passed over Libya at ground level (see Fig.3.22) where dust was lifted and made available for long range transport in the upper levels. The ascending character of the air masses arriving at 700 and 500 hPa and the descending character of those arriving at 900 and 850 hPa during their last day of travel, induced frontal mixing which may have enhanced the dispersion of material from the upper to the lower atmospheric levels. These phenomena resulted in episodic increase in the elemental concentrations. Since the air mass trajectories of October 30 and 31 were similar to those of October 29, the observed decrease in the elemental concentrations must have arisen from washout by local rainfall probably induced by the frontal mixing of the air masses.



Ca:3470 Mg:990 Na:500 Al:1820 Fe:1600 Mn:35 Co:0.60 V:7.2 Ni:5.9 Cr:11
Zn:17 Pb:30 Cd:0.18

Figure 3.22. Air mass back trajectories arriving at Erdemli at 900, 850, 700 and 500 hPa barometric levels on 29 October 1991. The right hand panel illustrates associated vertical motions of the trajectories (conc. in ng m^{-3}).

The patterns of the airflow in April, 1992 are presented in Figure 3.23. It will be seen that flows from the north-west and south-west directions were dominant.

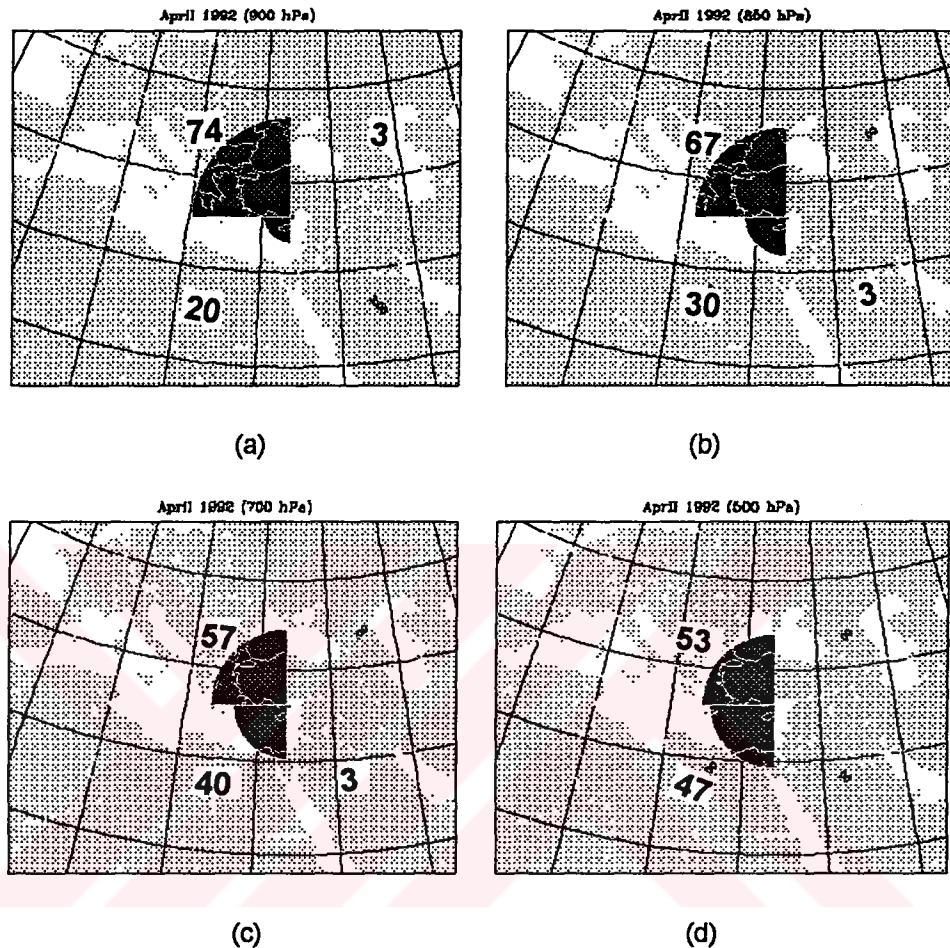


Figure 3.23. The percentage of mean air flow direction at various atmospheric pressure levels during April 1992.

(a) 900 hPa; (b) 850 hPa; (c) 700 hPa; (d) 500 hPa

Although only one local precipitation was recorded during April, 1992, the atmospheric concentrations of the elements at the sampling site show abrupt changes (see Table A9). Accordingly, these changes must be attributed to changes in the airflow patterns rather than the precipitation scavenging of the local atmosphere. It is necessary to emphasize here that a trajectory of a sample gives no indication of any precipitation that the air

may have encountered during its transport and, consequently, one has been able to consider the washout of atmospheric particles only by local rainfall. The probability of decrease in elemental concentrations in aerosols throughout their atmospheric transport has also been mentioned by Dulac et al. (1987) when studying the variability of the elemental concentrations in aerosols over the western Mediterranean. These authors pointed out also that even the grid size of the synoptic scale meteorological charts (200 km) is insufficient to permit consideration of local rain that might have be influenced the air masses during their transport.

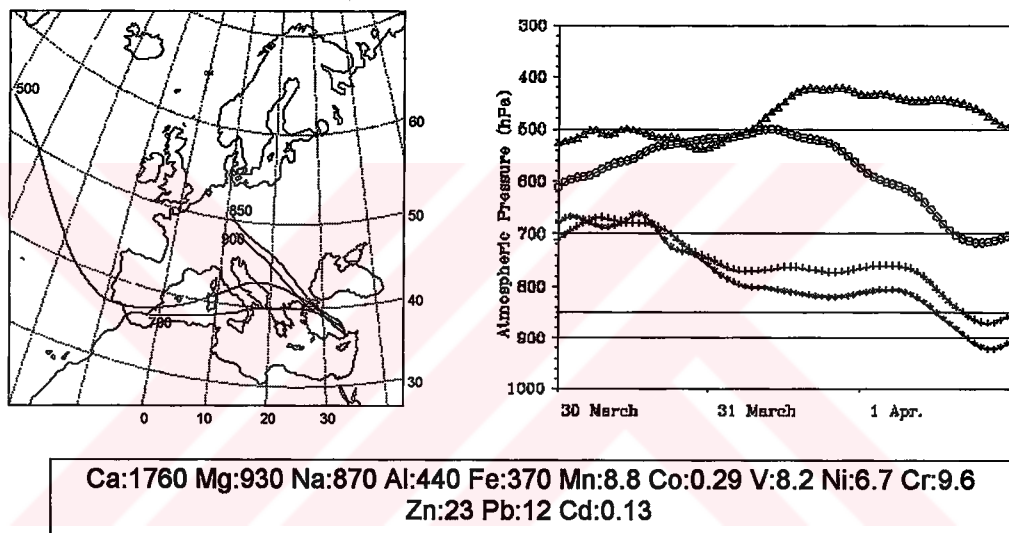
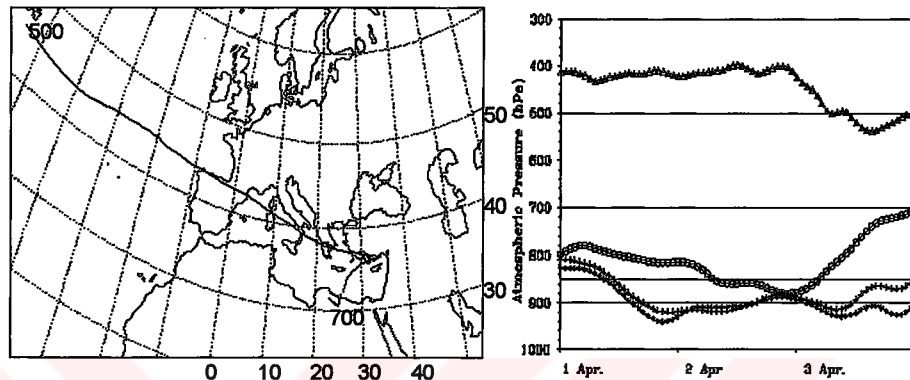


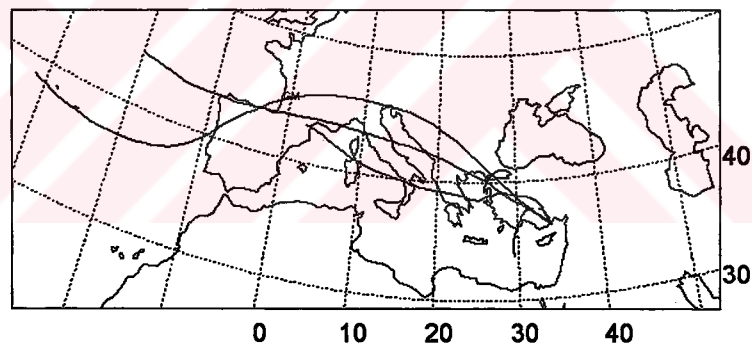
Figure 3.24. Air mass back trajectories arriving at Erdemli at 900, 850, 700 and 500 hPa barometric levels on 1 April 1992. The right hand panel illustrates associated vertical motions of the trajectories (conc. in ng m^{-3}).

The back trajectories for 1 April show that the air masses at each level underwent long range and descending transport (see Fig.3.24). Thus, the corresponding elemental concentrations observed at the sampling site and given in the same figure may be ascribed to the concentrations that persist from the European continent. Since the air masses had been transported within the upper troposphere, the influence of anthropogenic sources over the continents had been at a minimum throughout the transport

path and thus, for example, the associated Pb concentration, a well known label of anthropogenic activity, was at its minimum value. Although, the back trajectories on 2 April were similar to those of April 1 the air masses arriving at 900 and 850 hPa depict short range transport. The most pronounced difference in the elemental concentrations of the samples collected on April 1 and 2 was the sharp increase in the concentration of Cr in the later sample (see Table A9).



(a)



(b)

Ca:2330 Mg:1440 Na:1400 Al:1155 Fe:905 Mn:20 Co:0.47 V:16 Ni:10 Cr:44 Zn:30 Pb:60 Cd:0.16
--

Figure 3.25. Air mass back trajectories arriving at Erdemli at 900, 850, 700 and 500 hPa barometric. The right hand panel illustrate associated vertical motions of the trajectories (conc. in ng m^{-3}).

(a) 3 April 1992; (b) 4 April 1992

Continuous collection of a single sample throughout the two days of 3 and 4 April makes it difficult to assign the variation in the elemental concentrations to a single source. On 3 April the air parcel arriving at 700 hPa originated over Libya and its vertical movement verifies the existence of cyclonic activity which could enhance the transport of dust by the northeasterly component of the winds to the sampling site. This would induce an increase in the elemental concentrations observed in the particulates collected at the sampling site. In fact, an abrupt increase in concentrations was not observed on April 3 because of the dilution caused by subsequent air masses which arrived from the local sea and from the north-west on 4 April (Fig.3.25).

The concentrations of the elements on 7 April present a sharp increase with respect to samples collected on 1 and 2 April. On 7 April 1992 reduced visibility caused an aviation accident when a passenger plane carrying Yassir Arafat crashed in Libyan territory during a heavy dust storm (Ganor, 1994). The air mass back trajectories along with vertical movements (Fig.3.26) support the existence of a frontal process similar to that observed on April 3 generating dust transport to the sampling site.

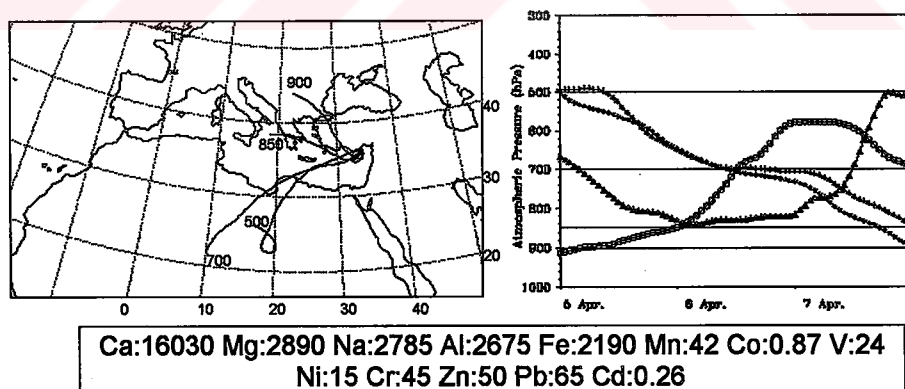
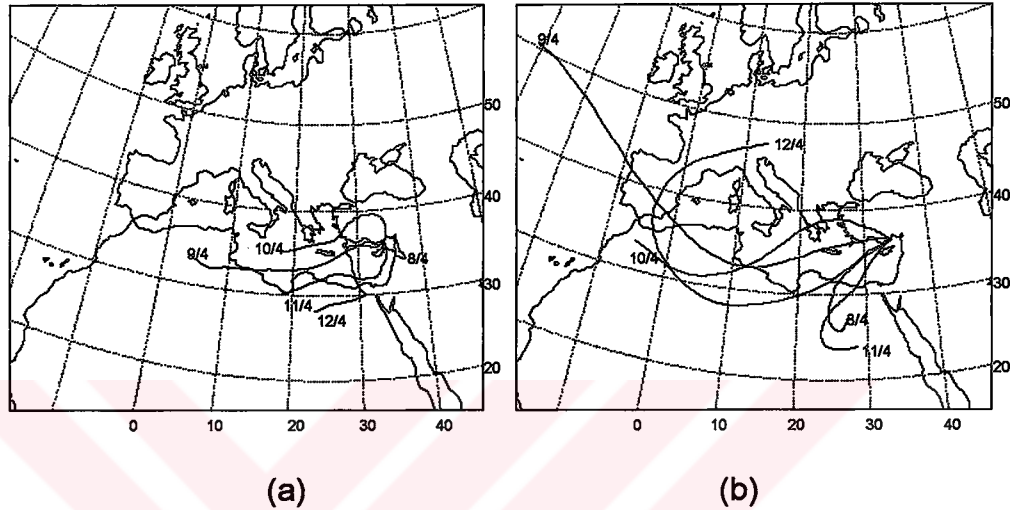


Figure 3.26. Air mass back trajectories arriving at Erdemli at 900, 850, 700 and 500 hPa barometric levels on 7 April 1992. The right hand panel illustrates associated vertical motions of the trajectories (conc. in ng m^{-3}).

This characteristic flow pattern, favorable to African dust transport, persisted until 13 April. The air mass trajectories arriving at 700 and 900 hPa and the concentrations from 8 to 12 April are shown in Figure 3.27.



Ca:7115 Mg:2545 Na:4960 Al:3485 Fe:1960 Mn:32 Co:0.50 V:13 Ni:10 Cr:20 Zn:18 Pb:80 Cd:0.11

Figure 3.27. Air mass back trajectories arriving at Erdemli during 8-12 April 1992 (conc. in ng m^{-3}).

(a) 900 hPa; (b) 500 hPa

The sudden decrease in the concentrations of the all elements - except Na and Pb - on 13 April must, in the absence of wash out by local rain, be ascribed to the change in the direction of all air flows to the Mediterranean (Fig.3.28). The increase in the concentrations of Na and Pb could be due to the transport of air masses arriving at 900 and 850 hPa within the boundary layer during the last day of their travel (see right hand panel of Fig.3.28).

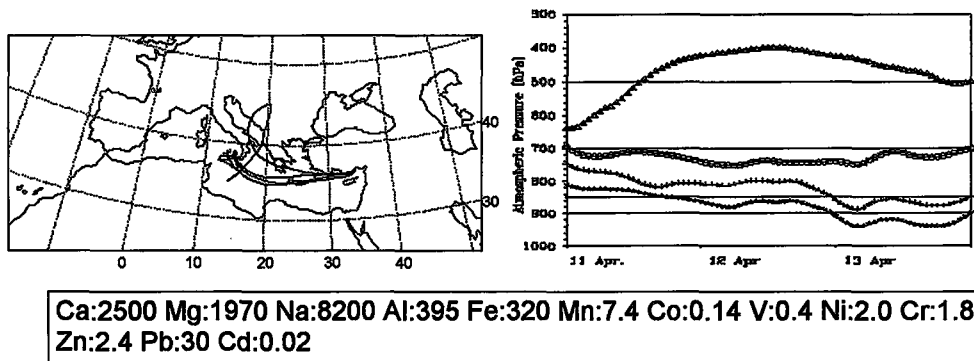


Figure 3.28. Air mass back trajectories arriving at Erdemli at 900, 850, 700 and 500 hPa barometric levels on 13 April 1992. The right hand panel illustrates associated vertical motions of the trajectories (conc. in ng m^{-3}).

The trajectories corresponding to samples collected between 14 and 16 April still possess the characteristics of maritime air. The higher concentration of Pb with respect to the sample collected on 13 April is the result of the boundary layer transport along the coast as displayed in Figure 3.29 for the 14 April.

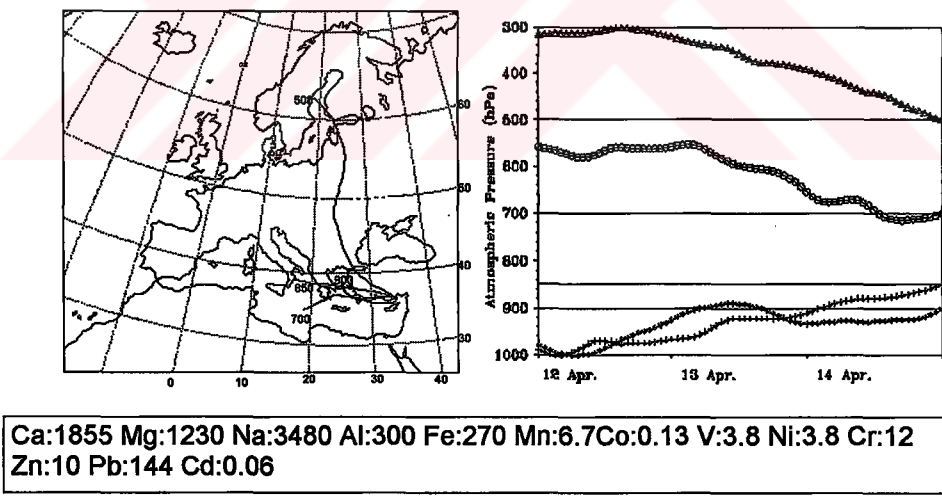


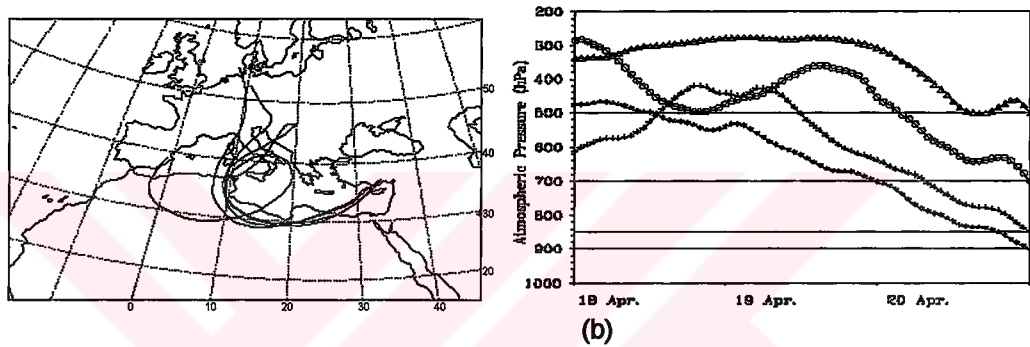
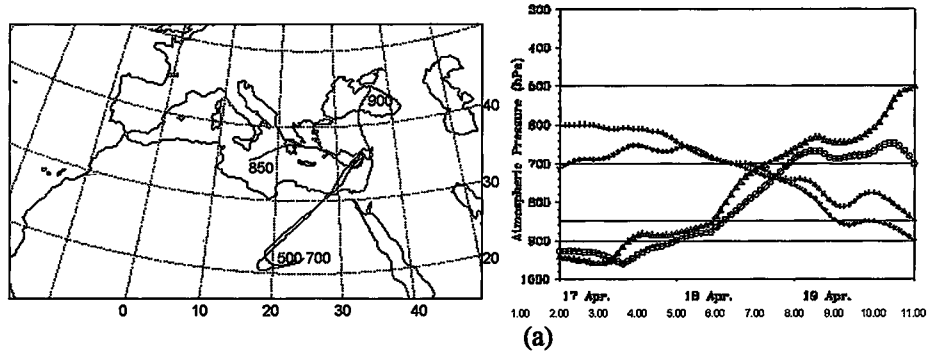
Figure 3.29. Air mass back trajectories arriving at Erdemli at 900, 850, 700 and 500 hPa barometric levels on 14 April 1992. The right hand panel illustrates associated vertical motions of the trajectories (conc. in ng m^{-3}).

On 19 April, (Figure 3.30a) ascending trajectories ending at 700 and 500 hPa transported material from the inner part of North Africa to Erdemli and the subsiding motions of the trajectories ending at 900 and 850 hPa transported material from Anatolia and from over the Mediterranean respectively. These trajectories suggest that the dust layer originating from North Africa was transported between the 700 and 500 hPa levels (at a mean altitude of between 3000 and 5000 m) and the observed frontal process induced strong vertical mixing which permitted the observation of dust at ground level despite its transport at higher levels. Since, the sample collected between 17 and the 19 April was composited the elemental concentrations cannot be used to verify the trajectory calculations on a synoptic scale.

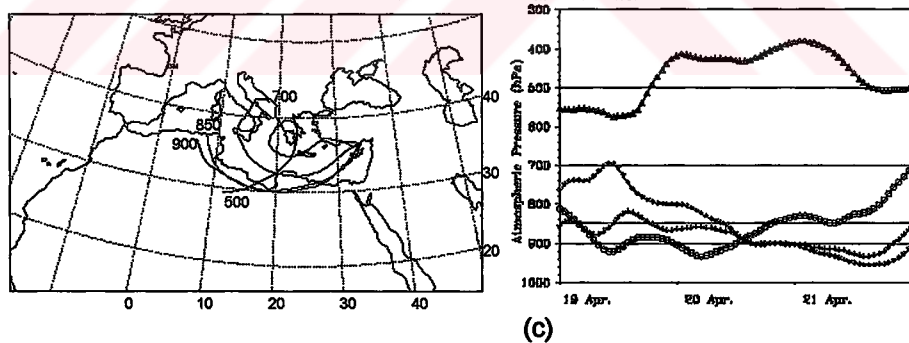
Figure 3.30b shows that on 20 April trajectories originating over western Europe and passed over the African continent before reaching the sampling site. The corresponding vertical motions of the air masses at all levels demonstrate that the long-range transport of the dust in the atmosphere (uplifted by the frontal process observed on 19 April) occurred in the upper atmospheric layer and this inhibited the addition of material from point emission sources on the continents over which the air masses had passed during their travel. Thus the sample collected on 20 April had an elemental composition representative of "pure" north African material as observed at the Erdemli site.

On 21 April air masses were still transported from North Africa at all four levels but the trajectories ending at the 850 and 900 hPa levels spent the last day of their travel within the lower atmosphere (see Fig.3.30c). The elemental composition of the sample collected on 21 April reveals that, except for the elements Pb, Zn and Cd, the concentrations of the elements decreased due, probably, to washout by local rain experienced during the night of 20 April. It is possible to ascribe the peak concentrations of the elements (especially of the one order of magnitude increase in Pb

concentration) observed in this sample to the contribution of local anthropogenic emissions.



Ca:16790 Mg:7310 Na:5885 Al:9860 Fe:4850 Mn:72Co:1.69 V:13 Ni:7.6 Cr:10
Zn:13 Pb:11 Cd:0.04

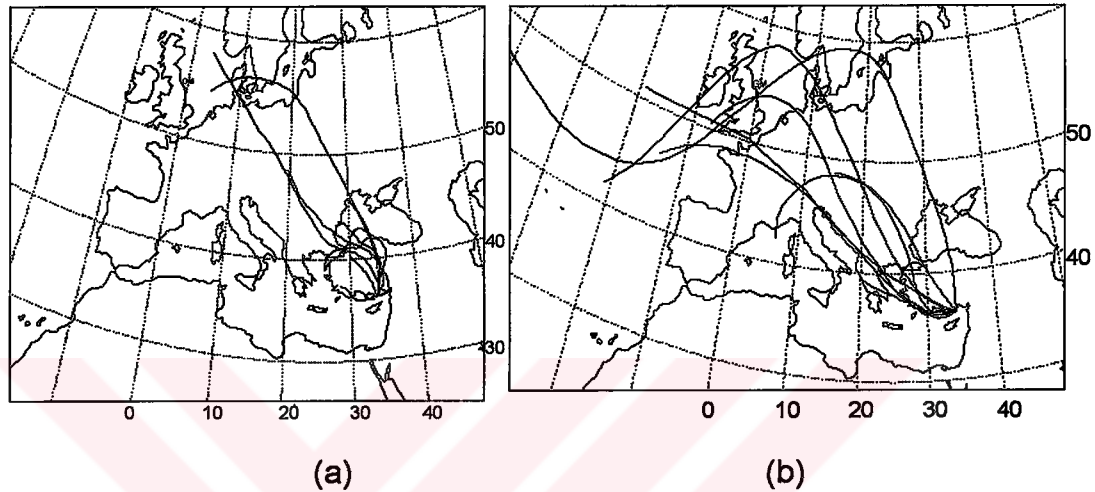


Ca:9465 Mg:2450 Na:3260 Al:4445 Fe:2160 Mn:29Co:0.47 V:6.7 Ni:5.7
Cr:4.8 Zn:15 Pb:106 Cd:0.06

Figure 3.30. Air mass back trajectories arriving at Erdemli at 900, 850, 700 and 500 hPa barometric levels. The right hand panel illustrates associated vertical motions of the trajectories (conc. in ng m^{-3}).

(a) 19 April 1992 (b) 20 April 1992 (c) 21 April 1992

From 22 April till 29 April the air masses arriving at all levels experienced a more steady flow from the north-west. Figure 3.31 depicts the trajectories at 900 and 500 hPa.



Ca:3090 Mg:1000 Na:1610 Al:670 Fe:585 Mn:12 Co:0.25 V:9.3 Ni:8.7 Cr:30 Zn:18 Pb:76 Cd:0.16

Figure 3.31. Air mass back trajectories arriving at Erdemli during 22-29 April 1992 (conc. in ng m^{-3}).

(a) 900 hPa; (b) 500 hPa

The composition of the sample collected on 27 April is the best example of long range transported continental material from the north-west sector. The associated continental trajectories represent an anticyclonic transport generating a permanent down-flow of air (Fig.3.32); that is, the air masses traveled above 900 hPa level or did not travel within the boundary layer.

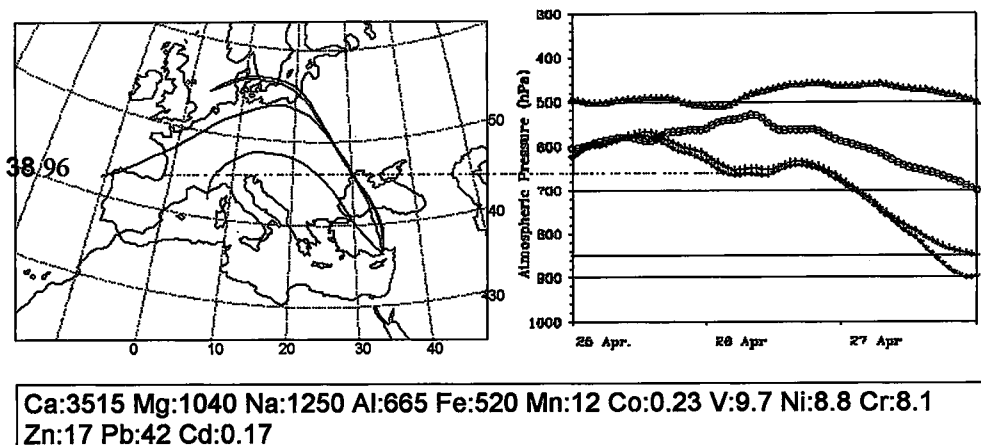


Figure 3.32. Air mass back trajectories arriving at Erdemli at 900, 850, 700 and 500 hPa barometric levels on 27 April 1992. The right hand panel illustrates associated vertical motions of the trajectories (conc. in ng m^{-3}).

On 30 April there was a three fold increase in the concentrations of Al, Fe, Co and a two fold increase in the concentrations of Ca and Mn with respect to the mean concentrations of the period 22-29 April (see Fig.3.33) and this was caused by the cyclonic transport of air masses arriving at 700 hPa from the SE direction.

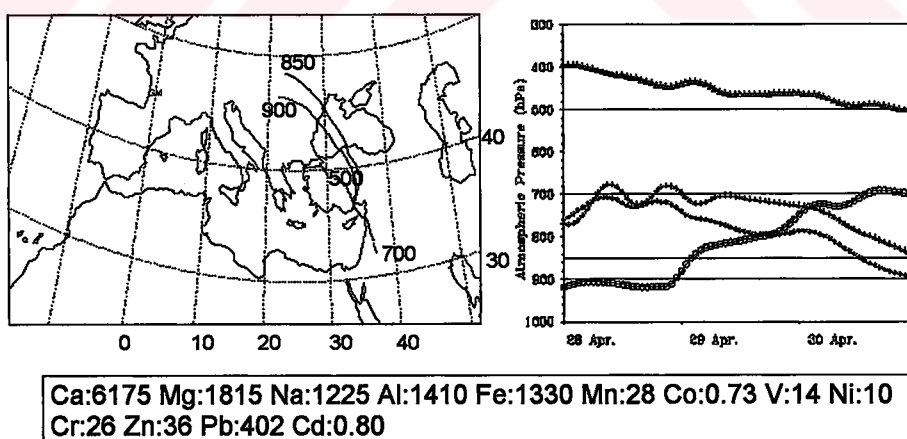


Figure 3.33. Air mass back trajectories arriving at Erdemli at 900, 850, 700 and 500 hPa barometric levels on 30 April 1992. The right hand panel illustrates associated vertical motions of the trajectories (conc. in ng m^{-3}).

An important finding has been the realization that dramatic changes in the direction of the air-mass trajectories over the eastern Mediterranean occur on rather short and unpredictable time scales accompanied by differences in the origins of the arriving air masses at different barometric levels. This sheds light on the extreme variability of the atmospheric concentrations of the elements observed on daily time scale. The vertical dimension of the trajectories is particularly useful in determining the boundary-layer transport of the air-masses where pollutants are predominantly emitted. During times of increased vertical motion, wind eroded crustal material can remain suspended and thus be transported over long distances. However, in a stratified atmosphere typical of stable atmospheric conditions most of the particles are removed by gravitational settling.

Now let us compare the data of October, 1992, with that of October, 1991 so as to demonstrate the interannual variation in the elemental concentrations of the aerosol. Since the sampling schedule started in August, 1991, chemical data for April 1991 is not available. For this reason October 1992 has been selected for an interannual comparison of the geochemical and meteorological data. Since local rain was observed but once in October 1992, the main parameter affecting the variability of the atmospheric concentrations was assumed to be the changes in airflow patterns. As discussed above, to explain the variability of atmospheric concentrations of the elements completely it is mandatory to consider the different levels of the air mass trajectories together with geochemical data. Figure 3.34 classifies the trajectories at each level with respect to geographical sectors for the month of October 1992. The main difference in airflow patterns between October 1991 (see Fig.3.12) and October 1992 is the comparative lack, in the latter month, of trajectories originating in the E-N and S-E. October 1992 was dominated by south-west flow at all levels of the atmosphere.

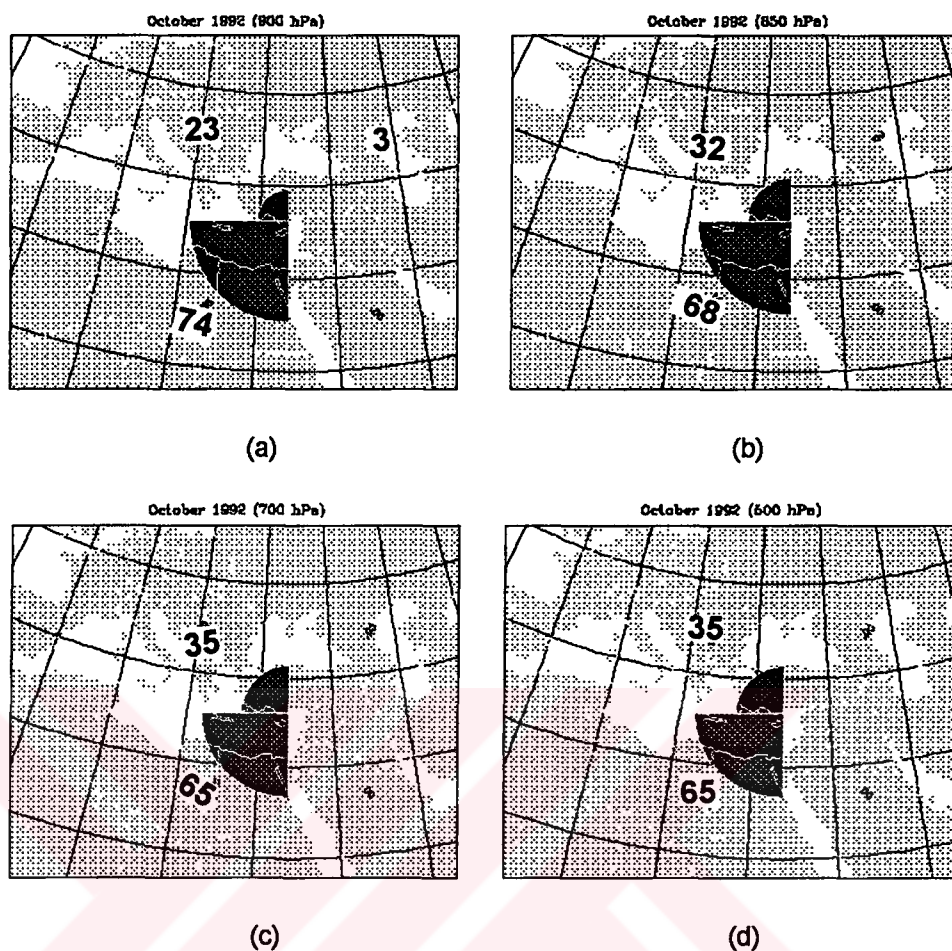
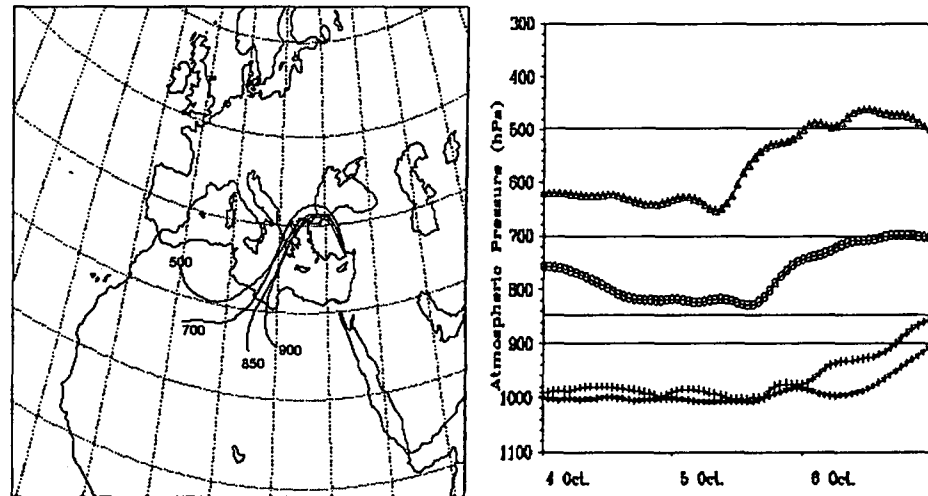


Figure 3.34. The percentage of mean air flow direction at various atmospheric pressure levels during October 1992.

(a) 900 hPa; (b) 850 hPa; (c) 700 hPa; (d) 500 hPa

Between 5-8 October 1992 the long range transport of air masses from North Africa resulted in an increase in the elemental concentrations. The air mass back trajectories on 6 October had their origin over the African continent and continuous upwelling of the air mass lifted dust into the upper troposphere where it was transported to the Erdemli site at 700 hPa (Fig.3.35). The presence of high concentrations of such anthropogenic elements as Pb and Cd in these samples can be attributed to local coastal sources. During the period from 2 to 5 October the air masses arriving at 900 hPa were relatively short, indicative of weak winds generating little

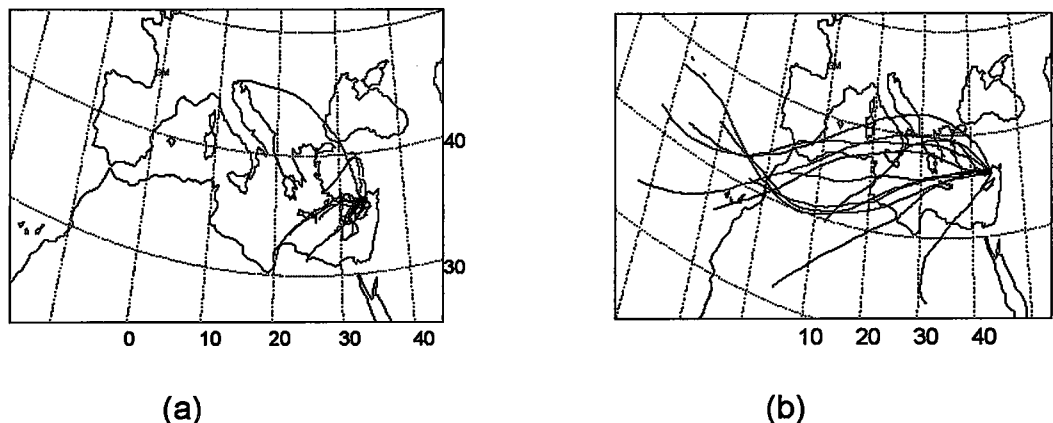
diffusion. Such meteorology favors the accumulation of local anthropogenic emissions in the atmosphere.



Ca: 10185 Mg: 4450 Na: 4425 Al: 3125 Fe: 2265 Mn: 43 Co: 2.7
V: 22 Ni: 14 Cr: 43 Zn: 26 Pb: 160 Cd: 0.33

Figure 3.35. Air mass back trajectories arriving at Erdemli at 900, 850, 700 and 500 hPa barometric levels on 6 October 1992. The right hand panel illustrates associated vertical motions of the trajectories (conc. in ng m^{-3}).

Between 12 and 23 October 1992 the airmasses arriving at Erdemli at 900 hPa traveled mostly over the sea whereas those arriving at 500 hPa originated from North Africa (Fig.3.36). The high mean elemental concentrations throughout this period indicate that the higher level airflow brought desert dust to Erdemli where it was, in fact, sampled. This situation, observed in both October 1991 and 1992, can be described as typical of the mixing of material from local sources with long range transported material. Consequently, the observed concentrations are not representative of "pure" material of African origin.



Ca:9065 Mg:2270 Na:1695 Al:1825 Fe:1405 Mn:24 Co:1.33 V:12 Ni:9.4 Cr:21 Zn:18 Pb:60 Cd:0.26
--

Figure 3.36. Air mass back trajectories arriving at Erdemli during 12–23 October 1992 (conc. in ng m^{-3}).

(a) 900 hPa; (b) 500 hPa

The most representative samples of long range material transported from the S-W and N-W sectors were those collected on 24 and 26 October 1992 respectively. On 24 October, 1992, trajectories arriving at four different levels originated from north Africa where they underwent continuous upwelling (see Fig.3.37). Although the air masses arriving at Erdemli at 850 and 900 hPa were at ground level over the African continent, the concentration of such anthropogenic tracers as Pb, Zn and Cd was lower than might have been expected. This is consistent with the dilution of the concentrations in the continental air masses by air masses from the open Mediterranean sea.

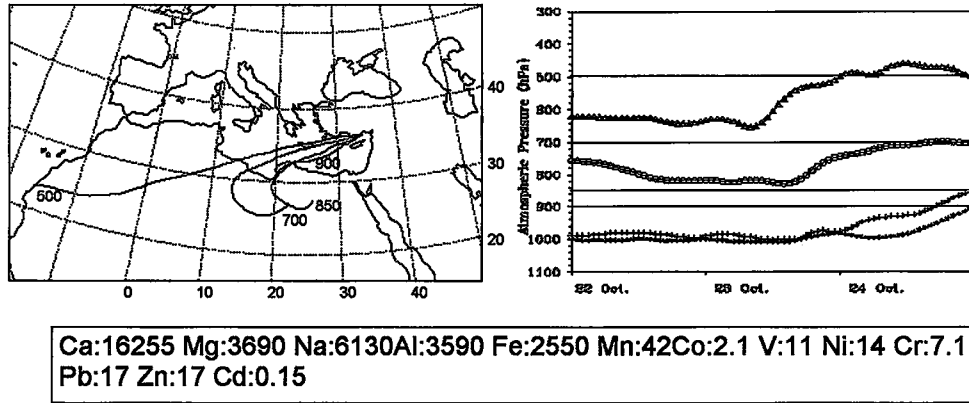
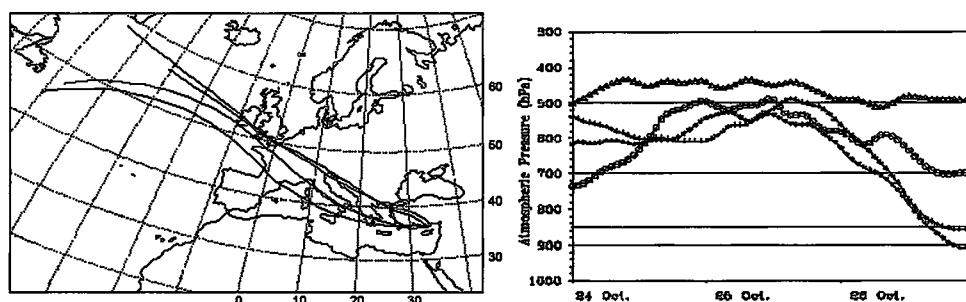


Figure 3.37. Air mass back trajectories arriving at Erdemli at 900, 850, 700 and 500 hPa barometric levels on 24 October 1992. The right hand panel illustrates associated vertical motions of the trajectories (conc. in ng m^{-3}).

On 26 October, 1992, air masses at all levels originated from the Atlantic and reached the sampling zone by passing over the European continent. Although this continent is populated and industrialized, the concentrations of anthropogenic tracers were still low. The associated trajectories (Fig.3.38) show the air masses traveling over Europe at more than 700 hPa and permanent down-flow of the air masses indicates anticyclonic transport. At all levels air parcels were transported above the boundary layer across a region where entrainment and removal by precipitation would be minimized and the elemental composition of this sample can therefore be assumed to be representative of the atmosphere of the Atlantic ocean.

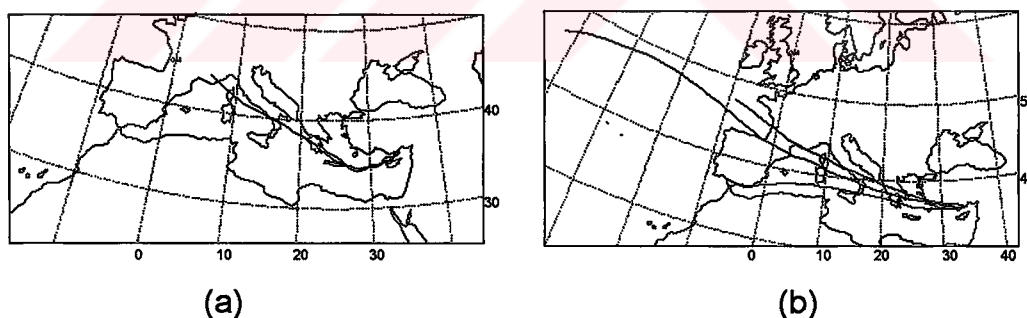
In summary, one has observed the eastward transport of air masses above the boundary layer from the Atlantic region passing over the European mainland and advecting material to the eastern Mediterranean atmosphere where it was delivered back to the surface in subsiding air. Further, as indicated by the elemental concentrations of the sample collected on 26 October, the vertical entrainment of free tropospheric air into the turbulent boundary layer serves to reduce the boundary layer concentrations by dilution.



Ca:4010 Mg:1320 Na:3545 Al:365 Fe:250 Mn:5.6 Co:0.27 V:1 Ni:2.3
Cr:0.8 Zn:6.1 Pb:9.7 Cd:0.03

Figure 3.38. Air mass back trajectories arriving at Erdemli at 900, 850, 700 and 500 hPa barometric levels on 26 October 1992. The right hand panel illustrates associated vertical motions of the trajectories (conc. in ng m^{-3}).

Between 27 and 29 October, 1992, the elemental concentrations reached their nadir for the month and the associated trajectories arriving at 900 and 500 hPa show that the sampling zone was under the influence of maritime air (Fig.3.39).



Ca:3365 Mg:1070 Na:1935 Al:180 Fe:210 Mn:3.8 Co:0.19 V:5 Ni: 3.3 Cr: 2.1
Zn:5 Pb:22 Cd:0.06

Figure 3.39. Air mass back trajectories arriving at Erdemli during 27-29 October 1992 (conc. in ng m^{-3}).

(a) 900 hPa; (b) 500 hPa

In these case studies of the months April, 1992, and October, 1991 and 1992, we have seen how, day by day, the elemental concentrations in the aerosols sampled at Erdemli can be correlated with the history of the air masses flowing over the eastern Mediterranean. The analysis has emphasized the utility of back trajectory studies in the Mediterranean region. The work has explained:

1. The abruptness of change observed in aerosol trace metal compositions,
2. The importance of using 3-D, variable level air mass back trajectories in considering not only the problem of altitudinal variations in wind speed and direction and but also the wider question of the usage of the vertical components of air motion to examine the association between air mass history and the fluctuations of both crustal and anthropogenic elemental concentrations in aerosols over the eastern Mediterranean.
3. How, infrequently, the composition of "pure" Atlantic, European and North African atmospheres can be separated.

In fact, 3-D air mass back trajectories corresponding to each sample have been obtained. These data, together with the associated elemental compositions are shown in Appendix. One could analyze the daily data for nearly the entire sampling period employing exactly the same philosophy and exactly the same methods as those used in the case studies. Although this would obviously provide much more detail one would find few, if any, phenomena that have not been considered in the case studies. Indeed, the months April and October were chosen since these months both belong to transitional seasons when intrusions of desert dust can enhance atmospheric Al concentrations to extraordinary magnitudes. Although both months lie in the transitional seasons they differ from each other in the following way. April follows the wet winter months whereas October succeeds the dry summer months. Thus, the atmosphere over the basin was scavenged more efficiently before the April sampling period but, on the other hand, accumulation of particles within the atmosphere was to be

expected before the sampling in October due to the lack of precipitation and the stagnation of air masses that is characteristic of the summer season.

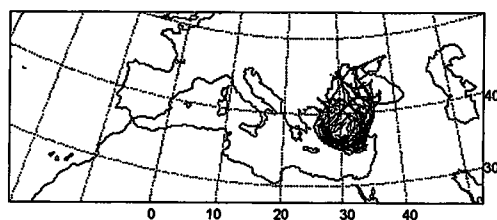
A daily analysis of the entire sampling period would permit consideration of the seasonal variation in aerosol composition. In fact, a discussion of the effects of seasonal variation on the sectorial composition is included in the next section.

3.3.2.2. Influence of Sectors of Air Trajectories on the Elemental Compositions of the Aerosols at the Erdemli Site

Having discussed the influence both of the origin of the air masses arriving at the sampling zone and of the scavenging of aerosols by local rainfall on the diel variation of the atmospheric concentrations of the elements, the characteristic seasonal concentrations of the N-W and the S-W geographical sectors will be discussed. This will enable one to see the effect of the temporal variation of the source strengths on the sectorial elemental concentrations. These two sectors were chosen since, throughout the investigations, they provided the dominant airflows to the sampling site.

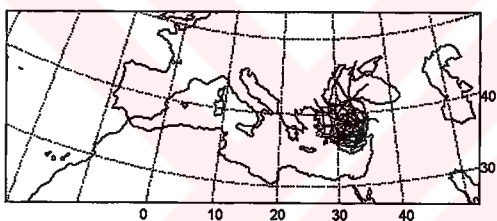
The calculated air trajectories will be used to classify the samples with respect to emission areas. Since the sampling was carried out at ground-level the samples were classified by observing their lowest level trajectories, which are those arriving at the sampling point at 900 hPa. The representative samples for each group were selected from those whose trajectories originated from the same sector at all four different levels. Since the geographical area that the trajectories covered during their transit is important in determining the composition of the atmospheric particulates, the trajectories have also been grouped within each sector as either long or short ranged.

Representative trajectories from western Anatolia (sector code 2a); Europe (sector code 2b); and their corresponding mean seasonal elemental concentrations are given in Figure 3.40 (a-b).



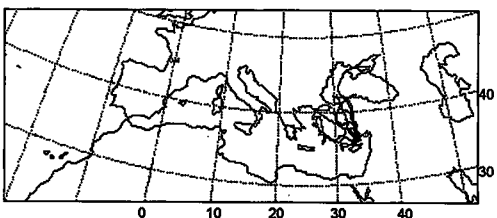
n=35
 Ca:5715±4000 Mg:1730±795 Na:4760±2390
 Al:1020±335 Fe:1075±333 Mn:23±7.1
 Co:0.65±0.28 V:10±4.8 Ni:6.8±2.4 Cr:8.5±3.7
 Zn:45±33 Pb:53±60 Cd:0.25±0.33

Summer



n=29
 Ca:2340±1535 Mg:665±445 Na:1300±1500
 Al:475±450 Fe:540±575 Mn:9.5±7.9
 Co:0.40±0.55 V:8.9±8.0 Ni:5.5±3.0 Cr:10±7.5
 Zn:20±16 Pb:37±33 Cd:0.20±0.12

Winter



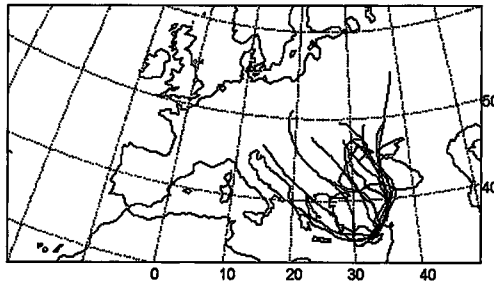
n=9
 Ca:2530±925 Mg:814±498 Na:1205±930
 Al:650±455 Fe:720±605 Mn:11±6.5
 Co:0.39±0.28 V:6.4±3.8 Ni:4.5±2.8 Cr:14±8.9
 Zn:25±15 Pb:100±220 Cd:0.23±0.1

Transitional seasons

(a)

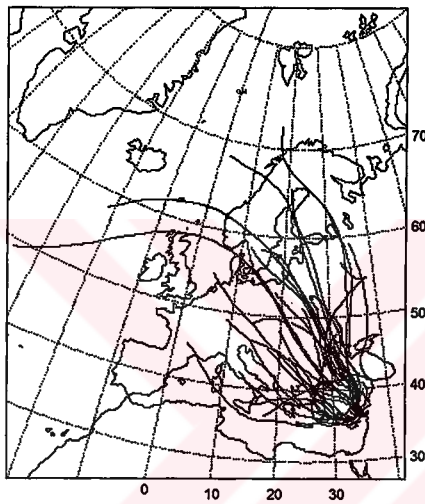
Figure 3.40. Representative trajectories and their mean elemental concentrations on seasonal basis from the N-W sector (conc. in ng m^{-3}).

(a) Western Anatolia; (b) Europe



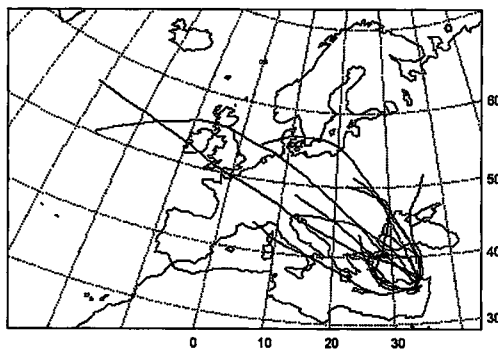
n=16
Ca:6470±4580 Mg:2000±975 Na:3465±2320
Al:1420±440 Fe:1360±530 Mn:21±8.5
Co:0.69±0.36 V:11±7.1 Ni:7.0±3.0 Cr:12±5.7
Zn:30±20 Pb:75±85 Cd:0.69±0.91

Summer



n=31
Ca:2170±1395 Mg:815±470 Na:2330±2025
Al:380±344 Fe:400±255 Mn:7.7±5.2
Co:0.35±0.31 V:8.0±3.9 Ni:4.5±2.4 Cr:12±8.6
Zn:15±11 Pb:37±38 Cd:0.25±0.22

Winter



n=14
Ca:3000±1995 Mg:1085±500 Na:1410±980
Al:635±440 Fe:765±730 Mn:15±12
Co:0.36±0.27 V:7.2±4.6 Ni:6.4±3.8 Cr:12±10
Zn:23±11 Pb:80±105 Cd:0.21±0.19

Transitional seasons

(b)

Fig.3.40. Cont.

Short trajectories from the N-W direction (Fig.3.40a) cover western Anatolia whereas the long ones (Fig.3.40b) mainly originate from Eastern Europe in summer but in winter and the transitional seasons they have a longer fetch over the continent, sometimes starting from the Atlantic. In spite of this large geographic coverage of the trajectories, there are no significant differences in the mean elemental concentrations of the samples associated with short and long trajectories within the seasons. The higher standard deviation of the mean concentrations of most of the elements in winter and the transitional seasons reveals precipitation scavenging of the atmosphere to be most effective in generating large fluctuations in the concentrations. Although most of the mean elemental concentrations have relatively low standard deviations in summer, the pollution-derived elements (e.g. Pb, Zn and Cd) still have higher standard deviations than the others.

Minimum atmospheric concentrations of crustal elements occurred during this study in winter when NW winds dominated the sampling site. Thus the elemental concentrations corresponding to long trajectories at 900 hPa (see Fig.3.40b) in winter can be accepted as providing the best possible values of the "European Background". Another important finding arises from the winter concentrations observed from short trajectories (see Fig.3.40a). In winter one observes that, when the trajectories extend towards Europe the average concentrations of individual elements in air masses are little different whether the trajectories are long or short ranged. In other words, the elemental composition of the material transported from Europe varies no more than when the trajectories are short ranged and the air mass traverses Anatolia only. During winter one expects local anthropogenic emission within the geographic coverage to be at its maximum, while particulates originating from crustal sources are at their minimum due to the wetness of the catchment regions. The same reasoning also applies to the catchment areas at European sites. Therefore, the winter observation of similar average elemental compositions in the particulates of long and short trajectories can be further interpreted as; the average composition of the

European background material that can be transported to the sampling site, if it exists, is the same as the local composition.

Irrespective of the sectors, the dispersion of material between the upper and lower layers of the troposphere over the Mediterranean is restricted in summer because of a strong subsidence inversion based about 1500 m (850 hPa barometric level) above ground that is well correlated with the depth of the mixing layer (UNEP/WMO, 1989). Such high-inversion stagnation interrupts vertical mixing and produces a persistent haze layer throughout the season (Reiter, 1975). The land-sea cooling cycle in this season results in the growth of the mixing height over the sea until the late evening. Thereafter, the aerosol in the upper layer has the possibility of downward mixing.

In summer some samples that have short coverage of the NW direction at 900 hPa have unusually high concentration of the crustal elements (see Fig.3.41a). The lower panel of the figure showing the trajectories arriving at 700 and 500 hPa demonstrates that at higher levels of the atmosphere airflow from North Africa which was able to bear mineral aerosol from this potential source area to the sampling site (see Fig.3.41b). The present investigation has shown that this mode of transport occurs in the higher levels in summer over the eastern Mediterranean and also over the Black Sea (Kubilay and Saydam, 1995c; Kubilay et al., 1995b). This result demonstrates the drawback which would arise when one uses trajectories only at one standard atmospheric level to represent the long-range transport of material. It also shows the importance of coupling geochemical tracer concentrations (e.g. in this study the Al concentration in the air was utilized) with air mass back trajectories in order to classify the origin of the aerosols arriving at receptor sites.

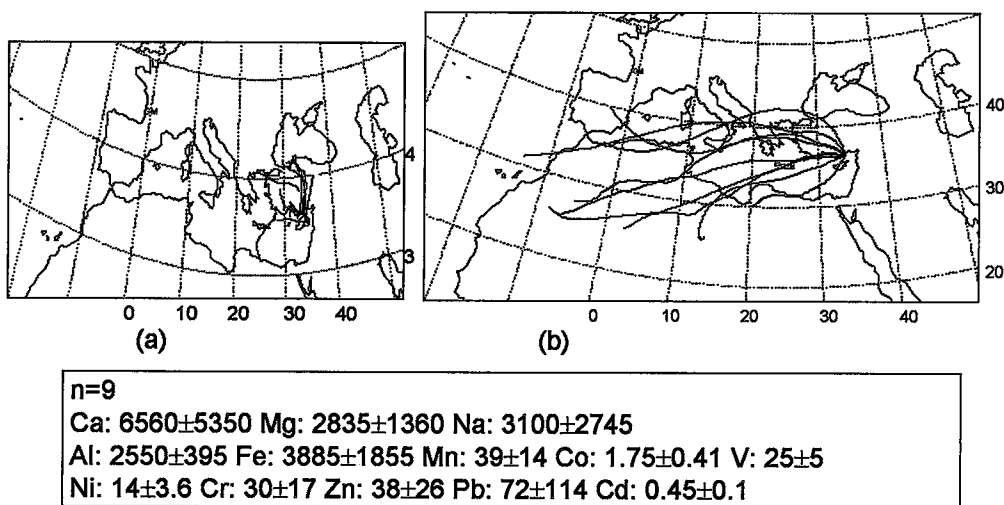


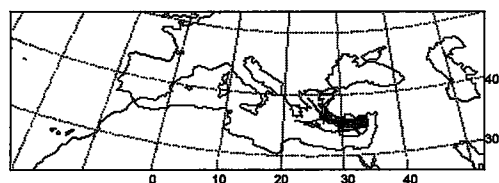
Figure 3.41. Saharan originated trajectories during summer time (conc. in ng m^{-3}).
 (a) 900 hPa; (b) 700 and 500 hPa

The geometric mean of the all elements (except Cr and Pb) given in Table 3.5. exhibit higher values in summer than in winter and the transitional seasons. Further, as can be seen from Figure 3.41a, the local lower layer trajectories may permit the accumulation of both continental and marine origin elements in the atmosphere. Consequently, restricted ventilation together with the deficit in precipitation during summer results in the accumulation of particles within the atmosphere.

The short range trajectories arriving at 900 hPa from the SW cover the Mediterranean Sea (see Fig.3.42). The elemental mean concentrations of the samples associated with marine trajectories generally decrease in the following order; summer>winter>transitional seasons. The higher mean concentrations of the crustal elements (e.g. Al, Fe) from this sector during the summer was result of diurnal heating and cooling cycles cause the

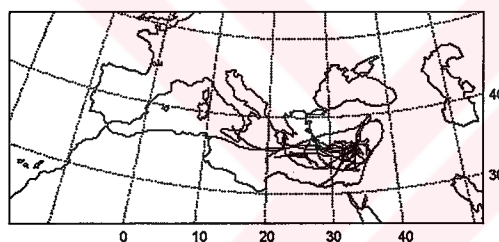
convective transport and circulation of the air between sea and land in the boundary layer.

There is no long range transport at 900 hPa from the S-W except during the transitional seasons when there were a few occasions when long-range continental transport from North Africa was observed.



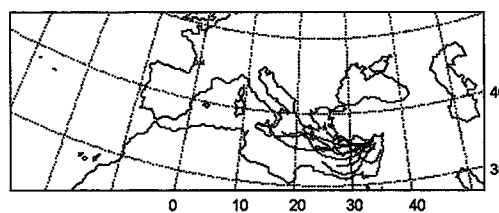
(a)

n=18
 Ca:5350±2935 Mg:1880±520 Na:4050±1770
 Al:920±425 Fe:930±395 Mn:19±7
 Co:0.69±0.28 V:11±4.5 Ni:5.3±1.7 Cr:10±5.1
 Zn:40±20 Pb:40±32 Cd:0.45±0.36



(b)

n=18
 Ca:1855±1065 Mg:795±415 Na:2325±3380
 Al:415±270 Fe:500±300 Mn:8.9±5.5
 Co:0.30±0.23 V:8±4.4 Ni:4±2.6 Cr:8.7±8.7
 Zn:17±15 Pb:30±27 Cd:0.19±0.13



(c)

n=11
 Ca:2250±1650 Mg:980±535 Na:2785±2125
 Al:350±170 Fe:290±258 Mn:4.4±2.5
 Co:0.23±0.13 V:3.1±2.2 Ni:3.3±1.6 Cr:6.1±4.4
 Zn:7.5±2.9 Pb:27±38 Cd:0.09±0.07

Figure 3.42. Representative short range trajectories and their mean elemental concentrations (ng m^{-3}) on seasonal basis from the S-W sector.

(a) Summer; (b) Winter; (c) Transitional seasons

A study conducted at a remote coastal station in the southeast of Sardinia, in the central Mediterranean revealed that Saharan dust transport to the region provided on average about $30 \mu\text{g m}^{-3}$ of the suspended particulate dust load in winds from the south (Guerzoni et al., 1992). Assuming an Al:mineral ratio of 0.08 (see Chester et al., 1991a) this mineral dust loading corresponds to an atmospheric Aluminum concentration of 2500 ng m^{-3} . This atmospheric Al concentration may be accepted as the threshold Al concentration representing the chemical signature of a desert dust intrusion or **pulse** to the region.

During the transitional seasons 21 samples were recorded having Al concentrations of $>2500 \text{ ng m}^{-3}$. Examination of the air mass back trajectories of these 21 samples arriving at 900 hPa shows that:

a) only 4 samples originated from the Sahara (see Fig.3.43),

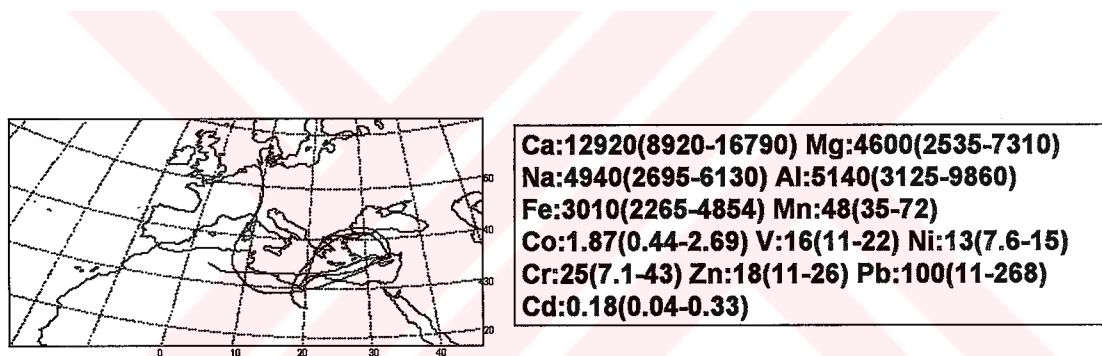
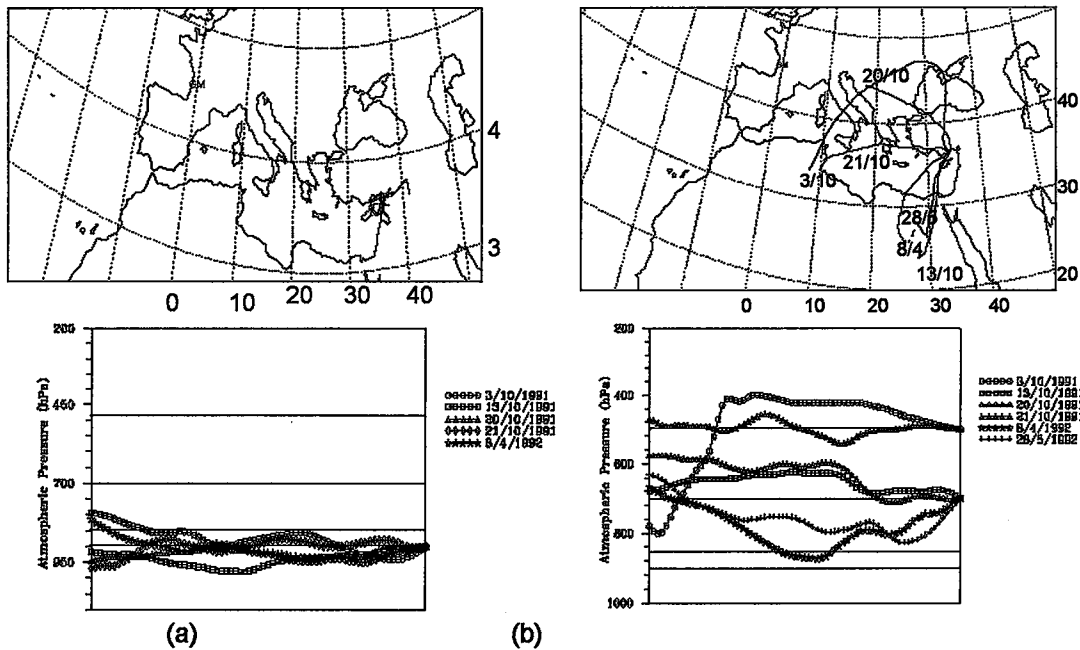


Figure 3.43. North-Africa originated trajectories arriving at 900 hPa to the Erdemli site (conc. in ng m^{-3}).

b) 6 of these 21 dust samples originated from Syrian deserts (see Fig.3.44a). The lower panel of the figure represents the vertical movement of the trajectories. At 900 hpa air masses are transported within the boundary layer that could carry dust from near Middle East. Trajectories arriving at higher barometric pressures (700 and 500 hPa) originated from North Africa except one that had its origin over Europe.

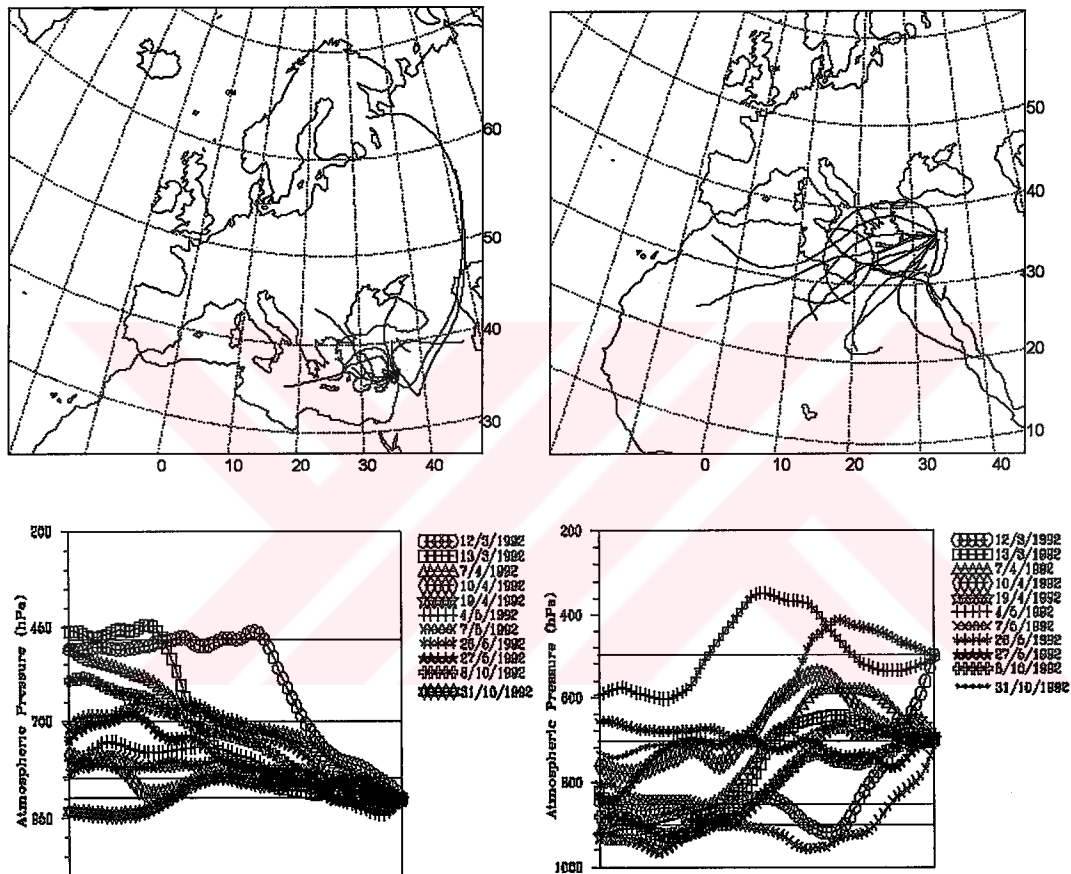


Ca:13145 (5115-37600) Mg:5640 (2170-14295) Na:2625 (850-5770)
 Al:7430(2527-22568) Fe:7125(1553-20045) Mn:97(28-306) Co:3.3(0.2-11) V:34(8.6-123)
 Ni:21(6-56) Cr:29(10-66) Zn:40(22-55) Pb:103(16-340) Cd:0.49(0.14-1.39)

Figure 3.44. Representative Middle East originated air-mass back trajectories and their corresponding vertical movements (conc. in ng m^{-3}).
 (a) 900 hPa (b) 700 hPa and 500 hPa

c) The 900 hPa trajectories of the remaining 11 samples in transitional seasons; gave very different origins of the air masses depending on the final barometric level. The lower layers of the local atmosphere were fed with air-masses coming from non desert sources, one trajectory reaching 60°N (see Fig. 3.45a). Only the trajectories ending at the 700 and 500 hPa barometric levels had their origin over North Africa (see Fig. 3.45b). The vertical motions of the trajectories are also shown at the bottom panel of the Figure 3.46. At the synoptic scale, there is a significant upward movement for the upper trajectories (700 and 500 hPa) and in contrast, a notable downward movement for the lower layer trajectories (900 hPa). The upward movement allows the dust to ascend and consequently to be taken in the cyclonic system.

So, these observations strongly suggest that the advection of the Saharan dusts is similar in character to a frontal system. The African dust transport event observed at the Erdemli site is quite similar to that previously described by Bergametti et al., (1989b); Martin et al., 1990; Dulac et al., (1992) as over the western Mediterranean and by Reiff et al., (1986) and Davies et al., (1992) as over Europe.



**Ca:16344(5285-52840) Mg:6560(1465-16745) Na:6935(405-44960)
 Al:6615(2675-14840) Fe:7350(1870-30390) Mn:76(11-190) Co:3(0.26-11) V:22(6.6-38)
 Ni:20(5.7-45) Cr:26(4.8-60) Zn:45(12-170) Pb:90(20-365) Cd:0.32(0.06-0.58)**

Figure 3.45. Representative North-Africa originated air-mass back trajectories and their corresponding vertical movements (conc. in ng m^{-3}).
 (a) 900 hPa (b) 700 and 500 hPa

Thus it can be seen that the long range transport from this sector has a pronounced influence on the atmospheric concentrations of the elements and as consistent with the discussion of the case studies in Section 3.3.2.1 one concludes that the long-range transport of desert dust from the S-W sector is the most important apparent source effecting the atmospheric concentrations of the elements at the Erdemli receptor.

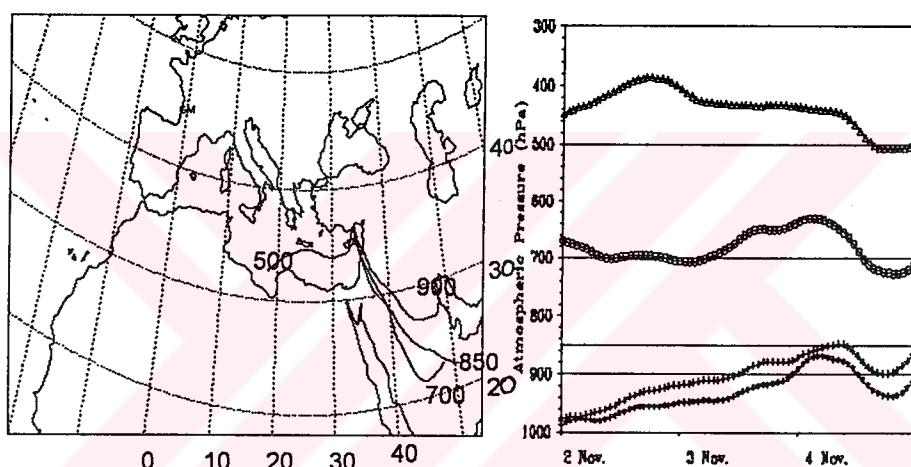
The assessment of atmospheric dust transport from North Africa to Atlantic is also in agreement with the frontal character of African dust transport to the Mediterranean and is further complicated by the non-uniform vertical distribution of the dust. Aircraft measurements made at Barbados (tropical North Atlantic) during the summer of 1969 (Prospero and Carlson, 1972) show the maximum aerosol concentrations to be above the marine boundary layer. The dust is confined to a layer between 550 and 750 hPa (Carlson and Prospero, 1972). This elevated layer, termed the Saharan air layer, is a persistent feature of the tropical North Atlantic during dust outbreaks. Aircraft studies above the coast of West Africa (Talbot et al., 1986) indicate a similar vertical distribution. Martin et al., (1990), conducted a study at a remote coastal station in Corsica in the western Mediterranean to determine the actual levels at which Saharan dust was transported. These authors found, by combining geochemical tracers of dust (Si,Al) with three-dimensional air-mass trajectories, temperature soundings of the World Meteorological Organization (WMO) along the path of the dust clouds and satellite imagery, that the dust layers were located mainly between 850 and 500 hPa which is what has been shown to be true in the eastern part of the Mediterranean throughout this study. Dust from the Saharan air layer settles into the marine boundary layer by gravity and by convective mixing across the inversion of the marine boundary layer. Because of these processes, dust concentrations in the marine boundary layer might be lower than in the Saharan air layer.

Dayan's (1986) five years (1978-1982) climatological study of airflows reaching Israel indicates a seasonal variation in the frequency of airflow

patterns at 850 hPa. He observed the long range transport of dust to the eastern Mediterranean from North Africa and from the Middle East deserts to occur in spring and fall, respectively. Mineral aerosol detection above Africa from the thermal infrared channel of the satellite between the period of 1984-1993 have described both the seasonal character of dust activity and allowed the sources of dust emission to be located (Legrand et al., 1994; Legrand, 1995). The produced dust climatology throughout the observational period revealed an annual cycle with a maximum in March-May and a minimum in October-December. The same seasonal rhythm of dust activity identified identified by Legrand et al., 1994 and Legrand, 1995 was also reflected in the statistics of dust-storm occurrence performed at Israel (Ganor, 1994). He analyzed the occurrence and duration of Saharan dust outbreaks to Israel during a period of 33 years and results show the following: The dusty season begins in late summer, episode frequency is uniform through autumn and early winter and rises to about double (maxima during April) the monthly average during March and April. Frequency drops sharply after May and July-August are dust free. The spring maximum in the dust transport from North Africa seen throughout Ganor's study is also in line with the maximum in the photometric measurements of back-scatter (turbidity) observed over North Africa between March and June (D'Almeida, 1986).

The air mass trajectories able to carry dust to the eastern Mediterranean have been classified into two types (Yaalon and Ganor, 1979; Ganor et al., 1991). First, those trajectories originating over North Africa as a result of the Saharan depression and secondly those originating over the Arabian Peninsula on the rare occasions when the 'Persian Gulf Depression' is situated over the Red Sea. Ganor et al., (1991) described the chemical composition of 23 severe dust intrusions to an eastern Mediterranean coastal site (Israel) and concluded that only one of the intrusions originated from the Arabian Peninsula.

During 3-5 November, 1992 a dust storm from the Arabian desert increased the elemental concentrations of the aerosol samples collected at Erdemli. On 4 November the air mass back trajectories at 900, 850 and 700 hPa arrived from the SE during this unique event so far as the present study is concerned and clearly indicate transport from the Arabian Peninsula, whereas the trajectory arriving at 500 hPa originated over the Mediterranean. The vertical movements of the trajectories arriving at 900 and 850 hPa demonstrate a typical cyclonic flow favoring the uplift of dust (see Fig.3.46).



Ca:14180	Mg:3150	Na:1635	Al:6114	Fe:6470	Mn:66	Co:4.3	V:17	Ni:17	Cr:35
Zn:30	Pb:126	Cd:0.46							

Figure 3.46. Air mass back trajectories arriving at Erdemli at 900, 850, 700 and 500 hPa barometric levels on 4 November 1992. The right hand panel illustrates associated vertical motions of the trajectories (conc. in ng m^{-3}).

3.3. Chemical Composition of Aerosols Over the Eastern Mediterranean

3.3.1. Enrichment Factors

As discussed previously (Section 3.2), the elemental concentrations of atmospheric particulates vary over several orders of magnitude depending on the geographic location of the sampling site, the local and meso-scale meteorological conditions (rain, long-range transport of air masses) and the seasonal changes in the intensities of the sources venting particulates into the atmosphere. There being many factors affecting the atmospheric concentrations of the elements over short time and space scales, it is difficult to characterize the composition of the aerosol by observing their regional atmospheric concentrations. This has been confirmed in Section 3.3.2.2. where one sought elemental concentrations characteristic of each of the potential sources surrounding the Erdemli site. The identification of source areas was found to be difficult because the origin of individual injections was masked by the mixing which occurs in the reservoir.

The primary constituent of the aerosols arriving at the sampling site was the crustal component transported both from the surrounding desert areas and from within the region - as a result of deforestation, agricultural activities and over-exploitation of vegetation for domestic use. Thus, the chemical composition of the Mediterranean aerosol is controlled by the mixing of various components and the extent to which the mixing occurs will vary both in space and time.

One way of evaluating the chemical character of the aerosol is by the use of Enrichment Factors (EFs) providing information on the extent to which trace metal concentrations in aerosols are enriched or depleted relative to crustal and marine sources. In this section EFs which are straightforward and informative parameters will be utilized for the characterization of aerosols. Generally, EFs are utilized to establish the expected contributions

of crustal and marine sources to the composition of aerosols (Zoller et al., 1974; Rahn, 1976). The EFs are conveniently calculated for the various elements in the aerosol by the general formula given below:

$$EF(X)_{\text{aerosol-source}} = \frac{\left(\frac{X}{\text{Ref.}} \right)_{\text{aerosol}}}{\left(\frac{X}{\text{Ref.}} \right)_{\text{source}}},$$

in which $EF(X)_{\text{aerosol-source}}$ is the enrichment factor of element X in the aerosol relative to a crustal or marine source and X/Ref is the ratio of the concentration of element X to the concentration of the reference (precursor of source material) element in the aerosol and in the source material. Elements commonly used as crustal indicators include aluminum, silicon, iron and scandium; for sea salt the nearly universal choice is sodium.

The definition of EF is based on the assumption that constituents from the source are found in the sample in the same proportion as they occur in the source. Since rocks have been analyzed more extensively than soils, in the calculation of EFs relative to crust, crustal rock is used instead of average soil. A number of estimates of the average composition of crustal rock are available; the present study uses that of Taylor (1964) which represents a 1:1 mixture of granite and basalt rocks. In fact, those rocks which undergo weathering around the eastern Mediterranean have been defined as ultrabasic, basic and limestone (Ergin et al., 1988). The elemental abundancies in such rocks, together with those in average rock, are given in Table 3.6. This Table shows local rocks to be enriched in certain elements (Ca, Co, Cr, Ni, Fe) relative to average rock. This discrepancy may introduce errors into the calculation of enrichment factors.

Rahn (1976), postulated three reasons as to why average rock rather than local rock must be chosen as a reference material when calculating EF_{crust} values:

- (1) most aerosol analyses are not accompanied by corresponding analyses of local soil
- (2) inter worker standardization of enrichment factor calculations are easier when only a handful of global reference materials are used
- (3) use of a constant reference material by each worker enables the direct comparison of enrichment factors.

Rahn (1976) compared several tables of elemental abundances in average crustal rock given by different authors and concluded that there was similarity of concentrations from estimate to estimate and that the uncertainty in enrichment factors due to the choice of reference rock was less than a factor of two.

Constituents that derive from sources other than the Earth's crust will have high crustal EFs though coals and even fly-ash possess relative concentrations of many trace metals similar to that of average crustal material (Bertine and Goldberg, 1971). Elements with low EFs are assumed to be of crustal origin only, whereas enrichments less than 1, signify depletion with respect to crustal sources. In this thesis elements with EF_{crust} (or EF_{sea}) values of less than 10 are considered to have approximately the same inter-element concentration ratios in the atmosphere as in average crustal material (or in bulk seawater). The upper limit of ten has been used for interpreting the crustal enrichment (seawater enrichment) factors because the proportions of trace elements in the actual crustal-aerosol (sea salt-aerosol) precursors may differ from those in average crustal material.

Since different types of crustal rock and soil exist in the various source areas and since there is uncertainty concerning the chemical fractionation which occurs during weathering, mean crustal rock ratios have been used as crude approximations of the relative composition of crustal material in the aerosols. Thus, if the values of elemental EFs do not exceed 10 they may be accepted as indicating a crustal source for the elements considered. However, this approach will not distinguish between crustal

material vented into the atmosphere by natural processes and injected as a result of such human activity as increased exposure of soil surfaces due to agriculture and other land-cleaning operations, stone crushing, sand and gravel operations and the suspension of soil particles by vehicular traffic. In polluted areas 90 % or more of the nonenriched elements in the atmosphere have an anthropogenic origin (Rahn, 1976).

Because of the various constraints involved in the calculation of EF values they should be treated as order-of-magnitude indicators of the type of potential sources.

In Section 3.2.2. it was concluded that concentrations of the elements in aerosols over the sampling site were derived from both crustal and marine sources. In these circumstances it may be of interest to use EFs to estimate the relative crustal and sea salt contributions to the abundance of each element. The average crustal (Taylor, 1964) and bulk seawater (Martin and Whitfield, 1983) compositions with respect to elements considered in this study are given in Table 3.6. Soil composition (Martin and Whitfield, 1983) is also indicated in the table. The main difference between the average composition of rock and soil is the lower concentration of Ca, Mg and Na in soil.

Table 3.6. The average composition of mean crust, various rocks types, soil and bulk sea water.

	Rock (a)	Ultrabasic (b)	Basic (b) ($\mu\text{g/g}$)	Limestones	Soils (c)	Sea Water (c) ($\mu\text{g/L}$)
Al	82300	4500	87600	4200	71000	0.5
Ca	41500	7000	72000	302300	15000	412000
Cd	0.2	-	0.2	0.035	0.35	0.01
Co	25	210	48	0.1	8	0.05
Cr	100	2000	200	11	70	0.3
Fe	56300	98500	85600	3800	40000	2
Mg	23300	-	45000	47000	5000	$1.29 \cdot 10^6$
Mn	950	1500	2000	1100	1000	0.2
Na	23600	5700	19400	400	5000	$1.077 \cdot 10^7$
Ni	75	2000	160	20	50	0.2
Pb	12.5	0.1	8	9-5	35	0.003
V	135	40	200	-	90	2.5
Zn	70	30	130	20	90	0.1

(a) Taylor, (1964).

(b) From Tables in Emelyanov and Shimkus (1986) and Ergin et al., (1988).

(c) Data from Martin & Whitfield (1983).

Figure 3.47 illustrates crustal enrichment factors calculated with respect to average rock (solid lines) and soil (dotted lines) composition of elements observed in the eastern Mediterranean aerosols. The type of variation differs from element to element and from sample to sample as can be clearly seen from the relatively high standard deviations of the geometric means. As shown in Section 3.2, the concentrations of the elements in the Erdemli aerosol are, to a good approximation, log-normally distributed. Any linear combination of normally distributed variables must itself be so distributed. Accordingly, to be representative, the geometric mean of the EFs was preferred to arithmetic means during the construction of Figure 3.47. Although the geometric means of the EF_{crust} values of elements Fe, Mn, Co, Mg, V, Ni, Ca, Na and Cr for the whole sample set are between 1 and 10, standard deviations - except for those of Fe, Mn and Co - reveal the

possibility of enrichments within the data set. Zn, Cd and Pb have mean EF values larger than 10 indicating the anthropogenic origin of these elements. The mean EF values of Co, Mg, Ca and Na relative to soil are higher than the mean EF values of the same elements calculated relative to average rock due to the depletion of these elements in soil relative to rock (see Fig.3.47). Since the abundances of the elements Zn, Cd and Pb in soil are higher than in average rock (see Table 3.6) their mean EF values with respect to soil are lower than those calculated for with respect to average rock.

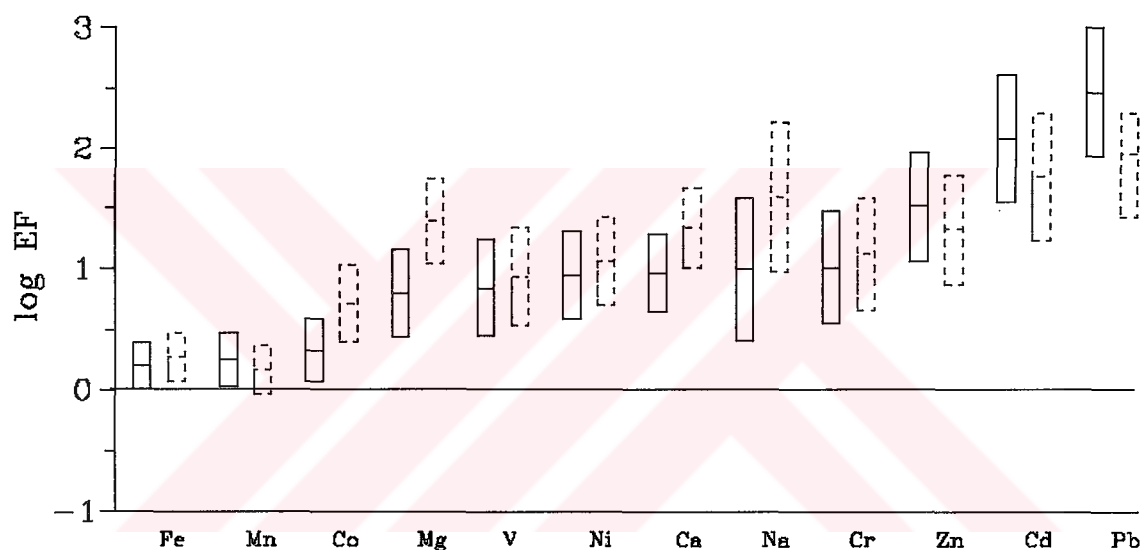


Figure 3.47. EF_{crust} values for atmospheric trace metals collected at the Erdemli site. The horizontal bars represent geometric mean enrichment factors, and vertical bars represent the geometric standard deviation (Solid bars for average crust composition and dashed bars for average soil composition).

The EF values of the elements calculated with respect to bulk sea composition are about 10^5 , save for Mg and Ca (see Fig.3.48) these being elements affected by sea salt. Dulac et al. (1987) also concluded that over the western Mediterranean recycling of sea salt from oceanic sources made

a negligible contribution to trace metal concentrations in the bulk particulate aerosol.

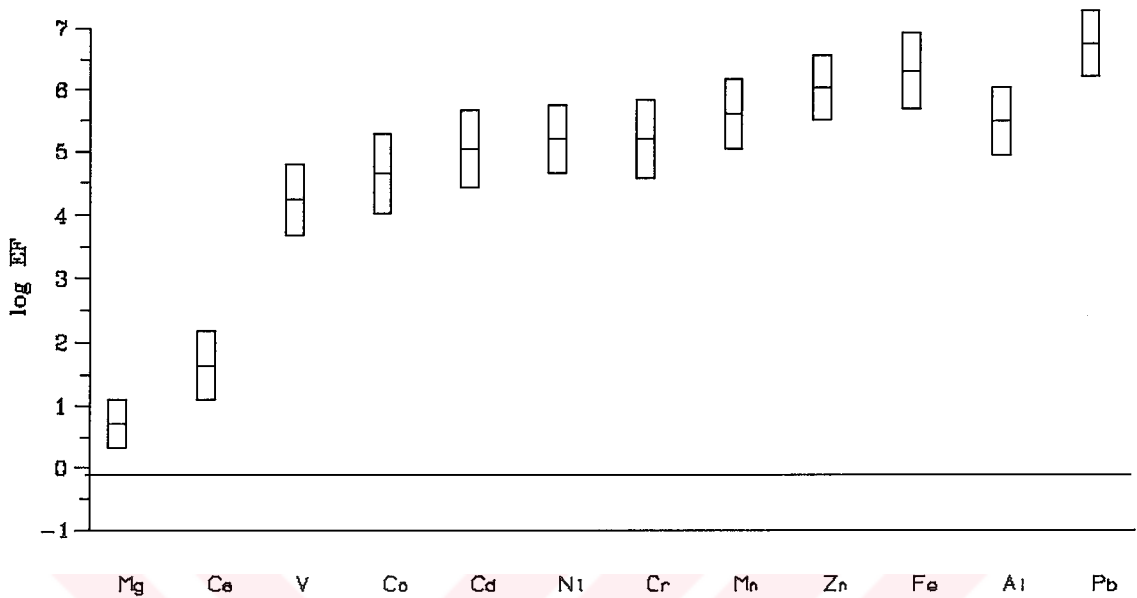


Figure 3.48. EF_{mar} values for atmospheric trace metals collected at the Erdemli site. The horizontal bars represent geometric mean enrichment factors, and vertical bars represent the geometric standard deviations.

These variations can be summarized more clearly if the data are grouped in three seasons (to compensate for temporal variation) as discussed in Section 3.2.4.1 describing the elemental concentrations in atmospheric particulates (see Table 3.7). On the basis of EF values, trace metals can be divided into three broad groups; i.e. non enriched elements (NEEs) and two categories of anomalously enriched elements (AEEs).

Group 1, the NEEs: Aluminum (by definition, the crustal indicator element), Fe, Mn, Co and Mg in all seasons; Ca, Na, Ni, Cr, V (in summer and transitional seasons), have geometric mean EF values which are <10 in the Erdemli aerosol population.

Group 2, the less significantly enriched AEEs: Ca, and Na (in winter); Ni, Cr, V (in winter) and Zn (in all seasons) have geometric mean EF values in the range >10 - $<10^2$.

Group 3, the more significantly enriched AEEs: Pb and Cd have geometric mean EF values in the range $>10^2$ - $<10^3$.

Table 3.7. Seasonal geometric mean enrichment factors (EFs) of the metals (number in parenthesis are the ranges of EFs).

	Winter	Summer	spring-fall
Fe	1.8(0.1-15)	1.5(0.3-5.3)	1.4(0.1-6)
Mn	2.0(0.2-17)	1.8(0.5-8.7)	1.5(0.1-6)
Ni	14(2-193)	6.5(1.7-22)	6.5(0.9-36)
Cr	16(0.7-668)	7.0(1.3-81)	8.0(0.2-97)
Co	2.7(0.1-35)	2.1(0.5-12)	1.9(0.1-6)
Cd	215(5-2942)	88(15-1816)	66(1.8-1370)
V	14(0.6-265)	5.4(0.4-55)	4.4(0.6-26)
Zn	44(6-359)	35(1-273)	20(1.6-212)
Pb	456(17-6590)	200(26-3537)	225(7-10080)
Ca	11(1.6-132)	8.3(0.9-60)	8(1.1-50)
Mg	8(1.4-142)	5.6(2-25)	4.9(1.0-46)
Na	14(0.3-542)	9.8(0.3-94)	5(0.1-171)

Although the trace metals have been grouped according to their seasonal geometric mean EFs, the EF ranges indicate that within the groups the NEEs may sometimes behave as AEEs and vice versa. From the magnitudes of the crustal EFs one may conclude that, in almost all samples, Fe and Mn have a mainly crustal origin; Co, Ca, Na, Mg, Ni, Cr and V have a mainly crustal origin in some samples but in others possess a substantial non-crustal component. In all samples the origin of Zn and especially Pb and Cd appear to be predominantly non-crustal. Table 3.7 shows the proportions of crustal/non-crustal components in the particulates to vary with the seasons. All the elements have their highest EFs in winter when the amount of dust (or the concentration of its precursor Al) is low. This

indicates that during dry and dusty periods (summer and transitional seasons) the concentrations of the elements in the aerosols was evidently controlled by the amount of dust but, as the levels of dust subsided, other sources became apparent and resulted in the enrichment of the elements relative to crustal sources.

3.3.2. The Average Compositions of the End Members of the Aerosols Over the Eastern Mediterranean

In previous studies carried out in the eastern and western Mediterranean, Chester et al., (1977; 1981; 1984; 1993a) made a series of particulate collections and found, on the basis of the meteorological conditions, the crustal EFs and the clay mineralogy, that there are two distinct end members over this regional sea; namely, materials brought to the atmosphere of the Mediterranean from the European continent, defined as the "European end Member" and from the North African continent, defined as the "Saharan end Member".

The elemental composition of the particulates is controlled by the mixing of these two components. However, in the absence of local pollution the composition of the end-members does not appear to vary geographically. There have been attempts to establish "average" characteristic EFs of the elements for individual end members of the atmospheric particulates over the Mediterranean basin, and in this section data obtained during the course of the present study will be used to define the characteristics of the end members for the eastern Mediterranean atmosphere.

In order to identify characteristic long-range material transported from the Eurasian continents to the atmosphere over the eastern Mediterranean, individual samples have been selected on the basis of their air mass back trajectories since these indicate the geographical origin (i.e.

the catchment area) of the particulates and also the land masses over which the air masses have passed before reaching the sampling coordinates.

The enrichment factors of the elements in "pure" Sahara dust outbreaks sampled at the various Mediterranean sites and off the coast of West Africa during the prevailing north east trades at the north Atlantic are listed in Table 3.8. Although a number of dust outbreaks from the surrounding desert regions have been sampled throughout the sample collection period of the present study only two have been included in the table, these being truly "desert" populations representing North African and Middle East and Arabian deserts, namely the episodes of 20 April, '92 and 4 Nov. '92. These two samples are the most representative examples of "pure desert" materials collected during the present work.

As demonstrated by Schutz and Rahn (1982), the basic assumption that the ratios of crustal abundancies are preserved from source to sampling site, is well founded for particles of less than 10 μm in diameter. And element concentrations in Saharan soils in this size fraction that is subject to long-range transport have relatively homogeneous composition. These findings support the non-enriched characteristic of elements in Sahara end member save for those, such as Zn, Pb and Cd, which are derived from pollution (see Table 3.8).

Table 3.8. EF_{crust} values of the elements in the samples collected from outbreaks of desert dust.

Element	(a)	(b)	(c)	(d)	(e)	(f)	(g)	(h1)	(h2)
Na	0.14	-	-	0.08-1.14	-	0.4	0.4	2.0	0.9
Ca	0.69	-	-	-	-	6.83	11	3.4	4.6
Mg	0.78	-	-	-	-	2.17	1.6	2.6	1.8
Fe	1	1	0.92	-	0.55	1.18	1.2	0.74	1.6
Al	0.93	1	1	1	1	1	1	1	1
Mn	1.07	1	0.84	0.26-0.44	0.92	1.15	5	0.59	0.87
Co	0.88	-	-	1.54	-	0.63	2.5	0.63	2.6
Ni	-	1.2	2.8	0.6-1.7	6.6	1.11	4	0.84	3.1
Cr	1.02	1.4	2.9	-	2.1	1.66	-	0.85	4.6
V	0.88	-	-	-	-	1.34	-	0.95	2.0
Zn	2.34	3.2	5.6	-	13	3.66	11	2	6
Pb	-	7.7	46	9-134	56	10.2	31	7	134
Cd	<200	8.3	96	-	26	1.4	255	4	76

(a) Rahn et al., (1979) (Atlantic north east trades).

(b) Murphy (1985) (Atlantic north east trades; mean of 6 Saharan dusts).

(c) Chester et al., (1984) (average of four Saharan dust episodes collected on board in the Tyrrhenian Sea).

(d) Tomadin et al., (1989).

(e) Chester et al., (1990) (Cap Ferrat; Saharan dust sample).

(f) Ganor et al., (1991) (Mean of 23 Sahara dust storm episodes in Israel).

(g) Guieu (1991b) (Tour du Valat).

(h1) present study (North African originated dust intrusion event observed on 20 Apr. 1992).

(h2) present study (Middle East originated dust intrusion event observed on 4 Nov. 1992)

The diffuse nature of the sources of the pollution derived elements, especially Pb, on the continents causes considerable variation within their EFs. The contamination of the desert material has been linked to the meteorological conditions during its long-range transport to the receptor regions. The data set obtained for the Arabian and Middle East desert origin end member contains considerable Pb and Cd. This result may be explained by the fact that the air masses originating from the Arabian Peninsula on 4 November passed over Middle Eastern countries

before reaching the sampling site, whereas the dust observed on 20 April, 1992 had traveled only over the sea. As mentioned in Section 2.3.4. the sample collected on 20 April 1992 was the most characteristic desert sample obtained during the course of the sampling period which did not suffer from local pollution.

The other end member of the atmosphere over the eastern Mediterranean, as described in Section 3.3.2.2., might consist of long-range material transported within air masses from Eurasia and possessing long transit times over the continent before reaching the sampling site. Table 3.9 displays both the mean atmospheric Al concentrations and the elemental EFs of the metals for those winter samples having long-range trajectories from the NW direction (see Fig.3.40b) together with the corresponding data for samples defining the European end member for the western Mediterranean atmosphere (Chester et al., 1984).

Table 3.9. EF_{crust} values of the elements in samples representative of the European end Member.

	Present study (n=31)	Chester et al. (1984) (n=5)
Al ng m ⁻³	384(26-1778)	112(75-216)
EF _{Fe}	2.3(0.45-15)	1.7(0.87-2.4)
EF _{Mn}	2.7(0.53-16)	3.5(2.8-5)
EF _{Cr}	63(2.6-668)	8.6(4.7-16)
EF _{Ni}	26(2.3-190)	15(7.2-29)
EF _{Zn}	86(8-304)	120(79-170)
EF _{Pb}	1070(17-6680)	767(275-1333)
EF _{Cd}	502(21-2269)	1219(445-3087)

The elemental characteristics of the samples named as European end member samples summarized in Table 3.9 arise from samples, none of which, during the the 3 days preceding their collection, received any contribution from desert sources. Any variation within the Al concentrations

is therefore due either to local crustal effects or to precipitation scavenging of the atmosphere. Thus, comparison of the composition of the local end member with that from the western Mediterranean atmosphere suffers from differences in local AI contributions that result in a variation in the EFs.

The data presented above can be used to draw one important conclusion. The eastern Mediterranean aerosol contains a "background" material which has a composition controlled by the extent to which it is diluted or mixed with regional crustal material rather than with anthropogenic material. Further, it appears that there exist two contrasting particulate catchment regions around the basin. However, European Background material brought by long range transport from the NW produces no significant change in the EFs of the elements compared to those of the Saharan end member and therefore no change in the trace metal composition of the aerosols in the lower troposphere over the eastern Mediterranean.

One sees that one of the end members of the region, a desert catchment, supplies large quantities of crustal material which dilute the background, whereas the other end member, consisting of urban and semi-industrialized catchments, does not supply "pollutant" or crustal material to enhance the local background composition.

It is apparent from the above discussion that the eastern Mediterranean represents an excellent example of a region in which both desert and non-desert catchments provide material superimposed on local background.

Table 3.10 provides EFs of the elements, relative to crust, in aerosols observed over contrasting marine environments. The atmospheric concentrations of the elements over the North Pacific are higher than those reported for the South Pacific ocean (see Section.3.3.2.2) due to the episodic influx of Asian dust to the former area (Duce et al., 1983). Table

3.10 shows, however, the EF_{crust} of the elements to be higher in the South Pacific Ocean than in the North Pacific region. This result reveals the composition of the aerosol over the North Pacific Ocean to be more affected by crustal sources than the aerosol over the South Pacific Ocean. Since the composition of the aerosols over the tropical North Atlantic is affected by Saharan dust the EFs of the elements, except for Pb, resemble those reported for the North rather than the South Pacific.

The lowest EFs reported in Table 3.10 for aerosols over coastal seas are for elements found over the Arabian sea. The similarity of the calculated mean EFs in the samples collected during the present study to those reported for North Sea aerosols, the North Sea being known to be a polluted region, confirms the presence of an anthropogenic effect in the Erdemli aerosol.

Table 3.10. Mean EF_{crust} for trace metals in aerosols representative of marine environments.

Element	Open Ocean		Coastal Seas		
	Tropical North Pacific (Enewetak) ¹	Tropical South Pacific (Samoa) ²	Tropical North Atlantic ³	North Sea ⁴	Arabian Sea ⁵
Al	1	1	1	1	1
Fe	0.84	1.9	0.9	1.5	1
Mn	0.96	7	1.1	3.6	1.4
Ni	-	-	4	12.4	2.3
Cr	2.7	-	2.4	11.5	2.4
Co	0.93	13	1.6	2.8	2.1
Cd	130	-	-	-	18
V	3.5	-	2	-	6
Zn	13	140	28	141.5	18
Pb	40	190	390	605	27

1. Duce et al., (1983).

2. Arimoto et al., (1987).

3. Buat-Menard and Chesselet (1979).

4. Chester and Bradshaw (1991) (close to pollutant sources).

5. Chester et al., (1991a) (close to crustal sources).

It is of interest to compare the mean EFs of trace metals found at the Erdemli site with those reported from other land based stations located in the north western Mediterranean at which aerosols have been collected over periods of several months. The data in Table 3.11 indicate that, on the basis of their EFs, the aerosols over the Erdemli site were less enriched in the elements Pb and Zn than aerosols sampled in the western part of the Mediterranean.

Table 3.11. EF_{crust} values in aerosols over the land-based stations at the Mediterranean Sea (sampling locations are indicated in Fig.3.7).

	Blanes ¹	Cap Ferrat ²	Tour du Valat ³	Corsica ⁴	Erdemli ⁵
Al	1	1	1	1	1
Fe	1.3	1.2	1.1	1.3	1.6
Mn	2.3	2.6	2.9	2.7	1.8
Cr	3.4	5.6	-	-	10
Ni	15	26	-	-	9
Zn	151	128	186	134	33
Pb	843	1024	982	631	295

1. Chester et al., (1991b).

2. Chester et al., (1990c).

3. Guieu (1991b).

4. Bergametti et al., (1989b).

5. Present study.

Most of the observed variation in EFs is caused by variability in the amount of crustal material (e.g. the Al concentration) present in the atmosphere. To discuss this, the elemental EFs for the samples collected in April 1992 are ranked in Table 3.12 according to their increasing Al concentration.

It is apparent that there are considerable variations in the concentrations of Al and these variations are strongly dependent on the origin of the air masses arriving at the collection site. Clearer insight as to

how the source controls the elemental composition of atmospheric particulates is provided by the air mass back trajectories corresponding to each sample (see Section 3.3.2.1).

Table 3.12. Enrichment Factors, ranked on the basis of Al concentrations, in atmospheric particulates collected in April 1992.

Sample No	Al ng m ⁻³	Ca	Mg	Na	Fe	Mn	Co	Ni	Cr	V	Zn	Pb	Cd
(EF _{crust})													
10	198	10	14	46	1.5	3.9	1.1	16	10	3.6	202	2047	491
11	200	14	11	27	1.7	3.5	1.3	23	97	14	132	7790	336
9	300	12	15	40	1.3	2.0	1.4	14	35	7.9	39	3157	82
8	396	13	18	71	1.2	1.7	1.1	5.5	3.8	0.6	7	501	18
1	443	8	8	7	1.2	1.8	2.1	16	18	11	61	178	117
15	599	8	5	7	1.4	1.6	0.9	8	7	3.9	21	1357	50
16	615	14	6	17	1.3	1.9	1.3	13	34	9.1	34	1019	205
17	664	11	6	7	1.1	1.6	1.1	15	10	9.1	31	417	103
2	753	7	3	2	0.8	1.2	0.4	3.5	33	2.6	37	113	41
18	816	5	5	4	1.3	1.6	1.3	19	22	11	36	353	44
3	1156	4	5	4	1.1	1.6	1.3	9.7	32	8.5	30	341	58
12	1203	10	5	14	1.4	1.9	1.1	11	28	8.7	61	948	134
19	1414	9	5	3	1.4	1.8	1.7	8	16	6.3	30	1871	233
20	2000	9	3	3	1.1	1.2	2.6	10	5	7.8	19	1163	294
4	2675	12	4	4	1.2	1.5	1.1	6	14	5.7	22	161	41
5	2755	5	3	7	0.8	0.9	0.6	2	3	2	12	409	20
7	2996	3	3	4	0.9	1.0	0.6	4	2	2.4	5	45	16
14	4446	4	2	3	0.7	0.6	0.3	1.4	0.9	0.9	4	157	6
6	4704	4	2	4	0.8	0.7	0.3	3.1	7.3	2.3	3	67	5
13	9859	3	3	2	0.7	0.7	0.6	0.9	0.9	0.8	2	7	2

There is no change within the EFs of Fe, Mn and Co with change in Al concentration. On the other hand, it is very clear from Table 3.12 that the EF's of the elements, Na, Ca and Mg, increase as the Al concentrations decrease. This is clearly consistent with the primarily marine origin of these

elements in atmospheric particulates. The EFs of the elements of Ni, Cr, V, Zn, Pb and Cd vary by up to three orders of magnitude and this confirms that for these elements there are sources other than crust. In general the EFs of these elements increase as the Al concentrations decrease. This would suggest that the background anthropogenic constituent of atmospheric particulates over the eastern Mediterranean is masked by an Al rich crust derived component. The present data shows this clearly with wide ranges of Al concentration i.e. 198-9859 ng m⁻³ for April 1992. This discussion is consistent with the idea of Chester et al. (1981) that the elemental composition of atmospheric particulates over the eastern Mediterranean is controlled largely by the dilution of the background anthropogenic component by the crustal component. In the following section this "dilution theory" will be tested using the enriched element, Pb, utilizing the concept of an EF diagram.

3.3.2. Enrichment Factor (EF) Diagrams

The relationship between aluminum and the other elements in aerosols can be expressed in the form of an EF diagram, in which the EF_{crust} is plotted against the concentration of aluminum in the air on a log-log scale (Rahn, 1976; Saydam, 1981; Chester et al., 1981; 1983; 1989; 1993a; Guerzoni et al., 1989). Generally, in this type of diagram enriched elements (e.g. Pb, Cd and Zn) fall in a triangular field in which the EF's increase as the concentration of aluminum decreases. The triangular field has a hypotenuse along a line of constant concentration which forms an apparent lower limit of concentration. In contrast, non-enriched elements (e.g. Fe, Mn) have EF's which generate a broad horizontal field with only a small vertical range, i.e. the EF's are largely independent of variations in the concentration of aluminum. The log-log scatter diagram pays an unexpected dividend - isopleths (lines of equal concentration) of the element whose

enrichment factor is being plotted appear as straight lines inclined at 45° counterclockwise from the vertical. Thus a single diagram shows the concentrations of elements X and Al, as well as the enrichment factor of X relative to the crust and Al (Rahn, 1976).

The benefit of EF diagrams for defining regions is apparent in Figure 3.49 where data from contrasting marine and coastal regions are plotted on a composite Pb EF diagram. This EF diagram incorporates a linear "mixing relationship" for the aerosol over the Mediterranean and surrounding marine regions (Chester et al., 1981; 1983; 1989; 1993a). This "mixing relationship" has been shown to hold within the relatively narrow region enclosed by lines at 45° to the axes, which represent minimum (C_{min}) and maximum (C_{max}) concentrations which constrain the limit of the field. For the purpose of assessing the effects of crustal and urban inputs in perturbing the linear mixing relationship, the positions of the C_{min} and C_{max} concentration of the enriched element have been identified from analyses of samples collected at various cruises in the Mediterranean and surrounding seas covering the North Atlantic westerlies/north east trades, the western Mediterranean, the Tyrrhenian Sea, the eastern Mediterranean, the Red Sea and the Arabian Sea (Chester et al., 1993a).

Data from atmospheres over the remote Southern and Northern Pacific where the dilution of the background noncrustal component of the atmospheric particulate by a crustal component is at a minimum (Duce et al., 1983; Arimoto et al., 1987) have been included in the figure. Although these particular Pb concentrations are lower than the C_{min} (1 ng m^{-3}) of the Mediterranean region they nevertheless correspond to enriched material (i.e. $EF > 10$). The enrichment of Pb relative to crust in these remote regions indicates the existence of an anthropogenic background component over the marine areas. These data provide an excellent contrast to the regional marine data set which is diluted by a crustal component.

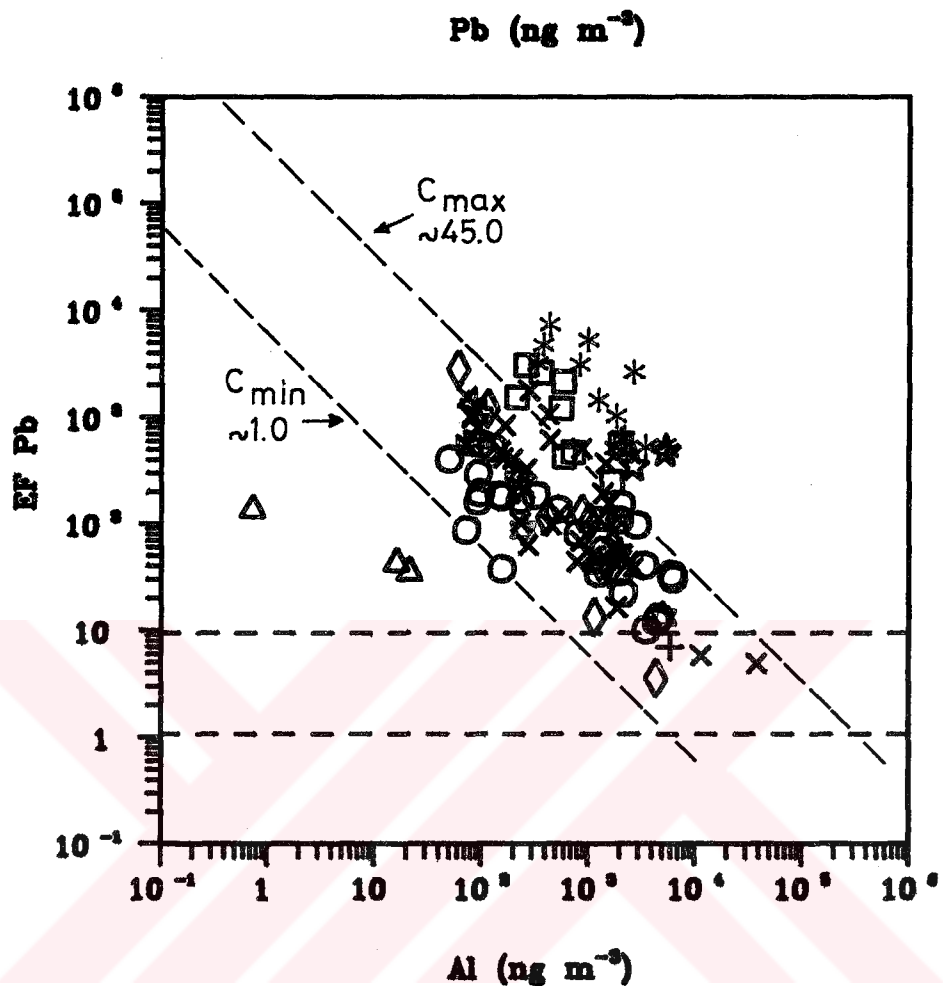


Figure 3.49. Composite enrichment factor diagram for Pb.

Data for the following aerosol samples are plotted. Mediterranean open ocean samples (circles, central Mediterranean, data from Correggiari et al., 1989; diamond, eastern Mediterranean, data from Chester et al., 1981; x, eastern Mediterranean, data from Karakoc, 1995); polluted samples (star; Istanbul, data from Kubilay et al., 1995b; green asterix, Bosphorus and the sea of Marmara, Karakoc, 1995; square, Cap Ferrat, data from Chester et al., 1989;); crustal end member (+, Atlantic ocean, Murphy, 1985; red filled star, Cap Ferrat, Chester et al., 1990c; blue symbol, Tyrrhenian Sea, Chester et al., 1984); European end member (brown symbol, Tyrrhenian Sea, Chester et al., 1984); remote region (triangle, north and south Pacific, Duce et al., 1983; Arimoto et al., 1987). The 45° broken lines enclose the dilution/mixing region in which the elemental chemistry of aerosols is controlled largely by the dilution of the European background material by crustal solids.

Data from different Saharan dust episodes, to the North Atlantic (Murphy, 1985), the western Mediterranean (Chester et al., 1990c) and the Tyrrhenian Sea (Chester et al., 1984) which define the "crustal end member" for the Mediterranean atmosphere have also been plotted. The episode reported by Murphy, (1985), defines a specific region in the high Al concentration and $EF < 10$ part of the diagram that delineates the perturbation of the mixing region by crustal components. The Saharan samples collected from the Tyrrhenian Sea (Chester et al., 1984) and from the Cap Ferrat station located at the southern coast of France (Chester et al., 1990c) plot in the region of mixing/dilution. This suggest that crustal perturbations of the composition of the aerosol are less significant over the western Mediterranean basin than over the Atlantic Ocean where the prevailing trade winds favor the transport of North African dust.

Chester et al., (1984) defined another constituent of the Mediterranean atmospheric particulate, the "European end member", as occupying the upper end of the dilution/mixing region along a 45 degree axis having low Al concentrations and relatively high Pb EF's.

The perturbation of the linear mixing relation by urban pollution is defined by two samples collected in Istanbul whose air-mass back trajectories verified that local anthropogenic emissions were the source of the atmospheric particulate (Kubilay et al.1995b) and by samples collected over the Sea of Marmara and along the Bosphorous (Karakoc, 1995) all of which are plotted on the same figure. These samples delineates a specific area that can be defined as the perturbation of linear mixing by local anthropogenic emissions. Atmospheric samples from a land-based station located at the Cap Ferrat station (Chester et al., 1989) are included in the diagram and generally also occupy the area to the right of the dilution region indicating the effect of local pollution (see Figure 3.49).

Samples collected on board ship during oceanographic cruises in the central and eastern Mediterranean (Correggiari et al., 1989, Chester et al., 1981; Karakoc, 1995) demonstrate the linear mixing/dilution relationship

perfectly. These samples also illustrate the effect of the perturbation of the relation by the crustal end member and by local pollution.

The Pb EFs and the Al concentrations of the twenty samples collected during April 1992 (see Table 3.12) have been plotted as an EF diagram in Figure 3.50. One sees that points falling on equal concentration lines may have EF values differing by two orders of magnitude. For example, the concentrations of Pb in samples 1 and 13 are 12 and 10.7 ng m^{-3} , whereas the corresponding EF values are 176 and 7, respectively. These two points clearly show that the concentration of an enriched element in atmospheric particulates is not a restraining parameter on the identification of the source of the atmospheric particulates.

Sample 13, which was collected at the sampling site from the dust storm of 20 April, is assumed to exemplify the true, crust-derived, desert component transported to the basin and its specific location on the EF diagram well represents the perturbation of the mixing region by the crust derived material. The controlling factor for the two order of magnitude change in EFs between samples 1 and 13 is the concentration of Al representing the amount of crustal material in the atmosphere. The concentrations of Al for samples 1 and 13 were 440 and 9860 ng m^{-3} , respectively. The higher concentration of Al for the point 13 is a result of the air mass having been swept over North Africa. The air-mass back trajectory for sample 1 originated from Eastern Europe (see Figure). These two points on the EF diagram provide an excellent example of the dilution of the anthropogenic component (Pb in this case) by the crustal component of the atmospheric particulate within the mixing/dilution region.

One sees that the enrichment of an element with respect to crust in atmospheric particulates is controlled by the concentration of Al (an indicator of crustal material). Examination of the elemental concentrations of the samples collected in April, 1992, together with their corresponding air mass back-trajectories at four different barometric levels, has shown that in this month there were two outbreaks of dust from North Africa (see Section

3.3.2.1). The second dust outbreak observed from 7 to 12 April 1992 (samples 4 to 7) had the longest duration of any dust pulses observed during the course of this study and is known to have suffered from urban pollution. The specific location of the samples known to have been affected by local urban inputs (samples 4 and 5) illustrates another use of the EF diagrams. In other words, local urban perturbation of the dominating air mass can be traced by the specific positions possessed by individual samples on the EF diagram.

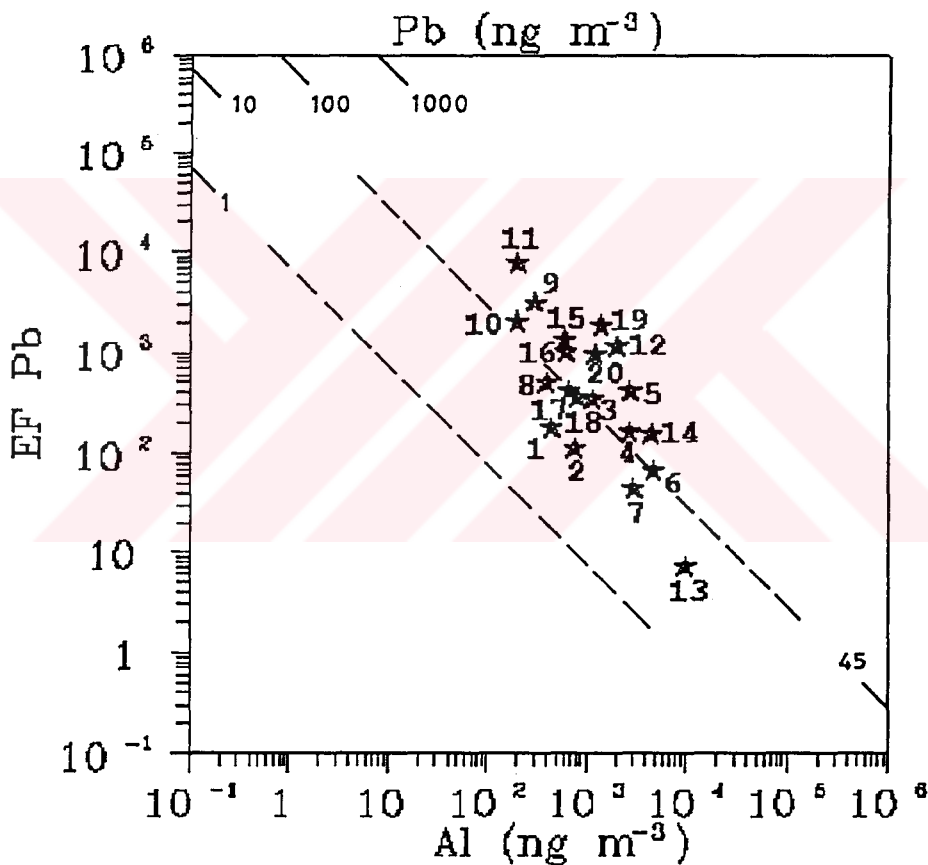


Figure 3.50. EF Diagram of Pb for the samples collected during April 1992.

The mean Al concentration of all the other samples was 670 ng m^{-3} ($100\text{-}2000 \text{ ng m}^{-3}$) and their positions on the EF diagrams were controlled mainly by the mutual proportions of the two components (crustal

and anthropogenic) superimposed on the composition of locally derived atmospheric particulates. The corresponding range of Pb EFs was 100-7690. EFs of samples collected from the same place can vary almost daily as materials from different catchments are collected. The Pb concentrations used for the construction of the EF diagram had a sufficiently wide range (10.7-402 ng m⁻³) to permit the construction of constant concentration lines (isolines).

The coupling of the collection sites of individual samples with the appropriate air mass back trajectories permits the definition of certain specific regions on the EF diagram. Samples 8,9, 10 and 11 arrived at the sampling site with trajectories indicating their previous 3 days travel over the Mediterranean Sea. The Al contents of these 4 samples were less than 400 ng m⁻³. This conflicts with the mean Al concentration corresponding to short range coverage of the trajectories at 900 hPa (since same order of magnitude Al measured at those samples reaching to sampling site from NW and SW irrespective of seasons as mentioned in the section

In other words, the only source that could be identified by the use of the EF diagram is the desert source. This region is defined on the EF diagrams by those samples whose Al concentration is greater than 2500 ng m⁻³ and whose Pb Efs are less than 10.

The Pb concentration may always be modified by the advection of the arriving air masses over various emission areas. Marine samples possess the highest EF values since the arriving air masses spent no time over the continents, dilution of the anthropogenic elements with crustal material was at a minimum. The positions on the EF diagram of samples originating from continental areas varies with the meteorological conditions, especially the amount of precipitation, they have suffered during their travel. The EF diagram for Pb indicates a linear inverse trend between this element and the concentration of Al in the eastern Mediterranean atmosphere. That is, the greater the concentration of Al, the smaller the Pb EF. Such a relationship verifies the conclusion in Section 3.3.2.2 that over the eastern

Mediterranean there is a 'background' component, or components, in which the atmospheric particulates have relatively high Pb EF's, but are mixed with, and diluted by, crustal components. This relationship is similar to that found for various different marine atmospheric particulates from the North and South Atlantic, the Red Sea, the Arabian Sea, the Mediterranean Sea and the Black Sea (Chester et al., 1981; 1983, 1989, 1993a; Kubilay et al., 1995b) and is important precisely because it has been shown to operate over many regions of the World Ocean.

The important conclusion to be drawn from the EF diagram of Pb is that the trace metals in atmospheric particulates over the eastern Mediterranean have at least two long-range transported aerosol components. These are the "Eurasian urban" and the "Saharan and Middle East crustal" sources. A knowledge of the characterization of atmospheric aerosol end-members is critical to our understanding of their oceanic fates. There is evidence that the source of a trace metal affects the extent to which it is soluble in seawater. In general, metals having an urban source are more soluble than those derived from crustal weathering that can act as re-scavenging substrates for dissolved constituents of seawater (Chester et al., 1986; 1993b; Kersten et al., 1991). As a result, it is important to identify the extent to which the aerosols from two different sources are mixed together in the eastern Mediterranean atmosphere. This could be achieved by the use of such parameters as enrichment factors and variations in the concentration of Al (which is a crustal indicator) or by air mass back trajectories.

As discussed previously, the elemental mean concentration, or the EFs, of atmospheric elements vary seasonally over the eastern Mediterranean. It must be stressed that the variation in the elemental concentrations or EFs is related to catchment areas (potential source regions supplying material to the atmosphere of the receptor region). When defining regions on the EF diagram the assumption must be made that the scavenging history and the rates of particle production of all the relevant

aerosols must be identical. Consequently, to maintain consistency EF diagrams must be constructed on a seasonal basis.

In the following sections, the elemental chemistry of atmospheric Pb concentrations over the eastern Mediterranean are discussed in terms of the EF diagram.

The data collected in three different seasons are plotted as Pb EF diagrams in Figs.3.51 (a-c). The general impression offered by these enrichment factor diagrams is that of independence of the lead and aluminum concentrations i.e. that the sources were noncrustal.

In the diagram for summer the data clusters in a narrow range of Al concentrations covering one order of magnitude (132-3435 ng m⁻³) whereas the Pb EF changes by two orders of magnitude (26-3589). The spread of enrichment factors within a relatively narrow range of aluminum concentrations seems to imply other enrichment processes are at work. For example, lead is used as an additive in certain gasolines, the combustion of these during summer when traffic activity increased could introduce sizable amounts of lead into the atmosphere. The absence of wet scavenging and stagnation of the air masses throughout this period causes accumulation of Pb in the atmosphere. The apparent minimum Pb concentration during summer was 6.7 ng m⁻³.

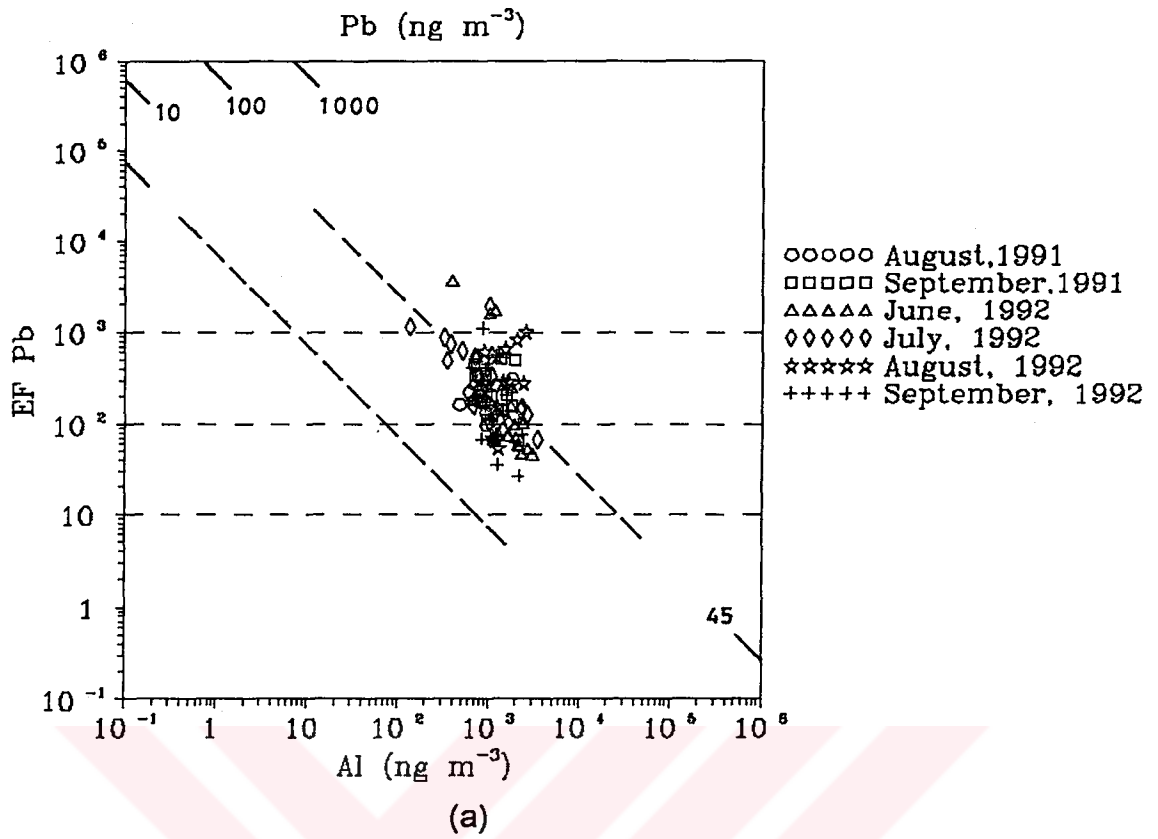
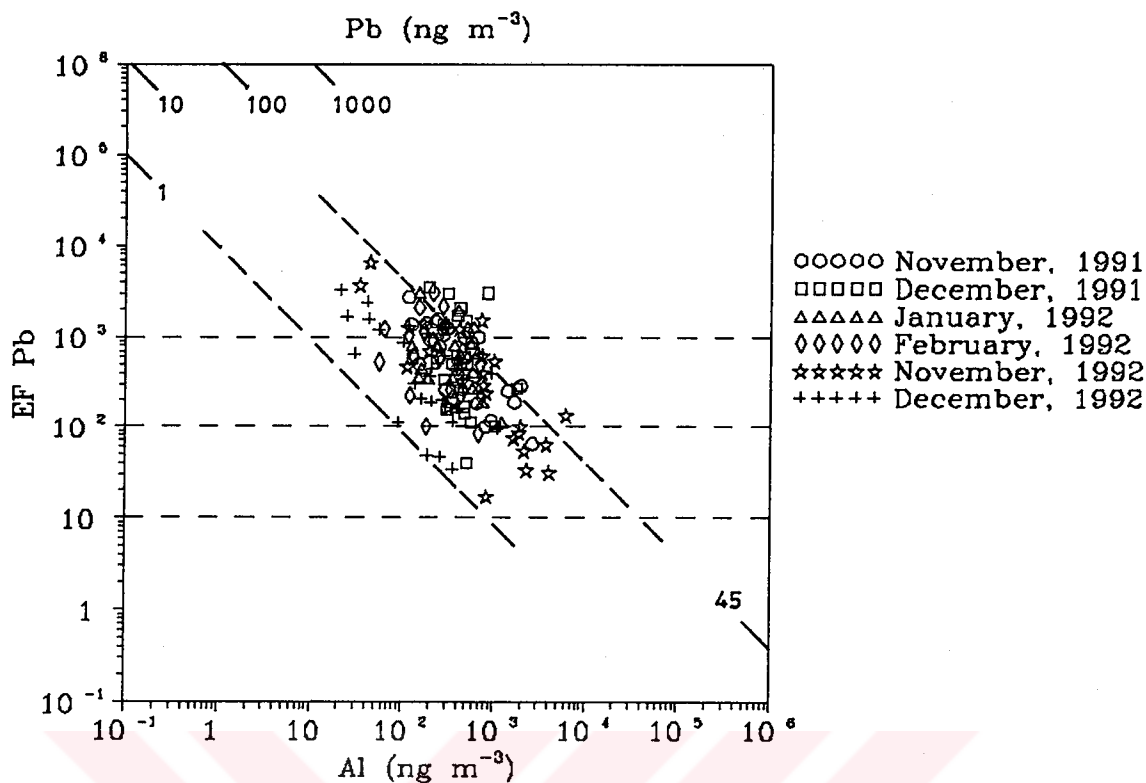


Figure 3.51. EF diagrams of Pb constructed on seasonal basis for the aerosols collected at the Erdemli site.

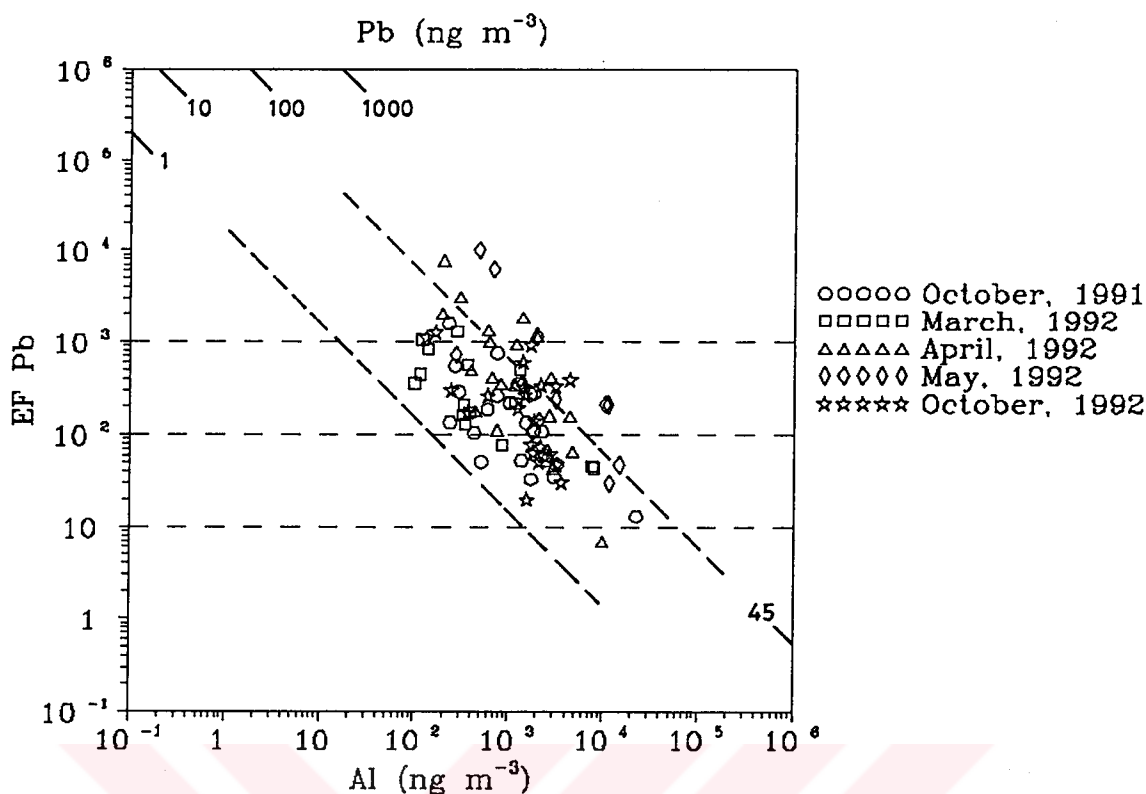
(a) summer (b) winter (c) transitional seasons



(b)

Fig.3.51. Cont.

During winter both Al concentration ($21\text{-}1778 \text{ ng m}^{-3}$) and Pb EF ($33\text{-}3510$) change by two orders of magnitude. The lowest lead concentration observed in winter was 1.4 ng m^{-3} .



(c)

Fig.3.51. Cont.

During transitional months the scatter of data points along the x and y axes is more obvious. Both the Al concentration ($33\text{-}22568 \text{ ng m}^{-3}$) and the Pb EF ($7\text{-}9950$) change by three orders of magnitude. During transitional months the majority of the points are aligned along constant concentration isolines, which is what one expects of enriched elements. Moreover, there appears to be a well-defined lower limit of concentration of about 2.1 ng m^{-3} .

Thus, one concludes that the EF variations observed during the transition seasons are representative of the annual variations of Al and Pb. The discussion has shown another way of presenting the interaction of the various source regions. The specific activities and associated transport efficiencies of particulates within the prevailing air mass is reflected in the

wide dispersion of sample points along the mixing/dilution region on the EF diagram.

3.4. Statistical Techniques in Studying the Relationships Between the Elements

3.4.1. Linear Correlation

The inter-relationship of the complete suite of the analyzed elements is shown by their calculated correlation coefficients in Table 3.13. The crust indicator, Al, is strongly correlated [p(see the correlation coefficient of each pair in Table 3.13,339) < 0.00001] with Fe, Co, V, Ca, Mg, Mn, Ni and Cr. The statistically significant correlation [p(0.25,339)<0.00001] of Al with Zn, which is an anthropogenic element, is surprising. Significant correlations also occur between Al and other anthropogenic elements Pb [p(0.17,339) < 0.002] and Cd [p(0.15,339) < 0.004]. The number of significant correlations which Al exhibits, including Zn, Pb and Cd confirms the common behavior of crustal and anthropogenic elements, either because of a common partial source or because of the mixing of those air masses that have different origins. There is no correlation between Al and Na which does show that these two elements originate from different sources. The significant correlation between Ca, Mg and Na indicates that Ca and Mg are influenced both by seawater and crust.

Table 3.13. Relationships between the elements in the atmospheric particulates

	Ca	Mg	Na	Al	Fe	Mn	Co	Ni	Cr	V	Zn	Pb	Cd
Ca	1	0.77	0.30	0.73	0.57	0.76	0.79	0.67	0.45	0.52	0.29	0.16	0.20
Mg		1	0.56	0.77	0.64	0.79	0.77	0.73	0.40	0.52	0.27	0.13	0.15
Na			1	0.08	0.08	0.15	0.24	0.19	0.04	0.04	0.18	0.03	0.02
Al				1	0.84	0.94	0.83	0.78	0.50	0.71	0.25	0.17	0.16
Fe					1	0.78	0.72	0.68	0.40	0.61	0.36	0.26	0.16
Mn						1	0.88	0.82	0.52	0.75	0.38	0.16	0.20
Co							1	0.79	0.54	0.68	0.27	0.16	0.17
Ni								1	0.63	0.74	0.33	0.35	0.21
Cr									1	0.65	0.20	0.31	0.16
V										1	0.31	0.29	0.27
Zn											1	0.16	0.34
Pb												1	0.13
Cd													1

3.4.2. Factor Analysis

The relationships between the elements have been further explored by factor analysis, which aims to reproduce the correlation matrix in its most emphatic form. In this work, factor analysis utilized the Statgraphic program package. Interpretation of the common factors is facilitated by performing Varimax rotation. As a general rule of thumb in factor analysis, only eigenvalues larger than 1 are retained. Although factors with eigenvalues less than 1 make no significant contribution to the variance of the data they can be retained if they are physically interpretable.

Table 3.14 shows the four factors which explain 80 % of the variance; the first three have eigenvalues greater than 1 and the fourth has an eigenvalue of 0.923. The first factor explains 53% of the variance. Ca, V, Co, Al, Fe, Mn, Ni, Cr, and Mg load heavily in this factor. This factor may be

interpreted as representing aerosols from crustal sources (either local or long distance sources).

Table 3.14. Varimax rotated factor matrix.

Variable	Factor Loading				Communality
	1	2	3	4	
Ca	0.78	0.13	0.32	0.06	0.73
Na	0.08	0.06	0.96	-0.01	0.93
V	0.75	0.22	-0.11	0.34	0.74
Co	0.90	0.09	0.17	0.09	0.86
Al	0.96	0.07	0.003	0.04	0.93
Fe	0.82	0.16	-0.02	0.10	0.71
Mn	0.95	0.17	0.07	0.05	0.94
Ni	0.82	0.14	0.13	0.35	0.83
Cr	0.55	0.07	-0.05	0.54	0.60
Zn	0.22	0.75	0.17	0.09	0.65
Pb	0.07	0.09	0.02	0.91	0.84
Cd	0.09	0.84	-0.06	0.05	0.72
Mg	0.78	0.07	0.55	0.04	0.91
Eigenvalue	6.8	1.4	1.2	0.92	
Cumulative % of variance	53	64	73	80	

The second factor explains a further 11% of the variance. Zn and Cd load heavily in this factor, which may be interpreted as aerosols containing elevated concentrations of trace metals due to the emission from Zn-Cd smelters. The third factor further explains 9% of the variance. Na, Mg and Na load heavily. This factor can be interpreted as aerosol derived from the sea surface (marine contribution). The fourth factor explains a further 7% of the variance. Pb, Cr, Ni and V load heavily and the factor is interpreted as aerosols possibly derived from oil burning and vehicular sources.

It should be noted that the correlation of Al with Zn, Pb and Cd cannot be explained by this factor analysis. The four factor solution is a reasonably good model of the individual variables, the column of communalities shows that the model explains well over 70 % of the variance of each variable, with the exception of Cr and Zn with communalities of about 0.60.

Correlation and factor analysis of the trace element data both indicate that components from crustal and anthropogenic sources behave quite similarly, suggesting that it is not possible to apportion sources on a sub-regional scale and that there is strong meteorological control which produces effective mixing of individual and subregional sources. This explains why a number of elements associated with crustal sources behave similarly to anomalously enriched (anthropogenic) elements and why attempts to apportion sources using elemental ratios have failed.

3.5. The Atmospheric Input of Trace Elements onto the Eastern Mediterranean

The deposition of atmospheric particulate species onto the sea surface can have a significant impact on biological processes and chemical cycling in the oceans (see Chapter 1.). A deficiency of 'bioactive' trace metals may limit oceanic plankton production (Brand et al., 1983). Mineral dust particles are of particular interest because they can provide limiting micronutrients that are required by phytoplankton for various metabolic reactions (Duce and Tindale, 1991). Excess of certain toxic metals especially in urban atmospheric particles may inhibit plankton growth when they deposited on to the sea-surface microlayer (Hardy and Crecellus, 1981).

In November 1987 an airborne pollution monitoring and modeling program was prepared during the WMO/UNEP Workshop on Airborne Pollution of the Mediterranean. This program was then initiated within the framework of the national MED POL monitoring projects of the participating nations. The major goals of the program were identified as follows: to evaluate the importance of the atmospheric transport and deposition of land-based contaminants to coastal and open Mediterranean waters, to assess the airborne contamination levels of potentially harmful substances, to identify source areas for these atmospheric contaminants and to develop predictive models for assessing airborne pollution loads. The program recommended that the priority measurement of trace elements in precipitation and aerosol should include Pb, Zn and Cd (UNEP/WMO, 1989). Results of the modeling effort for the atmospheric transport and deposition of these metals onto the Mediterranean obtained by utilizing emission inventories of the adjacent countries together with meteorological parameters, for the year of 1991, were published in (UNEP/WMO, 1994).

This section emphasizes the estimation of the deposition fluxes of the mineral dust indicator (e.g. Al, Fe and Mn) and pollutant indicator (e.g. Pb, Zn and Cd) elements.

3.5.1. Dry and Wet Deposition Fluxes

The total deposition of chemicals to the ocean from the atmosphere is the sum of the amounts transferred in gas, liquid and solid phases. Materials transferred in gas and solid phases are referred to as 'dry' deposition. Liquid deposition, often referred to as 'wet' deposition, will comprise water and its dissolved gases and

solutes, together with any insoluble material contained therein (GESAMP, 1989).

Since wet and dry deposition comprise the final portion of the atmospheric pathway of chemical constituents, deposition rates must be known in order to determine the eventual impact of continent to ocean and continent to continent transport. It is well known that knowledge of total concentrations alone is insufficient for understanding trace metal-biota interactions, since trace metal-biota interactions, including assimilation, biological limitation and toxicity, are related to the free metal-ion concentrations and their speciation within the sea water (Bruland et al., 1991). The data obtained during this thesis permit the determination only of the total deposition of trace metals which may provide an estimate of the importance of the atmospheric input to the eastern Mediterranean and of its temporal variability.

Recently, an attempt to estimate the yearly atmospheric input of trace elements and mineral aerosol to the world ocean and regional seas using state-of-the-art data and knowledge has shown important gaps and uncertainties (GESAMP, 1989).

Sampling of dry deposition fluxes of particles is generally based on the use of flat plate surfaces or bucket-like collectors, referred to as surrogate surfaces. In view of the drawbacks of such techniques which do not simulate natural surfaces properly, elemental dry deposition fluxes are often estimated using indirect approaches combining model and aerosol measurements techniques.

The dry deposition flux of a given element (F_D) is given by the product of the measured atmospheric particulate concentration of the element (C_p) and its deposition velocity (V_d),

$$F_D = V_d \times C_p$$

The term V_d comprises all the processes of deposition, such as gravitational settling, impaction and diffusion of particles to the water. It is very difficult to describe properly since each of these processes acts simultaneously and because each is dependent on a number of variables (i.e., wind speed, particle size, relative humidity, air viscosity, sea surface roughness). There are two ways to estimate V_d values of the trace metals in aerosols. One is based on field estimates of dry deposition using surrogate surface; the second is to estimate V_d s from the theoretical model of Slinn and Slinn (1980) together with distributions of mass particle sizes generally derived from cascade impactor samplers. Based on modeling efforts, a range of V_d values for various size classes of particles are given in GESAMP (1989) which are indicated below.

Submicrometer aerosol particles:

0.1 cm s^{-1} , \pm a factor of three

Supermicrometer crustal particles not associated with sea-salt:

1.0 cm s^{-1} , \pm a factor of three

Large sea salt particles and materials carried by them :

3.0 cm s^{-1} , \pm a factor of two

The large variation in the V_d values of various trace metals in particles over the Mediterranean have also been confirmed both by experiment and modeling techniques (Migon et al., 1995; Dulac et al., 1989).

The wet deposition flux (F_w) is formally expressed as the product of the precipitation rate (P) and the concentration (C_r) of the substance of interest in rain,

$$F_w = P \times C_r$$

This equation is often expressed not in terms of C_r , which effectively implies making direct flux estimates, but through a scavenging ratio (S) (also sometimes called a washout factor), which is the ratio C_r/C_p ; such that

$$F_w = P \times S \times C_p \times \rho^{-1}$$

in which ρ (the density of air) appears in order to make particle concentrations, which are expressed as mass per unit volume of air (often ng m^{-3}), dimensionless. The attractiveness of the concept is that one can take advantage of numerous ground-level air-concentration measurements to estimate precipitation concentration and wet deposition. The scavenging ratio concept has a limitation in that these ratios are often derived from ground-level air concentrations, which do not necessarily represent the air entering the frontal storms where there can be strong vertical gradients in ambient concentrations. The other factors known to affect the scavenging ratio include the size of the particles being scavenged, their physical and chemical form and such cloud properties as droplet size, temperature and cloud type (GESAMP, 1989). During calculation of the deposition fluxes of the elements in the present study the V_d and S values recommended for the regional seas in GESAMP, (1989) were utilized. That is;

for mineral dust indicator elements $V_d = 1 \text{ cm s}^{-1}$; $S = 1250$
and for pollution-derived elements $V_d = 0.1 \text{ cm s}^{-1}$; $S = 600$.

The contribution of each of the geographical wind sectors mentioned in Section 3.1.1. to the total depositional flux of the

elements considered in this thesis was determined by an approach developed by Vossler et al. (1989). The average fractional contribution of each geographical sector j on element k was calculated using the equation:

$$\frac{[C_{kj}]}{[C_k]} = \frac{1}{N} \sum (C_{ik} \times P_{ij}) / [C_k]$$

where C_{kj} is the concentration of element k from each geographical sector j , C_k is the average concentration of element k in all samples, C_{ik} is the concentration of element k , for sampling period i . Since trajectories were not confined to a single sector during their three days of travel, calculation of sector frequencies (P_{ij}) corresponding to each sample was performed according to the method outlined for grouping of the trajectories into geographical sectors (see Section 3.1.1). During calculation of P_{ij} values, trajectories arriving at 900 hPa were used and all the deposition and C_{kj} calculations performed by the spreadsheet calculation.

The total deposition fluxes of the elements during the year 1992 are presented on a seasonal basis in Table 3.15. The percentage of the total depositions for each season in wet and dry forms are indicated in parenthesis.

In winter 80% of the total deposition of Al, Fe and Mn and about 90% of the total deposition of Zn, Pb and Cd were deposited in the wet form.

In summer Al, Fe and Mn had about 70 % of their total deposition in the dry form. The anthropogenic indicator elements, Zn, Pb and Cd, had about equal percentages of their total deposition in wet and dry forms. This result verifies the findings of Dulac et al. (1992b) that the dry deposition flux of mineral aerosol may be

quantitatively dominant, on a seasonal scale, in marine regions like the Mediterranean having a marked dry season.

Table.3.15. Total atmospheric deposition fluxes of trace elements onto the eastern Mediterranean. The percentages of the total depositions in wet and dry forms are presented in parenthesis ($\text{mg m}^{-2} \text{ year}^{-1}$).

	Winter	Summer	Spring-Fall
Al	295(80,20)	201(27,73)	842(66,34)
Fe	358(81,19)	233(31,69)	1108(72,28)
Mn	5.8(80,20)	3.3(21,79)	9.9(65,35)
Zn	2.7(92,8)	0.9(50,50)	2.7(89,11)
Pb	5.3(94,6)	1.7(63,37)	13.6(91,9)
Cd	0.06(94,6)	0.01(55,45)	0.03(91,9)

During transitional seasons about 70 % of the total deposition of the elements, Al, Fe and Mn, are in wet form whereas this percentage increased to 90% for the elements Zn, Pb and Cd. The total deposition fluxes of Al, Fe, Mn and Zn are maximum in the transitional seasons. The higher Al flux (mineral dust indicator element) during transitional seasons relative to the other seasons is due to the intense Saharan dust outbreaks to the eastern Mediterranean. The effect of the episodic Saharan dust outbreaks on the atmospheric concentrations of the elements was described in Section 3.3. Bergametti et al., (1989b) have shown that in the western Mediterranean about 30 % of the total annual flux of the dust indicator elements (Al and Si) resulted from only one single Saharan dust outbreak to the region observed in March 1986. This indicates that a major fraction of the annual deposition can occur in a small number of the days, as observed also by Prospero et al., (1987) for Saharan dust deposited in Miami (Florida). Although the

mean atmospheric concentrations of the elements were higher in the summer than in the winter (see Section.3.2.4) their corresponding total deposition figures were higher in the winter. As shown in Section 3.1 the greatest percentage of the annual precipitation at the sampling site occurred in winter which confirms the higher efficiency of the wet deposition with respect to dry deposition.

The contributions of each geographical wind sector to the seasonal total deposition of elements at 900 hPa are given in Table 3.16. In winter the contribution from the SW sector to the total deposition of all the elements was minimum except for Pb which enjoyed equal contributions from both the SW and NW sectors.

Table 3.16. Percent contribution of the four geographical sectors at 900 hPa to the mean seasonal total deposition of the elements.

	Winter				Summer				Spring-Fall			
	NE	NW	SW	SE	NE	NW	SW	SE	NE	NW	SW	SE
Al	19	33	14	34	21	40	36	3	37	14	22	27
Fe	17	34	15	34	15	39	43	3	50	14	13	23
Mn	21	36	16	27	21	40	36	3	34	19	21	26
Zn	24	44	6	26	17	38	43	2	48	25	11	16
Pb	18	40	19	23	17	46	31	6	36	39	5	20
Cd	26	39	17	18	21	40	37	2	36	36	12	16

Bergametti (1987) used airflow climatology together with the atmospheric concentrations of the elements over Corsica (western Mediterranean) to evaluate the contributions of the different source regions on a yearly time scale. He suggested that the contribution of Al (mineral dust indicator) associated with flow from the south may have been underestimated because of the lofting of

warm African air masses to considerable height. He estimated that up to 70% of the annual Al deposition comes from Africa.

The percentage contribution of the sectors on the total deposition of Al was recalculated by utilizing 700 and 500 hPa trajectories. The most striking feature found was that during transitional seasons the contribution of the SW sector to the total deposition of Al increased to 68 and 72 % respectively. This result confirms the conclusion in Section.3.3.2.1. that the long-range transport of dust from the SW sector could be identified with the higher level trajectories.

The total deposition fluxes of the elements estimated during this study for the year 1992 are compared with the annual fluxes of the same elements to other regional seas reported in GESAMP, (1989) (see Table 3.17). The depositional flux of the elements are similar both for the North Sea and Baltic Seas and in general they are lower than those given for either the western or eastern Mediterranean.

Table.3.17. Total atmospheric depositions of trace elements onto the regional seas ($\text{mg m}^{-2} \text{yr}^{-1}$).

	North Sea	Baltic Sea	North Western Mediterranean	Eastern Mediterranean
Al	38-150	-	970	1338
Fe	38-150	87	720	1699
Mn	1-5	2.4	22	19
Zn	5-23	11	34	6.3
Pb	4-23	2.4	29	20.6
Cd	0.1-0.5	0.14	1	0.1

The total deposition fluxes of Al and Fe are higher in the eastern than in the western Mediterranean basin. In contrast, the

total deposition fluxes of the pollution derived elements, Zn, Pb and Cd, are lower in the eastern basin. The total deposition of Mn is of similar magnitude in both basins. This is connected with the higher excess concentration of Mn relative to crust in the western Mediterranean (see Section.3.3.2.2). That is, although the total deposition of Mn is the same in both basins, the percentage of pollution derived Mn may be higher in the western than in the eastern basin of the Mediterranean.



CHAPTER IV

CONCLUSIONS

The results obtained through the operation of the first continuous atmospheric sampling tower at the ERDEMLI site have shown clearly:

1. Atmospheric concentrations of elements vary greatly on time scales ranging from days to seasons. Day-to-day and season-to-season changes of one or two orders of magnitude are common especially in the transitional seasons. The variations in the chemical composition and the corresponding dust loading over the eastern Mediterranean basin throughout these seasons are governed by the inputs from desert regions and the Sahara is by far the most important remote source of atmospheric particulates over the basin.

The contrast between the rates of precipitation in Winter and Summer is reflected in the atmospheric concentrations of the elements. During the dry summer seasons the elemental concentrations in the samples were higher than in the wet winter seasons when precipitation scavenging of the atmosphere was effective both at the sampling site and the surrounding regions.

2. The most tedious but, nevertheless, the most scientific approach to understanding the variation in the elemental composition of the samples is to study their daily air mass trajectories. During this study facilities were made available through the LAND-3 project and the Italian Meteorological Office at Erice/Italy to reach ECMWF's (European Centre for Medium Range Weather Forecast, Reading, UK.) Mars archive and compute the air mass back trajectories at different barometric levels. The procedures for reaching

ECMWF's archive and the algorithms used to compute 3-D air mass trajectories for given geographical boundaries at 4 different barometric levels are included in detail in the Appendix. Thus it is possible for anyone to use the steps given herein to compute the air mass back trajectories.

ECMWF's trajectory model and data base were used to calculate three-day back, 3D trajectories arriving at the Erdemli site at 900, 850, 700 and 500 hPa pressure levels on a daily basis between the period of August 1991-December 1992. The calculated trajectories permitted identification of the mean airflow patterns and the origins of air masses in conjunction with the chemical characterization of the aerosols.

Classification of the trajectories into geographical sectors reveal that the dominant air flow pattern to the collection site throughout the sampling campaign was from the NW and SW directions. The contribution of NW flows to samples collected at Erdemli was uniform throughout the year. Southwest flow, especially along the North African coast, was most frequent during spring and autumn (defined as transitional seasons throughout this thesis). During the summer the frequency of air flow from this direction within the free atmosphere (500 hPa) was similar to that observed during transitional seasons. Northeast continental flow was most frequent during the summer and was usually confined within the boundary layer. SE flow from the Middle East was infrequent, occurring mainly within the boundary layer during winter and the transitional seasons. This review of the general circulation of the atmosphere over the eastern Mediterranean provided a starting point for the discussion of the long-range transport of material. Much evidence found in the literature and throughout this study supports the idea that long-range atmospheric transport is important in moving both natural and man-made substances around the world. Throughout the sampling period it was only the desert dust that gave a signal from a distant source that could be distinguished from the highly variable local background signal. The episodic influx of desert dust from the surrounding arid regions to the sampling site greatly increased our

awareness of how effective meteorological processes are in generating and distributing material throughout the environment. These meteorological events, by their episodic nature, do not appear explicitly in the average atmospheric circulation. However, they strongly influence the amount of dust transport and, depending on their strength and frequency, they may influence the long-term average of the atmospheric concentrations. The height to which dust is carried over the desert regions may have a large influence on its eventual range of transport. In addition, at the time of transport, mechanisms that vertically redistribute substances in the atmosphere, in particular from the planetary boundary layer where wet and dry removal processes are effective, to the region of the free troposphere where greater vertical stability and higher wind speeds prevail, have a significant influence on the efficiency of large-scale transport.

3. The vertical dimension of the air mass back trajectories is particularly essential in understanding the availability of desert dust for atmospheric transport. In such analyses it has been shown clearly that dust is transported if, and only if, the upper boundary trajectories were close to ground level over the source regions. In other words, consistent with the climatological analysis of the eastern Mediterranean depressions by Alpert et al., (1990,a,b) the presence of deep cyclonic meteorological events over the source regions, especially during the transition months, often results in upward movement of the upper trajectories. This is a necessary step for the uplift and possible long range transport of desert dust over the basin.

As a conclusion the uplift of dust above the atmospheric boundary layer over the source regions can be achieved by;

(a) synoptic-scale vertical motions (from a front or cyclone) which account for the intense events observed in transitional seasons.

(b) the vigorous convection processes over the North African continent which initiate the non-intense rarely observed events in summer.

3. Recent advances in remote-sensing technology and the associated data-analysis techniques have resulted in important new capabilities for verifying the long-range transport of desert dust. The use of satellite (METEOSAT-PDUS) data demonstrated the transport of desert dust during synoptic scale meteorological events. Various techniques can be used to manipulate digital data in order to understand the presence of dust over the continents and sea. The techniques used to differentiate dust over the continents also reveal the disturbances caused by dust pulses on the radiative processes of the planet. The observation of dust pulses by the NOAA AVHRR data collected at the Institute since 1994 has successfully demonstrated that satellite data can be used for the identification of dust transport over the sea or land. Other data from various satellites such as NOAA TIROS-N or METEOSAT can be used to predict and trace the hourly propagation of the clouds in association with synoptic scale meteorology. Since 1992 demodulators have also enabled us to receive synoptic scale surface meteorological charts from ECMWF/UK. These further support the real time satellite data and their description of dust transport. Thus it can be suggested that any atmospheric sampling program should always be supported by satellite data.

4. The 3 days air mass back trajectories are an essential tool for the understanding of atmospheric transport from a variety of sources. The study has further shown the necessity of the computation of air mass trajectories at different levels within the atmosphere. The barometric levels defining transport within the boundary layer (i.e. 900 and 850 hPa) are necessary in order to understand the perturbations caused by local sources.

5. The air masses arriving at the sampling station above the boundary levels (i.e. 700 and 500 hPa) were responsible for the observed fluctuations in the particulate matter concentrations. The knowledge of air mass history above the boundary levels is important, not only because these levels are the main

transport mechanism of desert dust but also because they introduce clear air masses over the sampling region especially during winter. During the course of low dust periods (i.e. during winter when the air mass mainly originates over the European continent with a long fetch, both above and below the boundary levels) the chemical composition of the particulates varies little compared to air mass originating from local sources. This highlights the fact that particulates originating from local sources during low dust periods appear to have the same composition as the air mass arriving from the European continent. It may be that the air mass originating from the European continent during winter contains insufficient material to alter the chemical composition of material transported below the boundary layer.

Although the geographical classification of the origin of the air-mass trajectories has shown there to be a potential for long-range transport of aerosols from Europe, the differences observed between the mean atmospheric elemental concentrations associated with short and long range transport from the NW geographical sector were insignificant compared with their large standard deviations.

6. Although precipitation scavenging of the atmosphere was effective during the transitional seasons, the arithmetic means of the atmospheric concentrations of the dust indicator elements (e.g. Al and Fe) were about four times higher than the winter means and twice as high as the summer means. That the long-range transport of Saharan dust dominates the chemical character of the aerosols over the basin in the transitional months and especially during March and May, further exemplifies the importance of the material over the basin which originates from the deserts. By utilizing the air mass back trajectory information and the atmospheric concentration of Al it was estimated that about 70 % the total deposition flux of this element in transitional seasons originated from the SW sector.

7. The concentration of dust in the atmosphere reaches its peak during the transition months and varies with the synoptic scale meteorology over the source region. The presence of dust masks all other local sources that are present along its path. Any local perturbations from anthropogenic sources can still be explained, however, from the vertical dimension of the trajectories arriving within the boundary level. Dust transport takes place as pulses even within the transitional seasons. This is another important peculiarity of dust transport which has been shown to affect the heat budget of the Mediterranean Sea (Garrett et.al., 1994). Thus it is important to know how each pulse of dust was transported; annual averages may cancel the importance of pulse transport. Further, the annual dust loadings of the eastern basin, although much more significant than those in the western basin, will underestimate the biological impact of dust pulses on the sea surface. Since Saharan crust-dominated aerosols are delivered in the form of pulses and can impose intermittent non-steady state conditions in the mixed layer when they are subsequently deposited to the sea surface, particular attention must be paid to estimating the input of Saharan aerosols to the eastern Mediterranean. Monitoring of dust pulses by satellite remote sensing available at the Institute has emphasized their impact on biological production within the sea surface and their possible effect on climatic variability.

8. Analysis has further shown the necessity for increased frequency of sampling especially during transitional seasons. It is well known that any synoptic scale cyclonic event approaches the sampling point in association with frontal systems which are often associated with abrupt rain and followed by drastic change in the direction of the winds following the depression. This study has shown that the air mass following the cyclonic events provides the main reason for the observed fluctuations in the dust loadings during transitional seasons when maximum dust loadings are followed by very low dust concentrations similar to those attained during winter. This

necessitates change in the frequency of the sampling strategy which may further complicate the logistics of the sampling. The position of the sampling tower used in this study, though by no means ideal for atmospheric sampling, was a wise choice logistically. The aim of a daily sampling frequency has not been satisfied but the rate of sampling was greater than that achieved at most other land based stations. The results of this study clearly show the need for refinement in the sampling strategy so that variations within each synoptic scale event could be sampled. This may be solved in future studies by the use of multiple samplers possibly operated automatically coupled to a wind sector controller or remotely operated. Such sampling might further highlight the importance of pulse transport since the present sampling strategy must have always underestimated the dust arriving at the sampling site.

Thus the importance of the dust episodes that originated from the Sahara - this desert being the largest single mineral aerosol source for the northern hemisphere - may be much more important than was thought before. Any increase in the global temperature due to the greenhouse effect can simply increase the aridity over the Sahara and make more dust available for long range transport, even with the present magnitude of the synoptic scale meteorological events. In fact recent statistics demonstrates that over the sub-Saharan the average rainfall has declined since 1970 (in Tucker et al., 1991). Therefore, long term statistics concerning the transport of Saharan dust could become even more important than previously thought and in this respect the present study could be an important milestone.

9. The analysis of the elemental concentrations can be discussed in many ways. The techniques involved in this study have shown various methodologies to be available for such discussion and all reach the same conclusions about the reasons for observed variations in elemental concentrations. In order to reduce the large amount of data and provide a

basis for the description and interpretation of the results, the method of factor analysis has been applied to the data set. The results of factor analysis have revealed that four factors together explain 80 % of the total variance in the data set. Factor 1 has high loadings for Ca, V, Co, Al, Fe, Mn, Ni, Mg and, to a smaller degree for Cr. This factor explains about 53 % of the variance. Aluminosilicates, both windblown soil dust from remote desert areas and local sources probably correspond to this factor. Factors 2 and 4 explain a further 18 % of the variance. Cd, Zn, Pb load heavily on these factors, as to a lesser extent do V, Ni and Cr. This factor is interpreted as the emissions from anthropogenic sources, which are possibly derived from metallurgical processes (Zn, Cd, Cr) and combustion processes (Pb, V, Ni). Factor 3 probably represents marine impact on the elemental concentrations of the aerosols over the Erdemli site (which is a rural location near the seaside) and explains 7 % of the variance.

10. The elemental data, as illustrated for lead, can also be expressed in terms of EF diagrams. Such diagrams can explain all the peculiarities of the variations in the dust loadings. It is possible to identify desert input regions as well as samples that have suffered from urban pollution that delineate a contrasting region. The majority of the samples are shown to occupy a region defined as the mixing-dilution region. The orientation of individual samples within this region further varies in accordance with the past history of the air mass corresponding to the specific element. It has been found possible to combine various published results together with the present data on the same figure, thus enabling one to see the effect of basinwide and even global variations of the elements.

Thus, although enrichment factors can be useful in differentiating the anthropogenic and natural elements the effects of different natural sources (e.g. the variable composition of local soil) can complicate any simple interpretation.

CHAPTER V

RECOMMENDATIONS FOR FUTURE RESEARCH

This work is based on studies confined to samples that have been collected from Aug 1991 to the end of Dec 1992. However, the sampling program at the institute has been continued till the present day. Thus, part of the recommended future work to understand the interannual variability in the long range transport of desert dust is already in progress. During the course of 1994 another step in the possible recommended work is being realized and the transport of dust pulses has been forecasted, using the NMC ETA step mountain model, by the team present at ERICE-Italy within the LAND-3 project. The establishment of the satellite remote sensing facilities at Erdemli, enabling the tracing of dust pulse transport using both NOAA TIROS-N series satellites and METEOSAT WEFAX data has also been realized at the institute. Satellite imagery can be used to identify major dust storms over the desert. Dust storms are most visible in the infrared (IR) spectrum. Because of the altitude of a dust cloud, it radiates at a temperature cooler than that at the earth's surface; hence, in the black-and-white photographs from the geostationary (METEOSAT) satellite, a dust cloud appears as a light-toned area against the black (hot) desert surface. The history of a dust cloud can be followed from the time that it appears until it crosses the northeast coast of Africa. Over the Mediterranean it can be followed in the imagery taken at visible-light wavelengths. Unfortunately, dust storms are difficult to identify when water clouds are present. Thus, the relative importance of dust sources and transport can not be qualitatively assessed on the basis of satellite imagery alone.

The continuation of the work at Erice within the Land-3 program has reached the stage that at present we are able to predict the occurrence of dust pulses by the model and subsequently observe them by satellites.

The knowledge gained during this study highlighted the importance of Saharan dust pulse events during April and one such event was recorded by satellite and by ground truth measurements (Karakoc, 1995) during 6-7 April 1994. The biological response of the eastern Mediterranean ecosystem was reflected in the blooming of coccolithophorid organisms (*Emiliana Huxleyi*) following the episodic influx of Saharan dust recorded in satellite data as high reflectance from the sea surface. Again, in April, 1995, it was proven by ground-truth that the observation of high reflectance from the seasurface following the episodic influx of Sahara dust was indeed caused by the blooming of *Emiliana Huxleyi* (Saydam 1995; Saydam et al. 1995 a,b).

Thus the biological impact of Saharan dust that would otherwise have been the subject of another recommendation has also been taken care of. Recent publications have further highlighted the importance of Fe on the marine biological cycle. The diurnal cycle in the dissolution of the Fe associated with desert dust within the clouds during day time is the prime suspect for the source of biologically available Fe. A latitudinal solar light dependency of the photochemical dissolution of Fe has been proposed and the distribution of the reported *Emiliana Huxleyi* blooms over the world ocean has been tested on this basis. This has conditioned the sampling strategy for dust pulses arriving at Erdemli during the spring of 1996.

Sulzberger and Laubscher, (1995) have demonstrated that an essential parameter in the photochemical dissolution of iron is its mineralogical form and these authors showed that it is the iron in lepidocrosite that can undergo photochemical dissolution. Ongoing international cooperation with Erice has further incorporated the

photochemistry and the biological uptake of Fe(II) by the microorganisms described by Johnson et al., (1994). Srdjan (1995) demonstrated that the high reflectance regions observed by satellite following the Saharan dust influx observed in April 1994 can be reproduced well by the model results.

It is therefore essential that further research should be devoted toward the characterization of the mineralogical state of the iron within the Saharan dust and the determination of the possible effect of the desert dust matrix on the bloom of specific organisms. It is also necessary to develop atmospheric models that incorporate the photochemistry of iron and its diurnal cycle during its transport.

As a general recommendation, it is time to begin planning an intensive desert dust transport field program over the Mediterranean. The experiment should include; (a) a network of ground stations at receptor sites (which would also study water column processes). More experimental data would be useful for the accurate determination of trace metal deposition on the Mediterranean Sea, especially continuous sets of concentrations for long periods of time, since concentrations of elements change vigorously during a time scale of days (b) remote sensing; (c) modellers; (d) biologists and meteorologists.

This proposed program should be carried out in at least 2 years. The coupling of atmospheric deposition and biological productivity in surface seawater is one of the most important consequences of the long-range transport of desert dust and the proposed programme would provide valuable data to the entire scientific community studying the long-range transport of dust and its possible effect on marine bio-geochemical cycles.

REFERENCES

Ackerman, S. A. and H. Chung (1992). Radiative Effects of Airborne Dust on Regional Energy Budgets at the Top of the Atmosphere. *Journal of Applied Meteorology*, **31**, 223-233.

Al-Momani, I.F. (1995). Long-Range Atmospheric Transport of Pollutants to the Eastern-Mediterranean Basin. *Ph.D. Dissertation*. METU Department of Environmental Engineering, Ankara, 223.pp.

Alpert, P., U. Neeman and Y. Shay-El (1990a). Intermonthly Variability of Cyclone Tracks in the Mediterranean. *Journal of Climate*, **3**, 1474-1478.

Alpert, P., U. Neeman and Y. Shay-El (1990b). Climatological Analysis of Mediterranean Cyclones Using ECMWF Data. *Tellus*, **42A**, 65-77.

Aslaner, M. (1973). Geology and Petrography of the Ophiolites in the Iskenderun-Kirikhan Region. *Publ. Min. Res. and Explor. Inst. Publ.*, Ankara, No. 50, 71p. & appendices.

Arimoto, A., R.A. Duce, B.J. Ray, A.D. Hewitt and J. Williams (1987). Trace Elements in the Atmosphere of American Samoa: Concentrations and Deposition to the Tropical South Pacific. *Journal of Geophysical Research*, **92**, 8465-8479.

Artz, R., R.A. Pielke and J. Galloway (1985). Comparison of the ARL/ATAD Constant Level and the NCAR Isentropic Trajectory Analyses for Selected Case Studies. *Atmospheric Environment*, **19**, 47-63.

Berg, W.W. and J.W. Winchester (1978). Aerosol Chemistry of the Marine Atmosphere. In: Chemical Oceanography, vol.7. J.P. Riley and R. Chester (eds.), Academic Press, London, pp.173-232.

Bergametti, G. (1987). Apports de matiere par voie atmospherique a la Mediterranee occidentale: Aspects geochimiques et meteorologiques. *Ph.D. Dissertation*. Univ. of Paris, 296 pp.

Bergametti, G., L. Gomes, E. Remoudaki, M. Desbois, D. Martin, P. Buat-Menard (1989a). Present Transport and Deposition Patterns of African Dusts to the North-Western Mediterranean. In: Paleoclimatology and Paleometeorology: Modern and Past Patterns of Global Atmospheric Transport, M. Leinen and M. Samthein (eds.), Kluwer Academic Publisher, pp.227-252.

Bergametti, G., A.L. Dutot, P. Buat-Menard, R. Losno and E. Remoudaki (1989b). Seasonal Variability of the Elemental Composition of Atmospheric Aerosol Particles over the Northwestern Mediterranean. *Tellus*, **41B**, 353-361.

Bergametti, G., E. Remoudaki, R. Losno, E. Steiner, B. Chatenet and P. Buat-Menard (1992). Source, Transport and Deposition of Atmospheric Phosphorus over the Northwestern Mediterranean. *Journal of Atmospheric Chemistry*, **14**, 501-513.

Bertine, K.K. and E.D. Goldberg (1971). Fossil Fuel Combustion and Major Sedimentary Cycle. *Science*, **173**, 233-235.

Bethoux, J.P., P. Courau, E. Nicolas and D. Ruiz-Pino (1990). Trace Metal Pollution in the Mediterranean Sea. *Oceanologica Acta*, **13**, 481-488.

Bethoux, J.P. and B. Gentili (1994). The Mediterranean Sea, A Test Area For Marine And Climatic Interactions. In: Ocean Processes in Climate Dynamics: Global and Mediterranean Examples P. Malanotte-Rizzoli and A.R. Robinson (eds.) NATO ASI Series, vol.419, Kluwer Academic Publishers. pp.239-254.

Betzer, P.R., K.L. Carder, R.A. Duce, J.T. Merrill, N.W. Tindale, M. Uematsu, D.K. Costello, R.W. Young, R.A. Feely, J.A. Breland, R.E. Bernstein and A.M. Greco (1988). Long-Range Transport of Giant Mineral Aerosol Particles. *Nature*, **336**, 568-571.

Biggins, P.D.E. and R.M. Harrison (1979). Atmospheric Chemistry of Automotive Lead. *Environmental Science and Technology*, **13**, 558-565.

Biostatistical Analysis (1984). Jerrold H. Zar. Prentice-Hall, 718 pp.

Brody, L.R. and M.J.R. Nestor (1980). Handbook for Forecasters in the Mediterranean, Part 2. Regional forecasting aids for the Mediterranean Basin. Naval Environmental Prediction Research Facility, Monterey, California, (Technical Report TR 80-10). pp.VII-1;VII-13.

Blank, M., M. Leinen and J.M. Prospero (1985). Major Asian Aeolian Inputs Indicated by the Mineralogy of Aerosols and Sediments in the Western North Pacific. *Nature*, **314**, 84-86.

Boutron, C.F., U. Gorlach, J.P. Candelone, M.A. Bolshov and R.J. Delmas (1991). Decrease in Anthropogenic Lead, Cadmium and Zinc in Greenland Snows Since the Late 1960s. *Nature*, **353**, 153-156.

Boyle, E.A., S.S. Husted and B. Grant (1982). The Chemical Mass Balance of the Amazon Plume-II. Copper, Nickel, and Cadmium. *Deep-Sea Research*, **29**, 1355-1364.

Brand, L.E., W.G. Sunda and R.R.L. Guillard (1983). Limitation of Marine Phytoplankton Reproductive Rates by Zinc, Manganese, and Iron. *Limnol. Oceanogr.*, **28**, 1182-1195.

Bruland, K.W. (1983). Trace Elements in Seawater. In: Chemical Oceanography, vol.8, J.P. Riley and R. Chester (eds), Academic Press, London, pp.157-221.

Bruland, K.W., J.R. Donat and D.A. Hutchins (1991). Interactive Influences of Bioactive Trace Metals on Biological Production in Oceanic Waters. *Limnol. Oceanogr.* **36**, 1555-1557.

Buat-Menard, P. and R. Chesselet (1979). Variable Influence of the Atmospheric Flux on the Trace Metal Chemistry of Oceanic Suspended Matter. *Earth and Planetary Science*, **42**, 399-411.

Buat-Menard, P., E. Remoudaki, J.C. Miquel, G., Bergametti, C.E. Lambert, U. Ezat, C. Quétel, J. La Rosa and S.W. Fowler (1989). Non-Steady-State Biological Removal of Atmospheric Particles from Mediterranean Surface Waters. ***Nature***, **340**, 131-134.

Carlson, T.N. and J.M. Prospero (1972). The Large-Scale Movement of Saharan Air Outbreaks Over the Northern Equatorial Atlantic. ***Appl. Meteorol.***, **11**, 283-297.

Cashetto, S. and R. Wollast (1979). Aluminium in Seawater: Control by Biological Activity. ***Marine Chemistry***, **7**, 141-155.

Chase, E.M. and F.L. Sayles (1980). Phosphorus in Suspended Sediments of the Amazon River. ***Estuarine Coastal Shelf Science***, **11**, 383-391.

Chen, L., R., Arimoto and R.A. Duce (1985). The Sources and Forms of Phosphorus in Marine Aerosol Particles and Rain From Northern New Zealand. ***Atmospheric Environment***, **19**, 779-787.

Chester, R., G.G. Baxter, A.K.A. Behairy, K. Conner, D. Cross, H. Elderfield and R.C. Padhgam (1977). Soil Sized Eolian Dusts from the Lower Troposphere of the Eastern Mediterranean Sea. ***Marine Geology***, **24**, 201-217.

Chester, R., A.C. Saydam and E.J. Sharples (1981). An Approach to the Assessment of Local Trace Metal Pollution in the Mediterranean Atmosphere. ***Marine Pollution Bulletin***, **12**, 426-431.

Chester, R., E.J. Sharples and G.S. Sanders (1984). Saharan Dust Incursion Over the Tyrrhenian Sea. ***Atmospheric Environment***, **18**, 101-123.

Chester, R. (1986). The Marine Aerosol. In: The Role of Air-Sea Exchange In Geochemical Cycling, P. Buat-Menard (ed). NATO ASI Series, vol.185, pp.443-476. D. Reidel Publishing Company.

Chester, R., K.J.T. Murphy, J. Towner and A. Thomas (1986). The Partitioning of Elements in Crust-Dominated Marine Aerosols. ***Chemical Geology***, **54**, 1-15.

Chester R., M. Nimmo and K.J.T. Murphy (1989). Atmospheric Inputs of Trace Metals and Nutrients to the Western Mediterranean - The EROS 2000 Programme. In: Water Pollution Research Reports, 13, J.M. Martin and H. Barth (eds.), pp.357-366. EROS 2000, First Workshop on the North-West Mediterranean Sea. Commission of the European Communities, Brussels.

Chester, R. (1990a). The Transport of Material to the Oceans: The Atmospheric Pathway. In: Marine Geochemistry, pp. 83-134. Chapman & Hall.

Chester, R. (1990b). The Atmospheric Transport of Clay Minerals to the World Ocean. In: *Proceeding of the 9th International Clay Conference*, Strasbourg, 1989, V.C. Farmer and Y. Tard (eds.), Sci. Geol. Mem., 88, Strasbourg, pp.23-32.

Chester, R., M. Nimmo, K.J.T. Murphy and E. Nicolas (1990c). Atmospheric Trace Metals Transported to the Western Mediterranean: Data From a Station on Cap Ferrat. In: Water Pollution Research Reports, 20, J.M. Martin and H. Barth (eds.), pp.597-612. EROS 2000, Second Workshop on the North-West Mediterranean Sea. Commission of the European Communities, Brussels.

Chester, R. and G.F. Bradshaw (1991). Source Control on the Distribution of Particulate Trace Metals in the North Sea Atmosphere. ***Marine Pollution Bulletin*, 22**, 30-36.

Chester, R., A.S. Berry and K.J.T. Murphy (1991a). The Distributions of Particulate Atmospheric Trace Metals and Mineral Aerosols Over the Indian Ocean. ***Marine Chemistry*, 34**, 261-290.

Chester, R., M. Nimmo, M. Alarcon and P. Corcoran (1991b). The Chemical Character of the North Western Mediterranean Aerosol. In: Water Pollution Research Reports, 28, J.M. Martin and H. Barth (eds.), pp.495-504. EROS 2000, Third Workshop on the North-West Mediterranean Sea. Commission of the European Communities, Brussels.

Chester, R., M. Nimmo, M. Alarcon, C. Saydam, K.J.T. Murphy, G.S. Sanders and P. Corcoran (1993a). Defining the Chemical Character of

Aerosols from the Atmosphere of the Mediterranean Sea and Surrounding Regions. *Oceanologica Acta*, **16**, 231-246.

Chester, R., K.J.T. Murphy, F.J. Lin, A.S. Berry, G.A. Bradshaw and P.A. Corcoran (1993b). Factors Controlling the Solubilities of Trace Metals From Non-Remote Aerosols Deposited to the Sea Surface by the 'Dry' Deposition Mode. *Marine Chemistry*, **42**, 107-126.

Chester, R., G.F. Bradshaw and P.A. Corcoran (1994). Trace Metal Chemistry of the North Sea Particulate Aerosol; Concentrations, Sources and Sea Water Fates. *Atmospheric Environment*, **28**, 2873-2883.

Chou, L. and R. Wollast (1989). Distribution And Geochemistry of Aluminium in the Mediterranean Sea. In: Water Pollution Research Reports, 13, J.M. Martin and H. Barth (eds.), pp.232-241. EROS 2000, First Workshop on the North-West Mediterranean Sea. Commission of the European Communities, Brussels.

Church, T.M., R. Arimoto, L.A. Barrie, F. Dehairs, F. Dulac, T.D. Jickells, L. Mart, W.T. Sturges and W.H. Zoller (1990). The Long-Range Atmospheric Transport of Trace Elements: A Critical Evaluation. In: The Long-Range Atmospheric Transport of Natural and Contaminant Substances A.H. Knap (ed.), Kluwer Academic Publishers, Netherlands, pp.37-58.

Copin-Montegut, G., P. Courau and E. Nicolas (1986). Distribution and Transfer of Trace Elements in the Western Mediterranean. *Marine Chemistry*, **18**, 189-195.

Correggiari, A., S. Guerzoni, R. Lenaz, G. Quarantotto and G. Rampazzo (1989). Dust Deposition in the Central Mediterranean (Tyrrhenian and Adriatic Seas): Relationships With Marine Sediments and Riverine Input. *Terra Nova*, **1**, 549-558.

Coude-Gaussen, G., P. Rognon, G. Bergametti, L. Gomes, B. Strauss, J.M. Gros and M.N. Le Corustumer (1987). Saharan Dust on Fuerteventura Island (Canaries): Chemical and Mineralogical Characteristics, Air Mass Trajectories, and Probable Sources. *Journal of Geophysical Research*, **92 (D8)**, 9753-9771.

D'Almeida, G.A. (1986). A Model for Saharan Dust Transport. ***Journal of Climatology and Applied Meteorology***, **25**, 903-916.

Davies, T.D., M. Tranter, T.D. Jickells, P.W. Abrahams, S. Landsberger, K. Jarvis and C.E. Pierce (1992). Heavily-Contaminated Snowfalls in the Remote Scottish Highlands: A Consequence of Regional Scale Mixing and Transport. ***Atmospheric Environment***, **26**, 95-112.

Dayan, U. (1986). Climatology of Back Trajectories from Israel Based on Synoptic Analysis. ***Journal of Climate and Applied Meteorology***, **25**, **5**, 591-595.

Dayan, U., J. Heffter, J. Miller and G. Gutman (1991). Dust Intrusion Events into the Mediterranean Basin. ***Journal of Applied Meteorology***, **30**, **8**, 1185-1199.

Devlet Meteoroloji İşleri Genel Müdürlüğü (1984). Ortalama, Ekstrem Sıcaklık ve Yağış Değerleri Bülteni (Günlük-Aylık). 678 sayfa.

Dobricic, S. (1995). A Simulation of Saharan Dust Transport and Its Influence on Phytoplankton Growth. Presented in the Workshop on Impact of Africa Dust Across the Mediterranean. Oristano, Sicily, Italy, 4-7 October 1995.

Donaghay, P.L., P.S. Liss, R.A. Duce, D.R. Kester, A.K. Hanson, T. Villareal, N.W. Tindale and D.J. Gifford, (1991). The Role of Episodic Atmospheric Nutrient Inputs in the Chemical and Biological Dynamics of Oceanic Ecosystems. ***Oceanography***, **4**, **2**, 62-70.

Duce, R.A., R. Arimoto, B.J. Ray, C.K. Unni and P.J. Harder (1983). Atmospheric Trace Elements at Enewatak Atoll: 1, Concentrations, Sources, and Temporal Variability. ***Journal of Geophysical Research***, **88**, 5321-5342.

Duce, R. (1986). The Impact of Atmospheric Nitrogen, Phosphorus and Iron Species on Marine Biological Productivity. In: The Role of Air-Sea Exchange in Geochemical Cycling, P. Buat-Menard (ed.). NATO ASI Series, vol.185, pp.497-529. D. Reidel Publishing Company.

Duce, R. (1989). SEAREX: The Sea-Air Exchange Program. In: Chemical Oceanography, vol.10. J.P. Riley and R. Chester (eds.), London, Academic Press Limited, pp.1-14.

Duce, R.A. and N.W. Tindale (1991). Atmospheric Transport of Iron and Its Deposition in the Ocean. *Limnology and Oceanography*, **36(8)**, 1715-1726.

Dulac, F., P. Buat-Menard, M. Arnold and U. Ezat, (1987). Atmospheric Input of Trace Metals to the Western Mediterranean Sea: 1. Factors Controlling the Variability of Atmospheric Concentrations. *Journal of Geophysical Research*, **92(D7)**, 8437-8453.

Dulac, F., P. Buat-Menard, U. Ezat, S. Melki and G. Bergametti (1989). Atmospheric Input of Trace Metals to the Western Mediterranean: Uncertainties in Modelling Dry Deposition From Cascade Impactor Data. *Tellus*, **41B**, 362-378.

Dulac, F., D. Tanre, G. Bergametti, P. Buat-Menard, M. Desbois and D. Sutton, (1992a). Assessment of the African Airborne Dust Mass Over the Western Mediterranean Sea Using Meteosat Data. *Journal of Geophysical Research*, **97(D2)**, 2489-2506.

Dulac, F., G. Bergametti, R. Losno, E. Remoudaki, L. Gomes, U. Ezat and P. Buat-Menard (1992b). Dry Deposition of Mineral Aerosol Particles in the Marine Atmosphere: Significance of the Large Size Fraction. In: Precipitation Scavenging and Atmosphere-Surface Exchange, S.E. Schwartz and W.G.N. Slinn (eds.), vol. 2, 841-854. Hemisphere Publishing Corp., Richland, WA.

Dulac, F., I. Jankowiak, M. Legrand, D. Tanre, C.T. N'Doume, F. Guillard, D. Lardieri, W. Guelle and J. Poitou (1994). Meteosat Imagery For Quantitative Studies of Saharan Dust Transport. In: Proceedings of the Meteosat Scientific Users Meeting, Cascais, Portugal, 5-9 Sept. 1994, EUMETSAT, Darmstadt, Germany, pp.391-400.

Emelyanov, E.M. and K.M. Shimkus (1986). Geochemistry and Sedimentology of the Mediterranean Sea, Dordrecht, D. Reidel Publishing Company, 553pp.

Ergin, M., S.N. Alavi, M.N. Bodur, V. Ediger, M. Okyar, (1988). A Review of the Geology and Geochemistry of the Northeastern Mediterranean Basins. IMS-METU Technical report.

Evans, G. (1972). Recent Sedimentation on the Southern Turkish Coast and Adjacent Mediterranean Between Turkey and Cyprus. Interim Report No.1, Imperial College, London.

Finden, D.A.S., E. Tipping, G.H.M. Jaworski and C.S. Reynolds (1984). Light-Induced Reduction of Natural Iron (III) Oxide and Its Relevance to Phytoplankton. *Nature*, **309**, 783-784.

Fowler, S.W., P. Buat-Menard, Y. Yokoyama, S.Ballestra, E. Holm and H.V. Nguyen (1987). Rapid Removal of Chernobyl Fallout from Mediterranean Surface Waters by Biological Activity. *Nature*, **329**, 56-58.

Fowler, S.W., S. Ballestra, J. La Rosa, E. Holm and J.J. Lopez (1990). Flux of Transuranium Nuclides in the Northwestern Mediterranean Following Chernobyl Accident. *Rapp. Comm. int. Mer Medit.*, **32**, 317.

Franzen L.G., M. Hjelmroos, P. Kallberg, E. Brorstrom-Lunden, S. Juntto and A.L. Savolainen (1994). The 'Yellow Snow' Episode of Northern Fennoscandia, March 1991-A Case Study of Long-Distance Transport of Soil, Pollen and Stable Organic Compounds. *Atmospheric Environment*, **28**, 3587-3604.

Froelich, P.N. (1988). Kinetic Control of Dissolved Phosphate in Natural Rivers and Estuaries: A Primer on the Phosphate Buffer Mechanism. *Limnology and Oceanography*, **33**, 649-668.

Ganor, E. and Y. Mamane (1982). Transport of Saharan Dust Across the Eastern Mediterranean. *Atmospheric Environment*, **16**, **3**, 581-587.

Ganor, E., H.A. Foner, S. Brenner, E. Neeman and N. Lavi (1991). The Chemical Composition of Aerosols Settling in Israel Following Dust Storms. *Atmospheric Environment*, **25A**, 2665-2670.

Ganor, E. (1994). The Frequency of Saharan Dust Episodes over Tel Aviv, Israel. *Atmospheric Environment*, **28**, 2867-2871.

GBC 906 and 908 Atomic Absorption Spectrophotometers Operation Manual (1990). Publication number: 01-0037-00. GBC Scientific Equipment Pty Ltd; Australia.

GESAMP (Joint Group of Experts on the Scientific Aspects of Marine Pollution) (1985). Atmospheric Transport of Contaminants into the Mediterranean Region. **Reports and Studies, No.26**, pp.53.

GESAMP (Joint Group of Experts on the Scientific Aspects of Marine Pollution) (1989). The Atmospheric Input of Trace Species to the World Ocean. **Reports and Studies, No. 38**, pp.111.

Gibson, R. (1991). Data Base for Trajectory Models. Basic Functional Design of ECMWF's Meteorological Operational System (EMOS): Data Bases. M1.1/6(1), pp.22.

Gilman, C. and C. Garrett (1994). Heat Flux Parameterizations for the Mediterranean Sea: The Role of Atmospheric Aerosols and Constraints from the Water Budget. **Journal of Geophysical Research, 99(C3)**, 5119-5134.

Graham W.F. and R. Duce (1979). Atmospheric Pathways of the Phosphorus Cycle. **Geochimica et Cosmochimica Acta, 43**, 1195-1208.

Guerzoni, S., R. Lenaz and G. Quarantotto (1989). Trace Metals Characterization of Airborne Particles from Different Mediterranean Areas. In: Airborne Pollution of the Mediterranean Sea. **MAP Technical Reports Series, No.31**, pp.65-73.

Guerzoni, S., R. Lenaz, G. Quarantotto, G. Rampazzo, A. Correggiari and P. Bonelli (1989). Trace Metal Composition of Airborne Particles over the Mediterranean Sea. **Giornale di Geologia, series 3a, 51(2)**, 117-130.

Guerzoni, S., G. Cesari, R. Lenaz and L. Cruciani (1992). A New Sampling Station at the Coastal Site of Capo Carbonara (Sardinia, central Mediterranean): Preliminary Data and Technical Proposals. In: Airborne Pollution of the Mediterranean Sea. **MAP Technical Reports Series, No:64**, pp.33-40.

Guieu, C., J.M. Martin and F. Elbaz-Poulichet (1990) Atmospheric Input of Trace Metals (Cd, Co, Cu, Fe, Mn, Ni and Pb) to the Gulf of Lions. In: Water Pollution Research Reports, 20, J.M. Martin and H. Barth (eds.), pp.613-621. EROS 2000, Second Workshop on the North-West Mediterranean Sea. Commission of the European Communities, Brussels.

Guieu, C., J.M. Martin, A.J. Thomas and F. Elbaz-Poulichet (1991a). Atmospheric Versus River Inputs of Metals to the Gulf of Lions. Total Concentrations, Partitioning and Fluxes. ***Marine Pollution Bulletin***, 22, 176-183.

Guieu, C. (1991b). Apports Atmospheriques a la Mediterranee Nord-Occidentale. These de doctorat de l'Universite de Paris, 225 pp.

Hardy, J.T. and E.A. Crecellus (1981). Is Atmospheric Particulate Matter Inhibiting Marine Primary Productivity? ***Environmental Science & Technology***, 15, 1103-1106.

Hydes, D.J., G.J. De Lange and H.J.W. De Baar (1988). Dissolved Aluminium in the Mediterranean. ***Geochimica et Cosmochimica Acta***, 52, 2107-2114.

Jankowiak, I. and D. Tanre (1992). Satellite Climatology of Saharan Dust Outbreaks: Method and Preliminary Results. ***Journal of Climate***, Vol. 5, No.6.

Johnson, K.S., K.H. Coale, V.A. Elrod and N. W. Tindale (1994). Iron Photochemistry in Seawater from the Equatorial Pacific. ***Marine Chemistry***, 46, 319-334.

Kallberg, P. (1984). Air Parcel Trajectories from Analyzed or Forecast Windfields. Workshop on Simplified Models for Short-Range Forecasting on the Mesoscale. SMHI R&D notes, No. 37. The Swedish Meteorological and Hydrological Institute.

Karakoç, F. (1995). Comparison of Atmospheric Trace Element Distributions over the Black Sea, Marmara Sea and Mediterranean Sea Regions. Ma.Sc. Thesis, pp. 130. METU-Inst. Mar. Sci., Erdemli.

Kendall, L.C., R.G. Steward, P.R. Betzer, D.L. Johnson and J.M. Prospero (1986). Dynamics and Composition of Particles from an Aeolian Input Event to the Sargasso Sea. *J. Geophys. Res.*, **91**, 1055-1066.

Kersten, M., M. Kriews and U. Förstner (1991). Partitioning of Trace Metals Released From Polluted Marine Aerosols in Coastal Seawater. *Marine Chemistry*, **36**, 165-182.

Khalef, F.I. (1989). Desertification and Aeolian Processes in the Kuwait Desert. *J. Arid Environ.*, **16**, 125-145.

Kremling, K. and P. Streu (1993). Saharan Dust Influenced Trace Element Fluxes in Deep North Atlantic Subtropical Waters. *Deep-Sea Research*, **40**, 1155-1168.

Krom, M.D., N. Kress and S. Brenner (1991). Phosphorus Limitation of Primary Productivity in the Eastern Mediterranean Sea. *Limnology and Oceanography*, **36(3)**, 424-432.

Kubilay, N., S. Yemenicioğlu and C. Saydam (1994). Trace Metal Characterization of Airborne Particles from the Northeastern Mediterranean. *Fresenius Environmental Bulletin*, **3**, 444-448.

Kubilay N., A.C. Saydam, S. Yemenicioğlu, G. Kelling, S. Kapur, C. Karaman and E. Akca (1995a). Long Term Observation of Atmospheric Particles and Their Chemical and Mineralogical Variability in the Coastal Region of the Northeast Mediterranean. *Cathena*, (in press).

Kubilay, N. S. Yemenicioğlu and A.C. Saydam (1995b). Airborne Material Collections and Their Chemical Composition over the Black Sea. *Marine Pollution Bulletin*, **30**, 475-483

Kubilay, N. and A.C. Saydam (1995c). Trace Elements in Atmospheric Particulates over the Eastern Mediterranean; Concentrations, Sources, and Temporal Variability. *Atmospheric Environment*, **29**, 2289-2300.

Kubilay, N., C. Saydam, S. Nickovic and S. Dobricic (1995d). Soil Derived Dust Particulates Over the Eastern Mediterranean. XXXIV Congress-Assemblée Plénière de la C.I.E.S.M., La Valetta (Malta), 27-31 March 1995. *Rapp. Comm.int. Mer Medit.*, **34**, pp.61.

Lantzy, R.J. and F.T. Mackenzie (1979). Atmospheric Trace Metals: Global Cycles and Assessment of Man's Impact.

***Geochim. Cosmochim. Acta*, 43, 511-525.**

Laumond, F., G. Copin-Montegut, P. Courau, E. Nicolas (1984). Cadmium, Copper and Lead in the Western Mediterranean Sea. ***Marine Chemistry*, 15, 251-261.**

Legrand, M., C.T. N'Doume (1992). Tracking the Dust Clouds over Africa by Means of the Meteosat Thermal IR Imagery. In: IRS'92: Current Problems in Atmospheric Radiation, Keevallik and Kerner (eds). 342-344. A. Deepak.

Legrand, M., C. N'doume and I. Jankowiak (1994). Satellite-Derived Climatology of the Saharan Aerosol. In: Passive Infrared Remote Sensing of Clouds and the Atmosphere II. D.K. Lfrich (ed.), Proceedings, SPIE 2309, pp.127-135.

Legrand, M. (1995). Climatology of desert aerosol from METEOSAT. In: Lettre pigb-pmrc France, French IGBP-WCRP Letter Daniel Cadet (ed.), pp.VII

Levin, Z. (1993). Potential Effects of Global Warming on the Microphysics of Clouds and Rain in the Middle East. In: Proceedings of an International Workshop on Regional Implications of Future Climate Change, (eds. M. Graber, A. Cohen and M. Magaritz), pp.229-239. April 28 - May 2, 1991.

Losno, R., G. Bergametti, P. Carlier and G. Mouvier (1991). Major Ions in Marine Rainwater With Attention to Sources of Alkaline and Acidic Species. ***Atmospheric Environment*, 25A, 763-770.**

Loye-Pilot, M.D., J.M. Martin and J. Morelli (1986). Influence of Sahara Dust on the Rain Acidity and Atmospheric Input to the Mediterranean. ***Nature*, 321, 6068, 427-428.**

Loye-Pilot, M.D. and J. Morelli (1988). Fluctuations of Ionic Composition of Precipitations Collected in Corsica Related to Changes in the Origins of Incoming Aerosols. ***J. Aerosol Sci.*, 19, 577-585.**

Loye-Pilot, M.D., J.M. Martin and J. Morelli (1989). Atmospheric Input of Particulate Matter and Inorganic Nitrogen to the North-Western Mediterranean. In: Water Pollution Research Reports, 13, J.M. Martin and H. Barth (eds.), pp. 368-376. EROS 2000, First Workshop on the North-West Mediterranean Sea. Commission of the European Communities, Brussels.

Mamane, Y., U. Dayan and J.M. Miller (1987). Contribution of Alkaline and Acidic Sources to Precipitation in Israel. *The Science of the Total Environment*, 61, 15-22.

Martin, D., C. Mithieux and B. Strauss (1987). On the Use of the Synoptic Vertical Wind Component in a Transport Trajectory Model. *Atmospheric Environment*, 21, 45-52.

Maring, H., D.M. Settle, P. Buat-Menard, F. Dulac and C.C. Patterson (1987). Stable Lead Isotope Tracers of Air-Mass Trajectories in the Mediterranean Region. *Nature*, 330, 154-156.

Martin, D., G. Bergametti and B. Strauss, (1990). On the Use of the Synoptic Vertical Velocity in Trajectory Model: Validation by Geochemical Tracers. *Atmospheric Environment*, 24A, 8, 2059-2069.

Martin, J.-M. & M. Whitfield (1983). The Significance of the River Input of Chemical Elements to the Ocean. In: Trace Metals in Sea Water, C.S. Wong, E. Boyle, K.W. Bruland, J.D. Burton and E.D. Goldberg (eds), New York: Plenum Publishing Corporation, pp.265-96.

Martin, J.M., F. Elbaz-Poulichet, C. Guieu, M.D. Loye-Pilot and G. Han, (1989). River Versus Atmospheric Input of Material to the Mediterranean Sea: An Overview. *Marine Chemistry*, 28, 159-182.

Martin, J.H. and S.E. Fitzwater (1988). Iron Deficiency Limits Phytoplankton Growth in the North-East Pacific Subarctic. *Nature* 331, 341-343.

Martin, J.H., R.M. Gordon and S.E. Fitzwater (1990). Iron In Arctic Waters. *Nature* 345, 156-158.

Martin, J.H. *et al.* (1994). Testing the Iron Hypothesis in Ecosystems of the Equatorial Pacific Ocean. *Nature*, 371, 123-128.

Mayewski, P.A., L.D. Meeker, S. Whitlow, M.S. Twickler, M.C. Morrison, R.B. Alley, P. Bloomfield and K. Taylor (1993). The Atmosphere During the Younger Dryas. *Science*, **261**, 195-197.

Merrill, J.T. (1985a). Atmospheric Pathways to the Oceans. In: The Role of Air-Sea Exchange in Geochemical Cycling, P. Buat-Menard (ed.). NATO-ASI series, D.Reidel Publishing Company, 549pp.

Merrill, J.T. (1985b). Modeling Atmospheric Transport to the Marshall Islands. *Journal of Geophysical Research*, **90**, **12**, 927-12, 936.

Migon, C., B. Journel and E. Nicolas (1995). Measurement of Trace Metal Wet, Dry and Total Atmospheric Fluxes over the Ligurian Sea. *Atmospheric Environment* (in press).

Miller, J.M. and J.M. Harris (1985). The Flow Climatology to Bermuda and Its Implications for Long-Range Transport. *Atmospheric Environment*, **19**, 409-414.

Milliman, J.D., L. Jetic and G. Sestini (1992). The Mediterranean Sea and Climate Change-An overview In: Climatic Change and Mediterranean, L. Jetic, J.D. Milliman and G. Sestini (eds.), UNEP, pp.1-14.

Moulin, C., F. Dulac, F.M. Breon, J.M. Andre, F. Guillard and W. Guelle (1994). Remote Sensing of Airborne Desert Dust Mass over Oceans Using MeteoSat and CZCS Imagery. *Memoires de l'Institut oceanographique*, Monaco, no.18, pp.35-43.

Murphy, K.J.T. (1985). The Trace Metal Chemistry of the Atlantic Aerosol. *Ph.D. Dissertation*. University of Liverpool.

Nicolas, E., Migon. C. and Alleman, L. (1992). Atmospheric Heavy Metal Concentrations and Pb Evolution from 1986 to 1992 over the Northwestern Mediterranean Sea. In: Water Pollution Research Reports, **30**, J.M. Martin and H.Barth (eds), pp. 279-286. EROS 2000, Fourth Workshop on the North-West Mediterranean Sea. Commission of the European Communities, Brussels.

Nolting, R.F. (1989). Dissolved and Particulate Trace Metals in Sediments of the Gulf of Lions. In: Water Pollution Research Reports, **13** J.M. Martin and H.Barth (eds.), pp. 314-340 pp. EROS 2000, First Workshop

on the North-West Mediterranean Sea. Commission of the European Communities, Brussels.

Özsoy, E. (1981). On the Atmospheric Factors Affecting the Levantine Sea. European Centre for Medium Range Weather Forecasts, Technical Report No:25; 29pp.

Özsoy, E., A. Hecht and Ü. Ünlüata (1989). Circulation and Hydrography of the Levantine Basin. Results of POEM Coordinated Experiments 1985-1986. *Progress in Oceanography*, **22**, 125-170.

Özsoy, E., A. Hecht, Ü. Ünlüata, S. Brener, H.İ. Sur, J. Bishop, M.A. Latif, Z. Rozenraub and T. Oguz (1993). A Synthesis of the Levantine Basin; Circulation and Hydrography 1985-1990. *Deep-Sea Research*, **40**, 1075-1019.

Pacyna, J. (1983). Trace Element Emission from Anthropogenic Sources in Europe. Technical report No. 10/82. Norwegian Institute for Air Research, 107pp..

Pacyna, J.M., A. Semb and J.E. Hanssen (1984). Emissions and Longrange Transport of Trace Elements in Europe. *Tellus*, **36B**, 163-178.

Pacyna, J.M. (1984). Estimation of the Atmospheric Emissions of Trace Elements from Anthropogenic Sources in Europe. *Atmospheric Environment*, **18**, 41-50.

Prospero, J.M. and T.N. Carlson (1972). Vertical and Areal Distribution of Saharan Dust over the Western Equatorial North Atlantic Ocean. *Journal of Geophysical Research*, **77**, 5255-5265.

Prospero, J.M. (1981a). Eolian Transport to the World Ocean. In: *The Sea* (ed.C.Emiliani), vol.7, The Oceanic Lithosphere, Wiley, New York, pp. 801-874.

Prospero, J.M, R.A. Glaccum and R.T. Nees (1981b). Atmospheric Transport of Soil Dust from Africa to South America. *Nature*, **289**, 57-572.

Prospero, J.M. (1985). Records of Past Continental Climates in Deep-Sea Sediments. *Nature*, **315**, 279-280.

Prospero, J. and R.B. Nees (1987). Deposition Rate of Particulate and Dissolved Aluminum Derived from Saharan Dust in Precipitation at Miami, Florida. *Journal of Geophysical Research*, **92(D12)**, 14723-14731.

Prospero, J.M. (1990). Mineral-Aerosol Transport to the North Atlantic and North Pacific: The Impact of African and Asian Sources. In: The Long-Range Atmospheric Transport of Natural and Contaminant Substances A.H. Knap (ed.), Kluwer Academic Publishers, Netherlands, pp.59-86.

Quetel C.R., E. Remoudaki, J.E. Davies, J.C. Miquel, S.W. Fowler, C.E. Lambert, G. Bergametti and P.B. Menard (1993). Impact of Atmospheric Deposition on Particulate Iron Flux and Distribution in Northwestern Mediterranean Waters. *Deep-Sea Research*, **40**, 989-1002.

Rahn, K.A. (1976). The Chemical Composition of the Atmospheric Aerosol. Technical Report. Graduate School of Oceanography, University of Rhode Island, Kingston, R.I., 265 pp.

Rahn, K.A., R.D. Borys, G.E. Shaw and L. Schutz (1979). Long-Range Impact of Desert Aerosol on Atmospheric Chemistry: Two Examples. In: Scope 14: Saharan Dust (Mobilization, Transport, Deposition) C. Morales (ed.), John Wiley, Chichester, pp.243-266.

Reiff J., G.S. Forbes, F.TH.M.Spieksma and J.J. Reynders (1986). African Dust Reaching Northwestern Europe: A Case Study to Verify Trajectory Calculations. *Journal of Climatology and Applied Meteorology*, **25**, 1543-1567.

Reiter, E.R (1975). Handbook for Forecasters in the Mediterranean, Weather Phenomena of the Mediterranean Basin, Part1: General Description of Meteorological Processes, Environmental Prediction Research Facility, Naval Postgraduate School, Monterey, California, Technical Paper No. 5-75, 344 pp.

Remoudaki, E., G.Bergametti and P. Buat-Menard (1991). Temporal Variability of Atmospheric Lead Concentrations and Fluxes Over the Northwestern Mediterranean Sea. *Journal of Geophysical Research*, **96**, 1043-1055.

Robinson, A.R. and M. Golnaraghi (1993). Circulation And Dynamics of the Eastern Mediterranean Sea; Quasi-Synoptic Data Driven Simulations. *Deep-Sea Research*, **40**, 1207-1246.

Savoie D.L., J.M. Prospero and E.S. Saltzman (1989). Non-Sea-Salt Sulphate and Nitrate in Trade Wind Aerosols at Barbados: Evidence for Long-Range Transport. *Journal of Geophysical Research*, **94**, 5069-5080.

Saydam, A.C. (1981). The Elemental Chemistry of Eastern Mediterranean Atmospheric Particulates. *Ph.D. Dissertation*. University of Liverpool, U.K., 214 pp.

Saydam, C. (1995). The Observation of Saharan Dust by Remote Sensing over the Mediterranean and its Impact on Climate. Presented in the Workshop on Applications of Remote Sensing over the Mediterranean Sea. Mondello, Sicily, Italy, 20-22 April 1995.

Saydam, A.C., N. Kubilay and E. Ozsoy (1995). Climate Processes Related to Saharan Dust over the Mediterranean. Presented in the Workshop on Impact of Africa Dust Across the Mediterranean. Oristano, Sicily, Italy, 4-7 October 1995.

Saydam, A.C. (1995). Saharan Dust Transport and Its Importance for the Black Sea. NATO-ARW on Sensitivity of North Sea and Black Sea to Anthropogenic and Climate Changes. Varna-Bulgaria, 14-18 November 1995.

Schneider, B. (1987). Source Characterization for Atmospheric Trace Metals over Kiel Bight. *Atmospheric Environment*, **21**, 1275-1283.

Schutz, L.W., P. Buat-Menard, R. A.C. Carvalho, A. Cruzado, J.M. Prospero, R. Harris, N.Z. Heidam, R. Jaenicke (1990). The Long-Range Transport of Mineral Aerosols: Group Report. In: The Long-Range Atmospheric Transport of Natural and Contaminant Substances A.H. Knap (ed.), Kluwer Academic Publishers, Netherlands, pp.197-229.

Shaw, H.F. and P.R. Bush (1978). The Mineralogy and Geochemistry of the Recent Surface Sediments of the Cilica Basin, Northeast Mediterranean. *Marine Geology*, **27**, 115-136.

Sherrell, R.M. and E.A. Boyle (1988). Zinc, Chromium, Vanadium and Iron in the Mediterranean Sea. *Deep-Sea Research*, **35**, 1319-1334.

Shiller, A.M. and E.A. Boyle (1987). Variability of Dissolved Trace Metals in the Mississippi River. *Geochimica et Cosmochimica Acta*, **51**: 3273-3277.

Shiller, A.M. and E.A. Boyle (1991). Trace Elements in the Mississippi River Delta Outflow Region: Behaviour at High Discharge. *Geochimica et Cosmochimica Acta*, **55**, 3241-3251.

Siffert, C. and B. Sulzberger (1989). The Effect of Light on the Geochemical Cycling of Iron and Manganese in Natural Waters. In: Water Pollution Research Reports, 13 J.M. Martin and H.Barth (eds.), pp. 251-257 pp. EROS 2000, First Workshop on the North-West Mediterranean Sea. Commission of the European Communities, Brussels.

Slinn, S.A. and W.G.N. Slinn (1980). Predictions for Particle Deposition on Natural Waters. *Atmospheric Environment*, **14**, 1013-1016.

Spokes L.J., T.D.Jickells and B. Lim (1994). Solubilisation of Aerosol Trace Metals by Cloud Processing: A Laboratory Study. *Geochimica et Cosmochimica Acta*, **58**, 3281-3287.

Sulzberger, B. (1992). The Role of Heterogeneous Photochemical Reactions for the Formation of Dissolved Iron Species in Aquatic Systems. Water Pollution Research Reports, 13 J.M. Martin and H.Barth (eds.), pp. 183-186 pp. EROS 2000, Fourth Workshop on the North-West Mediterranean Sea. Commission of the European Communities, Brussels.

Sulzberger, B. and H. Laubscher (1995). Reactivity of Various Types of Iron (III) (Hydr)oxides Towards Light-Induced Dissolution. *Marine Chemistry*, **50**, 103-115.

Sunda, W. G., S.A. Huntsman and G.R. Harvey (1983). Photoreduction of Manganese Oxides in Seawater and its Geochemical and Biological Implications. *Nature*, **301**, 234-236.

Swap R., M. Garstang, S. Greco, R. Talbot and P. Kalberg (1992). Saharan Dust in the Amazon Basin. *Tellus*, **44B**, 133-149.

Takashi, I. and K. Takeuchi (1987). Sulfur Dioxide Oxidation by Oxygen Catalyzed by Mixtures of Manganese (II) and Iron (III) in Aqueous Solutions at Environmental Reaction Conditions. ***Atmospheric Environment***, **21**, 1555-1560.

Talbot, R.W., R.C. Harriss, E.V. Browell, G.L. Gregory, D.I. Sebacher and S.M. Beck (1986). Distribution and Geochemistry of Aerosols in the Tropical North Atlantic Troposphere: Relationship to Saharan Dust. ***Journal of Geophysical Research***, **91**, 5173-5182.

Taylor, S.R. (1964). Abundance of Chemical Elements in the Continental Crust: A New Table. ***Geochimica et Cosmochimica Acta***, **28**, 1273-1285.

Tegen, I. and I. Fung (1994). Modeling of Mineral Dust in the Atmosphere: Sources, Transport, and Optical Thickness. ***Journal of Geophysical Research***, **99**, 22897-22914.

Tolun, N. and A.N. Pamir (1975). Explanatory Text of the Geological Map of Turkey, Hatay sheet. *Publ. Min. Res. and Explor. Inst. Publ.*, Ankara, 99 p. & appendices.

Tomadin, L., R. Lenaz, V. Landuzzi, A. Mazzucotelli and R. Vanucci (1984). Wind-Blown Dusts over the Central Mediterranean. ***Oceanologica Acta***, **7**, 13-23.

Tucker C.T., H.E. Dregne and W.W. Newcomb (1991). Expansion and Contraction of the Sahara Desert from 1980 to 1990. ***Science***, **253**, 299-301.

Uematsu M., A.R. Duce, J. Prospero, L. Chen, J.T. Merrill and R.J. McDonald (1983). Transport of Mineral Aerosol from Asia over the North Pacific Ocean. ***Journal of Geophysical Research***, **88**, 5343-5352.

Uematsu M., A.R. Duce and J. Prospero (1985). Deposition of Atmospheric Mineral Particles in the North Pacific Ocean. ***J. Atmos. Chem.***, **3**, 123-138.

United Nations Environment Program, World Meteorological Organization (UNEP,WMO) (1989a). Airborne pollution of the Mediterranean

Sea. Report and proceedings of a WMO/UNEP workshop. **MAP Technical Reports Series No.31.**

United Nations Environment Program, World Meteorological Organization (UNEP, WMO) (1989b). Meteorological and Climatological Data From Surface and Upper Air Measurements for the Assessment of Atmospheric Transport and Deposition of Pollutants in the Mediterranean Basin: A review. **MAP Technical Reports Series No.30**, Athens, UNEP, pp.137.

United Nations Environment Program, World Meteorological Organization (UNEP, WMO) (1992). Airborne Pollution of the Mediterranean Sea. Report and Proceedings of the second WMO/UNEP workshop. **MAP Technical Reports Series No.64.**

United Nations Environment Program, World Meteorological Organization (UNEP, WMO) (1994). Assessment of Airborne Pollution of the Mediterranean Sea by Sulphur and Nitrogen Compounds and Heavy Metals in 1991. **MAP Technical Reports Series No.85**, Athens, UNEP, pp.304.

Vossler T.L., C.W. Lewis, R.K. Stevens, T.G. Dzubay, G.E. Gordon, S.G. Tuncel, G.M. Russwurm and G.J.Keeler (1989). Composition and Origin of Summertime Air Pollutants at Deep Creek Lake, Maryland. **Atmospheric Environment**, **23**, 1535-1547.

Wells, M.L. (1994). Pumping Iron in the Pacific. **Nature** **368**, 295-296.

Whelpdale, D.M. and J.L. Moody (1990). Large-Scale Meteorological Regimes and Transport Processes. In: The Long-Range Atmospheric Transport of Natural and Contaminant Substances A.H. Knap (ed.), Kluwer Academic Publishers, Printed in Netherlands, pp.3-39.

Woodward, E.M.S., N.J.P. Owens, A.P. Rees and C.S. Law (1990). A Seasonal Survey of Nutrient Cycling and Primary Productivity in the Gulf of Lions, during 1988 and 1989. Water Pollution Research Reports, 13 J.M. Martin and H.Barth (eds.), pp. 83-91 pp. EROS 2000, Second Workshop on the North-West Mediterranean Sea. Commission of the European Communities, Brussels.

Xyla, A.G., H. Laubscher, B.M. Bartschat and B. Sulzberger (1991). Formation of Dissolved Iron and Manganese in Aquatic Systems: The Effect of pH, Light, and of the Thermodynamic Stability of the Solid Phase. Water Pollution Research Reports, 28, J.M. Martin and H.Barth (eds.), pp. 329-339 pp. EROS 2000, Third Workshop on the North-West Mediterranean Sea. Commission of the European Communities, Brussels.

Yaalon, D.H. and E. Ganor (1973). The Influence of Dust on Soils During the Quaternary. *Soil Science*, **116(3)**, 146-155.

Yaalon, D.H. and E. Ganor (1979). East Mediterranean Trajectories of Dust-Carrying Storms from the Sahara and Sinai. In: Saharan Dust, Chapter 9, (Ed by C.Morales), John Wiley and Sons, New York, pp.187-183.

Zhang, H. and R. Wollast (1990). Distributions of Dissolved Cobalt and Nickel in the Rhone and Gulf of Lions. Water Pollution Research Reports, 20 J.M. Martin and H.Barth (eds.), pp. 397-414 pp. EROS 2000, Second Workshop on the North-West Mediterranean Sea. Commission of the European Communities, Brussels.

Zhang, J. and M.G. Liu (1994). Observations on Nutrient Elements and Sulphate in Atmospheric Wet Depositions Over the Northwestern Pacific Coastal Oceans-Yellow Sea. *Mar. Chem.*, **47**, 173-189.

Zhu X., J.M. Prospero, F.J. Millero, D.L. Savoie, and G.W. Brass (1992). The Solubility of Ferric Iron in Marine Aerosol Solutions at Ambient Relative Humidities. *Mar. Chem.*, **38**, 91-107.

Zhuang G., Yi Z., Duce R.A. and Brown P.R.(1992). Link Between Iron and Sulphur Cycles Suggested by Detection of Fe(II) in Remote Marine Aerosols. *Nature* **355**, 537-539.

Zoller, W.H., E.S. Gladney and R.A. Duce (1974). Atmospheric Concentrations and Sources of Trace Metals at the South Pole. *Science*, **183**, 198-200.

APPENDIX



Table A1 The job utilized for retrieving air mass back trajectories from ECMWF

```
-----  
#QSUB/USER ="mcf"/PASSWORD=password"  
#QSUB/REQUEST=MRSANMA  
#QSUB/MERGE  
#QSUB/CPUTIME=1000  
#QSUB  
#  
set +v  
#  
PATH=$PATH  
export PATH  
#  
CRAYPACKLIB=/tmp/emos_sms/lib/craypacklib.a  
#FDB=/tmp/emos_sms/lib/libfdb.a  
TRAJDB=/tmp/emos_sms/lib/traj.a  
#  
pwd  
ls -l  
rm TERRY TMDB core fort.73 fort.74 fort.75 trab.out trdata  
# MARS request  
#  
mars << \EOF  
RET,      TYPE=an,  
          date=920324/TO/920327/BY/01,  
          time=00/06/12/18,  
          levtype=ML,  
          levelist=ALL,  
          repres=SH, RES=81,  
          param=U/V/W/LNSP,  
          TARGET="TERRY"  
  
END  
EOF  
#cp /tmp/emos_sms/bin/maketdb maketdb  
ls -l  
#  
# Create the database  
#  
/tmp/emos_sms/bin/maketdb -f TMDB -s NEW -o DELETE -u YES -m 31 TERRY  
#  
ls -l  
rm TERRY  
#  
# Defaults  
#  
set -exS  
#  
# Assign statements  
assign -a trdata fort.7  
# $FDB is not needed (ECMWF)
```

```
#segjdr -H 330000+1000 $TRAJ $CRAYPACKLIB $TRAJDB \
$ECLIB $EMOSLIB -o trab.out -e TRAMS
```

```
#
echo " 3 DIMENSIONAL TRAJECTORIES "
trab.out << *EOF*
&NATRAJ
```

```
LUDB=72, LUTR=75,
DAYS=3., IDT=-15, NTRAJ=4,
INIY=1992, INIM=3, INID=28, INIH=12
NLON=240., NLAT=121, NLEV=31, LEVLOW=31, LEVUPP=1,
STALAT= 36.33, 36.33, 36.33, 36.33,
STALON= 34.15, 34.15, 35.15, 34.15,
STALEV=900., 850., 700., 500.,
```

```
L3DIM=.TRUE., LTEST=.FALSE., LPRINT=.FALSE.,
```

```
&
*EOF*
```

(DAYS=number of days to follow the parcel; IDT=timestep in (integer) minutes, negative for backtracking; NTRAJ=number of trajectories (Max=20); NLON, NLAT=resolution of regular finite difference grid; NLEV=number of levels in the database (up to 16/9/91 it is 19 and beginning from 17/9/91 to onwards it is 31); LEVLOW, LEVUPP= limits (in level numbers) for calculation interval; INIY, INIM, INID, INIH=start(end) date; STALAT, STALON, STALEV=start (end)positions in degrees and hPa

Table A2. The trajectory data base obtained from the requestfile given in Table A1.

3-DIM T R A J E C T O R I E S

INITIAL DATE/TIME 1992- 3-27 12UT
ECMWF ANALYSES

STEP	HRS	U	V	W	LAT	LON	LEVEL
0	0	-2.60	4.73	0.24	36.33	34.15	900
4	-1	-3.45	4.55	0.21	36.18	34.27	892
8	-2	-3.69	4.35	0.15	36.03	34.41	885
12	-3	-3.65	4.23	0.09	35.89	34.55	881
16	-4	-3.54	4.01	0.03	35.76	34.69	878
20	-5	-3.51	3.65	-0.03	35.63	34.82	878
24	-6	-3.59	3.16	-0.08	35.52	34.96	880
28	-7	-3.28	2.96	-0.04	35.42	35.09	882
32	-8	-2.91	2.82	0.00	35.33	35.21	883
36	-9	-2.51	2.71	0.03	35.24	35.31	883
40	-10	-2.08	2.61	0.05	35.15	35.40	881
44	-11	-1.65	2.51	0.06	35.07	35.47	879
48	-12	-1.19	2.41	0.08	34.99	35.52	876
52	-13	-1.09	2.62	0.10	34.90	35.56	873
56	-14	-0.98	2.89	0.13	34.81	35.59	869
60	-15	-0.89	3.23	0.16	34.71	35.63	864

64	-16	-0.82	3.67	0.18	34.60	35.65	858
68	-17	-0.77	4.25	0.21	34.47	35.68	851
72	-18	-0.79	4.85	0.22	34.32	35.71	843
76	-19	-0.71	5.00	0.14	34.16	35.73	836
80	-20	-0.68	5.02	0.07	34.00	35.75	833
84	-21	-0.68	4.98	0.02	33.83	35.78	831
88	-22	-0.70	4.94	-0.03	33.67	35.80	831
92	-23	-0.73	4.96	-0.07	33.51	35.82	833
96	-24	-0.76	5.11	-0.10	33.35	35.85	836
100	-25	-0.68	4.88	-0.08	33.19	35.87	839
104	-26	-0.51	4.65	-0.08	33.03	35.89	842
108	-27	-0.37	4.20	-0.09	32.88	35.90	845
112	-28	-0.20	3.76	-0.10	32.75	35.91	848
116	-29	0.01	3.34	-0.12	32.64	35.90	852
120	-30	0.25	2.93	-0.13	32.53	35.89	856
124	-31	-0.04	2.71	-0.12	32.44	35.89	861
128	-32	-0.39	2.48	-0.10	32.36	35.89	865
132	-33	-0.79	2.19	-0.09	32.28	35.91	869
136	-34	-1.25	1.86	-0.08	32.21	35.94	872
140	-35	-1.78	1.48	-0.07	32.16	35.99	874
144	-36	-2.37	1.01	-0.05	32.11	36.07	876
148	-37	-3.06	0.93	-0.07	32.08	36.17	879
152	-38	-3.83	0.89	-0.09	32.05	36.29	881
156	-39	-4.63	0.90	-0.10	32.02	36.45	885
160	-40	-5.42	0.97	-0.11	31.99	36.64	888
164	-41	-6.19	1.16	-0.11	31.95	36.85	892
168	-42	-6.86	1.43	-0.09	31.91	37.10	896
172	-43	-6.54	2.17	-0.08	31.85	37.35	899
176	-44	-5.98	2.62	-0.08	31.76	37.59	902
180	-45	-5.21	2.74	-0.10	31.67	37.80	905
184	-46	-4.46	2.89	-0.12	31.58	37.98	908
188	-47	-3.70	3.04	-0.15	31.47	38.13	913
192	-48	-2.94	3.12	-0.17	31.37	38.26	919
196	-49	-3.00	2.89	-0.14	31.27	38.37	924
200	-50	-3.03	2.87	-0.12	31.17	38.48	927
204	-51	-3.25	3.06	-0.10	31.08	38.59	929
208	-52	-2.94	2.86	-0.08	30.99	38.69	931
212	-53	-3.12	3.00	-0.07	30.90	38.79	932
216	-54	-2.91	2.93	-0.06	30.81	38.88	934
220	-55	-2.97	2.40	-0.06	30.73	38.97	936
224	-56	-2.98	1.80	-0.06	30.67	39.07	937
228	-57	-3.31	1.31	-0.05	30.63	39.18	938
232	-58	-3.43	0.69	-0.04	30.60	39.29	939
236	-59	-3.61	0.05	-0.03	30.60	39.40	940
240	-60	-3.80	-0.61	-0.02	30.61	39.53	940
244	-61	-3.01	-1.10	-0.01	30.64	39.64	941
248	-62	-2.22	-1.55	0.00	30.69	39.72	940
252	-63	-1.43	-1.96	0.01	30.76	39.77	940
256	-64	-0.66	-2.31	0.02	30.83	39.80	939
260	-65	0.08	-2.62	0.02	30.92	39.79	938
264	-66	0.76	-2.88	0.03	31.01	39.76	937
268	-67	1.11	-2.58	0.01	31.11	39.71	935

272	-68	1.47	-2.23	-0.01	31.19	39.64	935
276	-69	1.82	-1.87	-0.03	31.27	39.57	935
280	-70	2.13	-1.53	-0.05	31.33	39.47	937
284	-71	2.44	-1.30	-0.07	31.38	39.37	938
288	-72	2.83	-1.18	-0.09	31.42	39.26	936

STEP	HRS	U	V	W	LAT	LON	LEVEL
0	0	-2.22	6.59	0.26	36.33	34.15	850
4	-1	-2.12	6.36	0.20	36.12	34.24	842
8	-2	-1.77	6.26	0.14	35.91	34.32	835
12	-3	-1.35	6.08	0.09	35.71	34.38	831
16	-4	-1.05	5.84	0.04	35.52	34.43	828
20	-5	-0.88	5.62	-0.03	35.33	34.46	828
24	-6	-0.86	5.38	-0.09	35.15	34.50	830
28	-7	-0.80	5.24	-0.02	34.98	34.53	832
32	-8	-0.53	5.19	0.05	34.81	34.56	831
36	-9	-0.08	5.24	0.12	34.64	34.57	828
40	-10	0.55	5.41	0.18	34.46	34.56	823
44	-11	1.19	5.69	0.22	34.28	34.53	815
48	-12	1.52	5.69	0.27	34.09	34.47	807
52	-13	1.16	5.38	0.28	33.91	34.42	797
56	-14	0.84	5.04	0.29	33.74	34.38	786
60	-15	0.47	4.53	0.30	33.58	34.35	776
64	-16	0.10	3.83	0.30	33.44	34.34	765
68	-17	-0.27	3.18	0.30	33.32	34.34	754
72	-18	-0.64	2.59	0.30	33.22	34.36	743
76	-19	-0.55	1.44	0.30	33.15	34.38	733
80	-20	-0.40	0.12	0.31	33.12	34.40	722
84	-21	-0.29	-1.25	0.32	33.14	34.41	710
88	-22	-0.25	-2.61	0.33	33.19	34.42	698
92	-23	-0.26	-3.75	0.35	33.29	34.43	686
96	-24	-0.37	-4.62	0.38	33.43	34.44	673
100	-25	0.35	-4.48	0.37	33.57	34.44	659
104	-26	0.95	-4.38	0.36	33.71	34.41	646
108	-27	1.42	-4.32	0.35	33.85	34.36	633
112	-28	1.74	-4.31	0.34	33.98	34.30	621
116	-29	1.92	-4.36	0.34	34.12	34.23	609
120	-30	1.92	-4.46	0.34	34.26	34.15	596
124	-31	1.58	-4.62	0.33	34.40	34.08	584
128	-32	1.17	-4.77	0.31	34.55	34.02	572
132	-33	0.77	-4.91	0.29	34.70	33.98	561
136	-34	0.34	-4.99	0.26	34.86	33.96	551
140	-35	-0.05	-5.00	0.24	35.02	33.95	542
144	-36	-0.46	-4.98	0.22	35.17	33.96	534
148	-37	-0.41	-4.69	0.18	35.33	33.98	527
152	-38	-0.36	-4.38	0.15	35.47	33.99	521
156	-39	-0.31	-4.08	0.12	35.60	34.00	516
160	-40	-0.23	-3.76	0.08	35.73	34.01	512
164	-41	-0.14	-3.44	0.04	35.84	34.02	510
168	-42	-0.02	-3.12	0.01	35.94	34.02	509
172	-43	-0.30	-3.32	-0.03	36.04	34.02	509
176	-44	-0.47	-3.60	-0.06	36.15	34.04	511

180	-45	-0.50	-3.88	-0.09	36.27	34.06	514
184	-46	-0.38	-4.15	-0.10	36.39	34.07	517
188	-47	-0.14	-4.40	-0.11	36.53	34.08	521
192	-48	0.20	-4.62	-0.11	36.67	34.08	524
196	-49	0.65	-4.68	-0.06	36.82	34.06	527
200	-50	0.98	-4.63	-0.01	36.96	34.03	529
204	-51	1.23	-4.50	0.03	37.11	33.98	528
208	-52	1.45	-4.30	0.06	37.25	33.92	527
212	-53	1.67	-4.02	0.09	37.38	33.86	524
216	-54	1.93	-3.67	0.12	37.50	33.78	520
220	-55	3.01	-4.16	0.08	37.62	33.68	516
224	-56	3.93	-4.55	0.05	37.76	33.54	514
228	-57	4.67	-4.83	0.02	37.91	33.36	512
232	-58	5.26	-5.00	-0.01	38.06	33.15	512
236	-59	5.68	-5.02	-0.04	38.22	32.93	513
240	-60	5.93	-4.89	-0.07	38.38	32.68	515
244	-61	6.20	-5.16	-0.05	38.54	32.43	517
248	-62	6.41	-5.40	-0.04	38.70	32.17	519
252	-63	6.50	-5.63	-0.02	38.88	31.90	520
256	-64	6.39	-5.72	-0.01	39.06	31.63	520
260	-65	6.28	-5.58	0.01	39.24	31.36	520
264	-66	6.33	-5.37	0.04	39.41	31.10	519
268	-67	7.13	-4.90	0.08	39.57	30.81	517
272	-68	7.89	-4.50	0.10	39.72	30.50	514
276	-69	8.60	-4.15	0.12	39.86	30.15	510
280	-70	9.18	-3.91	0.12	39.99	29.77	505
284	-71	9.61	-3.54	0.12	40.10	29.37	501
288	-72	9.86	-2.67	0.11	40.20	28.95	497

STEP	HRS	U	V	W	LAT	LON	LEVEL
0	0	4.61	7.31	0.30	36.33	34.15	700
4	-1	4.68	7.25	0.17	36.09	33.96	691
8	-2	4.87	6.80	0.07	35.87	33.77	686
12	-3	5.07	6.20	0.01	35.66	33.57	684
16	-4	5.23	5.62	-0.04	35.47	33.37	684
20	-5	5.37	5.10	-0.07	35.30	33.16	685
24	-6	5.49	4.62	-0.08	35.15	32.94	686
28	-7	5.39	4.26	0.01	35.01	32.73	687
32	-8	5.56	3.83	0.08	34.88	32.51	684
36	-9	5.94	3.44	0.14	34.76	32.28	679
40	-10	6.48	3.15	0.19	34.66	32.04	672
44	-11	7.08	3.03	0.21	34.56	31.77	664
48	-12	7.64	3.08	0.22	34.47	31.48	655
52	-13	8.07	1.87	0.16	34.39	31.17	648
56	-14	8.25	0.85	0.12	34.35	30.85	642
60	-15	8.23	0.05	0.10	34.34	30.52	637
64	-16	8.03	-0.55	0.10	34.35	30.20	633
68	-17	7.72	-0.93	0.11	34.38	29.89	628
72	-18	7.43	-1.22	0.11	34.42	29.60	623
76	-19	7.45	-0.96	0.06	34.46	29.30	619
80	-20	7.44	-0.67	0.01	34.49	29.01	617
84	-21	7.42	-0.34	-0.02	34.51	28.72	617

88	-22	7.41	-0.03	-0.04	34.52	28.43	617
92	-23	7.48	0.04	-0.03	34.52	28.13	618
96	-24	7.59	0.02	-0.01	34.52	27.84	617
100	-25	7.40	-0.81	0.03	34.54	27.54	616
104	-26	7.27	-1.44	0.06	34.58	27.25	614
108	-27	7.17	-1.90	0.07	34.64	26.97	610
112	-28	7.07	-2.23	0.08	34.71	26.69	607
116	-29	6.98	-2.42	0.08	34.79	26.41	603
120	-30	6.90	-2.49	0.07	34.87	26.14	600
124	-31	6.44	-2.69	0.04	34.96	25.87	597
128	-32	5.97	-2.82	0.01	35.05	25.63	595
132	-33	5.53	-2.92	-0.02	35.15	25.40	594
136	-34	5.07	-3.06	-0.03	35.25	25.19	595
140	-35	4.59	-3.22	-0.05	35.35	25.00	595
144	-36	4.09	-3.40	-0.06	35.46	24.82	596
148	-37	4.05	-3.46	-0.01	35.58	24.66	597
152	-38	4.01	-3.53	0.04	35.70	24.50	595
156	-39	3.96	-3.59	0.09	35.81	24.34	592
160	-40	3.91	-3.61	0.14	35.94	24.18	587
164	-41	3.91	-3.60	0.18	36.06	24.03	580
168	-42	4.06	-3.48	0.22	36.17	23.87	572
172	-43	3.94	-2.47	0.16	36.27	23.71	564
176	-44	3.76	-1.60	0.09	36.34	23.55	559
180	-45	3.50	-0.84	0.02	36.38	23.40	556
184	-46	3.14	-0.17	-0.05	36.40	23.27	556
188	-47	2.70	0.44	-0.12	36.40	23.15	558
192	-48	2.19	1.00	-0.19	36.38	23.05	563
196	-49	1.82	1.36	-0.12	36.35	22.97	567
200	-50	1.47	1.70	-0.06	36.30	22.91	570
204	-51	1.12	2.04	0.00	36.25	22.85	570
208	-52	0.75	2.42	0.07	36.18	22.82	568
212	-53	0.31	2.87	0.13	36.09	22.80	564
216	-54	-0.21	3.41	0.20	36.00	22.79	557
220	-55	-0.12	3.95	0.14	35.88	22.80	550
224	-56	-0.02	4.49	0.08	35.75	22.80	545
228	-57	0.02	5.09	0.01	35.60	22.80	543
232	-58	0.00	5.77	-0.08	35.43	22.80	543
236	-59	-0.12	6.52	-0.17	35.23	22.80	547
240	-60	-0.29	7.33	-0.27	35.01	22.81	554
244	-61	-0.08	6.99	-0.36	34.78	22.82	564
248	-62	0.26	6.86	-0.46	34.56	22.81	578
252	-63	0.93	6.85	-0.52	34.34	22.79	595
256	-64	1.71	7.11	-0.54	34.12	22.74	614
260	-65	2.54	7.85	-0.54	33.89	22.65	632
264	-66	3.57	8.92	-0.52	33.62	22.54	651
268	-67	5.33	9.22	-0.45	33.33	22.36	667
272	-68	6.94	9.29	-0.47	33.03	22.12	682
276	-69	8.12	9.39	-0.52	32.74	21.83	699
280	-70	8.87	10.28	-0.59	32.42	21.50	718
284	-71	9.78	12.76	-0.65	32.06	21.14	740
288	-72	10.37	16.53	-0.57	31.59	20.76	761

STEP	HRS	U	V	W	LAT	LON	LEVEL
0	0	14.53	3.58	0.23	36.33	34.15	500
4	-1	15.59	3.78	-0.09	36.21	33.55	496
8	-2	16.14	3.52	-0.29	36.10	32.92	501
12	-3	15.87	3.29	-0.40	35.99	32.29	511
16	-4	15.64	2.84	-0.40	35.89	31.68	523
20	-5	15.27	2.80	-0.23	35.80	31.08	533
24	-6	15.40	3.04	-0.03	35.71	30.48	535
28	-7	15.49	4.41	0.02	35.59	29.88	532
32	-8	15.59	5.31	0.01	35.43	29.28	529
36	-9	15.65	5.57	0.01	35.26	28.67	526
40	-10	15.85	5.34	0.00	35.08	28.07	523
44	-11	16.15	5.10	0.03	34.91	27.45	520
48	-12	16.83	5.28	0.07	34.75	26.81	515
52	-13	17.02	5.79	0.00	34.57	26.16	512
56	-14	17.33	5.72	-0.05	34.39	25.50	510
60	-15	18.16	5.44	-0.19	34.21	24.82	512
64	-16	19.52	5.05	-0.31	34.04	24.10	518
68	-17	20.48	5.53	-0.40	33.87	23.34	528
72	-18	21.93	6.57	-0.52	33.68	22.52	542
76	-19	21.35	8.84	-0.42	33.43	21.70	556
80	-20	21.28	10.23	-0.38	33.13	20.88	568
84	-21	21.12	11.38	-0.26	32.77	20.08	577
88	-22	21.65	11.98	-0.20	32.39	19.27	582
92	-23	22.27	12.47	-0.21	32.00	18.45	587
96	-24	22.51	12.82	-0.25	31.59	17.60	592
100	-25	21.23	14.02	-0.31	31.15	16.79	599
104	-26	20.56	14.69	-0.33	30.69	16.02	608
108	-27	20.23	15.33	-0.28	30.20	15.26	615
112	-28	20.02	16.30	-0.23	29.69	14.52	621
116	-29	19.59	17.24	-0.23	29.15	13.79	626
120	-30	18.76	17.38	-0.28	28.59	13.09	631
124	-31	18.63	16.26	-0.34	28.05	12.41	639
128	-32	18.22	15.15	-0.43	27.54	11.75	651
132	-33	17.68	13.76	-0.54	27.07	11.11	665
136	-34	16.93	12.11	-0.61	26.65	10.49	684
140	-35	16.54	10.83	-0.58	26.28	9.90	703
144	-36	16.01	9.51	-0.57	25.96	9.33	721
148	-37	15.69	8.57	-0.45	25.68	8.77	737
152	-38	15.50	8.77	-0.31	25.40	8.23	749
156	-39	15.38	9.04	-0.20	25.12	7.69	756
160	-40	15.05	9.44	-0.12	24.82	7.16	759
164	-41	14.40	9.75	-0.06	24.52	6.66	760
168	-42	13.49	9.70	-0.02	24.20	6.18	760
172	-43	12.57	9.14	0.01	23.90	5.74	758
176	-44	12.16	8.50	0.01	23.62	5.32	756
180	-45	11.98	8.07	-0.05	23.36	4.91	755
184	-46	11.59	7.81	-0.14	23.10	4.51	757
188	-47	11.13	7.46	-0.23	22.86	4.13	762
192	-48	10.57	7.38	-0.32	22.62	3.77	770
196	-49	9.62	7.43	-0.29	22.39	3.43	780
200	-50	8.96	7.61	-0.21	22.15	3.13	787

204	-51	8.51	7.62	-0.12	21.90	2.84	792
208	-52	8.23	7.48	-0.03	21.66	2.57	792
212	-53	8.06	7.33	0.05	21.43	2.30	790
216	-54	7.89	7.06	0.12	21.20	2.04	786
220	-55	7.02	6.24	0.06	20.99	1.80	781
224	-56	6.54	5.91	0.02	20.80	1.58	777
228	-57	6.16	5.70	-0.03	20.61	1.38	776
232	-58	5.83	5.59	-0.08	20.44	1.19	776
236	-59	5.51	5.59	-0.12	20.26	1.01	779
240	-60	5.18	5.68	-0.16	20.08	0.85	782
244	-61	5.10	4.88	-0.12	19.91	0.69	785
248	-62	4.86	4.03	-0.08	19.77	0.53	787
252	-63	4.53	3.18	-0.05	19.66	0.39	788
256	-64	4.15	2.38	-0.03	19.58	0.25	788
260	-65	3.76	1.66	0.00	19.52	0.14	787
264	-66	3.39	1.02	0.02	19.48	0.03	785
268	-67	3.77	0.85	0.05	19.45	359.92	782
272	-68	4.20	0.67	0.08	19.43	359.80	778
276	-69	4.61	0.49	0.10	19.42	359.67	773
280	-70	4.98	0.32	0.12	19.41	359.52	768
284	-71	5.28	0.18	0.13	19.40	359.36	762
288	-72	5.47	0.10	0.13	19.40	359.20	755

Table A3. Classification of the trajectories corresponding to the samples collected during August 1991-December 1992 with respect to their origins and meteorological conditions together with their elemental composition. The geographical coverage of trajectory codings is indicated in Figure 3.1. and the codes used for the type of airflow are as follows: A: Anticyclonic; C: Cyclonic; I: Isobaric (For the sake of space the sample number is given instead of date in the concentration tables).

A3.1. August 1991

Date	Sample No	900	850 hPa (mba)	700	500	Precipitation (mm)
01/8/1991	1	2a,A	2a,A	2b,A	3b,C	
05/8/1991	2	3a,C	2a,I	2b,A	2b,A	
06/8/1991	3	2a,C	2a,C	2a,C	3b,A	
07/8/1991	4	2a,I	2a,I	2a,I	3b,A	
08/8/1991	5	3a,C	3a,C	3a,A	3a,C	
09/8/1991	6	3a,C	3a,A	3b,A	3b,C	
10/8/1991	7	2a,C	2a,C	3b,I	2b,A	
12/8/1991	8	2b,C	2b,C	2b,A	2b,A	
14/8/1991	9	2a,A	2a,A	2a,A	3b,A	
15/8/1991	10	1a,A	1a,A	1a,A	3b,A	
16/8/1991	11	1a,I	1a,C	2a,A	2b,A	
19/8/1991	12	2a,I	2a,A	2a,A	2b,A	

20/8/1991	13	2a,A	2a,A	2a,A	2b,A
21/8/1991	14	2a,A	2a,A	2b,A	2b,A
22/8/1991	15	2a,C	2a,C	2a,A	3b,A
23/8/1991	16	2a,I	2a,I	3a,A	3b,A
26/8/1991	17	2b,A	2b,A	2b,A	2b,A
27/8/1991	18	2b,A	2b,A	2b,A	3b,A
28/8/1991	19	2a,I	2a,I	2a,A	3b,A
29/8/1991	20	2a,I	2a,I	2b,A	3b,A
30/8/1991	20	2a,I	2a,I	2b,A	2b,A
1/9/1991	20	2a,A	2a,A	2b,A	2b,A

August 1991

Sample No	Ca	Mg	Na	Al	Fe	Mn	Co (ng m ⁻³)	Ni	Cr	V	Zn	Pb	Cd
1	2445	1075	3075	925	1350	21	0.57	5.9	5.8	7.9	46	19	0.09
2	2190	1555	5300	770	625	12	0.49	4.5	3.5	8.4	17	21	0.08
3	2150	1111	4300	940	739	16	0.49	4.5	4.4	8.5	20	14	0.11
4	2130	1100	4200	820	1000	19	0.44	5.4	5.6	4.5	50	30	0.13
5	2055	940	4085	760	630	16	0.41	4.7	3.7	4.7	37	24	0.12
6	1980	1600	7385	930	1280	23	0.62	8.6	20	5.7	60	30	0.12
7	4680	1550	5085	1415	1445	32	0.86	9.1	12	15	45	30	0.18
8	7585	1590	3755	1800	1760	40	0.90	13	16	20	42	85	0.16
9	5365	1740	4185	1215	1965	22	0.75	9.8	19	22	35	50	0.09
10	2870	1960	7875	830	840	22	0.54	5.9	10	14	50	25	0.08
11	3565	1250	4520	750	725	17	0.38	5.4	7.7	10	33	40	0.06
12	3130	1300	4960	700	1115	21	0.50	4.1	8.1	8.5	58	20	0.07
13	1945	1160	4885	880	1525	22	0.49	5.1	5.3	3.8	49	25	0.07
14	3000	1245	3395	975	1090	25	0.54	6.6	8.8	8.3	47	25	0.10
15	2045	1210	5860	700	1120	22	0.40	4.5	8.3	4.9	57	29	0.07
16	2240	1265	5320	830	770	22	0.42	4.9	4.5	3.9	47	26	0.08
17	3635	1900	8890	825	1360	24	0.63	7.2	9.7	5.2	73	39	0.10
18	4300	1235	3280	1110	890	21	0.45	5.9	7.8	2.7	11	11	0.05
19	2350	1730	6300	605	520	15	0.29	5.4	8.2	9.1	41	21	0.06
20	2685	1150	3465	800	630	20	0.21	4.1	3.1	6.8	47	30	0.04

A3.2. September 1991

Date	Sample No	900 hPa	850 (mba)	700	500	Precipitation (mm)
02/9/1991	1	3a,A	3a,A	2b,A	2b,A	
03/9/1991	2	2b,A	2b,A	2b,A	2b,A	
04/9/1991	2	1b,A	1b,A	2b,A	3b,A	
05/9/1991	3	1b,A	1b,A	3b,A	3b,A	
06/9/1991	4	2a,C	2a,C	2b,A	3b,A	
07/9/1991	4	2a,C	2a,C	2b,A	3b,A	
08/9/1991	4	2a,A	2a,A	2b,A	3b,A	

09/9/1991	5	2a,A	2a,A	2b,A	3b,A
10/9/1991	6	2a,I	2a,I	3b,C	3b,A
16/9/1991	7	1a,A	1a,A	4a,C	3a,C
17/9/1991	8	3a,A	3a,A	3b,A	3b,A
18/9/1991	9	3a,A	3a,A	3b,A	3b,A
19/9/1991	10	3a,A	3a,A	3b,A	3b,A
23/9/1991	11	2a,A	2b,A	2b,A	2b,A
24/9/1991	12	2a,A	2a,A	2b,A	2b,A
25/9/1991	13	2a,A	2a,A	3a,A	3a,A
26/9/1991	14	2a,A	2a,A	2a,A	3b,A

September 1991

Sample No	Ca	Mg	Na	Al	Fe	Mn	Co (ng m ⁻³)	Ni	Cr	V	Zn	Pb	Cd
1	2900	1070	2720	1045	650	15	0.28	5.5	5.0	2.9	27	18	0.08
2	4410	1085	2250	935	805	19	0.59	5.2	4.1	2.3	14	16	0.05
3	4130	1325	3635	830	700	17	0.54	5.4	5.3	3.3	14	23	0.06
4	3200	1120	3445	710	620	16	0.46	4.6	3.7	7.9	28	37	0.05
5	4335	1010	2715	1060	860	22	0.88	7.0	6.8	16.2	30	33	0.06
6	4460	1050	4040	920	755	22	0.77	6.2	7.6	14.4	59	48	0.07
7	6815	2000	4865	1595	1595	36	1.75	9.5	6.5	17.7	64	51	0.08
8	5110	1345	3100	1790	1710	32	1.19	7.7	7.0	18.1	78	45	0.09
9	2300	1095	2040	845	775	22	0.62	5.2	4.5	4.4	73	35	0.07
10	4860	2555	4375	2120	1475	38	1.10	7.8	6.4	4.9	41	21	0.08
11	4235	970	415	675	895	22	0.66	7.2	8.1	11.9	25	47	0.06
12	5955	1100	5955	1320	1185	29	0.64	9.0	10.0	9.3	71	105	0.07
13	7050	1175	7050	1475	1295	32	0.79	11.0	15.0	22.1	51	137	0.10
14	9290	1625	9290	1895	1540	37	1.12	11.0	7.0	15.3	30	148	0.07

A3.3. October 1991

Date	Sample No	900	850 hPa (mba)	700	500	Precipitation (mm)
01/10/1991	1	1a,A	1a,A	1a,A	1a,I	
02/10/1991	2	1a,A	1a,A	1a,A	1a,I	
03/10/1991	3	4a,A	4a,A	1a,A	3b,C	
07/10/1991	4	3a,A	3a,I	3a,I	3a,C	17.5
08/10/1991	5	3a,C	3a,C	3a,C	3a,C	
09/10/1991	6	3a,C	3a,A	2a,C	2a,A	
10/10/1991	6	2a,A	2a,A	2a,A	2a,A	3.1
11/10/1991	7	1a,I	1a,I	2a,A	3b,C	
12/10/1991	7	1a,I	1a,I	3a,I	3b,C	
13/10/1991	8	4a,C	4a,C	3b,I	3b,I	
14/10/1991	9	2a,I	2a,A	2a,A	2a,A	
15/10/1991	10	1a,I	1a,A	1a,A	2a,I	
16/10/1991	10	2a,A	2a,A	3a,A	3b,A	

17/10/1991	11	2a,A	2b,A	2b,A	3b,A	
18/10/1991	12	2a,A	2a,A	3b,I	3b,C	
19/10/1991	13	3a,C	3a,C	2b,C	2b,I	30.2
20/10/1991	14	4a,C	4a,C	2b,A	2b,I	
21/10/1991	15	4a,C	2a,A	2b,A	3b,I	
22/10/1991	16	4a,I	4a,I	2a,A	3b,I	
23/10/1991	17	3a,A	3a,A	3b,A	3b,A	
24/10/1991	18	3a,C	3a,C	3b,C	3b,C	
25/10/1991	19	3a,I	3a,I	3b,C	3b,C	
26/10/1991	20	2b,A	2b,A	2b,I	2b,I	
27/10/1991	20	2b,A	2b,A	2b,A	2b,I	
28/10/1991	21	2a,A	2a,A	2b,A	3b,C	
29/10/1991	22	3a,A	3a,A	3b,C	3b,C	
30/10/1991	23	3a,A	3a,A	3b,C	3b,C	2.4
31/10/1991	24	3a,C	2a,C	3b,C	3b,C	0.3

October 1991

Sample No	Ca	Mg	Na	Al	Fe	Mn	Co	Ni	Cr	V	Zn	Pb	Cd
(ng m ⁻³)													
1	4370	1045	1815	2240	1065	21	0.43	11	11	9.2	19	37	0.25
2	3450	1120	1580	1865	1350	26	0.85	17	25	7.9	34	80	0.34
3	37600	14295	1745	22565	20045	305	1.00	55	65	122	54	47	1.39
4	325	225	830	430	110	2.5	0.25	3.5	3.4	2.4	11	6.9	0.07
5	300	190	1140	510	50	1.1	0.14	2.3	11.8	2.9	9.1	3.9	0.12
6	1535	215	480	230	140	2.5	0.01	2.2	5.0	4.6	8.6	56	0.08
7	4700	470	895	1540	2060	27	0.27	4.9	8.1	6.8	27	31	0.19
8	5115	2170	1875	3215	2470	41	0.88	10	21	14	21	23	0.40
9	2985	1145	1030	1370	1510	25	0.75	9.2	24	8.3	17	11	0.18
10	3445	855	815	1250	1115	20	0.67	6.3	15	11	46	66	0.24
11	4095	635	725	755	2485	51	0.51	10	14	10	47	87	0.30
12	1986	585	645	750	450	9.2	0.41	3.8	7.5	6.1	30	30	0.24
13	4025	655	405	1025	575	10	0.07	2.4	8.7	5.5	21	34	0.19
14	5650	2220	850	3030	2345	41	0.2	11	22	9.9	55	16	0.32
15	6015	2800	2160	2525	2155	37	0.82	12	16	8.8	35	20	0.21
16	6980	1420	185	1835	1545	25	0.93	12	17	8.7	17	31	0.16
17	7535	1770	615	1685	1730	28	0.62	15	29	18	32	70	0.27
18	2750	670	1370	235	165	1.8	0.28	4.7	9.3	1.9	5.0	4.9	0.04
19	3310	1035	1965	595	190	3.5	0.37	4.5	4.8	1.5	8.0	17	0.07
20	3460	765	2160	290	290	6.8	0.38	3.1	4.1	2.6	6.7	12	0.17
21	2930	555	3300	270	250	5.7	0.43	4.4	5.1	3.2	11	22	0.16
22	3740	990	495	1820	1600	35	0.60	5.9	10	7.2	16	30	0.18
23	5835	780	2485	1720	770	15	0.64	8.9	18	10	23	8.8	0.17
24	1265	620	745	650	630	8.5	0.24	1.9	2.4	10	6.9	18	0.11

A3.4. November 1991

Date	Sample No	900	850 hPa (mba)	700	500	Precipitation (mm)
01/11/1991	1	3a, I	3a, I	2b, A	2b, A	
02/11/1991	2	3a, C	3a, C	3b, C	3b, C	
03/11/1991	2	3a, C	3a, C	3a, C	3a, C	7.9
04/11/1991	3	3a, C	4a, C	2b, A	2b, I	
05/11/1991	4	3a, A	2a, A	2b, A	2b, A	
06/11/1991	5	2a, A	2a, A	2b, A	2b, A	
07/11/1991	6					
08/11/1991	7	3a, A	3a, A	3a, I	3b, I	
09/11/1991	7	3a, C	3a, C	3b, A	3b, A	
10/11/1991	8	3a, C	3a, C	3b, C	3b, A	
11/11/1991	9	2a, C	2a, C	2a, A	2b, A	
12/11/1991	10	3a, C	3a, C	3a, C	3b, C	
13/11/1991	11	2a, A	2a, A	3b, I	2b, A	
14/11/1991	12	2a, A	2a, A	2b, A	2b, A	
15/11/1991	13	2a, A	2a, A	2b, A	3b, A	
16/11/1991	14	3a, A	3a, A	3a, A	3b, A	
17/11/1991	15	3a, A	3a, A	3a, C	3b, I	
18/11/1991	16	3a, A	3a, A	3b, C	2b, C	
19/11/1991	17					21.6
20/11/1991	18	2b, A	2b, A	2b, A	2b, A	
21/11/1991	19	3a, A	3a, A	2b, A	3b, A	
22/11/1991	20	2a, A	2a, A	2b, C	3b, A	
23/11/1991	21	2a, A	2b, A	3b, A	3b, C	
24/11/1991	21	3a, A	3a, A	3b, C	3b, C	
25/11/1991	22	2b, A	2b, A	3a, C	3b, I	
27/11/1991	23	3a, C	3a, A	3b, I	2b, A	0.8
28/11/1991	24	3a, C	3a, C	3a, C	3a, C	8.4
29/11/1991	25	3a, C	3a, C	2b, A	2b, I	6.9
30/11/1991	25	3a, A	3a, A	3a, A	3a, A	1.8
1/12/1991	25	1a, C	4a, A	3b, A	3b, A	4.3

November 1991

Sample No	Ca	Mg	Na	Al	Fe	Mn (ng m ⁻³)	Co	Ni	Cr	V	Zn	Pb	Cd
1	1675	530	720	275	390	4.0	0.11	5.6	10	10	5.0	45	0.09
2	510	520	1745	120	195	3.3	0.04	1.8	4.5	3.1	8.0	26	0.07
3	230	185	445	200	80	1.7	0.22	1.9	4.8	5.9	1.0	28	0.01
4	440	275	560	150	115	1.9	0.01	2.3	3.5	1.7	1.7	12	0.05
5	935	315	600	180	260	5.0	0.10	6.6	8.7	9.4	7.3	38	0.08
6	1155	315	245	300	255	4.5	0.13	5.9	6.8	10	7.8	58	0.09
7	2260	700	740	465	710	11	0.16	5.9	7.3	14	37	71	0.22
8	2500	740	830	670	765	15	0.28	6.1	12	12	40	100	0.26
9	1930	620	530	575	745	10	0.17	6.3	6.2	16	29	65	0.22
10	2985	1060	345	1660	800	17	0.35	9.8	14	21	39	48	0.24

11	2575	640	150	315	655	12	0.20	4.3	8.0	9.7	50	59	0.04
12	1890	420	155	240	370	9.2	0.09	2.4	1.6	4.9	53	58	0.21
13	3650	990	840	570	880	16	0.27	5.1	0.7	3.4	49	76	0.23
14	6240	1840	645	1975	1880	30	0.82	8.4	16	17	42	88	0.26
15	6920	2520	360	2630	3030	35	0.56	9.4	18	19	28	26	0.31
16	3610	1790	2010	1410	1185	20	0.13	7.1	15	16	32	54	0.23
17	700	670	1980	230	235	5.5	0.13	2.1	3.6	9.7	24	51	0.14
18	530	510	1695	435	135	4.4	0.15	3.0	6.6	6.9	13	18	0.10
19	970	360	650	290	145	5.4	0.12	3.8	14	13	10	12	0.08
20	1240	335	395	115	200	2.4	0.04	5.7	17	41	11	49	0.19
21	1665	395	200	615	400	5.5	0.22	4.2	13	15	12	35	0.23
22	1665	610	365	805	710	9.8	0.34	3.2	2.5	9.6	10	12	0.18
23	1135	1270	3570	925	695	10	0.42	4.2	1.2	9.8	6.2	17	0.12
24	690	1160	3565	250	215	1.1	0.06	1.4	0.9	6.0	2.3	30	0.05
25	945	700	1565	350	410	5.1	0.11	2.5	4.0	5.9	3.5	27	0.06

A3.5. December 1991

Date	Sample No	900	850 hPa (mba)	700	500	Precipitation (mm)
03/12/1991	1	1b,A	1b,A	1b,A	1b,A	0.2
04/12/1991	2	2b,A	2b,A	2b,A	2b,A	0.1
05/12/1991	3	1b,A	2b,A	2b,A	2b,A	
06/12/1991	4	1a,A	1a,A	2b,A	3b,C	
07/12/1991	4	4a,A	4a,A	3b,C	3b,C	1.8
08/12/1991	4	3b,C	3b,C	3b,C	3b,C	22.2
09/12/1991	5	2b,C	2b,C	2b,C	2b,A	53.5
10/12/1991	6	2b,C	2b,A	2b,C	2b,C	9.2
11/12/1991	6	3a,A	3a,A	3a,A	3b,I	0.7
12/12/1991	7	3a,A	3a,A	2b,A	2b,A	18.5
13/12/1991	8	1a,C	1b,C	3a,A	3a,A	4.6
14/12/1991	8	1a,A	1a,A	4a,C	2b,I	
15/12/1991	8	1a,A	1a,A	1b,A	1b,A	
16/12/1991	9	2a,A	2a,A	2b,A	2b,A	
17/12/1991	10	2a,C	2b,C	2b,A	2b,A	
18/12/1991	11	2a,A	2a,A	2a,A	3b,I	
19/12/1991	12	2a,A	2a,A	2a,C	3b,C	
20/12/1991	13	3a,C	3a,C	3a,C	3a,C	
21/12/1991	13	4a,C	4a,C	3b,I	3b,C	0.3
22/12/1991	13	3b,I	3b,I	3b,I	3b,C	2.7
23/12/1991	14	3b,A	3b,A	3b,A	2b,C	41.4
24/12/1991	15	4a,C	4a,C	3b,A	3b,C	31.4
25/12/1991	16	4a,C	4a,C	3b,A	3b,C	
26/12/1991	17	4a,I	4a,I	3a,C	3a,A	0.6
27/12/1991	18	2b,A	2b,A	2b,C	2b,C	49.6
28/12/1991	18	2b,A	2b,A	2b,C	2b,A	0.9
29/12/1991	18	3b,C	3b,C	3b,C	2b,A	8.9
30/12/1991	19	3b,C	3b,C	3b,C	3b,C	8.1
31/12/1991	20	3a,I	3a,I	3b,C	3b,C	34.4
1/1/1992	20	2b,C	2b,C	2a,C	2b,C	

December 1991

Sample No	Ca	Mg	Na	Al	Fe	Mn (ng m ⁻³)	Co	Ni	Cr	V	Zn	Pb	Cd
1	675	395	745	470	230	2.9	0.23	3.1	7.6	1.5	4.5	12	0.04
2	2090	2215	6845	1775	565	13	0.08	4.3	6.2	11	11	74	0.09
3	2035	1605	4635	860	510	7.7	0.33	21	28	19	18	400	0.18
4	2215	7160	24755	515	455	11	0.09	8.7	9.0	5.1	17	39	0.13
5	620	1100	4070	285	120	1.8	0.03	5.4	9.3	4.6	7.0	15	0.05
6	935	1045	4765	475	87	2.5	0.03	2.9	5.8	7.6	6.4	45	0.07
7	420	220	1085	500	79	1.1	0.06	0.9	1.4	3.1	2.5	3.1	0.06
8	640	145	320	310	110	1.3	0.03	1.4	5.6	4.7	6.6	7.4	0.08
9	860	155	320	340	195	1.4	0.10	5.3	32	5.3	5.6	9.8	0.10
10	1300	240	220	560	240	5.3	0.09	3.0	11	7.8	13	9.8	0.01
11	2655	400	320	1020	320	8.1	0.19	4.9	20	19	18	15	0.20
12	2855	655	680	310	770	18	0.45	14	26	17	65	144	0.50
13	1780	3440	2950	190	400	9.4	0.41	34	19	9.7	30	104	0.53
14	1000	1375	5100	425	260	4.3	0.13	4.0	5.9	12	21	136	0.15
15	1800	2355	8930	395	370	4.6	0.13	3.0	0.3	6.1	10	103	0.31
16	1710	700	1280	495	570	8.1	0.19	4.6	2.9	16	19	112	0.29
17	920	3725	14540	385	195	2.7	0.08	4.0	1.7	6.5	5.8	20	0.05
18	1000	2785	10330	280	144	2.6	0.13	7.4	15	7.1	6.2	58	0.07
19	600	1885	7570	480	35	2.7	0.11	3.7	0.8	3.7	2.9	10	0.01
20	495	345	2400	125	170	2.6	0.10	4.7	13	10	4.3	11	0.07

A3.6. January 1992

Date	Sample No	900	850 hPa (mba)	700	500	Precipitation (mm)
02/1/1992	1	2b, A	2b, A	2b, A	2b, C	
03/1/1992	2	2b, A	2b, A	2b, I	2b, C	
04/1/1992	2	2b, C	2b, C	2b, C	2b, C	
05/1/1992	2	2b, A	2b, A	2b, A	2b, C	
06/1/1992	3	2a, I	2a, I	3a, C	2b, C	
07/1/1992	4	2b, A	2b, A	2b, C	2b, I	
08/1/1992	5	2b, A	2b, A	2b, C	2b, A	
09/1/1992	6	2b, A	2b, A	2b, A	2b, A	
10/1/1992	7	2a, A	2a, A	2b, A	2b, C	
11/1/1992	7	2b, A	2b, A	2b, A	3b, C	
12/1/1992	7	2a, A	2b, A	3b, A	3b, C	
13/1/1992	8	3a, C	3a, C	2b, C	3b, C	
14/1/1992	9	2a, I	2a, I	2b, C	2b, C	
15/1/1992	10	2b, I	2b, I	2b, C	2b, C	0.7
16/1/1992	11	2a, C	2a, C	2b, I	2b, C	
17/1/1992	12	2b, A	2b, A	2b, A	2b, C	
18/1/1992	12	2b, A	2b, A	2b, C	2b, A	
19/1/1992	12	2b, I	2b, I	2b, I	2b, C	
20/1/1992	13	2b, A	2b, A	2b, C	2b, C	0.1
21/1/1992	14	2a, I	2a, I	2b, I	2b, C	

22/1/1992	15	2a,C	2a,C	2b,C	2b,I
23/1/1992	16	2b,A	2b,A	2b,A	2b,I
24/1/1992	17	2b,A	2b,A	2b,I	2b,I
25/1/1992	17	1b,A	1b,A	1b,A	1b,I
26/1/1992	17	1b,A	1b,A	1b,A	1b,A
27/1/1992	18	1b,A	1b,A	1b,A	1b,A
28/1/1992	19	1b,A	1b,A	1b,I	1b,A
29/1/1992	20	1b,A	1b,A	1b,I	1b,A
30/1/1992	21	1a,A	1a,A	2b,I	2b,C
31/1/1992	22	2a,I	2a,I	2b,I	2b,C
1/2/1992	22	2b,A	2b,A	2b,A	2b,I
2/2/1992	22	2b,A	2b,I	2b,A	2b,I

9

January 1992

Sample No	Ca	Mg	Na	Al	Fe (ng m ⁻³)	Mn	Co	Ni	Cr	V	Zn	Pb	Cd
1	1765	880	1165	390	355	4.0	0.28	8.1	2.9	10	10	10	0.11
2	2370	665	2955	290	310	5.4	0.22	6.1	5.0	26	30	65	0.19
3	1550	385	465	160	200	3.4	0.13	4.9	2.1	4.9	20	11	0.24
4	1960	430	940	125	220	3.2	0.08	5.0	5.0	7.5	32	15	0.34
5	1885	490	1000	150	200	3.2	0.16	4.5	6.3	6.6	16	71	0.22
6	3825	1085	4760	230	565	11	0.42	10	3.9	19	56	29	1.05
7	7850	1810	6440	650	906	14	0.10	2.6	28	9.2	39	67	0.86
8	930	600	735	665	680	14	0.32	9.5	8.1	15	43	27	0.46
9	2585	1520	6275	575	590	7.9	0.27	9.0	12	21	25	36	0.47
10	4080	1700	7490	450	500	7.9	0.29	8.4	11	11	24	40	0.56
11	1825	480	610	240	260	6.7	0.20	4.2	10	5.6	28	30	0.22
12	4360	930	3015	370	345	7.2	0.27	5.7	12	27	28	46	0.08
13	1445	820	4475	150	180	3.1	0.12	4.2	16	9.6	38	8.2	0.09
14	1605	365	505	185	145	3.3	0.10	4.7	5.5	6.5	19	10	0.18
15	3255	1115	3625	590	500	9.8	0.32	8.1	8.9	12	23	116	0.10
16	2890	715	2590	405	330	5.1	0.26	6.3	5.8	12	27	122	0.48
17	4200	1400	4390	555	575	10	0.26	5.4	5.9	10	22	71	0.24
18	5465	1570	4980	570	610	10	0.44	7.9	9.2	9.1	16	23	0.28
19	7095	2475	8065	750	893	19	0.64	11	12	17	57	21	0.89
20	10160	4870	37800	1200	1045	15	0.90	13	5.2	9.4	27	21	0.81
21	2175	1500	5920	350	390	7.4	0.28	4.9	4.9	7.0	17	19	0.59
22	1630	1960	10200	215	272	11	0.49	2.6	11	8.8	16	29	0.41

A3.7. February 1992

Date	Sample No	900	850 hPa (mba)	700	500	Precipitation (mm)
03/2/1992	1	1b,I	1b,I	3a,I	3b,C	
04/2/1992	2	1a,A	1a,A	3a,C	1b,I	
05/2/1992	3	2a,A	2a,I	2b,I	2b,I	
06/2/1992	4	2b,A	2b,A	2b,A	2b,I	7.8

07/2/1992	5	2b, I	2b, I	2b, A	2b, C	
08/2/1992	5	2b, A	2b, A	2b, A	2b, C	
09/2/1992	5	2b, A	2b, A	2b, A	2b, C	
10/2/1992	6	1b, A	1b, A	1b, A	1b, A	
11/2/1992	7	2b, A	2b, A	2b, A	2b, A	
12/2/1992	8	2b, A	2b, A	2b, I	2b, I	
13/2/1992	9	2b, A	2b, A	2b, A	2b, C	
14/2/1992	10	2a, I	2b, I	2b, A	2b, I	
15/2/1992	10	2a, I	2a, I	2b, A	2b, A	
16/2/1992	10	2a, A	2a, A	3b, C	3b, C	
17/2/1992	11	4a, I	4a, I	3b, C	3b, C	
18/2/1992	12	3b, C	3b, C	3a, C	3b, C	
19/2/1992	13	3a, C	3a, C	2b, A	2b, I	17.2
20/2/1992	14	2b, I	2b, I	2b, A	2b, A	
21/2/1992	15	2b, A	2b, A	2b, A	3b, C	
22/2/1992	15	2a, A	2a, A	2a, C	3b, C	2.4
23/2/1992	15	2a, A	2b, A	2b, A	1b, A	5.4
24/2/1992	16	1b, A	2a, I	2a, C	2b, I	1.6
25/2/1992	17	3a, A	3a, A	3a, A	3a, I	
26/2/1992	18	1a, C	1a, C	1a, A	1a, A	0.2
27/2/1992	19	2b, A	2b, A	2b, A	2b, A	
28/2/1992	20	2b, A	2b, A	2b, C	2b, C	
1/3/1992	20	2b, I	2b, I	2b, I	2b, I	2.4

February 1992

Sample No	Ca	Mg	Na	Al	Fe	Mn	Co	Ni	Cr	V	Zn	Pb	Cd
(ng m ⁻³)													
1	4070	10260	34970	430	580	16	0.76	9.8	3.3	3.1	22	15	0.31
2	2900	1010	2070	250	290	7.3	0.25	5.6	5.2	5.2	15	22	0.20
3	2215	1360	4535	150	217	6.5	0.20	10	13	9.2	14	49	0.14
4	1360	1270	4925	115	135	5.2	0.09	4.1	5.8	6.1	20	18	0.11
5	2825	1085	2250	680	390	13	0.41	10	6.8	4.6	13	8.7	0.10
6	4125	910	570	720	515	10	0.30	4.9	5.4	4.0	8.7	24	0.12
7	2140	435	685	270	285	6.8	0.26	3.9	8.2	5.7	8.1	49	0.11
8	3550	1245	2845	450	500	11	0.31	6.8	12	9.5	37	48	0.19
9	3485	1165	2980	410	510	13	0.46	6.9	5.7	6.9	47	28	0.39
10	4965	1245	2070	510	1020	27	0.62	9.4	11	10	155	93	0.97
11	3650	1070	1645	710	1080	24	0.55	7.2	5.3	11	82	54	0.77
12	980	1255	4490	63	130	3.2	0.06	3.7	4.1	4.7	18	11	0.24
13	1280	1170	3830	132	115	1.1	0.12	2.3	1.4	1.6	7.3	12	0.08
14	1905	1145	3525	215	235	4.8	0.35	7.1	22	10	16	102	0.14
15	1980	2715	8065	340	400	6.6	0.27	4.2	8.2	7.6	13	13	0.38
16	550	390	1435	55	110	4.9	0.06	2.1	2.1	3.7	12	4.6	0.19
17	1270	390	635	120	175	4.1	0.17	3.1	2.2	3.7	13	4.1	0.26
18	1255	355	705	180	215	4.0	0.20	5.7	8.0	3.7	9.2	2.8	0.09
19	2535	630	1420	270	280	5.7	0.31	4.5	10	7.5	13	90	0.16
20	1775	495	875	170	220	6.7	0.10	2.0	7.0	3.4	18	29	0.23

A3.8. March 1992

Date	Sample No	900	850 hPa (mba)	700	500	Precipitation (mm)
02/3/1992	1	2a,C	2b,A	2b,I	2b,C	
03/3/1992	2	2b,A	2b,A	2b,A	2b,A	
04/3/1992	3	2a,A	2a,A	2b,I	2b,C	
05/3/1992	4	2b,A	2b,A	2b,A	2b,C	
06/3/1992	5	2b,A	2b,A	2b,A	2b,C	
07/3/1992	5	2b,A	2b,A	2b,A	2b,A	
08/3/1992	5	2b,A	2b,A	2b,C	1b,A	
09/3/1992	6	1b,A	1b,A	1b,A	2b,C	
10/3/1992	7	1b,A	1b,A	1b,A	2b,A	
11/3/1992	8	1b,A	1b,A	1b,C	1b,C	
12/3/1992	9	1b,A	1b,A	3b,C	3b,C	
13/3/1992	10	1b,A	1b,A	3b,C	2b,A	
14/3/1992	10	3b,A	3a,A	3b,A	2b,A	
15/3/1992	10	3a,A	3a,A	2b,A	2b,C	
17/3/1992	11	3a,C	3a,C	3b,C	2b,A	0.2
18/3/1992	12	3a,A	3a,A	2b,I	2b,C	9
19/3/1992	13	2b,C	2b,C	2b,A	2b,A	17.6
20/3/1992	14	2b,C	2b,A	2b,I	2b,C	
21/3/1992	14	3a,C	3a,C	2b,C	2b,C	
22/3/1992	14	2a,C	2a,C	2b,A	2b,A	3.6
23/3/1992	15	2a,C	2a,C	2a,C	3a,I	1.3

March 1992

Sample No	Ca	Mg	Na	Al	Fe	Mn	Co	Ni	Cr	V	Zn	Pb	
(ng m ⁻³)													
1	1695	210	295	325	320	6.3	0.16	1.4	10.5	2.9	23	8.1	0.18
2	2580	290	740	280	330	7.4	0.16	3.7	8.9	7.8	20	56	0.11
3	1760	1130	575	330	395	13	0.27	3.5	6.0	6.3	60	10	0.28
4	2065	2125	660	855	730	17	0.36	5.9	4.4	6.4	24	10	0.23
5	2135	880	2400	370	450	9.5	0.08	3.6	3.8	4.9	12	32	0.09
6	2550	1220	750	345	335	7.2	0.17	1.4	7.0	5.1	11	6.8	0.08
7	2355	1465	655	385	380	6.8	0.57	2.6	4.9	4.4	7.2	10	0.06
8	6945	11280	32315	1185	1570	40	1.5	13	6.9	9.8	57	39	0.16
9	52840	16745	44960	8100	6565	136	10.5	38	61	34	63	55	0.34
10	12860	5650	6585	7700	4355	72	0.27	12	19	16	36	54	0.52
11	3090	2040	5325	1315	1070	19	0.03	5.1	11	12	27	99	0.12
12	418	1280	4970	100	60	1.7	0.03	0.1	1.0	1.7	5.2	5.4	0.03
13	660	880	3130	115	105	3.4	0.20	0.1	2.7	1.8	14	7.9	0.10
14	845	580	1920	140	133	3.3	0.01	1.9	1.9	2.8	9.6	17	0.09
15	1135	280	870	120	155	3.4	0.04	0.8	4.4	4.0	7.5	19	0.40

A3.9. April 1992

Date	Sample No	900	850 hPa (mba)	700	500	Precipitation (mm)
01/4/1992	1	2b,A	2b,A	2b,A	2b,I	
02/4/1992	2	2a,A	2a,A	2b,A	3b,I	
03/4/1992	3	3a,A	3a,A	3b,C	2b,A	
04/4/1992	3	3a,I	2b,A	2b,A	2b,C	
07/4/1992	4	2b,A	2b,A	3b,C	3b,C	
08/4/1992	5	4a,A	4a,A	3b,I	3b,I	
09/4/1992	6	3b,A	3b,A	3b,A	3b,I	
10/4/1992	7	3a,A	3a,A	3b,C	3b,I	
11/4/1992	7	3b,A	3b,A	3b,C	3b,C	
12/4/1992	7	3b,A	3b,A	3b,A	3b,A	
13/4/1992	8	3a,A	3a,A	3a,I	3a,I	
14/4/1992	9	3a,C	3a,C	2b,A	2b,A	
15/4/1992	10	2b,A	2b,A	2b,A	2b,I	
16/4/1992	11	2b,A	2b,A	3b,A	3b,I	
17/4/1992	12	2a,A	2a,A	2b,A	2b,A	
18/4/1992	12	2a,A	2a,A	2a,A	3b,A	
19/4/1992	12	1a,A	3a,A	3b,C	3b,C	
20/4/1992	13	3b,A	3b,A	3b,A	3b,A	4
21/4/1992	14	3b,A	3b,A	3b,C	3b,C	
22/4/1992	15	2b,A	2b,A	2b,A	2b,A	
23/4/1992	15	2b,A	2b,A	2b,A	2b,A	
24/4/1992	16	2a,A	2b,A	2b,A	2b,I	
25/4/1992	16	2a,A	2a,A	2b,I	2b,I	
26/4/1992	16	2b,C	2b,C	2b,A	2b,I	
27/4/1992	17	2b,A	2b,A	2b,A	2b,I	
28/4/1992	18	2a,A	2b,A	2b,A	2b,A	
29/4/1992	19	2a,A	2b,A	2b,A	2b,A	
30/4/1992	20	2b,A	2b,A	4a,C	2a,A	

April 1992

Sample No	Ca	Mg	Na	Al	Fe	Mn	Co	Ni	Cr	V	Zn	Pb	Cd
	(ng m ⁻³)												
1	1760	930	865	440	365	8.8	0.29	6.7	9.6	8.2	22	12	0.13
2	2620	610	397	750	405	10	0.08	2.4	30	3.1	23	12	0.08
3	2325	1445	1400	1155	905	19	0.47	10	43	15	29	60	0.16
4	16030	2885	2785	2675	2190	42	0.87	14	44	24	50	65	0.26
5	7140	2280	5770	2755	1550	28	0.50	6.0	10	8.7	29	171	0.14
6	8920	2535	5560	4705	2445	34	0.45	13	41	17	11	47	0.06
7	5285	2815	3540	2995	1870	34	0.54	10	8.0	11	12	20	0.12
8	2500	1970	8200	395	325	7.4	0.14	2.0	1.8	0.4	2.4	30	0.02
9	1855	1230	3480	300	275	6.7	0.13	3.8	12	3.8	10	143	0.06
10	955	760	2665	195	200	8.6	0.06	2.9	2.4	1.1	33	61	0.24

11	1380	620	1600	200	240	7.7	0.08	4.2	23	4.5	22	238	0.1
12	5785	1730	4940	1200	1155	25	0.39	12	40	16	62	173	0.3
13	16790	7310	5885	9860	4855	72	1.69	7.6	10	12	13	10	0.0
14	9465	2455	3260	4445	2160	28	0.47	5.7	4.8	6.7	14	106	0.0
15	2400	875	1160	600	575	10	0.18	4.4	5.2	3.7	10	123	0.0
16	4255	1040	3000	615	535	12	0.25	7.3	25	9.0	17	95	0.3
17	3515	1040	1255	665	520	11	0.23	8.8	8.1	9.7	17	42	0.1
18	2185	1075	1020	815	725	14	0.33	14	21	14	24	43	0.0
19	6175	1815	1225	1415	1330	27	0.73	10	26	14	35	402	0.8
20	9060	1975	1565	2000	1555	27	1.60	18	11	25	32	354	1.4

A3.10. May 1992

Date	Sample No	900	850 hPa (mba)	700	500	Precipitation (mm)
04/5/1992	1	1b,A	1a,A	3b,A	3b,C	
05/5/1992	2	3a,C	3b,A	3b,A	3b,C	
06/5/1992	3	4a,C	4a,C	1a,C	3b,C	0.2
07/5/1992	4	1a,A	1a,A	3b,C	3b,A	
20/5/1992	5	2a,A	2a,A	2b,C	2b,A	
21/5/1992	6	2b,A	2b,A	2b,A	2b,C	
25/5/1992	7	2a,I	2a,I	2b,I	2b,A	
26/5/1992	8	2a,A	2a,A	2b,A	3b,C	
27/5/1992	9	3a,A	3a,A	3b,C	3b,C	
28/5/1992	10	4a,I	4a,I	3b,A	3b,A	

May 1992

Sample No	Ca	Mg	Na	Al	Fe	Mn (ng m ⁻³)	Co	Ni	Cr	V	Zn	Pb	Cd
1	10285	2720	3155	3145	7250	11	2.10	15	20	22	29	114	0.58
2	6150	1740	3720	275	950	7.3	0.54	6.0	10	7.7	11	30	0.29
3	2035	590	265	691	1497	7.3	0.60	22	45	29	17	655	0.42
4	17540	7055	6320	11255	30390	100	13	24	10	26	168	365	0.43
5	3310	885	2135	480	1990	10	0.48	8.0	16	15	26	733	0.32
6	760	635	44	1380	2215	22	0.53	8.8	6.5	8.9	32	74	0.30
7	5325	1860	1615	2100	5795	37	1.45	13	8.0	14	43	45	0.83
8	21865	14580	1000	14840	11455	190	8.52	44	38	38	47	110	0.41
9	20095	11825	435	11680	10600	139	2.86	36	44	31	41	54	0.43
10	17360	10085	3345	10495	14195	123	6.40	29	40	37	45	340	0.48

A3.11. June 1992

Date	Sample No	900	850 hPa (mba)	700	500	Precipitation (mm)
01/6/1992	1	3a,C	2a,A	2b,C	2b,C	
02/6/1992	2	2b,A	2b,A	2b,A	2b,C	0.1
03/6/1992	3	2b,A	2b,A	2b,A	3b,C	
04/6/1992	4	2b,A	2b,A	3b,C	3b,A	
05/6/1992	5	2b,A	2b,A	2b,I	3b,A	0.6
08/6/1992	6	2a,I	2a,I	2b,I	2b,I	
09/6/1992	7	2a,I	2a,I	3b,A	3b,C	
10/6/1992	8	3a,C	3a,C	3b,A	3b,I	
11/6/1992	8	3a,C	3a,C	3b,A	3b,A	
12/6/1992	9	3a,C	3a,C	3b,A	3b,C	
13/6/1992	10	2a,A	2a,A	3b,C	3b,C	
14/6/1992	11	3a,C	3a,C	3b,I	2b,A	
15/6/1992	12	3a,C	3a,C	3a,A	2b,A	
16/6/1992	13	2a,C	2a,C	2a,C	2b,C	
17/6/1992	14	2a,C	2a,C	2b,C	2b,C	0.2
18/6/1992	15	2b,A	2b,C	2b,I	3b,C	22.9
25/6/1992	16	1a,A	1a,A	1b,A	1b,A	
29/6/1992	17	2a,A	2a,A	2b,A	2b,A	
30/6/1992	18	3a,A	3a,A	2b,A	2b,A	

June 1992

Sample No	Ca	Mg	Na	Al	Fe	Mn	Co (ng m ⁻³)	Ni	Cr	V	Zn	Pb	Cd
1	2955	1285	2360	1955	1770	19	0.77	3.3	4.0	15	15	21	0.58
2	3190	1430	1515	1625	1335	21	0.93	7.5	14	18	7.5	19	0.52
3	3020	1435	2555	1750	1895	20	1.10	6.5	16	24	6.0	43	0.52
4	2548	1684	2123	1156	1356	26	1.44	14	18	20	53	306	0.60
5	1690	1025	2035	1760	1655	14	0.44	4.2	19	23	1.5	69	0.37
6	1190	1875	1965	2665	3745	31	1.65	10	41	32	9.7	22	0.46
7	1520	1535	1035	2135	5285	27	1.37	12	14	21	9.4	19	0.39
8	1565	1345	1140	2055	2255	26	1.06	11	27	15	47	19	0.33
9	2858	2130	1775	2360	4340	32	2.06	19	59	30	50	37	0.40
10	1885	2000	2600	3000	3310	28	1.28	11	17	21	21	21	0.32
11	3405	5940	10635	2295	8220	29	1.47	12	17	17	13	17	0.47
12	2155	2375	7705	1285	1700	12	0.58	5.8	7.0	9.0	10	15	0.24
13	3445	1310	2585	1070	1575	7.6	0.43	7.6	7.2	9.0	8.6	100	0.19
14	1000	670	1945	390	310	3.6	0.21	3.6	7.2	5.6	8.9	215	0.16
15	1430	880	2335	1010	1130	5.5	0.16	5.4	18	9.5	16	250	0.47
16	3700	1510	2010	1895	2500	23	0.99	14	20	17	52	29	1.27
17	2915	2575	8310	1585	2760	18	0.46	6.9	7.7	10	57	18	0.43
18	5055	2195	6995	700	855	32	0.81	2.3	21	12	89	59	0.56

A3.12. July 1992

Date	Sample No	900	850 hPa (mba)	700	500	Precipitation (mm)
01/7/1992	1	3a, I	2a, A	3b, A	2b, I	
02/7/1992	2	2a, A	3a, A	2b, A	2b, A	
06/7/1992	3	3a, I	2a, I	2a, A	2b, A	
07/7/1992	4	2a, A	2a, A	2b, A	2b, A	
08/7/1992	5	2a, A	2a, A	2b, A	3a, A	
09/7/1992	6	2a, I	2b, A	2b, A	3b, C	
14/7/1992	7	3a, A	3a, A	3a, A	3a, A	
16/7/1992	8	3a, A	3a, A	2b, A	2b, A	
19/7/1992	9	2a, A	2a, C	2b, I	3b, I	
20/7/1992	10	2a, C	2a, C	2a, C	2b, I	
21/7/1992	11	3a, A	3a, A	3a, A	2b, C	0.5
22/7/1992	12	3a, A	3a, A	2a, I	2b, A	0.7
23/7/1992	13	2a, A	2a, A	2b, A	2b, A	0.4
27/7/1992	14	1b, A	1b, A	2b, A	2b, A	
28/7/1992	15	2a, I	1b, I	2b, A	2a, A	
29/7/1992	16	2a, I	1a, I	2a, A	2b, A	
30/7/1992	17	1a, A	1a, A	2a, A	2b, A	

July 1992

Sample No	Ca	Mg	Na	Al	Fe	Mn	Co	Ni	Cr	V	Zn	Pb	Cd
(ng m ⁻³)													
1	4955	2075	6220	665	830	31	0.86	6.4	17	14	85	16	0.48
2	9640	2010	8695	320	810	25	0.94	2.3	16	12	49	43	0.33
3	11580	2795	3315	2630	2450	48	2.89	14	29	28	69	52	0.66
4	9935	2190	2170	2340	2120	41	2.15	13	58	31	67	55	0.57
5	8195	2085	2585	2220	1885	39	2.12	8.8	25	25	73	48	0.62
6	15225	3635	3540	3435	3765	75	2.41	17	29	25	74	36	0.52
7	6110	1725	2195	1405	1585	31	1.60	9.3	20	21	45	18	0.48
8	3860	1730	4455	370	740	18	0.95	4.3	7.9	15	41	42	0.26
9	4910	1745	3275	1000	1410	35	1.23	6.2	10	14	62	296	1.25
10	4085	2840	9800	765	970	27	0.85	6.5	7.6	13	49	39	0.76
11	2770	1520	4890	345	450	12	0.41	5.3	8.2	16	46	26	1.52
12	1800	935	2430	130	400	12	0.48	2.6	12	11	30	23	0.52
13	3920	1265	3380	510	535	15	0.58	4.8	4.5	7.8	27	50	0.27
14	5390	1730	4385	1000	1150	32	1.48	11	16	15	83	16	0.57
15	5350	2625	9255	1080	1100	30	0.39	12	8.8	0.6	86	55	0.65
16	3245	2630	11085	1170	1045	36	0.76	6.8	5.8	15	205	24	1.54
17	6435	2230	4825	1630	355	37	1.79	12	8.8	14	90	25	0.69

A3.13. August 1992

Date	Sample No	900 hPa	850 (mba)	700	500	Precipitation (mm)
03/8/1992	1	1a,A	1a,A	1a,A	2b,A	
04/8/1992	2	2a,A	2a,A	3a,A	3b,A	
05/8/1992	3	2a,C	2a,A	1a,A	3b,A	
10/8/1992	4	1b,C	1b,I	1b,C	2b,A	
11/8/1992	5	1b,A	1b,A	1b,A	2b,A	
12/8/1992	6	4a,I	1b,A	b,A	2b,A	
13/8/1992	7	1a,A	1a,A	3b,I	3b,I	
17/8/1992	8	2a,I	2a,I	2a,A	3b,A	
18/8/1992	9	2a,A	2a,C	2b,A	2b,C	
19/8/1992	10	2a,A	2a,A	2a,A	2b,A	
20/8/1992	11	2b,C	2b,C	2b,A	2b,A	5
24/8/1992	12	3a,A	3a,A	2a,C	2b,I	
25/8/1992	13	3a,C	3a,A	2b,A	2b,A	
26/8/1992	14	2a,A	2b,A	2b,I	2b,C	
27/8/1992	15	2b,A	2b,A	2b,A	2b,A	
31/8/1992	16					

August 1992

Sample No	Ca	Mg	Na	Al	Fe (ng m ⁻³)	Mn	Co	Ni	Cr	V	Zn	Pb	Cd
1	6830	2175	5415	1085	800	18	0.45	4.8	3.4	6.4	26	11	0.21
2	9070	2565	4370	1115	980	24	0.76	10	18	10	80	14	0.56
3	7115	1905	3045	1185	1075	25	0.52	10	8.1	14	66	13	0.59
4	8540	2640	955	2406	2030	36	1.43	14	16	14	39	104	0.43
5	4025	1445	150	1420	1100	21	0.62	6.3	9.0	8.2	19	65	0.24
6	7215	1840	170	2015	1860	35	1.26	15	11	10	16	257	0.20
7	14850	4130	1600	2530	2285	44	1.28	19	11	20	22	393	0.39
8	5545	2480	2300	1260	1000	19	0.54	7.5	8.4	8.4	25	10	0.19
9	6975	3150	2435	1145	975	18	0.67	8.5	10	9.4	17	11	0.14
10	18390	4450	3810	1640	1440	28	0.72	9.2	6.4	9.8	22	73	0.19
11	8360	2585	2900	1500	1165	24	0.59	10	19	9.7	23	152	0.43
12	5065	1545	3695	655	460	10	0.30	4.1	6.8	5.1	29	19	0.07
13	6960	2570	1400	890	730	16	0.57	6.1	8.4	7.8	44	84	0.98
14	10075	1985	3145	1240	880	17	0.53	6.1	14	8.7	44	29	0.77
15	8685	2505	4090	1210	900	17	0.70	6.8	16	7.6	30	100	0.38
16	7610	2330	3220	900	775	16	0.45	5.0	10	7.4	44	22	1.2

A3.14. September 1992

Date	Sample No	900	850 hPa (mba)	700	500
01/9/1992	1	3a,C	3a,C	3a,A	3a,A
02/9/1992	2	3a,C	3a,A	2b,A	2b,A
07/9/1992	3	3a,A	3a,A	3b,A	2b,A
08/9/1992	4	2b,A	2b,A	2b,A	2b,A
09/9/1992	5	2b,A	2b,A	2b,A	2b,A
10/9/1992	6	2a,A	2b,A	2b,A	2b,A
14/9/1992	7	2a,A	2a,A	2a,A	2b,A
15/9/1992	8	2a,A	2a,A	2b,A	2b,A
16/9/1992	9	2a,I	2a,A	2a,A	2b,I
17/9/1992	10	2a,I	2a,A	2b,A	2b,C
21/9/1992	11	3a,A	3a,C	3a,A	2b,I
22/9/1992	12	3a,A	3a,A	3a,I	3b,A
23/12/1992	13	3a,A	3a,A	3a,I	3b,I
24/9/1992	14	3a,A	3a,A	2b,A	2b,A
28/9/1992	15	1b,A	1b,A	2b,A	2b,I
29/9/1992	16	1b,A	1b,A	2b,A	2b,A
30/9/1992	17	2b,A	2b,A	2b,A	2b,A

September 1992

Sample No	Ca	Mg	Na	Al	Fe	Mn (ng m ⁻³)	Co	Ni	Cr	V	Zn	Pb	Cd
1	4050	2460	3525	650	630	12	0.68	5.3	9.6	7.3	29	18	0.20
2	12615	1895	2185	845	840	15	0.54	8.8	10	12	24	143	0.26
3	5765	1880	3110	1565	1300	26	0.84	5.4	9.7	8.3	36	50	0.30
4	19415	4810	2530	2310	1730	34	0.96	3.7	3.5	5.9	30	27	0.21
5	12115	3425	6300	2130	1660	31	1.26	6.1	7.4	6.4	30	32	0.23
6	20780	3715	1915	2140	1525	30	1.12	6.7	3.5	5.8	32	8.5	0.16
7	16295	2630	2390	1400	1310	26	1.76	6.9	4.4	5.2	49	27	0.43
8	14120	2235	4635	1010	900	19	0.52	3.2	3.4	5.5	21	17	0.16
9	6560	2100	4200	1245	1085	21	0.76	4.4	10	5.5	22	6.7	0.25
10	10040	2720	3800	1235	1205	25	0.74	4.7	8.3	9.3	28	13	0.14
11	11765	2935	4350	1090	980	20	0.64	4.5	11	7.8	46	11	0.13
12	7150	1815	2410	900	1060	22	0.86	6.4	17	10	63	56	0.79
13	8145	1930	4830	955	980	21	0.70	6.4	8.3	7.3	60	66	0.76
14	5375	2425	6155	975	945	20	0.72	4.8	9.7	5.8	32	40	0.29
15	7510	1535	1695	640	615	10	0.31	2.5	5.8	3.9	19	40	1.95
16	6820	1355	1125	895	630	12	0.26	5.4	6.2	5.2	42	21	3.65
17	7700	1525	560	830	685	13	0.24	3.0	2.6	2.7	23	8.7	2.30

A3.15. October 1992

Date	Sample No	900	850 hPa (mba)	700	500	Precipitation (mm)
01/10/1992	1	1a,A	2a,A	2a,A	2b,I	
05/10/1992	2	3a,I	3a,I	3a,I	3b,I	
06/10/1992	3	3b,C	3b,C	3b,C	3b,C	
07/10/1992	4	3b,A	3b,A	3b,C	3b,I	
08/10/1992	5	3a,A	3a,A	3b,C	3b,I	
12/10/1992	6	2b,A	2b,A	3b,C	3b,C	
13/10/1992	7	3a,A	3a,A	3b,I	3b,C	
14/10/1992	8	3a,I	3b,I	3b,C	3b,A	
15/10/1992	9	3a,I	3b,I	3b,C	3b,I	
16/10/1992	10	3a,A	3a,A	3b,A	3b,C	
17/10/1992	11	3a,I	3a,I	3b,A	2b,A	
18/10/1992	12	3b,A	3b,A	3b,A	3b,A	
19/10/1992	13	3a,A	3a,A	3a,A	3b,C	
20/10/1992	14	3a,A	3a,A	3b,C	3b,I	
22/10/1992	15	2a,I	2a,I	3b,I	3b,I	
23/10/1992	16	3a,A	3a,A	3b,A	3b,C	
24/10/1992	17	3b,C	3b,C	3b,C	3b,C	
25/10/1992	18	3b,A	3b,A	2b,A	2b,A	
26/10/1992	19	2b,A	2b,A	2b,I	2b,I	
27/10/1992	20	2b,A	2b,A	2b,A	2b,C	
28/10/1992	21	3a,A	3a,A	3a,I	3a,I	
29/10/1992	22	3a,C	3a,C	2b,C	2b,A	0.1
30/10/1992	22	3a,C	3a,C	3b,I	3b,I	
31/10/1992	23	3a,I	3b,I	3b,I	3b,I	

October 1992

Sample No	Ca	Mg	Na	Al	Fe	Mn (ng m ⁻³)	Co	Ni	Cr	V	Zn	Pb	Cd
1	5085	3585	515	595	585	12	0.75	6.0	3.0	7.2	12	24	0.17
2	11530	2675	2925	1400	1165	19	1.10	13	20	13	20	130	0.31
3	10185	4450	4425	3125	2265	42	2.70	13	42	21	25	160	0.33
4	12440	5020	2690	4420	2930	48	2.41	15	23	19	20	267	0.33
5	7835	3965	3820	2735	1970	37	1.59	7.6	20	14	17	26	0.22
6	7605	1690	705	1245	1040	16	1.08	8.2	33	11	12	37	0.28
7	12555	2840	1895	1705	1475	26	1.49	13	53	20	23	246	0.40
8	10480	3090	2460	2190	1620	28	1.35	11	18	14	26	113	0.33
9	7155	1900	1445	2095	1540	27	1.50	6.7	15	9.7	19	16	0.20
10	13395	2750	1030	2335	1845	31	1.64	8.9	3.5	8.2	17	22	0.17
11	12620	2460	2188	2195	1570	27	1.63	9.1	7.4	10	14	24	0.18
12	10025	2660	1645	1870	1450	24	1.55	10	8.1	10	15	40	0.30
13	9735	3125	2750	1815	1305	23	1.47	10	17	14	14	18	0.25
14	9205	1810	2170	1435	1065	18	1.01	11	26	16	13	71	0.33

15	4325	1915	1605	1475	1025	18	0.93	6.8	20	8.0	14	60	0.24
16	2624	745	755	1735	1500	20	1.00	6.1	25	8.6	24	20	0.22
17	16255	3690	6130	3590	2555	41	2.12	14	7.1	10	17	17	0.15
18	18540	3070	2345	1555	1225	24	1.09	9.7	0.7	4.0	7.9	4.8	0.07
19	4010	1320	3545	365	250	5.6	0.27	2.3	0.8	1.0	6.1	9.7	0.03
20	4185	1390	1585	165	190	3.4	0.16	2.8	3.5	1.3	5.1	32	0.03
21	2965	1000	2310	130	190	3.7	0.17	4.1	9.0	3.2	6.3	22	0.09
22	2955	825	1920	245	245	4.2	0.25	3.0	0.1	1.7	3.5	11	0.05
23	5675	1465	410	3210	2050	38	1.73	14	9.5	11.4	15.3	23	0.19

A3.16. November 1992

Date	Sample No	900	850 hPa (mba)	700	500	Precipitation (mm)
02/11/1992	1	2b,A	3b,A	3b,A	3b,I	
03/11/1992	2	2b,A	4b,C	4b,C	2b,I	
04/11/1992	3	4b,C	4b,C	4b,I	3a,I	
05/11/1992	4	4b,C	4b,C	4b,I	3a,C	
06/11/1992	5	2b,I	2b,I	2b,C	2b,I	
07/11/1992	6	2b,A	2b,A	2b,A	2b,C	
08/11/1992	7	2b,I	2b,I	2b,I	2b,I	
09/11/1992	8	2a,C	2a,C	2b,A	2b,A	
10/11/1992	9	2a,A	2a,A	2b,C	2b,C	
11/11/1992	10	2a,C	2a,C	2b,A	2b,A	
12/11/1992	11	2a,A	2a,A	2b,A	2b,A	
13/11/1992	12	4a,C	4a,C	3a,I	2b,I	
14/11/1992	12	3a,C	3a,A	3a,C	2b,C	6
15/11/1992	13	2b,C	2b,C	2b,A	2b,I	60.8
16/11/1992	14	2b,A	2b,A	2b,C	2b,A	1.5
17/11/1992	15	2b,A	2b,A	2b,A	2b,I	
18/11/1992	16	3a,A	3a,A	3b,A	2b,A	
19/11/1992	17	4b,A	4b,A	4b,C	3b,A	0.7
20/11/1992	18	4b,C	3b,C	3b,C	3b,A	11.7
21/11/1992	19	3a,C	3a,C	3a,C	2b,A	58.7
23/11/1992	20	2b,A	2b,A	2b,C	2b,C	
24/11/1992	21	2b,A	2b,A	2b,A	2b,A	0.3
25/11/1992	22	2b,A	2b,A	2b,A	2b,A	
26/11/1992	23	2b,A	2b,A	2b,I	2b,I	
27/11/1992	24	2b,A	2b,A	2b,I	2b,I	
28/11/1992	25	3a,C	3a,C	2b,C	2b,C	
29/11/1992	26	2b,A	2b,A	2b,A	2b,C	
30/11/1992	27	2b,A	2b,A	2b,I	2b,I	

November 1992

Sample No	Ca	Mg	Na	Al	Fe	Mn	Co (ng m ⁻³)	Ni	Cr	V	Zn	Pb	Cd
1	6330	1390	603	2140	2520	33	2.05	8.3	5.7	1.8	16	17	0.24
2	10195	2120	1020	3725	3880	48	1.91	13	23	7.8	24	36	0.39
3	14180	3145	1638	6115	6470	66	4.33	17	34	16	30	126	0.46
4	8860	2300	1555	3990	4580	50	3.85	10	9.5	13	24	18	0.23
5	8840	1690	2555	2290	2680	29	3.30	12	15	7.7	15	11	0.23
6	4445	1070	1880	810	1095	18	1.30	4.0	6.8	4.8	7.7	29	0.09
7	3165	520	185	385	585	11	0.80	6.5	6.6	4.7	7.9	34	0.13
8	3940	600	750	765	1210	20	1.66	8.1	8.4	5.2	10	34	0.04
9	5440	980	490	740	1455	23	1.86	9.9	18	8.4	12	69	0.25
10	5380	1240	390	1870	2250	27	1.68	4.4	10	7.3	11	24	0.32
11	6615	1710	2385	1940	2340	31	1.83	7.4	9.2	7.8	16	30	0.20
12	3135	1950	5600	1010	1335	17	1.23	9.0	14	5.8	17	84	0.19
13	1315	625	2290	115	190	2.3	0.13	1.9	24	5.9	5.3	22	0.09
14	1120	290	605	110	140	1.9	0.10	4.0	24	6.5	3.6	8.0	0.15
15	2500	570	1520	165	510	9.8	0.46	5.0	23	8.5	16	36	0.28
16	3475	625	780	195	485	9.4	0.58	0.9	26	7.7	12	21	0.24
17	3220	2235	9595	485	700	13	0.63	1.7	3.7	3.6	11	31	0.24
18	3675	2135	9975	1650	1770	19	1.06	4.3	6.0	5.7	11	19	0.23
19	925	895	3165	34	232	3.8	0.22	0.4	6.0	3.1	3.5	19	0.09
20	2960	915	2740	44	455	8.4	0.42	7.6	35	11	11	44	0.24
21	1760	595	76	835	685	12	0.76	4.4	8.4	5.6	5.7	2.1	0.22
22	1285	390	695	445	260	4.4	0.23	1.1	8.3	4.0	6.4	22	0.09
23	1030	390	1540	315	205	4.2	0.21	0.9	17	6.5	17	8.1	0.20
24	3065	515	1510	285	685	17	0.42	0.8	14	6.8	23	53	0.36
25	4730	735	1580	415	735	12	0.71	1.0	34	12	20	78	0.43
26	7320	1335	1755	725	1000	20	1.10	2.1	32	14	25	168	0.80
27	3165	1960	6775	745	715	17.	0.94	1.6	15	6.6	22	45	0.45

A3.17. December 1992

Date	Sample No	900	850 hPa (mba)	700	500	Precipitation (mm)
01/12/1992	1	4a,C	4a,C	3a,C	3a,C	2.1
02/12/1992	2	4a,A	4a,A	3b,C	3b,C	53.3
03/12/1992	3	4a,C	4a,C	1b,A	2b,A	5.2
04/12/1992	4	2a,A	2a,A	1b,A	3b,C	
05/12/1992	5	2a,A	2b,A	2b,C	2b,C	
06/12/1992	6	2b,A	2b,I	3b,C	3b,I	
07/12/1992	7	3a,A	3a,A	3a,C	3b,C	
08/12/1992	8	3a,C	3a,C	2b,I	2b,I	59
09/12/1992	9	3a,C	3a,C	2b,I	3b,I	3.3
10/12/1992	10	3a,I	3a,I	3b,I	3b,I	
11/12/1992	11	4a,I	4a,I	3b,C	3b,I	
12/12/1992	12	4a,C	4a,C	3b,A	3b,A	
13/12/1992	13	2b,C	2b,A	2b,A	2b,A	1.7
14/12/1992	13	3a,C	3a,C	3a,C	3a,C	12.4
15/12/1992	14	2b,C	2b,I	2b,I	2b,I	33.9
16/12/1992	15	2a,I	2a,I	2a,C	2b,I	13.8
17/12/1992	16	2a,I	2a,I	2a,I	2b,I	1.6
18/12/1992	17	2a,A	2a,A	2a,A	2a,A	
19/12/1992	18	1b,C	1b,C	1b,C	1b,I	
20/12/1992	19	1b,A	1b,A	1b,A	1b,A	
21/12/1992	20	1b,A	1b,A	1b,A	1b,I	
22/12/1992	21	1b,A	1b,A	2b,I	2b,C	
23/12/1992	22	2b,C	2b,C	2b,C	2b,C	
24/12/1992	23	2b,A	2b,A	2b,A	2b,A	
25/12/1992	24	1b,A	1b,A	1b,A	1b,A	0.2
26/12/1992	25	1b,I	1b,I	1b,C	1b,A	
27/12/1992	26	1b,I	1b,I	1b,C	1b,C	
28/12/1992	27	1a,A	1a,A	1b,A	3b,C	
29/12/1992	28	1a,A	2a,A	3a,I	3b,C	
30/12/1992	29	2a,I	2a,I	2b,C	2b,C	

December 1992

Sample No	Ca	Mg	Na	Al	Fe	Mn	Co (ng m ⁻³)	Ni	Cr	V	Zn	Pb	Cd
1	1495	1565	16635	210	125	6.2	0.46	6.0	8.8	1.0	3.7	14	0.11
2	600	245	245	55	160	3.8	0.24	2.9	2.7	1.3	1.7	10	0.21
3	695	67	52	160	130	1.8	0.16	2.6	3.9	0.3	3.2	5.1	0.08
4	1165	220	455	205	190	3.8	0.20	0.4	4.8	2.7	5.9	6.1	0.10
5	2035	275	80	243	234	4.5	0.24	2.2	5.5	4.7	8.9	19	0.21
6	2190	480	930	180	410	8.5	0.46	4.7	12	14	14	30	0.29
7	1710	1770	15160	285	280	9.4	0.70	9.2	9.6	3.5	7.1	27	0.16
8	2860	1560	3920	1100	1125	17	0.84	4.3	3.8	4.9	7.7	16	0.10
9	1570	380	285	350	620	9.1	0.07	4.4	2.5	2.4	7.4	6.1	0.30
10	2420	580	420	465	960	18	0.32	5.1	6.5	9.8	21	17	0.42
11	2530	550	955	200	480	8.3	0.18	3.9	2.8	3.9	13	11	0.24
12	1485	540	1320	40	380	6.6	0.18	1.2	0.6	7.5	10	15	0.29
13	560	820	3320	20	115	2.4	0.07	3.0	2.0	3.3	5.1	10	0.10
14	475	680	2300	25	37	1.8	0.02	0.7	2.9	1.6	1.7	6.6	0.09
15	630	920	3355	43	65	1.4	0.02	2.6	2.4	1.7	3.5	10	0.17
16	520	105	505	30	80	2.7	0.03	2.2	3.3	0.4	4.0	3.0	0.11
17	710	245	470	90	118	2.4	0.27	3.2	8.6	2.0	5.8	1.6	0.07
18	1500	650	1465	395	275	6.3	0.24	5.3	5.0	1.6	8.9	9.7	0.11
19	1095	235	330	185	180	4.7	0.05	3.6	3.4	1.9	5.9	1.4	0.16
20	1670	365	940	355	200	4.1	0.06	3.9	1.8	1.5	8.2	1.9	0.20
21	1700	375	230	455	265	6.5	0.20	4.0	8.0	9.9	13	24	2.75
22	1330	495	130	260	295	8.9	0.28	3.7	3.7	4.0	5.2	1.8	0.17
23	990	450	1255	135	315	6.6	0.10	6.8	7.0	5.3	2.5	6.4	0.36
24	955	170	325	275	224	6.3	0.24	4.8	4.0	4.3	10	8.4	0.30
25	790	120	245	100	100	2.7	0.04	3.7	1.2	3.4	5.4	13	0.23
26	1320	335	1215	205	180	5.9	0.12	3.1	2.3	4.1	6.1	19	0.19
27	3885	2315	8700	345	835	18	0.54	9.3	8.9	7.1	22	31	0.49
28	4410	1195	3000	950	795	14	0.50	7.9	10	6.9	19	57	0.39
29	1465	565	1390	385	495	11	0.11	6.0	18	8.7	18	27	0.45